The development of improved GFP mutants: Protein tagging and visualisation of gene expression patterns in mammalian cells and transgenic mice

GUOR MOUR HER

PhD

University of Edinburgh

1998

EX BIBL UNIV. EDINBURGEN

Declaration

I declare that this thesis was composed by myself.

Acknowledgments.

I never think that I can manage my work without so much support. First, I would like to thank for the opportunity of Ph.D. training provided by Prof. Nick Hastie and Dr. Bob Hill in the MRC Human Genetics.

Thanks very much for those experts who give enormous help and technical assistance: they are Mr. Brendan Doe, Dr.Paul Perry, Dr.Penny Rashbass and Ms. Allyson Ross. I also feel gratitude to Dr. Aswin Menke, Dr Colin Miles and Dr Duncan Davidson for their advises and suggestions for the writing of my thesis. Of course, I particularly thank for Dr. Bob Hill to give me a direction for my research, and his patience for correcting my thesis. I also want to express thankness to the members of MRC Human Genetics for all kinds of help.

Finally, I would like to thank my parents. Without their support, it is impossible for me to finish my Ph.D. degree.

June, 1998

Quote

For the invisible things of Him, both His eternal power and divine characteristics, have been clearly seen since the creation of the world, being perceived by the things made, so that they would be without excuse. **(Romans 1:20)**

Abstract

Green fluorescent protein (GFP), is a small and stable jellyfish (*Aequorea victoria*) protein with unique fluorescent properties. GFP can absorb UV or blue light and emit green fluorescence without the participation of other cofactors due to efficient autocatalytic formation of the GFP. These properties have enabled GFP labelling to be successfully used as a marker in many organisms. To increase fluorescent activity of GFP in the mammalian environment, mutations were created in a humanised form of GFP (containing mammalian codon-usage preferences). The fluorescence and expression efficiency of these mutants was characterised in mammalian cells and three of them showed strong fluorescence. In addition, stable green fluorescence was seen in established cell lines expressing these mutants with no obvious detrimental effect. In a study of WT1 nuclear function, three distinct nuclear patterns were seen in Cos7 cells depending on the isoform of WT1 in the GFP-WT1 fusions. These patterns were very similar to those reported for native forms of WT1 and the fluorescent signal provided a means to study these patterns at a high resolution. Functional domain analysis of WT1 was performed by expressing GFP and truncated WT1 fusions which suggested that the C-terminus (zinc finger regions) of WT1 had nuclear localisation signal(s) and additional signals which determined the specificity of the nuclear pattern. In addition, altered nuclear patterns of GFP-WT1 fusion were seen where coexpressed with truncated native WT1. These altered patterns implied that there was an association between native and truncated WT1 which may result in a dominant negative behaviour and the

mutated proteins caused dysfunctions of WT1 in cells. GFP transgenic mice were generated containing double-reporter constructs with either GFP fused to β-galactosidase (βGFP) or a dicistronic gene expressing GFP and β-galactosidase by a viral IRES sequence (dicistronic vector). Expression of these were driven by the Msx-1 promoter. Five GFP transgenic lines were generated and expressed both GFP fluorescence and x-gal enzymatic activity in embryos from E9.5 to E12.5. Both reporter activities were seen in many embryonic tissues including, maxillary and mandibular arches, eye, dorsal neural tube, somites, limbs and mid brain. In cryosections of E10.5 embryos, green fluorescence could be detected at a single cell level. In addition, optical sections of unfixed (E9.5 and E10.5) or culture embryos (E8.5) were taken by confocal analysis. Green fluorescent embryonic tissues were clearly seen at E10.5 embryos and in the neural fold at E8.5 embryos. In this thesis, GFP mutants are stable, non toxic and expressed with high efficiency. These proteins show strong green fluorescence and therefore are suitable for further studies. These GFP mutants were used as a protein tag to produce GFP-WT1 fusions and as a fluorescent marker under the control of the Msx-1 promoter to establish biological living systems in both mammalian cells and mouse embryos and to preliminary visualise expression of developmentally regulated genes. These results provide a foundation for further studies on developmental gene expression, protein localisation and protein-protein interaction in real time and space.

Table of Contents

Chapter 1 Introduction 1

1.1 Background: a short story about the development of GFP 1

1.2 The role of GFP in the formation of bioluminescence 2

1.2.1 Structure and formation of GFP chromophore 2
1.2.2 The bioluminescent pathway in *Renilla* and *Aequorea* 4

1.3 Properties of GFP 6

1.3.1 The structure of GFP 6
1.3.2 The spectra of GFP 8
1.3.3 The stability of GFP 9
1.3.4 Photoisomerisation and Photobleaching 11

1.4 GFP variants (mutants) 11

1.4.1 Wavelength-shifted variants 12
1.4.2 Codon-optimized variants 14
1.4.3 Enhanced solubility variants 16

1.5 Application 18

1.5.1 Visualisation of intracellular structure 19
1.5.2 Cellular protein trafficking events 22
1.5.3 Cell movement 23
1.5.4 Protein protein interaction 24
1.5.5 Host pathogen interaction 25
1.5.6 Vital marker in animals 26

1.6 The cellular function of WT1 33

1.6.1 Introduction 33
1.6.2 Structure of WT1 34
1.6.3 Cellular function of WT1 isoforms 35
1.6.4 WT1 mutations in Wilmis tumors 37

1.7 The functional role of Msx genes in mouse development 38

1.7.1 Introduction 38
1.7.2 Developmental expression of Msx genes in mouse embryos 39
1.7.3 The Msx-1 deficient phenotype 43

1.8 The aim of thesis 43

1.8.1 Optimised GFP fluorescent activity in mammalian enviroment 43
1.8.2 Visualisation of nuclear sublocalisation of GFP -WT1 (GW) isoforms and their mutants to predict the WT1 functional role in cells 44
1.8.3 Using an optimised GFP as an embryonic specific marker in developing mouse embryos 44

Chapter 2 Materials and Methods 46

2.1 Bacterial strains and media 46

2.1.2 Plasmid DNA and cloning vectors 47
2.1.3 Manipulation of plasmid 48

2.1.3.1 Preparation of *E.coli* competent cells 48
2.1.3.2 Bacterial transformation 49
2.1.3.3 Quick screening bacterial colonies 49
2.1.3.4 Plasmid DNA preparation and manipulation of plasmid DNA by enzymes 50

2.1.4 PCR reactions for subclonning of DNA fragment into vectors 50

2.2 In vitro PCR mutagenesis for GFP mutants 51

2.3 Nondenaturing gel electrophoresis analysis of GFP 51

2.4 Manipulation of mammalian culture cells 52

2.4.1 Cell culture 52
2.4.2 Transfection 53
2.4.3 Isolation of transfectants 53
2.4.4 X-Gal Staining of cell 54

2.5 Immunological and imaging techniques 54

2.5.1 Immunocytochemistry 54
2.5.2 Microscopy analysis 55
2.5.3 Western blot analysis 56

2.6 Techniques for animal experimentation 57

2.6.1 Transgenic mouse produce 57

2.6.1.1 DNA preparation 57

2.6.1.2 Microneedles preparation 58
2.6.1.3 Generation and collection of 2-cell stage of mouse embryos 58
2.6.1.4 Microinjection 58
2.6.1.5 Oviductal transfer 59
2.6.1.6 Tail biopsy and PCR analysis 60

2.6.2 Manipulation of Mouse embryos 60
2.6.2.1 X-Gal staining of mouse embryos 61
2.6.2.2 Vibratome sections of mouse embryos 61
2.6.2.3 Cryostat sections of mouse embryos 61

2.7 Whole mice embryo culture **62**

Chapter 3 Molecular characterisation of optimised GFPs **63**

3.1 Introduction **63**

3.2 The biological limitation of wild-type GFP **65**

3.3 The generation of GFP mutants **70**

3.4 Functional analysis of the GFP mutants **74**

3.4.1 GFP mutant with altered wavelength of excitation 74
3.4.2 Enhanced fluorescent GFP mutants 77

3.5 The molecular characteristics of GFP variants **84**

3.5.1 Comparison of the fluorescent intensity of GFP variants in BL21(DE)3 84
3.5.2 Comparison of the fluorescent activity of GFP variants in mammalian cells 85
3.5.3 Comparison of altered wavelength of GFP mutants 91
3.5.4 Stable expression in mammalian cells 94
3.5.5 The green fluorescence in two-cell stage of embryos 97

3.6 Discussion **99**

3.6.1 F64L mutation has a critical role for increasing GFP activity 99
3.6.2 The requirement for the optimal levels of GFP expression in mammalian cells 101
3.6.3 The stability of hGFP variants in mammalian cells 102

Chapter 4 Visualisation of subnuclear localisation of WT1 isoforms by using GFP as a vital fluorescent tag **104**

4.1 Introduction 104

4.2 Construction of GW expression vectors 105

4.3 Green fluorescent GW chimeras expressed in Cos7 cells 107

4.4 Molecular characteristic of GW isoforms 113
4.5 The functional analysis of GW isoforms 120

4.5.1 Comparison of subnuclear localisation of GW isoforms and WT1s 120
4.5.2 The unique nuclear patterns in Cos7 cells 124
4.5.3 GW isoforms may also associate with some nuclear proteins 124

4.6 Discussion 128

4.6.1 The consideration for design of GW constructs 128
4.6.2 A functional comparison of GW isoforms compared to WT1s 132
4.6.3 Cos7 cells may provide an similar environment for GW and WT1 isoform expression 133
4.6.4 The natural fluorescence of GW isoforms provide a detailed and sensitive signal 133

Chapter 5 Analysis of WT1 functional domains and the altered subnuclear localisations of mutated WT1 135

5.1 Introduction 135

5.2 Identification of putative NLS sequence for GW isoforms 136

5.2.1 The construction of the truncated GW isoforms 137
5.2.2 A putative NLS within the zinc finger regions 139

5.3 The zinc fingers are required for the nuclear patterns 141

5.4 Altered nuclear patterns caused by GW mutants 143

5.4.1 Dimerisation via the self-association domain of WT1 may cause a dominant negative behavior in the nucleus 143
5.4.2 The missense mutations of zinc fingers result in an altered subnuclear localisation 146

5.5 Discussion 152

5.5.1 The functional motifs for the nuclear localisation 152
5.4.2 The altered nuclear patterns caused by dominant negative mutations or missense mutations of the zinc finger regions of WT1 153

Chapter 6 Green fluorescent protein as a lineage specific marker in transgenic mouse embryos 157

6.1 Introduction 157

6.2 αGFP and βGFP constructs 159

6.3 Construction of transgenic vector 160

6.4 The production of GFP transgenic mice 164
6.5 Identification of GFP transgenic embryos 166

6.6 Detection of GFP expression in transgenic mice 174

6.6.1 A comparison of GFP fluorescent activity in βGFP, TFP and wild-type GFP 174
6.6.2 Identification of single green fluorescent cells in embryonic tissues 180

6.7 GFP fluorescence in living or unfixed transgenic embryos 187

6.8 Discussion 192

6.8.1 β–GFP behaves as a dual functional marker 192
6.8.2 Sensitivity of green fluorescence in βGFP transgenic embryos 192
6.8.3 The Msx1 promoter expressed in a similar embryonic patterns during embryogenesis as the endogenous Msx1 gene 194
6.8.4 The requirement of GFP fluorescent detection in the transgenic mouse embryos 194

Chapter 7 Conclusion and Perspective 197

Bibliography 203

Chapter 1 Introduction

1.1 Background a short story about the development of GFP

Bioluminescence is a common phenomenon in biology and organisms which display this feature have specialised proteins involved in fluorescence. One of these which has become of general interest recently is a jellyfish (*Aequorea victria*) fluorescent protein, green fluorescent protein (GFP). The importance of this protein is seen by the exponential increase in used of its biological and chemical properties.

The cDNA and genomic DNA from *A. victoria* was first reported by Prasher et al. (1992). Further, Chalfie et al. (1994) published results on the use of GFP as a genetic marker and protein tag in *C.elegans*. These reports opened the way for an immediate interest in GFP technology.

GFP technology became popular and useful in experimental biology because the jellyfish protein made it possible to visually trace gene expression or label proteins in cells, tissues and animals without any other exogenous factors. Furthermore, GFP techniques combined already existing analysis equipment and imaging methods (Galbraith 1995; Lybarger 1996; Niswender et al. 1995; Potter 1996; Terry et al. 1995; Valdivia et al. 1996; Yang et al. 1996; Zylka et al. 1996).

Traditional labelling techniques such as radioactive or immunochemical labelling are time consuming and labour-intensive. GFP labelling does not require antibodies or additional substrates which

make GFP ideal for directly labelling living cells. GFP makes real-time molecular studies of living cells possible and there are numerous applications for using GFP as a reporter for gene expression in different organisms (Cubitt et al. 1995; Gerdes et al. 1996).

1.2 The role of GFP in the formation of bioluminescence

Green fluorescent proteins exist in many bioluminescent organisms. Most of those organisms are metazoans and GFP can be identified in many Cnidarians such as *Aequorea, Renilla, hydra*, sea anemones and soft corals, Hydrozoans such as *Obelia, Phiallidium, Mitrocoma, Campanularia, Clytia, Lovenella, Diphyes* and Anthozoans such as *Ptilosarcus, Stylatula, Acanthoptilum* (Prasher 1995). However, amongst the numerous bioluminescent organisms the jelly fish *Aequorea victoria* has been of recent interest. *Aequorea victoria* , a Pacific Northwest species of jellyfish, shows green fluorescence from the light organ, photocytes, at the margin of its umbrella (Gerdes et al. 1996; Prasher 1995).

1.2.1 Structure and formation of GFP chromophore

The fluorescence of GFP is due to the unique chemical structure of the hexapeptide region (FSYGVQ) that constitutes the chromophore (Cody et al. 1993; Niwa 1996; Prasher et al. 1992) **(Fig.1.1)** of the protein. GFP absorbs light maximally at 395 nm with a smaller absorbance peak at 470 nm and the emission spectrum peaks at 509 nm with a shoulder at 540 nm (Inouye et al. 1994; Morise et al. 1974). GFP appears to be resistant to harsh environments and

denatured GFP can renature completely (Bokman et al. 1981; Ward et al. 1982). This suggest that the chromophore is quite stable and remains intact even if GFP is inactivated. When GFP refolds properly, the chromophore returns to a suitable environment and fluorescence is restored.

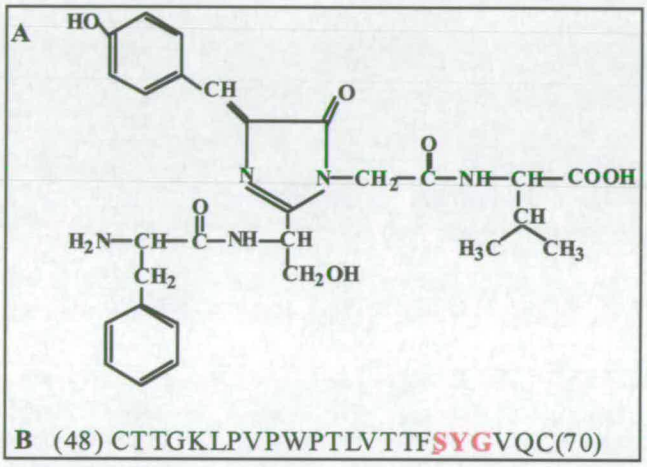

Fig.1.1 Structure of the GFP chromophore and nearby sequence.**A)** The structure of *Aequora* GFP hexapetide chromophoe was proposed by Cody et al. 1993. **B)** The cyclised chromophoe is formed from the 3 amino acids (underline) within the sequence.

This hexapeptide undergoes an autocatalytic cyclisation reaction of the tripeptide, Ser-Tyr-Gly, and a subsequent oxidation reaction at the cyclised tyrosyl side chain which are necessary to convert the nascent GFP (not fluorescent) to fluorescent GFP (Cody et al. 1993; Heim et al. 1994). The possible mechanism of this post-translational modification contains serial and complex biochemical steps. It is also crucial in determining the speed of formation of active GFP. The first step is a nucleophilic attack of the amino group of Gly67 on the carbonyl group of Ser65 to form a five-membered ring, followed by loss of water to form an imidazolin-5-one intermediate. The secondary step is the oxidation of the hydroxybenzyl side chain of

Tyr66 by atmospheric oxygen (Cubitt et al. 1995) **(Fig.1.2)**. So far, the catalyst for the cyclisation is unknown. However, the oxidation is an oxygen-dependent step. In wild-type GFP, it occurs spontaneously in the presence of air in about two hours (Coxon et al. 1995; Heim et al. 1994). In some GFP mutants, this oxidation only takes about 30 min. (Cormack et al. 1996; Heim et al. 1995)

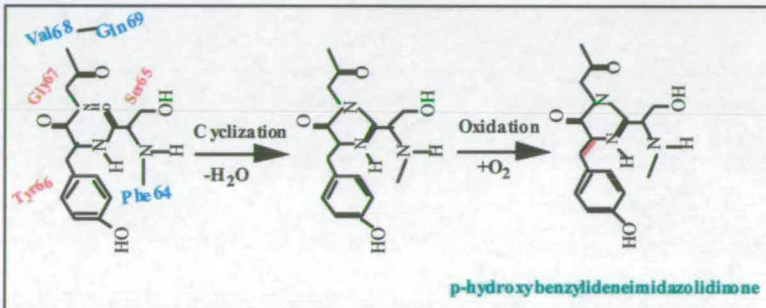

Fig.1.2 The biosynthetic mechanism for green fluorescent protein (GFP) chromophore contained cyclization and oxidation steps and formed a p-hydroxybenzylideneimidazolidinone chromophore.

1.2.2 The bioluminescent pathway in *Renilla* and *Aequorea*

Two well known GFP proteins are from marine invertebrates, *Aequorea victoria* (Pacific North-west jellyfish), and *Renilla reniformis* (Cubitt et al. 1995). The two systems are good examples of green fluorescence in cnidarians. The fluorescence from *A. victoria* and *R. reniformis* both follow similar biochemical pathways (Prasher 1995). They emit green light in vivo due to an energy transfer process from their photoproteins to GFPs.

In the jellyfish, the green light is formed by the intermolecular energy transfer between two closely associated proteins, aequorin, consisting of a Ca^{2+} -binding apoprotein or apoaequorin, and its

organic substrate, coelenterazine, and GFP. The Ca^{2+} bound aequorin induces a serial reaction in which coelenterazine is oxidised to coelenteramide, yielding blue fluorescence (λ_{max}=470 nm) from Blue Fluorescent Protein (BFP) (Inouye et al. 1985; Inouye et al. 1991; Tanahashi et al. 1990), and CO_2. One component of the BFP, the excited state coelenterazine, serves as an emitter or energy donor and GFP acts as the energy acceptor. When GFP is involved in the reaction, a bluish-green light (λ_{max}=508 nm) is emitted from the jellyfish due to the energy transfer from BFP (Inouye et al. 1994; Morise et al. 1974; Prasher et al. 1992; Ward et al. 1976; Ward 1979). However, in *Renilla* bioluminescence, a different photoprotein called luciferin-binding protein (LBP) is used. When LBP binds to Ca^{2+}, it becomes an oxidised coelenterazine (coelenteramide) transferring energy to *Renilla* GFP (Prasher 1995) **(Fig. 1.3)**.

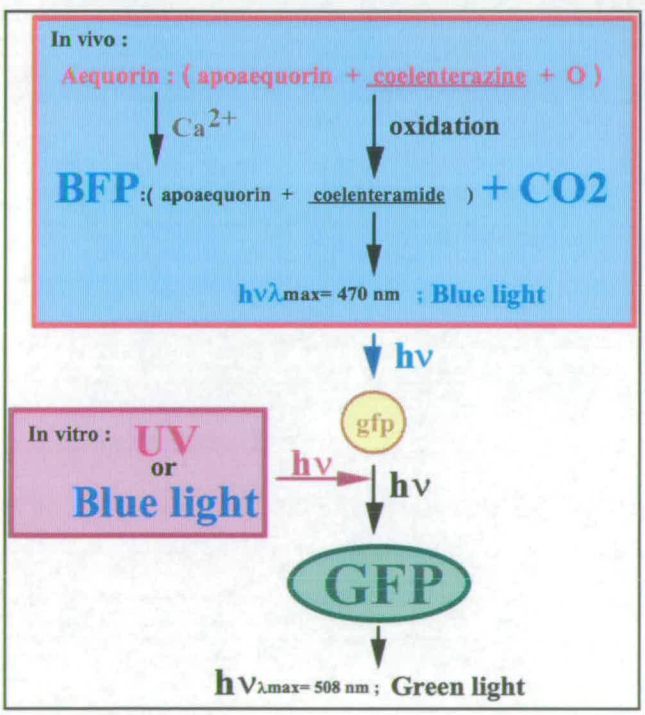

Fig.1.3 The scheme of green fluorescent pathway of *Aequorea victroria* GFP. In vivo, aequorin binds directly to Ca^{2+} by oxiding the coelenterazine and the energy released on oxidation of coelenterazine or coelenteramide stimulates GFP to emit green light. However, the photprotein, aequorin will release blue light in vitro in the absent of GFP. In vitro, GFP can also accept the energy directly from other light sources such as UV or blight light and emits the same green fluorescence.

In vitro, the aequorin is not an essential part of the green-light producing reaction in *Aequorea* because the purified GFP can be made to emit green light by exciting it directly with UV or blue light (Inouye et al. 1994). This ability to fluoresce in the absence of a natural energy transfer system is the trait which enables GFP to be used as a marker in heterogeneous systems. However, using the purified *Renilla* protein, green light is generated as a result of protein-protein interactions between *renilla* GFP and luciferase (Prasher 1995; Ward et al. 1976; Ward 1979).

1.3 Properties of GFP

1.3.1 The structure of GFP

Prasher et al. (1992) first reported the cloning and sequencing of both cDNA and genomic DNA of *Aequorea* GFP. The GFP gene has at least three exons in a 2.6 kb genomic sequence. The nucleotide sequence of *Aequorea victoria* cDNA contains a 720 bp coding region and northern analysis of GFP mRNA reveals it is 1.05 kb. The deduced translation indicates that GFP is a 238-aa protein having a calculated M_r of 26888. The estimated GFP molecular weight is equivalent to the 30 kd of native GFP (determined by SDS gel electrophoresis) (Inouye et al. 1994; Prendergast et al. 1978).

The crystal structure of GFP has also been reported by two independent research groups (Ormo et al. 1996; Yang et al. 1996). Yang et al. (1996) proposed the crystal structure of recombinant wild-type green fluorescent protein at a resolution of 1.9 Å using seleniomethionyl-substituted protein and multiwavelength anomalous dispersion (MAD) phasing methods. In S. J. Remington's group, they

showed the structure of the GFP mutant, S65T-GFP, using multiple isomorphous replacement and anomalous scattering method (Ormo et al. 1996).

Both groups proposed a very similar three-dimensional (3D) molecular structure of GFP. The main feature of the 3D structure of GFP indicated that the protein is in the shape of a cylinder, comprised of 11 strands of β-sheet or barrel with an α-helix inside and short helical segments on the ends of the cylinder resulting in a specific protein fold, β-can (Yang et al. 1996).

The mature active GFP protein has a hydrophobic surface, on the outside face of the cylinder structure and the chromophore is highly protected, located on the geometric centre of the cylinder (Ormo et al. 1996). These unusual structural features may explain the Stokes' shift (wavelength difference between excitation and emission maxim), the high quantum yield of fluorescence, the inability of O_2 to quench the excited state and the resistance to external pH (Bokman et al. 1981; Prendergast et al. 1978; Ward et al. 1982). The tight structure must be formed without a catalyst, since there is no entrance sites for enzymes taking substrate (Heim et al. 1994).

Dopf et al. (1996) made N-terminal and C-terminal truncations of GFP to study of the primary structural requirements for chromophore formation and subsequent GFP fluorescence. They showed that the minimal domain required for fluorescence extends from amino acid 2 to 232 in wild-type GFP. Since the last seven or more amino acids of the C-terminus of GFP cylinder are disordered, they do not play a critical role in the structure. However, the N-terminal

segment seems important for folding GFP or in protecting the chromophore (Yang et al. 1996). Truncation of segments may not allow for proper folding or positioning of the chromophore. Thus, it is impossible to make a mini-GFP or smaller GFP; however, it is possible to make either a N-terminal or C-terminal fusion of GFP to create a larger GFP or GFP chimera (Wang et al. 1994).

Furthermore, the 3D structure of GFP explains some properties of the GFP mutants. The GFP chromophore is highly protected and surrounded by a cylinder structure and several mutations in this regions have been reported (Cormack et al. 1996; Delagrave et al. 1995; Heim et al. 1994; Heim et al. 1995). Some mutants cause significant wavelength shifts and increase the fluorescent activity. For example, an important mutation within the chromophore of GFP affected the structure and thus altered the spectral features. This changed serine at position 65 for a threonine, refereed to as S65T, which increased fluorescent intensity and changed the excitation wavelength (Heim et al. 1995). The mechanism for increased fluorescence may be due to reduce collisional quenching, because an amino acid replacement may provide an additional side chain or functional group resulting in a better packing in the interior of the protein (Delagrave et al. 1995).

1.3.2 The spectra of GFP

Aequorea GFP or purified recombinant wild-type GFP has two excitation peaks, the larger excitation peak at 395 nm and the smaller peak at 475 nm. The emission maximum is at 508 nm (Chalfie

et al. 1994; Inouye et al. 1994). However, GFP mutations can alter excitation (Heim et al. 1995; Heim et al. 1996) and emission spectra (Heim et al. 1994). Some GFP mutations in the chromophore region shift the excitation maximum to about 490 nm (Heim et al. 1995). Some mutants have the substitutions outside of the chromophore and show a single excitation peak at either UV or FITC wavelengths (Anderson et al. 1996; Ehrig et al. 1995) (also see 1.4.1 for more discussion).

1.3.3 The stability of GFP

The unique chemical structure of the GFP chromophore results in a small but extraordinarily stable protein. The GFP chromophore can resist a variety of harsh conditions including heat, extreme pH (Bokman et al. 1981), and some chemical denaturing reagents (Cody et al. 1993; Robart et al. 1990). In these situations, the chromophore remains intact while the extra-chromophoric regions denature. However, once a suitable environment is re-established, the GFP refolds properly and returns its fluorescent activity (Bokman et al. 1981; Ward et al. 1982)

This unusual stability means that GFP fluorescence can be detected when subjected to relatively harsh conditions. For example, fluorescence of GFP is detected in expressing cells of *C.elegans* (Chalfie et al. 1994), *D.melanogaster* (Wang et al. 1994), HEK293 cell (Marshall et al. 1995), CHO cell (Kitts et al. 1995; Olmsted et al. 1994) and in recombinant GFP isolated from *E.coli* (Chalfie et al. 1994), when subjected to fixatives such as glutaraldehyde, formaldehyde or paraformaldehyde. GFP remains active in a broad pH range (pH7-12),

but loses its fluorescence at low pH (pH5.5-7) (Bokman et al. 1981). Many organic solvents do not significantly change its fluorescence (Bokman et al. 1981). However, some chemicals such as nail polish used to seal coverslips (Chalfie et al. 1994; Wang et al. 1994), nematode anesthetic phenoxypropanol (Chalfie et al. 1994), H_2O_2, , DTNB (5, 5'-dithio-bis-{2-nitrobenzoic acid}) (Inouye et al. 1994) and acetone (personal observation) have severe effects.

The formation of the GFP chromophore (active GFP) is very sensitive to temperature. However, mature GFP proteins are highly stable, and remain fluorescent up to 65°C (Ward et al. 1982). In microbes, wild-type GFP fluorescence was strongest when cells were grown at low temperature (<37°C) while low fluorescence was seen at higher temperature (>37°C). For example, yeast cells had only about 25% GFP fluorescent activity when they grew at 37°C rather than at 15°C (Lim et al. 1995). In *E.coli* cells, they showed stronger fluorescence when grown at 24°C / 30°C compared to 37°C (Heim et al. 1994). Mammalian cells expressing wild-type GFP have been seen to exhibit stronger fluorescence when grown at 30-33°C compared to 37°C (Ogawa et al. 1995; Pines 1995). Some GFP mutations have an ability to suppress the thermosensitivity and obtain a high fluorescent activity when the cells are incubated at 37°C (Cormack et al. 1996; Crameri et al. 1996; Matsumura et al. 1996; Siemering et al. 1996; Yang et al. 1996).

GFP seems quite stable when expressed in various organisms (Cubitt et al. 1995; Gerdes et al. 1996; Prasher 1995). Niswender et al. (1995) quantified the expression of GFP in mammalian cells. They used

three different imaging methods to identify GFP fluorescence and found that GFP fluorescence was reduced to half its original brightness after about 20 min of continuous illumination using blue light and the half-life of wild-type GFP was determined to be about 2-7 min. The concentration of wild-type GFP required to detect fluorescence in HeLa cells was found to be about 1μM estimated under the same condition.

1.3.4 Photoisomerisation and Photobleaching

Illumination of wild-type GFP can cause two distinct spectral changes over time. First, a photoisomerisation that progressively decreases at the 395 nm absorption peak and increases at the 475 nm peak. Secondly, a photobleaching process occurs that causes both peaks to decline by approximately equal proportions (Cubitt et al. 1995). This phenomena had been seen in Chalfie's early studies (Chalfie et al. 1994) using GFP as a marker in *C.elegans*. He found the exposure of GFP to a wavelength of 395 nm causes rapid loss of intensity and results in greater fluorescence when illuminated at 475nm. In fact, wild-type GFP has less fluorescent detection caused by photobleaching when GFP is illuminated by UV light in mammalian cells (Niswender et al. 1995). Fortunately, there are several FITC-shifted GFP mutants which have been recently reported (Delagrave et al. 1995; Heim et al. 1995). These mutants do not have a UV excitation peak and only have an excitation wavelength at blue light but still maintain their stable green fluorescent activity without detectable photobleaching.

1.4 GFP variants (mutants)

Despite Chalfie et al. (1994) showed wild-type GFP is useful as an experimental marker in *C.elegans*. Wild-type GFP still may have some biological limitations. For example, wild-type GFP is temperature sensitive and has photobleaching problems when stimulated by UV light (Heim et al. 1994; Kaether et al. 1995; Lim et al. 1995; Ogawa et al. 1995; Pines 1995; Webb et al. 1995). The most significant limitations have been found in mammalian cells (Pines 1995). The reasons may be due to inactive GFP forms (Crameri et al. 1996; Siemering et al. 1996), low translation efficiency (Chiu et al. 1996; Haas et al. 1996; Yang et al. 1996; Zolotukhin et al. 1996; Zylka et al. 1996), low intensity (Crameri et al. 1996; Heim et al. 1995; Siemering et al. 1996), complex photobleaching (Chalfie et al. 1994), and a significant lag in the development of fluorescence after protein synthesis (Cubitt et al. 1995). In some plants, the coding sequence of wild-type GFP has a cryptic plant intron that also interferes with the GFP expression (Haseloff et al. 1995). Thus, the development of stronger and more stable GFP variants became a way of optimising the system. In fact, a group of different GFP variants which overcame the limitations of wild-type GFP were created (Chiu et al. 1996; Cormack et al. 1996; Cormack et al. 1997; Crameri et al. 1996; Delagrave et al. 1995; Heim et al. 1995; Siemering et al. 1996; Yang et al. 1996; Zylka et al. 1996).

1.4.1 Wavelength-shifted variants

Heim et al. (1995) first reported the increased fluorescent activity of GFP mutants in which the Ser65 of the GFP chromophore region could be mutated by one of four amino acids, Ala, Leu, Cys and

Thr resulting in a single excitation peaks at 470-490nm with 4-6 times the amplitude of wild-type GFP. Especially, GFP-S65T which had the longest wavelength of excitation (490 nm) with emission at 510 nm. In addition, the crucial post-translational oxidation which produces the active chromophore proceeded about 4 times more rapidly than wild-type GFP. Delagrave et al. (1995) found a very similar mutant called Red-Shifted GFP (RSGFP) based on its excitation spectra similar to *Renilla reniformis* GFP and also had 3 mutations (F64M/S65G/Q69L) in the chromophore region. However, the RSGFP also showed similar spectral and intensity features to GFP-S65T. Another striking mutant had blue fluorescence due to the histidine in place of tyrosine at position 66 of the chromophore region and shifted the emission maxima to 448nm (Heim et al. 1994). Ehrig et al. (1995) proposed two GFP mutants with altered excitation spectra, GFP_{T203I} and GFP_{E222G}. In GFP_{T203I} , a threoine in place of an isolucine at position 203, shifted the excitation maxima to 390 nm. In GFP_{E222G}, a glutamine in place of a glycine at position 222, shifted the excitation maxima to 470 nm. Similar spectral mutants (GFP-Vex1 and GFP-Bex1) were also produced by Anderson et al. (1996). The GFP-Vex1 had S202F, T203I and V163A changes and showed a similar excitation peak as GFP_{T203I}. The GFP-Bex1 had S65T and V163A change and showed the similar excitation peak compared to GFP_{E222G}. All these wavelength GFP mutants are summarised in **Table 1.1**.

Table 1.1 Spectral properties of wavelength GFP mutants				
Clone	Mutations	Excitation Maximum (nm)	Emission Maximum (nm)	Reference
Aequorea GFP	None	396(476)	508(503)	(Chalfie et al. 1994)
Renilla GFP	None	489	507	(Delagrave et al. 1995)
S65T	S65T	489	511	(Heim et al. 1995)
RSGFP	F64M	490	505	(Delagrave et al. 1995; Yang et al. 1996)
	S65G			
	Q69L			
H9	S202F	398	511	(Heim et al. 1994)
	T203I			
P9	I167V	471(396)	502(507)	(Heim et al. 1994)
p11	I167t	471(396)	502(507)	(Heim et al. 1994)
P4	Y66H	381	445	(Heim et al. 1994)
P4-1	S65T	504(396)	511	(Heim et al. 1996)
	M253A			
	K238E			
P4-3	Y66H	381	445	(Heim et al. 1996)
	Y145F			
W	Y66T	458	480	(Heim et al. 1994)
W2	Y66W	432(453)	480	(Heim et al. 1996)
	I123V			
	Y145H			
	H148R			
	M153T			
	V163A			
	N212K			
W7	Y66W	433(453)	475(501)	(Heim et al. 1996)
	N146I			
	M153T			
	V163A			
	N212K			
GFP-T203I	T203I	400	512	(Ehrig et al. 1995)
GFP-VEX1	S202F	406(488)	495-535	(Anderson et al. 1996)
	T203I			
	V163A			
GFP-E222G	E222G	481	495-535	(Ehrig et al. 1995)
GFP-BEX1	S65T	395(488)	495-535	(Anderson et al. 1996)
	V163A			
5B,9B	T203H	512	524	(Ormo et al. 1996)
	S65T			
6C	T203Y	513	525	(Ormo et al. 1996)
	S65T			
10B	T203Y	513	525	(Ormo et al. 1996)
	F64L			
	S65G			
	S72A			
10C	T203Y	513	527	(Ormo et al. 1996)
	S65G			
	V68L			
	S72A			
11	T203W	502	521	(Ormo et al. 1996)
	S65G			
	S72A			

1.4.2 Codon-optimized variants

It is known that the codon usage in both prokaryotic and eukaryotic genes is strongly biased (Grantham et al. 1981; Zhang et al.

1991). Similarly, one of the reasons for low expression of wild-type GFP in the mammalian cells was the poor translational efficiency of the mRNA. In fact, translation in mammalian cells is characterised by a set of isoacceptor tRNAs that are different than those used in the jellyfish (Zolotukhin et al. 1996). Haas et al. (1996) and Zolotukhin et al. (1996) analysedd the sequence of *Aequorea* GFP cDNA and found that codon usage frequencies of the jellyfish gene is quite different from those prevalent in the human genome.

Recently, there were four independent research groups which re-engineered GFP coding sequences to contain codons preferred in human genes (Chiu et al. 1996; Haas et al. 1996; Yang et al. 1996; Zolotukhin et al. 1996). The re-engineered GFP proteins were called codon-optimised GFP or humanised GFP (Yang et al. 1996; Zolotukhin et al. 1996). Zolotukhin et al. (1996) made 92 base substitutions for 88 codons in wild-type GFP coding sequence and the re-engineered GFP, gfp$_{h}$, produced 5 to 10 times more fluorescent activity compared to wild-type GFP. Chiu et al. (1996) also proposed a mammalian codon-optimised GFP, synthetic GFP (sGFP), and showed 20-fold higher GFP expression in plant (maize leaf) cells than jellyfish GFP. In fact, a combination of the codon usage with some mutations with GFP can dramatically increase the fluorescent activity. For example, Hass et al. (1996) showed a mammalian codon-optimised GFP combined with S65T mutation and had a fluorescent improvement between 40-120 fold. Yang et al. (1996) made more than 190 silent base mutations (mammalian codon) in the GFP-m1 (a wild-type GFP combined with F64L and S65T mutation) (Cormack et al. 1996) to produce EGFP. The EGFP showed a increased fluorescent activity for over 350 fold (Yang

et al. 1996). Generally, the humanised codon usage of GFP increases by 5-10 times the fluorescent activity in mammalian cells. However, a combination with other mutations can further increase fluorescence more than 100 times.

1.4.3 Enhanced solubility variants

The majority of wild-type GFP expressed in *E.coli* at 37°C is inactive and becomes incorporated into inclusion bodies (Cormack et al. 1996; Crameri et al. 1996). Similarly, formation of inactive GFP may happen in mammalian cells (Crameri et al. 1996; Siemering et al. 1996). In jellyfish, GFP is known to bind aequorin through a hydrophobic contact area (Crameri et al. 1996; Ormo et al. 1996). When GFP is expressed in other organisms without the involvement of aequorin, the hydrophobic surface protein may cause aggregation and interfere with the formation of active GFP (Crameri et al. 1996). In addition proper protein folding of GFP may be particularly sensitive to the high temperatures required for mammalian cells (Cody et al. 1993). In jellyfish, green fluorescence is produced in a low temperature environment (sea water) (Cubitt et al. 1995; Ogawa et al. 1995). Thus production at higher temperature may interfere with the post-translational maturation of GFP. The insolubility and thermosensitivity feature of wild-type GFP may be linked to some amino acids which play a critical role in GFP structure (Kimata et al. 1997; Ormo et al. 1996; Siemering et al. 1996; Yang et al. 1996). Thus , appropriate mutations in wild-type GFP were predicted to increase solubility at higher temperatures.

Recently, two remarkable GFP mutants were reported (Cormack et al. 1996; Crameri et al. 1996). Combining the DNA shuffling technique for mutagenesis and FACS screen for mutation selection, an enhanced solubility mutant called GFP-C3 which enhanced protein solubility was produced (Crameri et al. 1996). GFP-C3 mutant involved 3 hydrophilic mutations, F100S, M154T and V164A, and which were suggested to reduce aggregation and increase chromophore activation (Crameri et al. 1996). In SDS-PAGE analysis, they found that wild-type GFP was contained mostly in the form of inactive inclusion bodies, whereas GFP-C3 remained mostly soluble in the lysates of *E.coli* . As compared to wild-type GFP, GFP-C3 had a 45 fold increase in fluorescence in *E.coli* and a 46 fold increase in fluorescence in CHO cells under UV light. Cormack et al. (1996) reported GFP mutants in which random amino acid (aa) substitutions were introduced in the twenty amino acids flanking the chromophore Ser-Tyr-Gly sequence at positions 65-67. FACS was used to select GFP mutants that fluoresce between 20-35 fold more intensely than wild-type GFP, when excited at 488 nm. One of these mutants, GFP-mut1, the mutations F64L and S65T enhanced fluorescence about 35 times at 488 nm. GFP-mut1 expressed higher fluorescence in *E.coli* at 37°C than wild-type GFP. The improvement in formation of active GFP seem to increase solubility due to more efficient protein folding at higher temperature.

The above mutants produce a more soluble GFP protein when produced at temperatures required for mammalian cell maintenance at 37°C and therefore provide a more useful GFP tag or vital marker for

study in mammalian cells. The features of all these mutants and other similar mutants are summarised in **Table 1.2**.

Table 1.2 The enhanced fluorescent intensity of GFP mutants

GFP mutants	Mutated positions	Codon usage	Excitation maximum	Emission maximum	relative activity	reference
wtGFP	None	wt	395(475)	508	1[a] (4-6)[b]	(Chalfie et al. 1994; Heim et al. 1996)
S65T	S65T	wt	489	511	6[a]	(Heim et al. 1995; Ormo et al. 1996)
RSGFP4	F64M	wt	490	505	6[a]	(Delagrave et al. 1995; Yang et al. 1996)
	S65G					
	Q69L					
GFP-C3	F100S	wt	385(490)	510	45[b](10)[a]	(Crameri et al. 1996)
	M154T					
	V164A					
GFP-m1	F64L	wt	488(395)	507	35[a](0.8[b]	(Cormack et al. 1996)
	S65T					
GFP5	V163A	plant	395(473)	507	20[a]	(Siemering et al. 1996)
	S175G					
GFP-5-S65T	S65T V163A	plant	490	510	33[a]	(Siemering et al. 1996)
	S175G					
GFP-S147P	S65T S147P	wt	480	510	6[c]	(Kimata et al. 1997)
hGFP	S65T	mammal	489	511	10[a]	(Yang et al. 1996)
GFPh	S65T	mammal	489	511	10[a]	(Zolotukhin et al. 1996)
sGFP	S65T	mammal	490	511	>100[d]	(Chiu et al. 1996)
EGFP	F64L	mammal	488	510	>350	(Cormack et al. 1996; Yang et al. 1996)
	S65T					
EBFP	F64L	mammal	380	440	2-3[e]	Clontech
	S65T					
	Y66H					
	Y145P					
PGFP	S65T/C	plant	490	510	>100[a]	(Pang et al. 1996)
YEGFP	S65G	yeast	488	510	>10[f]	(Cormack et al. 1997)

a. The value of relative fluorescent intensity was compared with GFP illuminated by FITC or blue light. **b.** The value of relative fluorescent intensity was compared with GFP illuminated by UV light. **c.** The value of relative fluorescent intensity was compared with GFP-S65T. **d.** The value of relative fluorescent intensity was obtained in plant cells(*Maize mesophyll protoplasts*). **e.** The value of relative fluorescent intensity was compared with other wild-type BFP. **F.** The value of relative fluorescent intensity was obtained in yeast cells (*Candida albicans*).

1.5 Application

The pioneering work by Chalfie et al. (1994) demonstrated that GFP could be used as a vital marker in heterogeneous expression. Subsequently, Wang et al. (1994) showed that GFP could be also used as a fluorescent tag for the N- or C-termini of protein to produce chimeric proteins which maintain both fluorescence and specific biological activity. Researchers from many fields now use GFP in their work and have shown that GFP can produce green fluorescence in a variety of organisms such as bacteria, slime molds, fungus, yeasts, insects, invertebrates, mammals and plants. There are many applications for the use of GFP as a protein tag such as to study protein localisation and function, as a reporter to monitor gene expression and as a vital marker to follow cell lineage in organisms.

1.5.1 Visualisation of intracellular structure

GFP has been fused with peptides that target the protein to subcellular structures such as, mitochondria (Rizzuto et al. 1996; Venerando et al. 1996), peroxisome (Kalish et al. 1996; Monosov et al. 1996), lysosome (Wubbolts et al. 1996), and endoplasmic reticulum (Boevink et al. 1996; Terasaki et al. 1996) and cell membrane (Hampton et al. 1996; Moriyoshi et al. 1996) providing a specific way to visualise organelle structure and dynamic events.

Rizzuto et al. (1995) fused GFP with a fragment encoding the amino-terminal 31 amino acids of the precursor of cytochrome c oxidase subunit VIII (mtGFP). When Hela cells were transiently transfected with the mtGFP, strong signals were visible in about 20-30 % of the cells with many rod-like fluorescent patterns, a typical shape

of mitochondria. Further, Venerando et al. (1996) treated mtGFP transfected hepatocytes with 2-5 mM acetylsalicylate (ASA) and visualised dramatic alterations in single living cells of the mitochondria morphology from the fluorescent 'spaghetti like' pattern of the untreated cells to large cisternal or vacuolar structures.

Recently, Monosov et al. (1996) constructed a peroxisomal targeting vector by fusion with C-terminal tripeptide peroxisomal targeting signal, SKL, driven by a methanol-inducible, alcohol oxidase (AOX1) promoter in the methylotrophic yeast *Pichia pastoris*. They targeted the GFP-SKL into the peroxisome-like structure of living *Pichia pastoris*. To visualise the detailed structure (ultrastructure) of peroxisome under the electron microscope, they used GFP fluorescence to photo-oxidise of diaminobenzidine (DAB) and produced a deposition of electron-dense oxidized DAB at intracellular locations such as a granular pattern in peroxisome. This GFP photo-oxidation procedure permitted facile ultrastructural localisation of GFP in cells by electron microscopy, and provided further evidence that GFP labeled peroxisomal structures in *Pichia pastoris*.

There are two examples of the structural analysis of endoplasmic reticulum (ER) using fusions to ER targeting signals. Terasaki et al. (1996) targeted GFP to the lumen of the ER of starfish eggs by injecting mRNA coding for a chimerical protein containing a signal sequence (N terminus) and the KDEL ER retention sequence (C terminus). They found that unfertilised eggs formed circular profiles (spherical shells of ER associated with yolk platelets) and a transient loss of continuity of the ER profiles at fertilisation. Similarly, Boevink

et al. (1996) used the signal peptide of patatin, a storage protein, to tag the N terminus of GFP in combination with the ER retention signal. The chimerical DNA cassette was then inserted into a potato virus X-based expression system. The virus then infected *Nicotiana benthamiana* and *N. clevelandii*. In virus infected cells, circular fluorescent inclusions were visualized both in the cortical ER and they moved and were restricted to the ER network and some in the streaming cytoplasm.

Moriyoshi et al. (1996) constructed adenoviral vectors containing membrane-targeted GFP, a GFP-S65T fusion with the two targeting signals, the first 20 amino acids of both growth-associated protein-43 (GAP-43) and c-Ha-Ras. They used the GFP recombinant adenovirus to infect cells in rat living brain slices in culture and analysed the neuronal processes of cortical neurons such as moving axonal and dendrtic cells.

There are also several examples using GFP tagged intracellular proteins to study the dynamic behaviours and functions of the proteins. Olson et al. (1995) tagged GFP with MAP4 (a ubiquitous microtubule-associated protein) and the subdomains of MAP4. They found that the GFP-MAP4 formed fluorescent microtubule arrays but the GFP tagged basic domain of MAP4 showed rearrangements of the microtubule in cellular cytoskeletons when these chimeras were transfected into BHK cells. Similarly, Ludin et al. (1996) produced GFP tagged versions of the neuronal microtubule-associated proteins (MAP), MAP2c and Tau34 and these chimeras had the similar ability to form fluorescent microtubules and cytoskeletal structure. By using these chimeric proteins, they could first see the dynamic behaviors of

cytoskeletal structure such as polymerisation and microtubule formation.

GFP tagged proteins retain biological features of the native protein and do not interfere with the normal cellular function. These subcellular targeting signals provide not only a specific way for subcellular localisation of GFP into organelles but also allow examination of the cellular function and the gene regulation in living cells.

1.5.2 Cellular protein trafficking events

There are many cellular proteins which shuttle within the cytoplasm to different organelles or to the nucleus. Trafficking proteins have functional domains or targeting signals for the translocation or movement. These functional domains may be controlled by different factors such as hormone, pH value of local environment and temperature. Cellular translocation has been analyzed by immunolabelling or histochemical methods. However, dynamic events are difficult by using these traditional methods. Recently, several researchers used GFP or its variants as a reporter or protein tag to directly visualise the translocation events.

Htun et al. (1996) and Carey et al. (1996) independently constructed chimeras, GFP-GR, with GFP-S65T fused to glucocorticoid receptor (GR) and they showed that GFP-GR translocated from cytoplasm to the nucleus in a hormone-dependent manner compared to native GR receptor (Carey et al. 1996). In fact, the fluorescence of GFP-

GR was first seen in the cytoplasm and translocation of GFP-GR occurred within a few minutes (4-10 min). Hanakam et al. (1996) studied the myristoylated proteins, hisactophilins, which exist in *Dictyostelium* cells in both a plasma membrane-bound and a soluble cytoplasmic state with a pH switch mechanism. They engineered a GFP tagged hisactophilin chimera, HsII-GFP, to monitor pH-dependent protein shuttling within living *D. discoideum* cells and showed the subcellular location of a strong green fluorescent HsII-GFP in a pH dependent manner.

1.5.3 Cell movement

Dictyostelium discoideum is commonly used to study cell movement during cell development. Cell movement is driven by chemoattractant-controlled processes involving the actin filament system (Gerisch et al. 1995; Maniak et al. 1995). One of the chemoattactants, cAMP, cause the accumulation of various actin-binding proteins in *Dictyostelium discoideum*. One of these actin-binding proteins is coronin which accumulates at the leading edge or the cortical sites of moving cells and contributes to the dynamics of the actin system (Gerisch et al. 1995; Maniak et al. 1995). Recently, several research groups used GFP tagged coronin to examine the dynamic process of the actin system during cell movement (Gerisch et al. 1995; Maniak et al. 1995). By directly using GFP or GFP chimeras to label moving cells, some dynamic properties of *Dictyostelium discoideum* such as the velocity and periodicity can be really measured.

Gerisch et al. (1995) generated a coronin-GFP fusion protein and expressed the protein in the aggregation stage of *Dictyostelium* cells. They used the GFP fusion to see the formation of multiple fluorescent pseudopodia of the moving cells and demonstrate that the coronin moiety of the fusion protein is responsible for chemoattractant-induced relocalisation at the alternating leading edge of *Dictyostelium* cells. Similarly, Maniak et al. (1995) made coronin-GFP fusion proteins to study coronin-involved phagocytosis and found that the fusion proteins were enriched and relocated in phagocytic cups during cell movement. To determine the movement of individual *Dictyostelium* cells, Rietdorf et al. (1996) mixed a subpopulation of GFP labeled cells at the stages of aggregates and mounds to measure cell movement speed.

1.5.4 Protein protein interaction

Mitra et al. (1996) reported an intracellular system of fluorescent resonance energy transfer (FRET) between two linked mutants of GFP. Using a concatamer of two GFP mutants, blue fluorescent protein (BFP) (Heim et al. 1994) and red-shifted GFP (RSGFP4) (Delagrave et al. 1995), RSGFP4::BFP5, they attempted to determine whether the two different spectral wavelengths (both in excitation and emission wavelength) mutants could be used in FRET when brought in close proximity. The idea was that when illuminated with UV light , the excited state energy from the excitation of BFP (the energy donor) transferred its energy to RSGFP, the acceptor. This transfer of energy is non-radiative, due to a dipole-dipole or protein protein interaction between the donor and acceptor.

Very recently, Miyawaki et al. (1997) designed fluorescent indicators, cameleons, which consisted of tandem fusions of two different GFP mutants which had different spectral maxima and calmodulin (a Ca^{2+} binding domain) was at the middle of cameleons. When cameleon bound Ca^{2+} , an increase of the fluorescent resonance energy transfer between the flanking GFPs was also measured. By using these cameleons, they were able to measure the concentration of cellular Ca^{2+}. For further application, the FRET may allow detection of other physiological changes such as enzymatic reaction between the enzyme and substrates, the dimerization of cellular proteins or other protein-protein or protein-ligand interaction in living cells.

1.5.5 Host pathogen interaction

GFP may be used as a novel indicator for the study of pathogen host interactions. Traditional methods of labelling pathogens for the study of pathogenicity has limitations because it is difficult to follow the pathogens within live host cells and the labelling signals will be diluted in dividing cells during long-term infection. The non toxic and stable nature of GFP in cells does not interfere the normal infectious process or the propagation of the pathogens. There are several successful applications in bacterial (Dhandayuthapani et al. 1995; Gage et al. 1996; Luo et al. 1996; Valdivia et al. 1996) , fungal (Spelling et al. 1996), and viral (Baulcombe et al. 1995; Casper et al. 1996; Epel et al. 1996; Heinlein et al. 1995; Oparka et al. 1996; Oparka et al. 1996) pathogenicity. To study the bacterial pathogenicity of enteric pathogens, *Salmonella typhimurium* (*St*), *Yersinia*

pseudotubersulosis (*Yp*), and *Mycobacterium marinum* (*Mm*), Valdivia et al. (1996) made two different constructs, pFPV1 (GFP driven by *lacZ po* promoter) and pFPV2 (GFP driven by mycobacterial *hsp60* heat shock promoter). They transformed *St* and *Yp* with pFPV1 and *Mm* with pFPV2 and infected animal tissue with these GFP expressing bacteria and visualised the expression for long-term, real-time interactions between live bacteria and live host cells with no obvious dilution of the fluorescence signal. A similar application of GFP for analysis of fundamental biological and pathogenesis-related phenomena was also seen in mycobacteria (Dhandayuthapani et al. 1995; Luo et al. 1996). Using different mycobacterial promoters fused with GFP cDNA to produce transcriptional fusion vectors and these vectors were used to assess gene expression in individual cells and to monitor mycobacterial fluorescence in infected macrophages (Dhandayuthapani et al. 1995) and murine cells (Luo et al. 1996).

Thus, the uses of GFP are not only as an in vivo marker but also as a biological tracer for allowing the pathologist to monitor colonisation, multiplication, persistence and transmission of pathogens in live animals.

1.5.6 Vital marker in animals

Animal development is a cumulative effect of dynamic events. Developmentally regulated genes have been widely studied by enzyme reporters such as, β-galactosidase, CAT and luciferase, in addition to antibody staining techniques in fixed samples. However, developmentally regulated genes undergo rapid temporal and spatial

changes during embryogenesis. It is difficult to follow gene expression in specific cell types during complex morphogenetic changes. Chalfie et al. (1994) reported results on the use of GFP as a genetic marker and protein tag in *C.elegans*. They successfully labelled neural cells in *C.elegans* by expressing GFP under the control of a neural specific promoter. So far, GFP techniques have been applied to many biological experiments as a vital genetic marker for real-time analysis in animals, including *Drosophila melanogaster*, *Caenorhabditis elegans*, xenopus, zebrafish and mice.

Drosophila melanogaster

Wang et al. (1994) showed that GFP had great potential as a marker in *Drosophila*. To study the subcellular distribution of *exuperantia* protein (Exu) in *Drosophila* oogenesis, they constructed a p-element vector by fusing GFP with the N- and C- termini of Exu. They demonstrated that the GFP tagged proteins behave like native GFP and retain the protein functions during the development of *Drosophila* oogenesis. Yeh et al. (1995) used GFP as a vital reporter under the control of the yeast upstream activating sequence (UAS) and generated transgenic flies. They showed that GFP could be detected in a variety of tissues, including ovaries, imaginal discs, and the larval nervous system during *Drosophila* oogenesis.

There are also several reports showing the utility of GFP as a cell lineage marker in visualising the development of specific tissues or organs in *Drosophila* (Barthmaier et al. 1995; Endow et al. 1996; Plautz et al. 1996; Shiga et al. 1996). Plautz et al. (1996) used GFP as a spatial

maker under the control of a multimeric cis-acting target site of the glass gene in living adult *Drosophila melanogaster*. They examined the fluorescence of glass-responsive GFP fusions in *Drosophila* and found the clearly distinguishable fluorescent signal in the pseudopupil of each eye and in three ocelli. GFP reporter constructs under the control of flight muscle-specific Act88F actin promoter (Barthmaier et al. 1995) was used to monitor indirect flight muscle development in normal and mutant *Drosophila*. They could visualise fluorescence in myoblast fusions during normal muscle development and also examined the morphological changes in fibers of a mutation caused by a single amino acid change in troponin-T.

Mosquito

Higgs et al. (1996) constructed a recombinant sindbis (dsSIN) virus expressing GFP to study development in living arthropods. They infected *Aedes aegypti* mosquitoes with GFP expressing dsSIN virus. After 48 h post-infection, the fluorescence could be observed in tissues of living larvae such as the ventral nerve cord, brain, and fine nerve fibers. In the stage of pupae, fluorescence was also visualised in the head, eyes, nervous system and occasionally reproductive system.

Caenorhabditis elegans

Recently, GFP was used to label chemosensory neurons of *C. elegans*. to examine responses to a variety of chemicals (Carey et al. 1996; Coburn et al. 1996; Komatsu et al. 1996; Schackwitz et al. 1996; Troemel et al. 1995), providing a better understanding of neuronal

processing at the genetic and cellular levels. Chalfie et al. (1994) first showed GFP can be a vital marker in living nematode *C.elegans*. GFP was expressed in a small number of neurons under the control of the mec7 promoter, an abundant neural specific promoter.

A family of transmembrane receptor genes whose products might mediate chemosensation in *C.elegans* were studied by tagging 22 candidate genes (Troemel et al. 1995) and introduced into the germline of *C.elegans* to produce transgenic animals. The chemically responsive sensory neurons were determined by the expression of these fusion proteins. A similar strategy examined the function of neuronal genes that mediate a pheromone response in *C.elegans* (Schackwitz et al. 1996) which showed the responsiveness to pheromone in some dauer-repressing neuronal genes.

The study of sensory neuron development in *Caenorhabditis elegans* provides a basic model to explain how the nervous systems can generate appropriate responses to complex environmental signals such as pheromone, chemical, scarce food and high temperature.

Xenopus

In *Xenopus laevis* oocytes, GFP was used as a vital marker under the control of the adenovirus major late promoter to study development (Matheson et al. 1996). The fluorescence first could be detected in some injected oocytes within 24 hr and fluorescent signal also continued to accumulate over a 7-day period. Tannahill et al. (1995) investigated the phenotype of misexpression of *Drosophila*

Enhancer of split E (spl) bHLH protein, md, in developing *Xenopus* embryos by coinjecting md mRNA with GFP mRNA. They examined the phenotype and found an obvious abnormal phenotype such as enlarged neural masses, distorted brains and incomplete eyes expressing GFP.

Zebrafish

Similar to the application of GFP in *Xenopus* embryos, mRNA from a glutathione S-transferase/GFP fusion construct (GST-GFP) was injected into individual blastomeres of early zebrafish embryos (Peter et al. 1995). A rapid production of green fluorescence was seen in one-cell embryos and later in a wide range of embryonic tissues including eye, brain, heart, blood, epithelium, and skeletal muscle in further development of embryos. These are the first few successful experiments for expressing GFP in vertebrates and provide evidence that stable GFP fluorescence can be seen in different tissues during development of vertebrates.

Alternatively, an GFP expression vector (Xex-GFP) driven by a *Xenopus* elongation factor 1a enhancer-promoter can confer fluorescence in living zebrafish (Amsterdam et al. 1995). The Xex-GFP construct was used to make transgenic zebrafishes and fluorescent cells could be seen in many tissue types at different embryonic stages. By comparing the fluorescence in different transgenic lines, they concluded that a single copy transgene was capable of producing sufficient GFP to be detected in zebrafish embryos and also estimated the minimum requirement of GFP to be 5-40 X 10^4 molecules per cell.

To express GFP in specific tissues of zebrafish, Moss et al. (1996) made a GFP fusion construct (MLC-GFP) driven by the rat myosin light-chain enhancer to generate GFP transgenic lines. A muscle -restricted green fluorescence was first observed after 24 hours of development and no fluorescence was observed in any other tissue of the transgenic lines. They demonstrated that the GFP gene either continues to be expressed or the protein is particularly stable in skeletal muscle.

Mice

Although GFP was successfully shown to be a protein tag in the mammalian cells and a vital marker in other vertebrates, it still has not been shown as a useful reporter in mammals. So far, only a few several reports have attempted to show GFP as a potential vital marker in transgenic mice (Akagi et al. 1997; Ikawa et al. 1995; Ikawa et al. 1995; Z.-Goetz et al. 1997). The first GFP transgenic mice were demonstrated by M. Okabe's research team (Ikawa et al. 1995). They used wild-type GFP as a marker under the control of the chicken β-actin promoter (pCX-GFP). The fluorescence could be first detected in fingers and the tail of a new born transgenic mouse under the fluorescent microscope. Frozen sections of tissue from the transgenic mice showed green fluorescence in many organs and tissues, including the heart, lung ,pancreas, kidney and muscle. Histochemical examination of tissue from 12 week old transgenic mouse also showed that no abnormality was found in any organs or tissue demonstrating that expression of GFP in mice was non-toxic. Most interestingly, in the

quantitative analysis of GFP expression in these organs and tissues, they estimated that the GFP expression was most dominant in muscle (when total cellular protein were extracted from these muscle tissues, the concentration of GFP was found at 200ng/ml of total protein). They subsequently reported the intrarenal microscopic expression of the GFP construct in kidney of several transgenic mice (Akagi et al. 1997). Green fluorescence was observed in the glomeruli, but not in the tubules, arteries and interstitium of the kidney. Furthermore, Okabe et al. (1997) used an enhanced fluorescent GFP, EGFP (Yang et al. 1996), as a reporter under the control of the same promoter and they obtained uniformly green fluorescent expression in the whole new born mice and in the tissues of adult mice such as brain, liver, kidney, heart, spleen thymus, adrenal gland , testis, testicular cells and adipose tissue. They also showed that GFP is non-toxic at 12 weeks old finding no abnormality in any tissue examined. The above reports show that GFP is potentially a valuable marker in transgenic mice. These reports also suggested the possibility of using GFP as a marker in mammals.

Very recently, GFP fluorescence was shown in specific embryonic tissues. Chiocchetti et al. (1997) used wild-type GFP as a reporter driven by a human liver specific promoter and generated transgenic mice. They detected green fluorescent signal in the central veins of the liver lobule in adult mice. Peel et al. (1997) used a humanized GFP as marker under the control of the tissue specific promoters, neuron-specific enolase and platelet-derived growth factor B chain promoter, and made a recombinant adenoviral vector through a viral infectious process to generate GFP transgenic rats. Zhuo et al. (1997) also used the humanised GFP as a marker under the control of

the astrocyte-specific glial fibrillary acidic protein (GFAP) promoter and showed green fluorescent patterns in the optic nerve, brain, and retina tissues of adult mice. These results suggest that some GFP mutants can enhance the sensitivity of the green fluorescent activity even under the control of weak promoters.

1.6 The cellular function of WT1

WT1 is an example of a developmental gene which has a role in organogenesis and when mutated results in a common childhood cancer. Of particular interest is the nuclear localisation of different WT1 isoforms which depending on the isoform are located in different subcellur localisation and are directed to well characterised subnuclear compartments. Studies on the WT1 cellular localisation suggest that WT1 is a multi-functional protein which interacts with cellular factors. In order to establish a model for a study in real-time of the dynamic cellular events of a developmentally regulated gene in living cells, WT1 isoforms were used because of their novel biological features. Of equal importance the protein is well studied in the unit and all the reagents were available.

1.6.1 Introduction

Wilms' tumour (WT) is a pediatric kidney cancer that arises from mesenchymal stem cells that would normally differentiate into epithelial components of the nephron (Haber et al. 1992; Heyningen et al. 1992; Miyagawa et al. 1994). A tumor suppressor gene for this disease, WT1 on chromosome 11p13, was isolated by position cloning

(Gessler et al. 1990; Royer-Pokora et al. 1991). WT1 expression during nephrogenesis in the kidneys is limited to the condensed mesenchyme, renal vesicle, and glomerular epithelial cell and therefore is likely to play a specific role in glomerular development during kidney organogenesis (Pritchard-Jones et al. 1990).

Structural analysis of WT1 showed that it has different binding, transactivation and repression domains in the protein molecule (Buckler et al. 1991; Kennedy et al. 1996). In vitro characterisation of WT1 shows DNA binding specificity (Hamilton et al. 1995; Wang et al. 1995) and that it interacts with nuclear proteins (Wang et al. 1995). In vivo, WT1 mediates cellular function through association with cellular specific proteins such as P^{53} (Maheswaran et al. 1993), CDK complexes (Kudoh et al. 1995) and epidermal growth factor receptor (EGF) (Englert et al. 1995). Furthermore, Mundlos et al. (1993) showed the nuclear location of WT1 protein in embryonic and adult tissues. Later, Larsson et al. (1995) showed WT1 splicing isoforms associated with different nuclear factors and showed some specific subnuclear localisation in Cos7 cells. This evidence suggests than WT1 is a transcription factor and plays an important role for specific cellular functions during kidney development.

1.6.2 Structure of WT1

WT1 spans about 50 kb of genomic DNA at the position of human chromosome 11p13 and encodes a protein with a glutamine /proline-rich amino terminus (Call et al. 1990), two signals for nuclear localisation (Bruening et al. 1996), and four Cys_2-His_2 zinc finger

motifs (Buckler et al. 1991; Haber et al. 1991). These characteristics suggest that WT1 is a transcription factor. Actually, WT1 protein is a multi-functional protein containing several motifs including a DNA binding domain (Rausher et al. 1990), a transcriptional repression domain (Wang et al. 1993), activation domain (Wang et al. 1993), self-dimerisation domain (Englert et al. 1995; Moffett et al. 1995; Reddy et al. 1995), and RNA recognition motif (Kennedy et al. 1996).

1.6.3 Cellular function of WT1 isoforms

WT1 mRNA contains two alternative sites of translation (Bruening et al. 1996), two alternatively spliced exons (Haber et al. 1990; Haber et al. 1991) and undergoes RNA editing (Bruening et al. 1996; Kennedy et al. 1996). Thus, in vivo WT1 may have 16 protein isoforms (Bruening et al. 1996). However, four major isoforms (++/+-/--/+/--) had been found to mediate the most important cellular functions (Charlieu et al. 1995; Englert et al. 1995; Kudoh et al. 1995; Larsson et al. 1995; Maheswaran et al. 1993; Mundlos et al. 1993; Wang et al. 1993; Wang et al. 1995). The WT1 proteins use two different splicing sites to produce two extra inserts (exon 5 and three amino acids KTS) resulting in four different isforms containing either one or two of the two inserts or neither insert. Specifically, the WT1+/+ isoform contains both exon 5 and the KTS while the WT1-/- isoform has none of them. The WT1-/+ isoform only contains the KTS and the WT1+/- isoform has only the exon 5 (Larsson et al. 1995). In normal human fetal kidney, the ratio of these four spliced mRNA maintains a constant value (++/+-/-+/-- = 8.3/3.8/2.5/1) during development and some kidney cancer had been found to have a disruption of the ratio (Reddy et al. 1995).

In vitro WT1 isoforms prefer to target some genes (Wang et al. 1995) and bind to some DNA sequences (Drummond et al. 1994).

In vivo WT1 proteins showed nuclear localisation in developing and mature podocytes of embryonic kidney (Mundlos et al. 1993). Lately, Larsson et al. (1995) demonstrate that the localisation of WT1 protein is splice form dependent. Three unique nuclear patterns were demonstrated, when Cos7 cells were transfected with vectors expressing one of the four WT1 isoforms. In the analysis of approximately 200 transfected cells in separate experiments, they showed that the four WT1 isoforms (+/+, -/-, -/+, +/-) (Larsson et al. 1995) were nuclear localised but with distinct patterns of speckles, diffuse stain, and domains. WT1 isoforms containing three amino acid sequences KTS (+/+ and -/+) showed mainly speckled patterns which were characterised by strongly stained irregular foci set against a diffuse nuclear background. The (-/-) form showed mainly domain patterns which were characterised by distinct areas of diffuse stain with little or no background. The (+/-) form showed mainly diffuse patterns which were defined as whole nuclear stain. Some osteosarcoma cell lines carrying WT1 isoforms and WT1 mutants under the control of a tetracycline-regulated promoter showed very similar nuclear patterns when tetracyline was absent in medium (Englert et al. 1995). However, WT1 isoforms do not give these unique nuclear patterns in some other mammalian cells (Chapter 4).

These unique nuclear patterns implied that WT1 associated with some nuclear factors when WT1 was ectopically expressed in Cos7

cells (Larsson et al. 1995). To further examine the association, WT1 isoforms were transfected into Cos7 cells. Two isoforms containing the three amino acid sequences KTS (+/+, -/+) mainly colocalised with transcription factors whereas two isoforms in which KTS is spliced out (-/+, -/-) mainly colocalised with splicing factors. The colocalisation of WT1 and splicing factors were then shown by coimmunoprecipitation of WT1 proteins with splicing proteins, indicating direct association between WT1 and splicing complexes in M15 cells (a mouse mesonephric cell line which expresses high amounts of WT1 mRNA and protein). In some WT1 mutants (Englert et al. 1995), a WT1 mutant WTAR (an in-frame deletion of zinc finger 3) showed a mixed speckled and diffuse nuclear pattern. Another mutant WT1-del Z (lacking the entire zinc-finger domain) showed a loss of the diffuse pattern with subnuclear clusters. Perhaps, these WT1 mutants showed altered nuclear patterns as some functional motifs or binding domains were lost. Thus, WT1's specific nuclear patterns may give strong evidence for cellular functions involved kidney development.

1.6.4 WT1 mutations in Wilms' tumors

Human mutations showed that the loss of one WT1 allele can disrupt development and cause different severity levels of Wilms' tumors (Kreidberg et al. 1993; Pelletier et al. 1991) which include gondola abnormalities (Pelletier et al. 1991). Male children with a deleted WT1 allele are diagnosed with WAGR (Wilms' Tumor / Aniridia / Genitourinary abnormalities / Retardation) syndrome (Haber et al. 1990) and one dysfunctional mutation occurs in Denys-Drash syndrome (DDS) that has severe abnormalities of renal and sexual

development (Pelletier et al. 1991). However, heterozygous mice undergo normal development and do not display any malignancies; however, the homozygotes die at 13-15 days gestation with heart and lung abnormalities (Kreidberg et al. 1993). These genetic data suggest that WT1 may play an important role during kidney development.

1.7 The functional role of Msx-1 gene in mouse development

*Msx*1 is expressed in regions, in particular craniofacial structures and limbs, that undergo mesenchymal epithelia interaction during embryogenesis. The expression of this gene and the enhancer elements that are responsible for the expression pattern have been well studied in the lab. In order to establish an animal model for a real-time study of a developmentally regulated gene during embryogenesis, I used established features of the *Msx*1 controlling elements in combination with GFP to mark regions in transgenic mouse embryos.

1.7.1 Introduction

The Hox-7 or Msx-1 gene was originally isolated from a λgt10 cDNA library of 8.5-day embryos by Hill et al. (1989) and a cosmid library of mouse genomic DNA by Robert et al. (1989). The Msx-1 gene is located on mouse chromosome 5 (Hill et al. 1989; Robert et al. 1989) or human chromosome 4 (Ivens et al. 1990) and is composed of two exons and one intron in chicken (Yokouch et al. 1991), mouse (Kuzuoka 1994), and human (Hewitt et al. 1991). DNA sequence analysis suggests that exon 1 consists of 5' untranslated region and the coding sequences for the first 151 amino acids in human

or 196 amino acids in mouse and exon 2 contains the homeobox and the 3' untranslated region.

The Msx-1 gene proved to have quite different developmental roles than the other members of the Hox gene family (class 1) and have been reported for other vertebrates, including human (Hewitt et al. 1991), chicken (Yokouch et al. 1991), quail (Takahashi et al. 1990), Xenopus and zebrafish plus a homology in *Ciona intestinalis* (Takahashi et al. 1990). These homeobox containing genes encode transcription factors containing a highly conserved 61 amino acid DNA-binding motif. These genes may play a role in controlling morphogenesis in vertebrates (Gaunt 1991; Tabin 1991).

1.7.2 Developmental expression of Msx genes in mouse embryos

By in situ hybridization, expression of Msx-1 was detected in broad areas at different stages of the mouse embryo from early expression at E6.5 (extra embryonic tissue) to later expression at E15.5 (Hill et al. 1989; Robert et al. 1989). These regions are in the developing embryonic cranium and nervous system during early developmental periods and later expression has been associated with mesenchymal-epithelia interaction in the developing teeth and limbs. Msx-1 expression has also been associated with neural crest ectomesenchymal cell migration and most recently in myoblast migration. The other areas of expression include the developing heart, the nasal pits and the forming Jacobson's organs. However, Msx-1 expression pattern occurs mainly in craniofacial and limb development (Brown et al. 1993; Davidson et al. 1991; I.-Belmonte et al. 1992;

Lyons et al. 1992; Mackenzie et al. 1991; Mackenzie et al. 1991; Yokouch et al. 1991).

Expression in forebrain and craniofacial structures

The cells that express Msx-1 during craniofacial formation from E9.5 to E15.5 mouse embryos were detected by in situ hybridization. These expression patterns suggest a possible involvement in cellular differentiation leading to the formation of a number of craniofacial structures, including the anterior pituitary (Rathke's pouch), choroid plexus, external ear, brain meninges, and skull bones, nasal pits and forming Jacobson's organs (Hill et al. 1989; Mackenzie et al. 1991; Robert et al. 1989)

At E9.5, Msx-1 is expressed in the mesenchyme of the brachial arches, components of the forming heart, and in the mesenchyme and epithelium of the progress zones of the developing forelimb and hindlimb buds (Hill et al. 1989; Robert et al. 1989) A band of intense expression is also seen in a narrow streak running from the most rostral areas of the forebrain to the tail neuropore along the line of neural tube closure. At E11.5, Msx-1 expression shows an extensive area of expression in the mesenchymal cells separating the head epidermis from neuroectoderm. This pattern of expression persists at least until E15.5 and delineates the future meninges, the fields of later ossification that form the skull bones. The other expression areas included tela choroida (posterior choroid plexus), anterior pituitary and cranial precursors.

From E12.5 to E13.5, Msx-1 is obvious in the thinning and convoluting areas of neuroepithelium differentiating into the choroid plexus and in the immediately adjacent mesenchyme cells. Msx-1 expression is also in the ventral aspect of the forming forebrain in the region of the tuberculum posterius. At E14.5, Msx-1 is expressed in the plexus extending from the rostral aspect of the telencephalon-forebrain junction and into the ventricles of the cerebral hemispheres. At E15, Msx-1 expression becomes detectable in mesenchyme derived from the second and third branchial arches, which later forms components of the middle ear and the styloid process. Msx-1 is also found in mesenchyme adjacent to the thinning epithelium of Jacobsons organ.

Limb expression

The other area of interest of Msx-1 expression in the mouse embryo is the developing limb buds. At E9.5, in the developing mouse limb, Msx-1 could be detected in the entire forming limb bud (Hill et al. 1989; Robert et al. 1989). Subsequently, at E11.5, the Msx-1 expression region is concentrated in the mesoderm and very weakly in the apical ectodermal ridge (AER) (Davidson et al. 1991; Robert et al. 1989). At E13.5, Msx-1 was present in the interdigital soft mesenchymal tissue (Hill et al. 1989).

One of the striking phenomena is that the Msx-1 and another msx family member, Msx-2 (another msh-like homeobox containing gene and very closely related with Msx-1) (Davidson et al. 1991), are expressed in many embryonic tissues which undergo epithelial-mesenchymal interaction during morphogenesis, including the limb,

atrioventricular cushion, Rathke's pouch, the genital tubercle, and the developing mandible and teeth (Hill et al. 1989; Lyons et al. 1992; Mackenzie et al. 1991; Mackenzie et al. 1991; Mackenzie et al. 1992; Robert et al. 1989; Robert et al. 1991; Suzuki et al. 1991; Wang et al. 1995). In the developing limb, the AER, an epithelial component, is a specialised thickening of the distal limb that has been demonstrated to support limb outgrowth and proper limb development which specifically regulates the underlying mesenchyme (Coelho et al. 1993; Davidson et al. 1991; I.-Belmonte et al. 1992; Jowett et al. 1993; Richman et al. 1992; Robert et al. 1991; Wang et al. 1995). Msx-1 and Msx-2, have been reported to be expressed in the limb bud, in and under the ridge (Davidson et al. 1991; Davidson et al. 1991). In 11.5 day old embryo, Msx-2 was expressed in the AER and only weakly in the most distal cells of the mesoderm, while Msx-1 was expressed mainly in the mesoderm and only very weakly in the AER (Davidson et al. 1991). Davidson et al. (1991) proposed a position-dependence of Msx-1 and Msx-2 expression. When non-expressing proximal limb mesoderm was grafted under the apical ectoderm, the grafted tissue responded by expressing Msx-1 and Msx-2. The results suggested that the genes respond directly to graded signals in the mesoderm produced by the AER.

Expression in other areas

Msx-1 is also expressed in some specific regions such as developing heart, tooth and eye. In 10.5-day embryos, Msx-1 could be detected in the mesenchyme of the branchial arches and endocardiac cushions (components of the forming heart) (Mackenzie et al. 1991;

Robert et al. 1989). Msx-1 expression in tooth germs is dependent on the stage of development of the individual tooth (bud, cap and bell) (Mackenzie et al. 1991). In the developing mouse eye (E15.6-E16.5), Msx-1 was expressed after formation of the optic cup, making the domain that will give rise to the ciliary body (Monaghan et al. 1991).

1.7.3 The Msx-1 deficient phenotype

In a targeted disruption of Msx-1, the heterozygous mice showed no obvious phenotype (Satokata et al. 1994). The homozygous msx-1-/- mice die in the immediate postnatal period and exhibit marked abnormalities in craniofacial development, including a complete cleft of the secondary palate, a failure of tooth and alveolar bone development in the mandible and maxilla and abnormalities of the skull, malleus, nasal bones and conchae. The best explanation for the limited severity in the null mutant phenotype is functional redundancy between Msx-1 and Msx-2 such that Msx-2 may compensate for the loss of the Msx-1 function (Catron et al. 1996) which is supported by the overlapping expression patterns of Msx-1 and Msx-2 during embryogenesis (Catron et al. 1996; Houzelstein et al. 1997).

1.8 The aim of thesis

1.8.1 Optimised GFP fluorescent activity in mammalian environment

The first idea of using the jellyfish green fluorescent protein (GFP) was demonstrated by Chalfie et al. (1994). They showed that wild-type GFP functioned as a marker in both of *E. coli* and *C elegans*.

However, it became apparent to me and others that wild-type GFP would be equally valuable in mammalian cells. This limitation of GFP however was the heat sensitivity and low expression efficiency of the jellyfish protein in mammalian environment as discussed above.

The aims of this study was to use GFP as a protein tag in living mammalian cells and a genetic marker in transgenic animals. Thus, developing a more effective GFP marker became the initial aim of this study. To generate GFP variants which were more effectively expressed in a mammalian environment, a PCR based in vitro mutagenesis method was developed to generate GFP mutations.

1.8.2 Visualisation of the nuclear sublocalisation of GFP-WT1 (GW) isoforms and their mutants to predict the WT1 functional role in cells.

The cellular functions of WT1 protein isoforms had been predicted by their specific nuclear patterns using immunocytochemistrical labelling (Larsson et al. 1995). To visualise nuclear patterns of WT1 in vivo, GFP-WT1 (GW) fusion isoforms were generated and introduced into Cos7 cells to display green fluorescent nuclear patterns. In addition, to establish a useful system for further analysis of the nuclear behaviour of native and mutated protein isoforms, GW was expressed and examined in living Cos7 cells to provide a non-invasive means to follow dynamic cellular events.

1.8.3 Using an optimised GFP as an embryonic specific marker in developing mouse embryos

A defined Msx1 promoter had been used in transgenic mice to drive a reporter enzyme, β-galactosidase, which showed many typical features of the native gene in developing mouse embryos (MacKenzie et al. 1997). To make GFP transgenic mice for studying cell behaviours during different aspects of development, GFP variants with β-galactosidase either as a dicistronic encoding gene using a viral IRES sequence or as a fusion gene were put under the control of the Msx-1 promoter.

Chapter 2 Materials and Methods

2.1 Bacterial strains and media

JM109: F`{traD36proAB$^+$lacI^{q}lacZÆM15}endA1 recA1 hsdR17(r_K^- ,m_K^+)supE44 thi-1 gyrA96 relA1 Æ(lac-proAB) (Biolabs)

XL1-Blue 1: F`::Tn10 proA$^+$B$^+$ lacI^q lacZÆM15/recA1 endA1 gyrA96 (Na^r) hsdR17(r_K^-,m_K^+) supE44 relA1 lac (Stratagene).

These *E.coi* strains are the host for pUC or pBR322 based plasmids and used for the blue/white selection of colonies in agar plates containing X-Gal and IPTG and general plasmid preparation.

BL21(DE)3: F$^-$ ompT [lon] hsdS$_B$ (r_B^-,m_B^+; an *E.coli* B strain) with DE3, a l prophage carrying T7 RNA polymerase gene (Biolabs). It is a general protein expression strain that lacks both the *ompT* and *lon* proteases and encodes T7 RNA polymerase under the control of the *lacUV5* promoter. T7 RNA polymerase is encoded on a lysogenic lambda bacteriophage under *lacUV5* control. Induction of the polymerase with IPTG allows controlled protein expression of genes placed downstream of the T7 RNA polymerase binding site. Thus, BL21(DE)3)cells are good host for all plasmids expressinglevels of proteins which may be toxic.

MC1061/P3: F` hsdR (r_K^- ,m_K^+) araD139 Æ (araABC-leu) 7679 galU galK ÆlacX74 rpsL thi mcrB {P3: Kan^R Amp^R(am) Tet^R(am)} (Invitrogene). This strain harboring the plasmid P3 (a low-copy 60kb

episomal plasmid, encodes the kanamycin resistance gene as well as amber mutant of the tetracycline and ampicillin resistance genes) permit selection and maintenance of plasmids that encode the tRNA suppressor F gene. Thus, this strain is used for the transformation with supF plasmid. The usual condition for selection is 25-40μg/ml ampicillin and 7.5-10μg/ml of tetracycline.

LB (Luria-Bertoni) broth and agar: 10g bacto-tryptone (Difco), 5g bacto-yeast extract (Difco), 10g Nacl, pH7.5. In LB agar containes 15 g agar (difco) per liter.

Antibiotic and other chemical stocks: Ampicillin (Sigma), 100μg/ml; Tetracyclin (Sigma), 25μg/ml; Kanamycin (Sigma), 50μg/ml; IPTG, 0.1M; X-Gal, 50mg/ml (in dimethylformamide).

2.1.2 Plasmid DNA and cloning vectors

General cloning vector: Bluescript (Stratagene): this vector is used for general purpose cloning. pTA vector (Invitrogen): this vector is used for the purpose of cloning PCR products.

Prokaryotic expression vector: pE11d (Stratagene).

Eukaryotic expression vector: pCI (Promega), pCMV (Invitrogen), and pCAG (Niwa et al. 1991). The other plasmid constructs in the study are summarized in **Table 2.1**.

Table 2.1 The summary of plasmid constructs in this study						
Vectors	**Eukaryotic promoter**	**Prokaryotic promoter**	**Antibiotic resistance**	**Eukaryotic selection**	**Bacterial hosts**	**Map**
pET11d		T7[a]	Amp		BL21(DE)3	Fig.3.2
pETGFP		T7	Amp		BL21(DE)3	Fig.3.2
pJ4W	LTR[b]		Amp		XL-Blue1	Fig.6.3
pCI	CMV[c]	T7	Amp		XL-Blue1	Fig.5.6
pCIhGZn	CMV	T7	Amp		XL-Blue1	Fig.3.13
pCGW	CAG[d]		Amp/Kan	G418	XL-Blue1	Fig.5.6
pCGWIWT1 -dC1+ hN	CAG		Amp/Kan	G418	XL-Blue1	Fig.5.6
pCMV	CMV		Amp/Kan	G418	XL-Blue1	Fig.3.5
pCMVGFP	CMV		Amp/Kan	G418	XL-Blue1	Fig.3.5
pCMVbGFP	CMV		Amp/Kan	G418	XL-Blue1	Fig.6.1
pCAG	CAG		Amp/Kan	G418	XL-Blue1	Fig.3.18
pCAGaGFP	CAG		Amp/Kan	G418	XL-Blue1	Fig.3.18
phGFP-S65T	CMV		Amp/ Kan / Tc		MC1061 / P3:	
pCoslNco5'	Msx-1[e]		Amp		XL-Blue1	Fig.6.3
pMZ	Msx-1		Amp		XL-Blue1	Fig.6.5
pMTZ	Msx-1		Amp		XL-Blue1	Fig.6.3
pMaG	Msx-1		Amp		XL-Blue1	Fig.6.4
pMbG	Msx-1		Amp		XL-Blue1	Fig.6.4
pTA		T7	Amp/Kan		JM109	Fig.3.2

a. T7, T7 promoter (Rosenberg et al. 1987) **b.** Mo MuLV LTR, promoter (Morgenstern et al. 1990). **c.** CMV, promoter. **d.** CAG, promoter (Matayoshi et al. 1990). **c.** Msx-1, Msx-1 promoter (MacKenzie et al. 1997).

2.1.3 Manipulation of plasmid DNA

2.1.3.1 Preparation of *E.coli* competent cells

Competent cells of *E. coli* strains suitable for plasmid DNA transformation were made by the Hanahan method (Hanahan 1985). A bacterial colony was inoculated into 5ml LB broth and incubated at 37°C overnight. The 5ml overnight culture was poured into 500ml LB broth containing 10m $MgCl_2$, 10mM NaCl and 25mM KCl, and shaken at 37°C until the culture reached mid log phase at OD_{560} = 0.5. The culture was chilled in an ice bucket for 15 min. and then centrifuged at 5,000 rpm for 10 min. The bacterial pellet was resuspended in 150ml of TFB I solution (35mM NaOAc, 10mM $CaCl_2$, 100mM RbCl, 50mM

MnCl in 15% glycerol, pH 5.8) and incubated on ice 10-15 min. After centrifuging at 5,000 rpm for 10 min, the pellet was resuspended in 20ml of TFB II solution (10mM MOPS, 75mM $CaCl_2$, 100mM RbCl in 15% glycerol, pH 6.8) and chilled in an ice bucket for 20 min. Finally, the bacterial cells were frozen in liquid nitrogen in 200ml aliquots and stored at -70°C.

2.1.3.2 Bacterial transformation

200ml frozen competent cells were thawed on ice and then 20ng plasmid DNA or 10ml ligated reaction mixture was added, and left on ice for 40-60 min. Cells were heat-shocked at 42°C for 1 min and then placed on ice for another 1 min. Then 800ml LB broth was added to the cells and incubated at 37°C for 1 hour. Finally, 100ml of the transformation was plated on agar plate containing the relevant antibiotic for the selection of colonies.

2.1.3.3 Quick screening of bacterial colonies

To screen GFP mutants in a short period of time, a modified method from Liu et al. (1995) was used to isolate the recombinant DNA in individual clones and identify the recombinant DNA by restriction enzyme analysis. Bacterial colonies were picked with a sterile toothpick and inoculated into 1ml LB broth containing the appropriate antibiotic and grown overnight. 200ml of each bacterial suspension was aliquoted into a 1.5ml centrifuge tube and spun down Each pellet was resuspended into 20ml quick-screen lysing buffer (8% sucrose, 50mM Tris-HCl, pH8.0, 5% Triton® X-100, lysozyme 0.1-2.0mg).

Resuspended pellets were incubated for 30 min at room temperature and then heated in a boiling water bath for 1 min. The lysate was centrifuged at 1500rpm for 5 min. 4-5ml of each supernatant was loaded directly onto the agarose gel to analyse the recombinant plasmid DNA. Then the recombinant DNA samples could be also digested by restriction enzymes to examine the inserts.

2.1.3.4 Plasmid DNA preparation and manipulation of plasmid DNA by enzymes

All plasmid DNA preparation were performed with Qiagen kits (Invitrogen) and the enzymes for manipulation of plasmid DNA were bought from Boehringer Mannheim. All procedures and conditions for enzyme reaction were followed by standard techniques of molecular biology.

2.1.4 PCR reactions for subclonning of DNA fragment into vectors.

Synthetic primers which contained specific restriction enzyme sites and complementary sequences at either end of the interesting region were designed for using in PCR reactions. 100ml of PCR reaction mixture contained 1-10ng of DNA template, 10mM of each primer, 2.5ml of 2.5mM dNTPs, 10ml of 10X PCR reaction buffer, 10ml of 20mM $MgCl_2$, and 0.5ml Taq polymerase (2.5unit/ ml). The reactions were performed using the following conditions: 94°C, 2 min. for 1 cycle, 94°C, 1 min., 55°C, 1min, 72°C, 1 min. (< 1kb; 2 min. for 1-2kb) for 40 cycles, and 72°C, 10 min. for 1 cycle. The PCR products were purified by the Qiagen kit and examined on a mini agarose gel.

Then PCR products were digested by the relevant restriction enzyme and ligated into cloning vector. Alternatively, 2ml of PCR reaction mixture could be used in the direct ligation of TA cloning (TA cloning system, Invitrogen).

2.2 In vitro PCR mutagenesis for GFP mutants

All PCR steps were carried out by using Vent® (exo+) DNA polymerase (New England Biolabs), a high-fidelity amplification enzyme. Conditions for the first PCR reaction were: 1ng GFP plasmid, phGFP-S65T (bought from Clontech), 20 ng/μl of each primer, 250μM dNTP, 1X polymerase buffer (supplied with Vent® (exo+) DNA polymerase), 2mM $MgSO_4$, and 1unit Vent® (exo+) DNA polymerase in 25μl reaction volume . The reaction mixture was subjected to 15 amplification cycles at 94°C for 1 min., 55°C for 1 min. and 72°C for 30 min. The PCR products were purified using microcon 30 (Microcon) and digested with the appropriate restriction enzyme in 20μl reactions at 37°C for 30 min. The digested mixture was incubated at 65°C for 5 min. Next, 2μl of inactivated mixture was religated by adding 2 units T4 DNA ligase at room temperature for 10 min. in a 10μl reaction. Finally, 1μl of religation mixture was used as temple for the second PCR reaction. The reaction mixture was subjected to 40 amplification cycles at 94°C for 1 min., 55°C for 1 min. and 72°C for 1 min. and then another a single cycle of elongation step at 72°C 1 min. The final amplified fragments were about 720bp and were the same size as the wild-type GFP fragment.

2.3 Nondenaturing gel electrophoresis analysis of GFP

EX BIBL UNIV. EDINBURGEN

Total cellular protein was prepared from overnight cultures of BL21(DE)3 expressing GFP variants. 1.5ml of bacterial culture cells was spun down. The cell pellet was washed twice with PBS and resuspended in 1ml PBS containing 10% glycerol and sonicated four times on an ice bath at intervals of 5-10 seconds. The extract was centrifuged at top speed for 20 min. Supernatants were transferred into clear tubes and kept at 4°C. The concentration of protein samples was determined by using a modified Lowry assay (Bio-Rad reagent) and spectrophotometer. The concentration of each sample was calculated from a standard curve which was determined several at different concentrations of BSA.

10mg of total protein from each of the samples was mixed with loading buffer (10% glycerol, 60mM Tris-HCl, 0.001% bromophenol blue, pH 8.3). Samples were loaded on a 12% PAGE (polyacrylamide gel) without any SDS or other denaturing reagent. GFP samples were very easily visualised as a green band during the electrophoresis.

The non-denaturing gels were stained with 0.1% Coomassie brilliant R250 (Bio-Rad) dissolved in 5% Trichloroacetic acid/water (w/v) and destained in ethanol / acetic acid / water (1:1:8) by gently shaking at room temperature.

2.4 Manipulation of mammalian culture cells

2.4.1 Cell culture

CHO-K1, NIH3T3, COS-7 and M15 cell lines were all maintained in DMEM containing high glucose plus 10% fetal calf serum (Gibco-BRL). The cell line G7 was maintained in Dulbecco's Modified Eagle's Medium (DMEM) containing high glucose plus 10% fetal calf serum (Gibco-BRL) and 5% horse serum (Sigma). Cells were grown in T25 tissue culture flasks in a 5% CO_2 humidified incubator at 37°C, harvested using trypsin-EDTA (0.05% Trypsin, 0.53mM EDTA/4Na; GIBCO/BRL) and subcultured at a 1:10 dilution, every 3 days.

2.4.2 Transfection

Transfection was performed by liposome mediated transfection (lipofectamine™ reagent, Gibco-BRL). Cells were plated at a density of 1 $X10^5$ in each well in a 4-well chamber slide (GibcoBRL). For each well, 250ng DNA and 0.4µl lipofectamine™ reagent were mixed well in 200µl of OPTI-MEM®I reduced serum medium (Gibco-BRL) and incubated at room temperature for 20 min. Before transfection, cells were washed twice with PBS and once with OPTI-MEM®I reduced serum medium. The mixture was then combined with another 200µl of OPTI-MEM®I reduced serum medium and loaded into a well in the chamber slide and incubated for 6 hr at 37°C in a CO_2 incubator.

2.4.3 Isolation of transfectants

75% confluent cells (5 x 10^6 cells) in a 10cm culture dish were transfected with 5μg of the linearised construct containing a Neo selection marker. After 24 hr, the transfected cells were trypsinised, diluted 100 times (this assumes that the G418 resistant clones was approximately 100; however, this dilution factor was a reasonable guess according to several previous experiments), and then transferred into 96 wells. After another 24 hr, the cells were selected by G418 at the final concentration of 200-500 μg/ml. After 2-3 weeks of selection, the surviving clones were examined for their gene products or reporter activity. Once positive clones were identified, the clones could be diluted again and subcloned as clonal cell lines.

2.4.4 X-Gal Staining of cells

Transiently transfected cells were replaced 2 times with PBS, buffer, 137mM NaCl, 2.7mM KCl, 4.3mM Na_2HPO_4, 1.4mM KH_2PO_4, 0.1M Sodium phosphate buffer, pH 7.3) and then fixed with 4% paraformaldehyde (in PBS) for 20-30 min at room temperature. The fixed cells were rinsed 3 times with PBS. Then the cells were stained with X-Gal staining solution (150mM NaCl, 1mM $MgCl_2$, 3.3mM $K_3Fe(CN)_6$, 3.3mM $K_4Fe(CN)_6$, 50 mg/ml X-gal, in PBS) for 1 hr at 37°C. Finally cells were covered with 70 % glycerol in PBS.

2.5 Immunological and imaging techniques

2.5.1 Immunocytochemistry

The transiently transfected cells in the chamber slide containing 8 or 4 wells were incubated at 37°C for 24-48 hours. To fix cells, medium was removed from the chamber slide and washed twice with PBS. Then, the cells in the chambers were fixed in 250ml of -20°C acetone: methanol 1:1 for 5-10 min. and rehydrated in PBS for 30 min. To fix GFP expressing cells, and to perform immunocytochemistry, cells were fixed with 4% paraformaldehyde and permeabilised with 1% NP-40 in 10mM glycine and 3% BSA for 10 min. at room temperature. Then the cells were washed twice with PBS for the following staining steps.

To stain cells, PBS was removed from the fixed cells and replaced by blocking solution (2% BSA, 0.2% Tween 20, 6.7% glycerol) for 1hr at room temperature. The cells were then incubated with primary antibodies (1: 200 dilution) for 1 hr at room temperature. After washing with PBS 3 times, cells were incubated with secondary antibodies (1: 100 dilution) conjugated with FITC, Texas Red (Jackson Immunoresearch Laboratories) for 30 min and then washed 3 times with PBS. The slides containing the fixed cells were finally mounted with 90% glycerol containing DAPI (0.1µg/ml) and covered with a coverslip for the analysis of immunofluorescence.

2.5.2 Microscopy analysis

Fluorescent images were captured on a photometric cooled charge-coupled device (CCD) camera using IPlab imaging software and a standard fluorescein filter cube. Optical sections of the mouse embryos were obtain by confocal microscopy (Bio-Rad, MRC 600). For

x-gal stained whole mount embryos, the images of the embryos were obtained by used conventional colour photography with bright field illumination on a dissection microscope. Then the images were processed by using Adobe Photoshop and Macpro software.

2.5.3 Western blot analysis

COS-7 cells were transfected as in the previous method (liposome-mediated transfection) with CMV-based expression vectors which produced WT1-GFP chimeras (GW++, GW--, GW-+ and GW+-) or other GFP fusion proteins. Total cellular protein was prepared 24-48 hours after transfection. 1 x 10^5 cells from 6 well 30-mm culture dish were collected by scraping in PBS and centrifuged for 5 min at low speed (1000-2000 rpm). The cell pellet was resuspend into sonication buffer (0.5M NaCl in PBS) and sonicated twice every 10-20 seconds. Alternatively, cells were lysed in 250µl of 2% SDS/50 mM Tris 7.5 by heating in a boiling water bath for 5-10 min and centrifuged at top speed for 10 min. The supernatants were transferred into clear tubes and kept at 4°C. The concentration of protein samples was determined by using the Bio-Rad DC Protein Assay Kit assay (Bio-Rad).

10-50 µg of total protein was combined loading buffer (2% SDS, 10% glycerol, 60mM Tris-HCl, 100 mM DTT, 0.001% bromophenol blue, pH 8.3) and boiled for 5 min. Then the samples were loaded on a 12% SDS-PAGE (polyacrylamide gel) and transferred onto nitrocellulose (Hybond ECL, Amersham). The blot was blocked with 1% blocking reagent (Boehringer Mannheim) in TBS-T (150mM NaCl, 20mM Tris-HCl, 0.1% Tween 20, pH7.6) at room temperature for 1 hr

and then incubated with the diluted primary antibody (1: 10,000 to 15,000 in 0.5% TBS-T) overnight at 4°C. The blot was washed 3 X 10 min in TBS-T at room temperature and then incubated with secondary antibody (1: 1000 dilution in 0.5% TBS-T) at room temperature for 1 hr. After 4 washes, the signal of immunoreactive proteins in the blot was detected using enhanced chemiluminescence assay (ECL, Amersham). The blot was placed on ECL-film and exposed for 1-5 min.

2.6 Techniques for animal experimentation

2.6.1 Transgenic mouse production

2.6.1.1 DNA preparation

10μg transgenic vector DNA was digested with the relevant restriction enzyme and run on an agarose gel to separate the transgenic cassette from cloning vector sequences. The transgenic DNA fragment recovered from agarose gels was purified with Gene Clean II Kit (BIO 101) and concentrated using a MICROCON 30 (Microcon). The concentration of DNA was determined by spectrophotometry and redissolved in microinjection buffer (10mM Tris-HCl, pH 7.5, 0.2mM EDTA, pH7.5) to a final concentration of 10-50 ng/ml (this concentration is about 5-25 fold higher than standard concentration of 2ng/ml, but this concentration let me get a higher rate of transgenic mouse production). Before microinjection, 1-5μl of the transgenic DNA solution is examined by agarose gel electrophoresis to confirm the presence of intact DNA fragment without any contamination from

cloning vector fragments. The working DNA solution or stock solution could be maintained at 4°C for several weeks.

2.6.1.2 Microneedle preparation

The holding pipettes were used to suck and hold the eggs to be injected, and were made on a microforge. The holding pipettes ready to be used must have one terminal blunt end with a diameter slightly smaller than the eggs. This prevents injuring or sucking in the eggs during the microinjection procedure. The injection needles had a sharp and enclosed end was pulled by pipette puller.

2.6.1.3 Generation and collection of 2-cell stage of mouse embryos

Vaginal plugs of F1 female mice (C57BL/10 X CBA, purchased form C. River) were sacrificed at the appropriate time. A small portion of oviducts was removed and washed into a 30-mm tissue culture dish containing 0.9% saline. The ampulla, a cumulus masses, were carefully released from the oviducts into small glass cell blocks containing the M2 medium (Sigma) and then were treated with 0.1M Hyaluronidase (Sigma). The Hyaluronidase treated masses became the individual eggs and washed them several times with M2 medium. Finally, the fertilised eggs were transferred into 30-mm tissue culture dish containing M16 medium (Sigma) which had been preequilibrated to the correct temperature and pH in the incubator and covered with paraffin oil.

2.6.1.4 Microinjection

The microinjection was performed under an inverted microscope specially designed for injection. About 30 eggs were placed on the centre of the injection slide containing M2 medium and covered by paraffin oil on the surface of the medium. The tip of the injection needles were filled with 10µl DNA solution. The holding needle was connected with a tubing containing an adaptor and the holding pressure was controlled by mouth. The injection needle was connected with another tubing linking to an empty 50ml syringe and the injection pressure controlled by hand. To initiate flow of DNA solution, the tip of the injection needle was slightly touched against the holding needle to break off the end. Then the injection needle was inserted into the male pronucleus (it is usually bigger and located close to the cell membrane) until the swelling pronucleus was observed. After injection, the surviving eggs were transferred into M16 medium for overnight incubation at 37°C incubator.

2.6.1.5 Oviductal transfer

Recipient CD1 female mice were plugged by vasectomised male mice and dissected to expose one side of oviducts for transferring injected eggs. For each implantation, about 30 cultured eggs which had became 2- cell stage embryos were transferred into both sides of oviducts in the recipient mouse. A Pasteur pipette was heated and pulled by hand to produce a long extensive end. The end was carefully broken to yield no protruding shards. 30 cultured eggs were loaded into the prepared pipette between two small air bubbles. Then the pipette was inserted into the infundibulum of the oviduct to release the eggs.

The implanted recipient female mouse was transferred into a clean cage with food and water for recovery and pregnancy.

2.6.1.6 Tail biopsy and PCR analysis

3-4 weeks of mice which were born from the recipient female mice were examined by PCR analysis of transgenes from a tail biopsy. The tails of those mice were cut and each placed in a labelled 1.5 ml centrifuge tube containing 500µl of the lysis buffer (10mM NaCl, 10mM Tris-HCl, pH8.0, 10mM EDTA, pH8.0, 2% SDS, proteinase K 2mg/ml), and then incubated at 55°C overnight. The tubes contained the lysate were centrifuged at top speed for 15 min. 400µl of each supernatant were individually transfer into a new tube and added 1 ml 100% alcohol for precipitation. The precipitated DNA pellets were wash twice with 70% alcohol and resuspended in 200µl TE buffer (10mM Tris-HCl, pH8.0, 0.1mM EDTA, pH8.0).

Synthetic primers which covered a 300-400bp region of the transgene were designed to use in PCR reactions. 20 µl of PCR reaction mixture containing 50 ng of DNA template, 10mM of each primer, 0.5µl of 2.5mM dNTPs, 2µl of 10X PCR reaction buffer, 2µl of 20mM $MgCl_2$, and 0.1µl Taq polymerase (2.5unit/µl). The reactions were performed under the following conditions: 94°C, 2 min. for 1 cycle, 94°C, 40 seconds, 55°C, 35 seconds, 72°C, 30 seconds for 40 cycles. The PCR products were examined by electrophoresis on a 3% agarose gel.

2.6.2 Manipulation of Mouse embryos

2.6.2.1 X-Gal staining of mouse embryos

Mouse embryos were fixed with 4% paraformaldehyde (in PBS; phosphate buffered saline buffer, 137mM NaCl, 2.7 mMKCl, 4.3mM Na_2HPO_4, 1.4 mM KH_2PO_4, 0.1M Sodium phosphate buffer, pH 7.3) for 30-60 min at 4°C. These embryos then were rinsed once with PBS buffer and washed 3 times in detergent wash (2mM $MgCl_2$, 0.1% Sodium desoxycholate, 0.02% NP-40, 0.05% BSA) for 30 min. Then the embryos were stained with X-Gal staining solution (0.085% NaCl, 5 mM $K_3Fe(CN)_6$,$K_4Fe(CN)_6$,X-Gal, in detergent wash) for 3-6hr at 37°C. Then embryos were fixed again with 4 % PFA for 3-4hr at room temperature or overnight at 4°C. The stained embryos were rinsed with PBS and kept at in 4°C for several weeks for further analysis.

2.6.2.2 Vibratome sections of mouse embryos

Mouse embryos were treated by same method for X-Gal staining (or without the step of X-Gal staining) and equilibrated for 1h each step in 5%, 10%,15% and 20% sucrose in PBS. Then mouse embryos were transferred into vibratome solution (14% BSA, 20% sucrose, 0.5% gelatin in PBS) overnight. Next day the embryos were embedded in fresh vibratome solution mixed with 2.5% gluteraldehyde and 100 mm thick sections were cut by a VIBRATOME 1000 (TPI).

2.6.2.3 Cryostat sections of mouse embryos

Mouse embryos were fixed with 4% PFA for 1 hour and were embedded in 2% agarose. The embedded blocks were transfered into 30% sucrose in PBS overnight. Then embedded blocks were covered with OCT (tissue-Tek) and frozen by liquid nitrogen. 10μm thick cryostat sections were cut with a CRYOSTAT CM 3000 (LEICA) and mounted in 70% glycerol for further analysis.

2.7 Whole mice embryo culture

For culturing living embryos, all the following steps were sterile. Pregnant mice at E8.5 was killed by cervical dislocation and uterus containing the embryos was washed twice with ice-cold PBS buffer. To collect embryos, the uterus were dissected in ice-cold nutrient medium (Gibco/BRL) plus 10% FCS (Gibco/BRL). Then the embryos were transferred into DMEM (Gibco BRL) containing 50% rat serum (Sigma) and were incubated at 37°C, 5% CO_2 for 6-24 hours.

Chapter 3 Molecular characterisation of optimised GFPs

3.1 Introduction

Green fluorescent protein (GFP) has the capacity to be a marker in many species, including microorganisms (bacteria, fungi, mold and yeast) (Chalfie et al. 1994; Dhandayuthapani et al. 1995; Fire et al. 1990; Gage et al. 1996; Gerisch et al. 1995; Lim et al. 1995; Luo et al. 1996; Maniak et al. 1995; Rietdorf et al. 1996; Sidorova et al. 1995; Spelling et al. 1996 ; Valdivia et al. 1996) and invertebrates (*C. elegans*, moth, *D. melanogaster*, mosquito) (B.-Fraser 1986; Barthmaier et al. 1995; Carey et al. 1996; Coburn et al. 1996; Endow et al. 1996; Higgs et al. 1996; Komatsu et al. 1996; Plautz et al. 1996; Schackwitz et al. 1996; Shiga et al. 1996; Troemel et al. 1995; Wang et al. 1994; Yeh et al. 1995), and vertebrates (xenopus, zebrafish) (Akagi et al. 1997; Amsterdam et al. 1995; Amsterdam et al. 1996; Matheson et al. 1996; Moss et al. 1996; Peter et al. 1995; Tannahill et al. 1995; Z.-Goetz et al. 1996; Z.-Goetz et al. 1997). Although successful application of GFP was shown previously in these organisms, there were only a few reports of its use in mammals (mice). The recent reports describing GFP transgenic mice (Akagi et al. 1997; Ikawa et al. 1995; Okabe et al. 1997; Z.-Goetz et al. 1997) showed ectopic expression in transgenic adult mice under the control of either a strong ubiquitous promoter or a tissue specific promoter (Chiocchetti et al. 1997; Peel et al. 1997; Zhuo et al. 1997). So far, there are no reports of GFP transgenic mice using a weak promoter or an embryonic specific promoter. To perform such a study requires a GFP variant which has increased fluorescent activity. The aim of this study was to identified

and characterize an optimised GFP to use as a marker in individual cells and mouse embryos **(Fig.3.1)**.

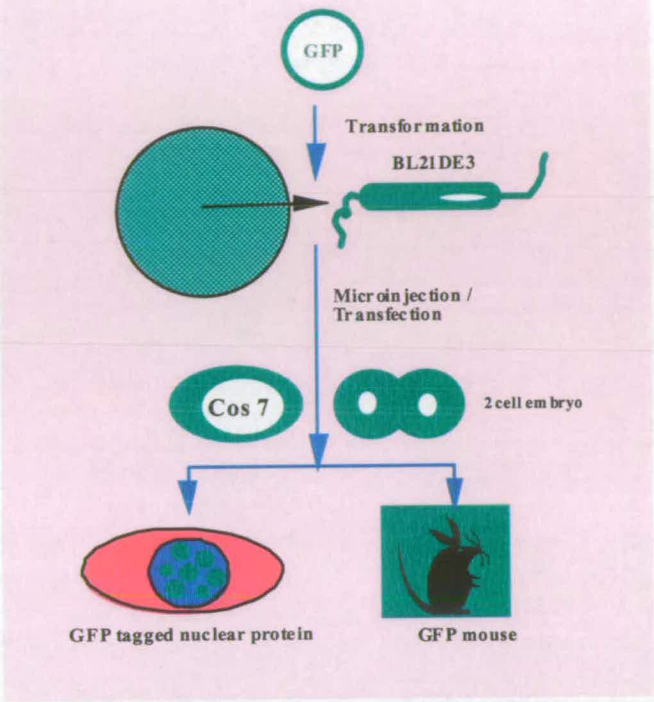

Fig.3.1 The strategy of using GFP as a marker in mammalian cells and in transgenic mice.

To generate this GFP, modification of the GFP coding sequence was performed by in vitro mutagenesis and the fluorescent activities of these mutants analysed in a series of assays. The modifications of GFP were based on Table 1.1 & 1.2 and consisted of different combinations of single mutations within the gene using either jellyfish or human codon preferences. The properties of the modified GFP variants were analysed in both prokaryotic and eukaryotic cells. Further, to examine the stability and toxicity of the GFP variants, they were transfected into mammalian cells to establish stable cell lines. Several cell lines were established that showed continuing and stable GFP fluorescence. These modified GFP variants showed features of

increased fluorescence and stability and were non-toxic in mammalian cells for further studies in mammalian embryos using weak or embryo-specific promoters.

3.2 The biological limitation of wild-type GFP

The cDNA of jellyfish GFP was first isolated by Prasher et al. (1992) and its ubiquitous activity was then demonstrated by Chalfie et al. (1994). However, the jellyfish protein is normally synthesised at low temperature and is not suitable for expressing in other organisms living in higher temperature (Heim et al. 1994; Kaether et al. 1995; Lim et al. 1995; Ogawa et al. 1995; Pines 1995; Webb et al. 1995). To further understand the nature of wild-type GFP, its fluorescent activity was examined in bacterial and mammalian cells.

GFP was produced in *E. coli* which showed a very intense green fluorescence in bacterial colonies (Chalfie et al. 1994). To first examine the wild-type GFP activity, fluorescence was analysed in a bacterial expression system (Rosenberg et al. 1987; Studier et al. 1990). First, pGFP10.1 (Prasher et al. 1992), a wild-type GFP cDNA containing plasmid, was used as a template for PCR amplification. The PCR products were directly cloned into the pTA vector (Invitrogene) and the recombinant was named pTAGFP. To check the fluorescent activity of the PCR products, the GFP fragment was digested from pTAGFP and was subcloned into the prokaryotic expression vector, pET11d (**Fig.3.2A**) (Rosenberg et al. 1987; Studier et al. 1986; Studier 1990), and the recombinant was named pETGFP (**Fig.3.2B**). pETGFP was then transformed into the *E.coli* strain BL21(DE)3 and the resulting

transformants observed under UV light. Some faint green fluorescent colonies were present without the inducer IPTG after 12-16 hours of incubation at 37°C and exposure to UV light (**Fig.3.3A**). A slightly increased number of green fluorescent colonies was seen after incubating at room temperature without IPTG for another 36 hours (**Fig.3.3B**). However, many strong green fluorescent colonies were detected after incubating at 37°C without IPTG for 24 hours and a further incubation at 4°C for several days (3-7 days) (**Fig.3.3D**). There was no detectable fluorescence in the control bacterial colonies (**Fig.3.3C**). This indicated that active wild-type GFP was more efficiently produced at a lower temperature. In fact, later publications confirmed that increased temperatures led to production of inactive GFP (Cormack et al. 1996; Crameri et al. 1996; Kimata et al. 1997).

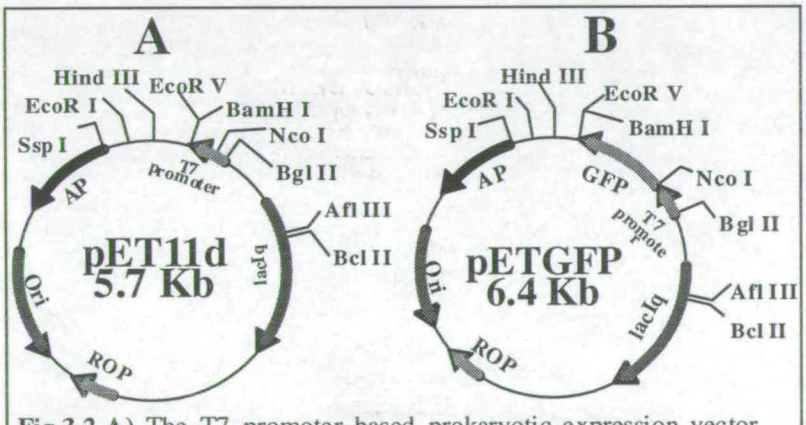

Fig.3.2 A) The T7 promoter based prokaryotic expression vector, pET11d. **B)** Wild type GFP cDNA was inserted into the Nco I / BamH I of pElld to produce pETGFP.

As shown above, the green fluorescent colonies had a bright intensity indicating that GFP molecules were highly expressed in bacterial cells. In fact, green fluorescent cells were seen as many green spots at low magnification (**Fig.3.9A**). Interestingly, at high magnification, a single GFP expressing bacterium showed a saturated

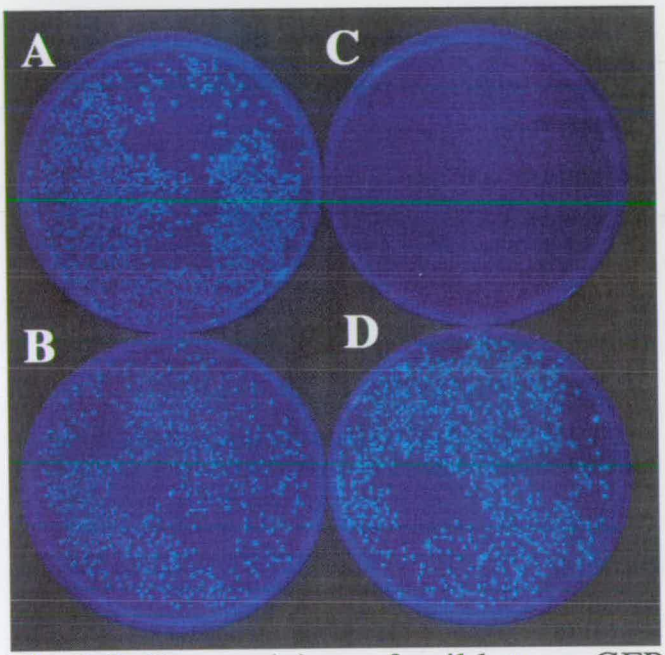

Fig.3.3 Comparision of wild type GFP fluorescent at various temperatures. pETGFP transformed bacterial colonies under UV light showing different levels of green fluorescent activity after incubting at **A)** 37 °C for 24 hours; **B)** 25 °C for 36 hours; **D)** 37°C for 24 hours and a further incubation at 4°C for 3 days. **C)** A negative control of bacterial colonies showed no detectable fluorescent activity after incubating with the same condition as **D)**.

green fluorescent colour throughout except for the chromosomal region (**Fig.3.5A**). Thus, GFP is produced at a high level and is distributed evenly throughout most of the cell.

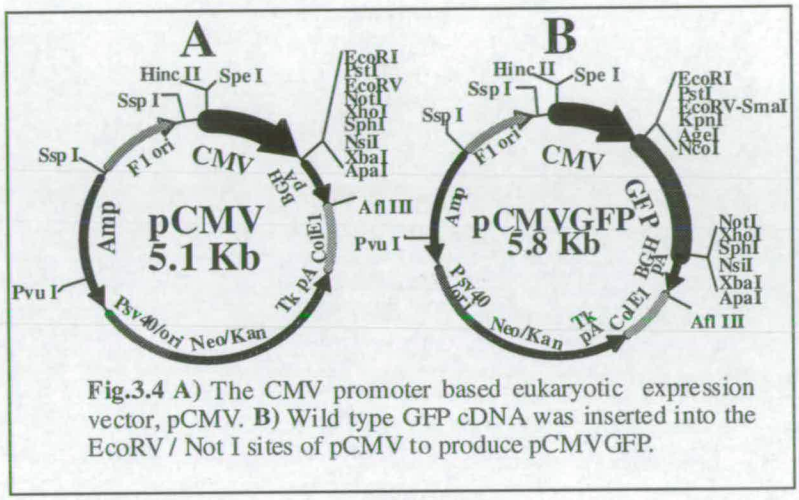

Fig.3.4 A) The CMV promoter based eukaryotic expression vector, pCMV. **B)** Wild type GFP cDNA was inserted into the EcoRV / Not I sites of pCMV to produce pCMVGFP.

To measure GFP fluorescent activity in mammalian cells, the wild-type GFP cDNA fragment was then subcloned into a eukaryotic expression vector, pCMV (**Fig.3.4A**). The resultant was named pCMVGFP (**Fig.3.4B**). pCMVGFP was then transfected into Cos7 cells. After transient transfection, only very weak fluorescence was seen in a small number of cells using either FITC filter or UV light under fluorescence microscopy. At high magnification, the fluorescing cells showed a ubiquitous distribution of GFP in the cytoplasm (**Fig.3.5B**). However, the green fluorescence in the Cos7 cells faded very quickly (photobleaching) within a few minutes. Furthermore, selecting for neo^r stable lines showed no detectable fluorescence under the same conditions. This suggested that wild-type GFP may be a useful marker in prokaryotic cells but was an inadequate means for detection in mammalian cells.

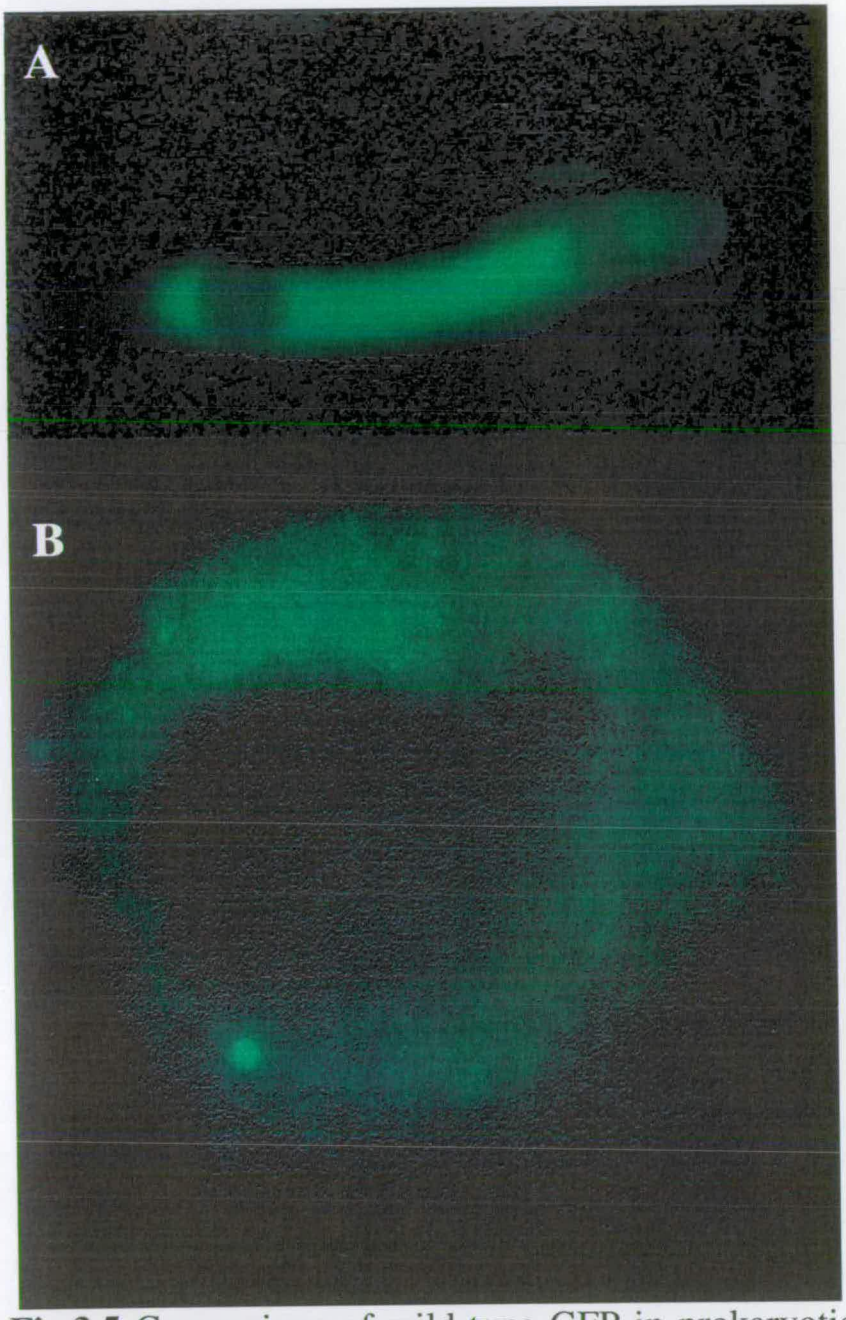

Fig.3.5 Comparison of wild type GFP in prokaryotic and eukaryotic cells. **A**) High magnification of a single green fluorescent bacteria cell, BL21(DE)3 in A) and a single green fluorescent mammalian cell, Cos7 in **B)** Visualised under UV illumination at the same exposure.

3.3 The generation of GFP mutants

As discussed above, wild-type GFP showed strong fluorescent activity in bacterial cells but did not function efficiently in a mammalian cell. The reason may be such that high levels of GFP molecules were produced in bacterial cells while low levels of GFP molecules were produced in mammalian cells.

Initially, I attempted to increase the fluorescent signals of GFP by concentration of the protein into subcellular compartments within the cell. Some polypeptides responsible for localisation of subcellular proteins can be fused to GFP to target the fusion into small cellular spaces. In fact, wild-type GFP tagged with nuclear localisation signal did slightly increase a detectable green fluorescence under UV light but not under blue light. However, the instability of the fluorescence (GFP fluorescence can be lost within a minute under UV light) of the wild-type GFP is undesirable. Thus, targeting wild-type GFP into the nucleus did increase fluorescence but not enough to enhance detection. Subsequently, it became clear that the fluorescent activity of jellyfish protein is affected by higher temperature and the stability is reduced by UV light. Obviously, the number of active and stable protein molecules is a critical requirement for detection in mammalian cells.

Hence, it was necessary to modify GFP by generating GFP mutants that would overcome the limitation of wild-type GFP. Since GFP green fluorescence was readily detected in bacterial cells, this provided a sensitive and efficient way to screen a GFP mutant among

thousands of colonies. By taking advantage of this, three classes of GFP mutants were generated by PCR mediated mutagenesis as described in section 2.2 and were then examined for their green fluorescent activity in bacteria. These mutants (GFP-S65T, GFP-S65C and GFP-S65A) shown in **Fig.3.6A** were more photostable and significantly enhanced the fluorescence of GFP when analysed using FITC filter for fluorescent microscopy. The other GFP mutants resulted in increased solubility of the protein and are described in the **Fig.3.6B**. Furthermore, to increase the translation efficiency in mammalian cells, similar mutants were generated by PCR from a humanised GFP template, hGFP-S65T (Clontech), in which the codon usage has been altered to optimise translational efficiency in a mammalian environment (**Fig.3.6C**).

A more rapid and efficient strategy to mutate GFP was modified from a PCR mutagenesis method (Dorrell et al. 1995; Vilardaga et al. 1995). This was ideal for making multiple substitutions in a given DNA fragment without the necessity of subcloning steps. Using this method, a series of substitutions were introduced into GFP coding sequences.

The procedure is outlined in **Fig.3.7**. Two sets of primers, PL/PA and PR/PB were designed from both ends of the DNA fragment of interest (GFP cDNA). PA and PB were designed to carry a mutant codon with an appropriate restriction site (x) or any recognition site recognised by a class 2S restriction enzyme (for example, Bbs I). The first PCR reaction consisted of a step for preamplification (below 20 cycle) using the two sets of primers. The two amplified fragments were digested with the appropriate restriction enzyme (X) and religated at

room temperature. Finally, the religation mixtures were used as a template for secondary amplification. The final PCR products could be analysed by checking for the introduced restriction sites (x) introduced by PCR. To analyse the contribution of the mutations, the PCR products were than subcloned to examine GFP fluorescent activity and the effect of the mutations.

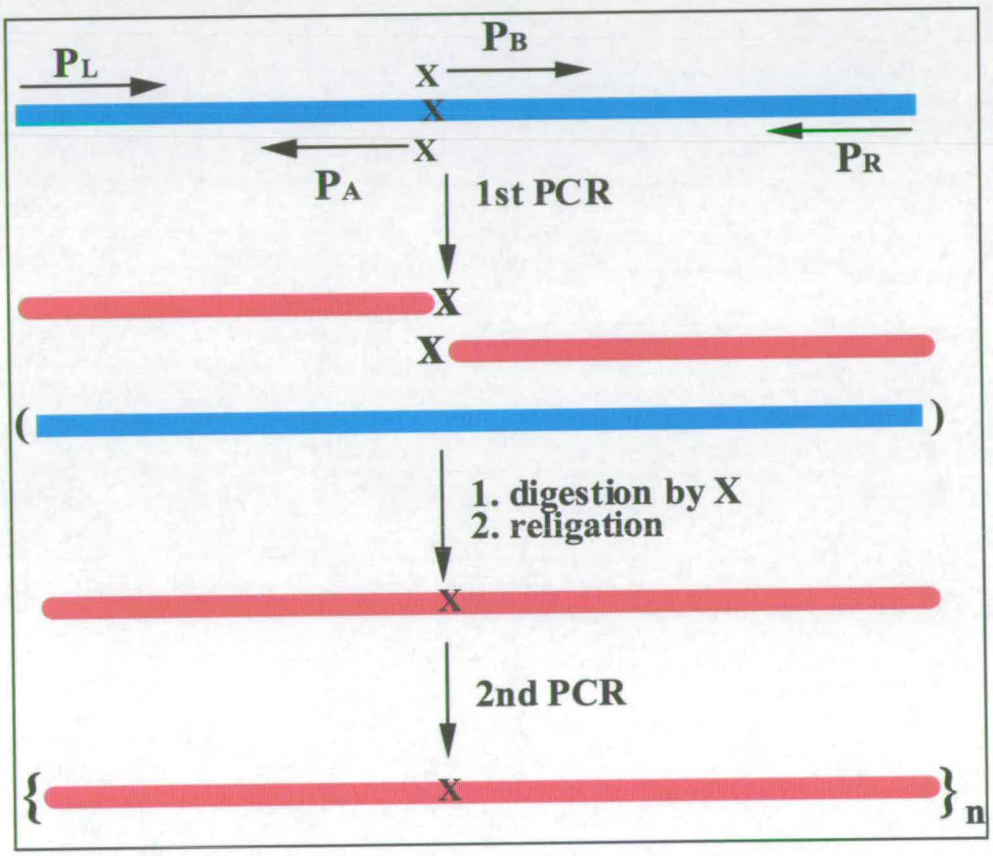

Fig.3.7 The strategy of PCR based mutagenesis

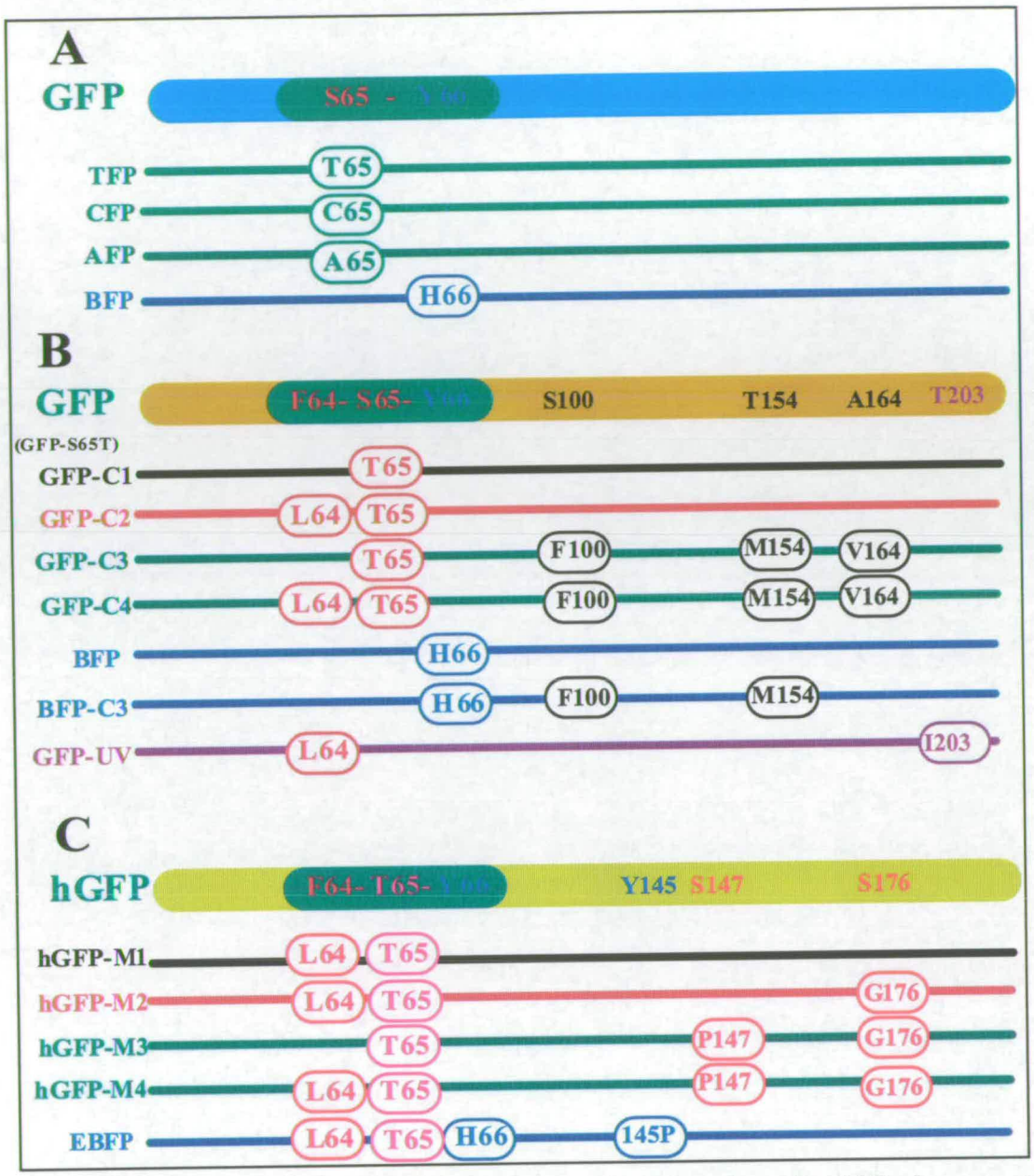

Fig.3.6 The summary of GFP variants. **A)** Wavelength shifted mutants: TFP, GFP-S65T; CFP, GFP-S65C; AFP, GFP-S65A; BFP, GFP-Y66H. **B)** Enchanced fluorescent wild-type GFP mutants: GFP-C1 (TFP), GFP-S65T; GFP-C2, GFP-F64L / S65T; GFP-C3, GFP-S65T / F100S / M154T / V163A; GFP-C4, GFP-F64L / S65T / F100S / M154T / V163A; BFP, GFP-Y66H; BFP-C3, GFP-Y66H / F100S / M154T / V163A; GFP-UV, GFP-F64L / T203I. **C)** Enchanced fluorescent humanised GFP mutants: hGFP-M1, hGFP-F64L / S65T; hGFP-M2, hGFP-F64L / S65T / S176G; hGFP-M3, hGFP-S65T / S147P / S176G; hGFP-M4, hGFP-S64L / S65T / S147P / S176G; EBFP, hGFP-F64L / S65T / Y66H / Y147P (Clontech).

3.4 Functional analysis of the GFP mutants

3.4.1 GFP mutant with altered wavelength of excitation

In bacteria under normal growth conditions, wild-type GFP fluorescence was stronger than that of TFP (GFP-S65T) and CFP (GFP-S65C) mutants directly exposed to the UV transilluminator (**Fig.3.8A**). However, wild-type GFP and TFP or CFP fluorescence showed no significant differences when visualising single cells under fluorescent microscopy using an FITC filter (**Fig.3.9**). I postulated that this may be due to GFP having reached saturating levels of fluorescence within the bacterial cell. Sequence analysis of the Thr mutant chromophore in TFP showed that indeed the mutation of T to A (TCT to ACT) was present causing the predicted conversion of Ser to Thr (the conversion of Ser to Cys was also identified in CFP). The results presented here suggest that these mutants do shift their excitation wavelength from the UV wavelength (390 nm) toward the visible or blue wavelength at 490 nm.

Analysis of the mutant which shifted the emission wavelength from green (508 nm) to blue (480 nm) (BFP or GFP-Y66H, **Fig.3.6A**) showed weak blue fluorescence compared to green fluorescence when directly exposed to the transilluminator (**Fig.3.8**). However, at the single cell level, the blue mutant showed substantial blue fluorescence when excited with UV light (**Fig.3.9**) but the fluorescent intensity was slightly weaker than wild-type GFP as predicted by Heim et al. (1994).

When transfected into Cos7 cells, slightly stronger fluorescent activity was detected for TFP, CFP or AFP (GFP-S65A, **Fig.3.6A**)

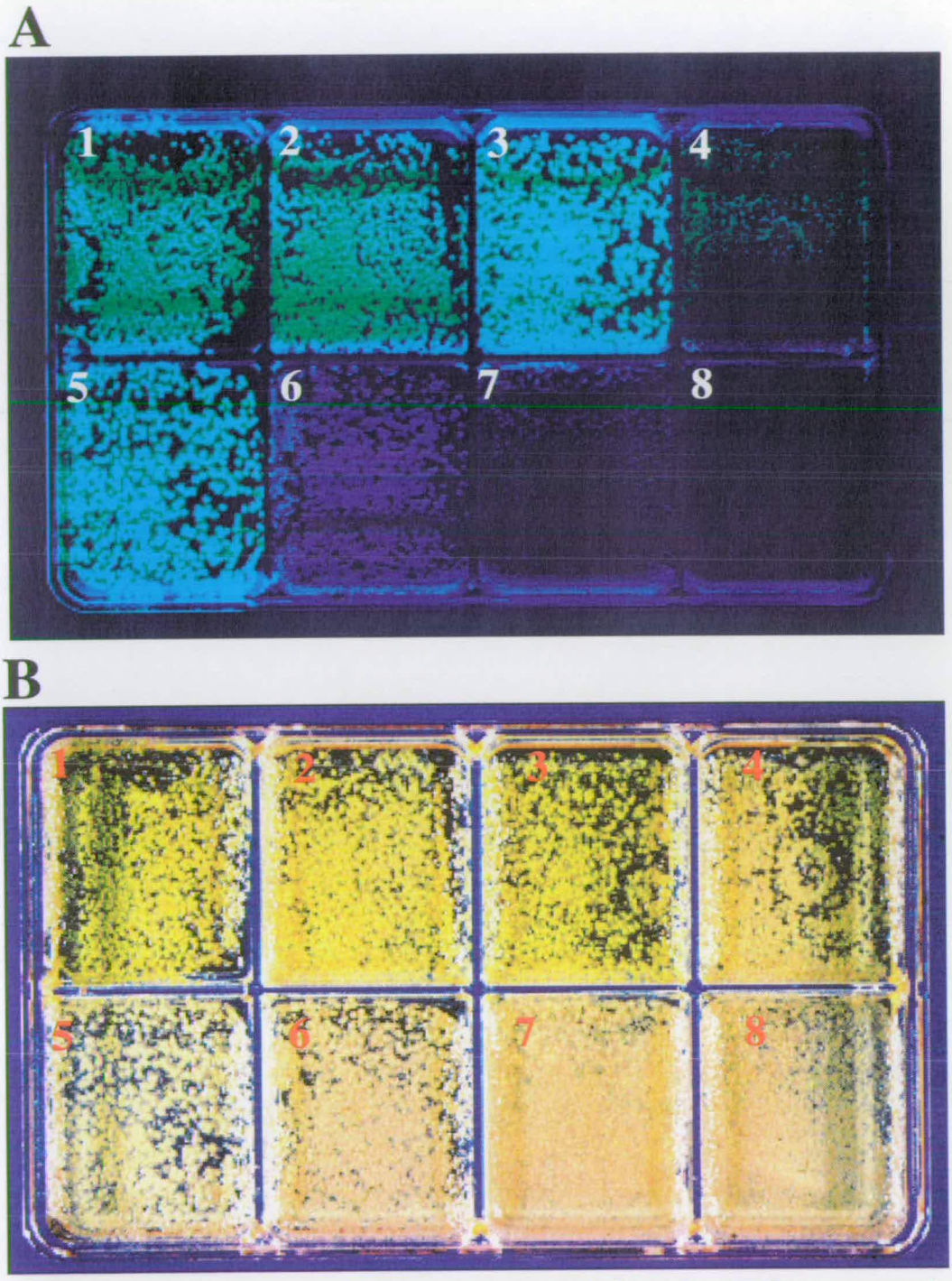

Fig.3.8 Comparison of fluorescent activity of GFP mutants in transformed bacterial colonies shown in **A)** UV light; **B)** visible light. 1, GFP-C4; 2, GFP-C3; 3, GFP-C2; 4, TFP; 5,GFP; 6, BFP-C3; 7, BFP; 8, BL21(DE)3.

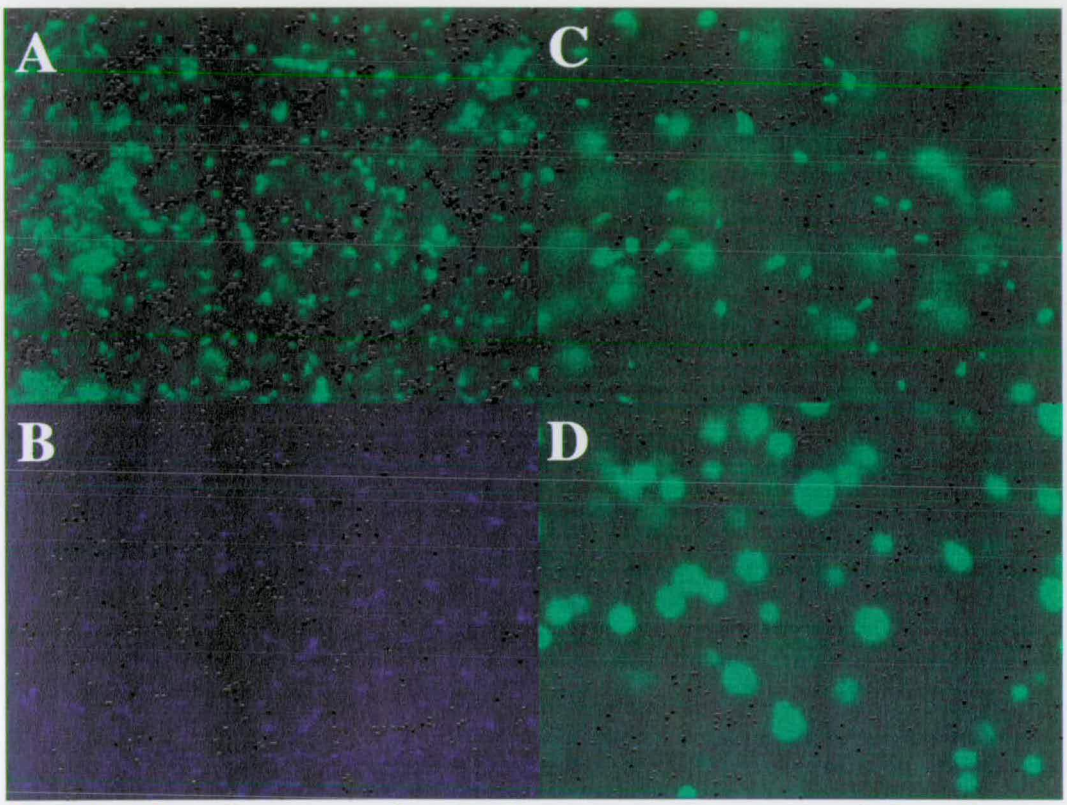

Fig.3.9 Visualisation of GFP mutants in bacterial cells under fluorescent microscopy. **A)** GFP, wild-type GFP; **B)** BFP (GFP-Y66H); **C)** CFP (GFP-S65-C); **D)** TFP, (GFP-S65T). GFP, CFP and TFP cells were illummiated at 490 nm. BFP cells were illummiated at 380 nm.

using the FITC filter compared to wild-type GFP under UV light (**Fig.3.10**) (GFP showed dim green fluorescence using FITC filter). Although these mutants had detectable fluorescence in bacterial cells at 490 nm and under UV (380 nm) light; the fluorescent signal was barely detectable in mammalian cells under UV light. These mutants probably do not overexpress in mammalian cells to the same extent as bacterial cells and other physiological conditions differ between prokaryotic and eukaryotic cells.

3.4.2 Enhanced fluorescent GFP mutants

The previous results were in agreement with Heim et al. (1995) that the advantage of TFP was to shift the major excitation wavelength from the UV range to 490 nm. In order to find a GFP variant with increased activity in mammalian cells, it was necessary to incorporate other reported mutations which affected heat sensitivity, solubility, and efficiency of translation.

Wild-type GFP mutants

First, the wild-type GFP coding regions were used as templates for mutagenesis. Six mutations (F64L, S65T, Y66H, F100S, M154T, V163A) (Cormack et al. 1996; Crameri et al. 1996; Haas et al. 1996; Heim et al. 1994; Heim et al. 1995; Heim et al. 1996) which had previously been reported as enhancing the fluorescent activity or shifting the emission wavelength in wild-type GFP were introduced into GFP. The resulting mutants were based on GFP-C1 or TFP which carried the S65T mutation responsible for shift of the excitation

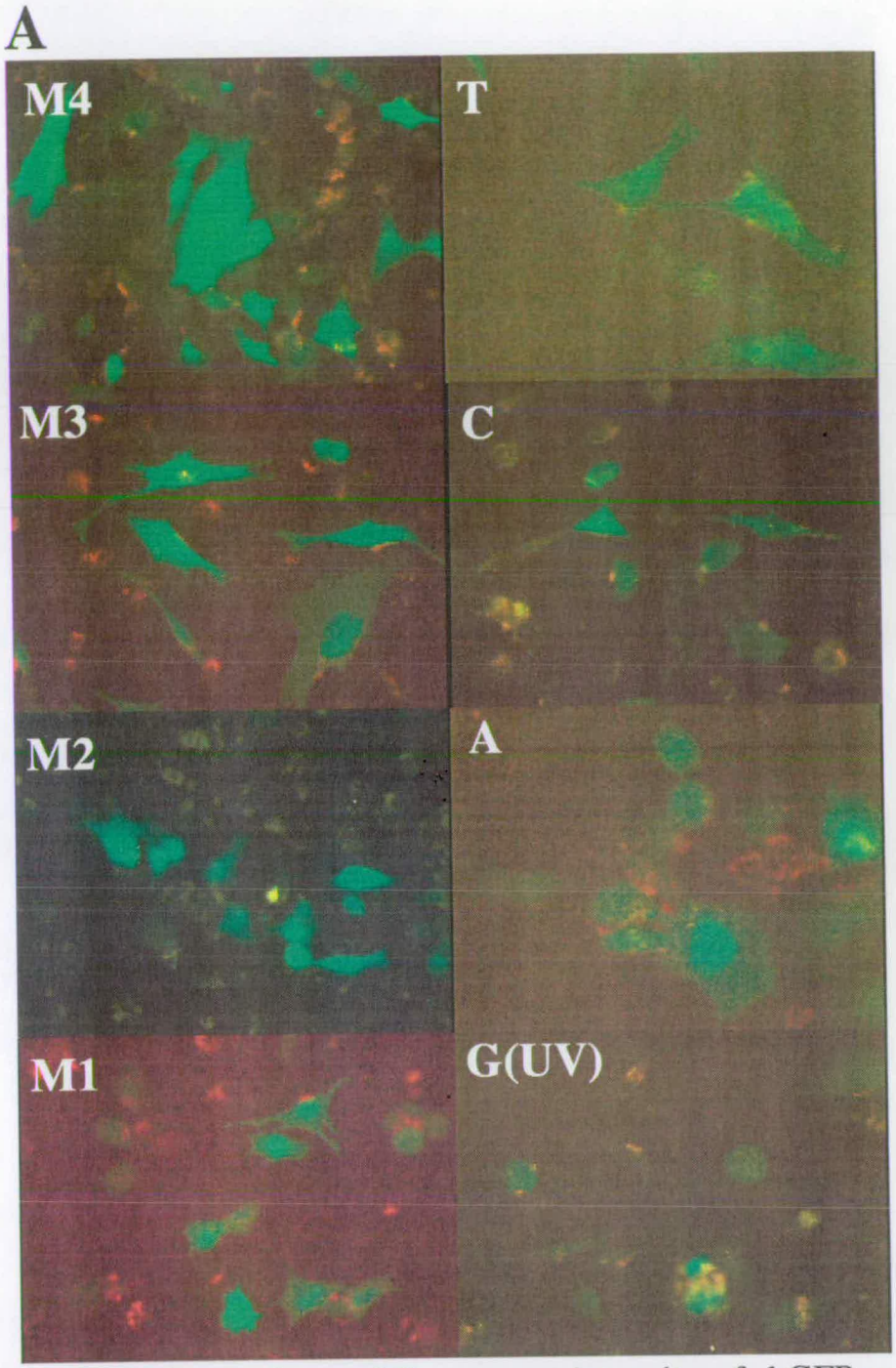

Fig.3.10 Comparison of fluorescent intensity of hGFP and GFPmutants in transiently transfected Cos7 cells. **A**) at low magnification; **B)** at high magnification (100X). hGFP mutants: M4, hGFP-M4; M3, hGFP-M3; M2, hGFP-M2; M1, hGFP-M1. GFP mutants: T, TFP; C, CFP; A, AFP; G, GFP. Green fluorescent cells shown in hGFP-M4, hGFP-M3, hGFP-M2, hGFP-M1 ,TFP, CFP and AFP were illuminated by blue light. Wild type GFP fluorescence was illuminated by UV light.

B

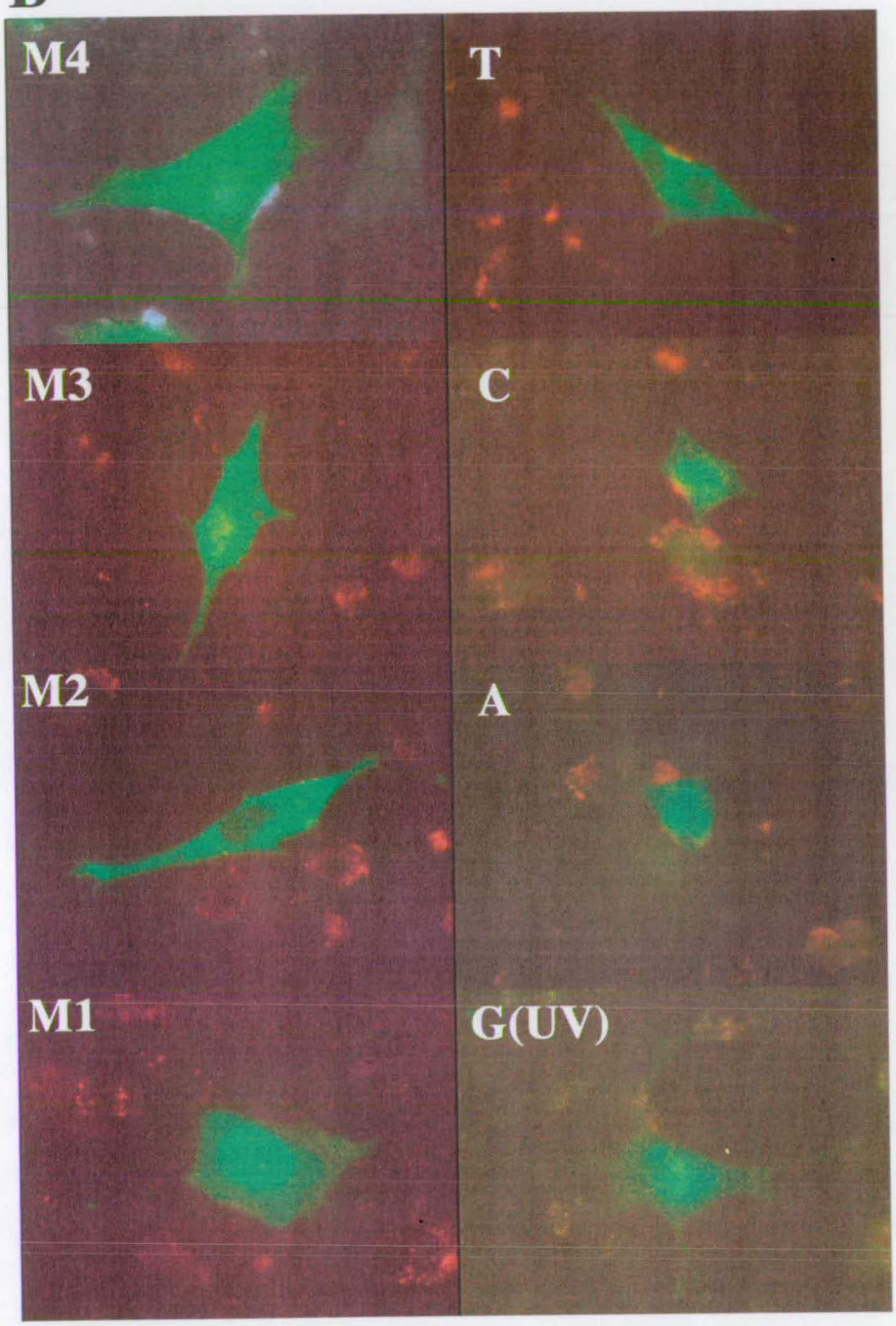

wavelength. Thus GFP-C2 was GFP-C1 plus the F64L mutation, GFP-C3 was GFP-C1 plus the F100S, M154T, and V163a, and GFP-C4 carried all the mutations in GFP-C3 plus the F64L mutation. The blue fluorescent mutation (BFP) carried the Y66H mutation responsible for shift of emission wavelength and was further modified to BFP-C3 (BFP+F100S, M154T and V163A) to determine the affects of the mutations on blue fluorescent activity (**Fig.3.6B**). These mutants were first examined for green fluorescent intensity in bacteria. When these GFP expressing colonies were illuminated by UV light, GFP-C4, GFP-C3, GFP-C2 and GFP showed a very bright fluorescence. Whereas, GFP-C1 showed only a faint fluorescence. The two blue mutants showed blue fluorescence and the BFP-C3 was brighter than BFP (**Fig.3.8A**). No fluorescence was detected in bacterial cells which did not express any GFP variants. Although those bacterial colonies expressing GFP-C4, GFP-C3 and GFP-C2 showed a comparable fluorescent intensity as wild-type GFP, GFP-C4, GFP-C3 and GFP-C2 showed fluorescent activities at 37°C for overnight incubation while GFP-C1 and wild-type GFP showed fluorescence at lower temperature (4-25°C) for another 2-3 days of incubation. A similarly enhanced fluorescence was seen in BFP-C3 compared to BFP but increased blue fluorescent activity of BFP-C3 in BFP is much lower than that of GFP-C3 in GFP-C1.

GFP-C2 and wild-type GFP showed a similar fluorescent activity which was stronger than both GFP-C4 and GFP-C3. Interestingly, a visible green color also could be seen in the colonies under a normal light source. GFP-C4 and GFP-C2 showed a deep yellow green color and GFP-C3 showed pure green. However, GFP-C1

and GFP showed only a light-green color and BFP-C3 and BFP showed a brown color (**Fig.3.8B**). To make a more clear comparison, bacterial lysates prepared from these mutants showed more clear features of the mutated protein under UV light and visible light (**Fig.3.11**).

Thus, these mutations play an important role in increasing GFP fluorescence. The features of these GFP variants in bacterial cells are summarised on **Table 3.1**. In particular, GFP-C4, GFP-C3 and GFP-C2 proteins may have increased solubility in bacterial cells as previously reported (Cormack et al.1996; Matsumura et al. 1996) resulting in stronger fluorescent activity than the GFP-C1 which contained only the S65T (Heim et al. 1995). Perhaps, these mutations involved in GFP-C4, C3 & C2 not only have a contribution in producing active protein but also increase the fluorescent intensity resulting in higher fluorescent activity than wild-type GFP.

Table 3.1 The features of GFP variants in BL21(DE)3 cells.

GFP variants	Colony color	Fluorescent intensity[a]	Fluorescent stability	Temperature requirement
GFP-C4	yellow green	High	Yes	37°C.
GFP-C3	deep green	High	Yes	37°C
GFP-C2	yellow green	High	Yes	37°C
TFP	light green	Weak	Yes	25°C
CFP	light green	Weak	Yes	25°C
AFP	light green	Weak	Yes	25°C
GFP	Green	High	Yes	4°C
BFP-C3[c]	Normal	Weak[b]	No	37°C
BFP	Normal	Weak	No	4°C

a. The fluorescent colonies were measured under UV light. **b.** The weak fluorescence was due to the blue intensity and photobreaching. **c.** It only very few colonies could be seen when cells were incubated at 37°C.

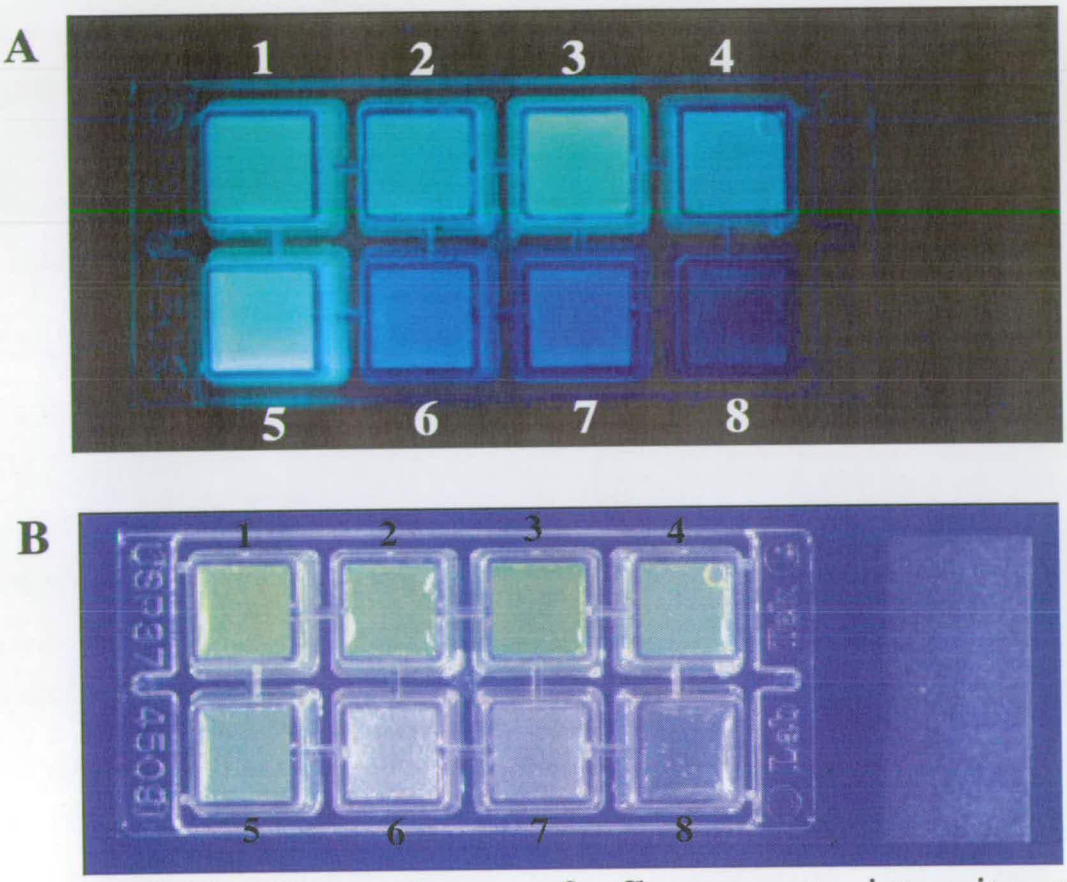

Fig.3.11 Comparison of fluorescent intensity of bacterial lysates from GFP mutants shown in **Fig.3.8**. . **A)** UV light. **B)** visible light. 1, GFP-C4; 2, GFP-C3; 3, GFP-C2; 4, TFP; 5,GFP; 6, BFP-C3; 7, BFP; 8 BL21(DE)3.

Humanised GFP mutants

Three classes of mutations were made using the GFP gene containing human preferred codons, hGFP-S65T (Clontech). As in the previous analysis, GFP-C2 containing the F64L and S65T mutations showed a significant in creased fluorescence. For comparison, an hGFP-M2 containing the F64L and S65T was generated by the same method as above. Furthermore, two other mutations S176G and S147P were incorporated into the hGFP-M1 template to generate three different humanised forms. I refer to these as hGFP-M4, hGFP-M3, hGFP-M2 and hGFP-M1 (**Fig.3.6C**). Thus hGFP-M2 was hGFP-M1 plus the S176G mutation, hGFP-M3 carried S65T, S147P and G176G and hGFP-M4 carried all the mutations in hGFP-M3 plus the F64L mutation.

To examine the fluorescent activity, the hGFP variants were transiently expressed in Cos7 cells under the control of the CMV promoter. Generally, all hGFP variants showed strong and stable green fluorescence using the FITC filter, in contrast to the other wild-type GFP mutants. However, wild-type GFP only showed a very weak fluorescent intensity under UV light (**Fig.3.10**). hGFP variants showed a high fluorescent activity in mammalian cells suggested that these highly fluorescent cells contained large numbers of active proteins. In fact, the number of green fluorescent cells expressing hGFP mutants was higher than that of GFP mutants (See 3.5.2). Most interestingly, most of the hGFP-M4 expressing cells had the strongest fluorescence (**Fig.3.10A**).

Thus, the combination of mutations in either hGFP-M1, M2, M3 & M4 or GFP-C2 C3 & C4 may show similar fluorescence at the level of a single protein. However, hGFP variants can produce a high level of these proteins in cells resulting in increased fluorescence. Thus, these new features make hGFP proteins better than their counterparts using jellyfish codons in mammalian cells.

3.5 The molecular characteristics of GFP variants

3.5.1 Comparison of the fluorescent intensity of GFP variants in BL21(DE)3

To quantitatively measure the relative fluorescent intensity of each mutant, each recombinant GFP mutant protein was prepared from protein lysates of BL21(DE)3 cells expressing these mutants and 10mg of the proteins were directly loaded on a non-denaturing gel (12% polyacrylamide). Five visible green bands could be detected on the gel before exposing under UV light (transilluminator). As discussed above, GFP-C4, C3, C2, and C1 do not absorb at UV wavelengths; however, the spectral bandwidth is probably quite broad from the transilluminator. Thus, five green fluorescent bands were seen at the same position on the gel under UV light (**Fig.3.12A**). Even under these conditions, GFP-C2 showed a strong fluorescent band similar to wild-type GFP. GFP-C4 and GFP-C3 also showed a strong but slightly weaker intensity. The GFP with the equivalent excitation wavelength, GFP-C1 (TFP) and CFP (CFP is a similar mutant as the TFP with a S65C mutation) gave a very weak intensity. Therefore, the additional mutations added to GFP-C4, C3 & C2 increased fluorescence

appreciably. A strong blue fluorescent band could also be seen in the BFP-C3 (**Fig.3.12B**). The relative amounts of each GFP were at a similar level when normalised to the amount of cellular proteins by staining with the coomassie blue (**Fig.3.12C**). GFP-C4 and GFP-C2 showed more fluorescence compared to TFP (GFP-S65T) and CFP (GFP-S65C) since the F64L mutation could not only increases the protein solubility but also reconverts the protein to UV excitability (Cormack et al. 1996). TFP and CFP could only be illuminated at the blue wavelength (490 nm) (Heim et al. 1994). However, F100S/M154T/V163A mutations contributed to increase the fluorescent activity but do not alter the spectral specificity in GFP-C3. In addition, there was no advantage of combining mutations in GFP-C4 in bacterial cells as GFP-C2 gave the strongest activity of these mutants.

3.5.2 Comparison of the fluorescent activity of GFP variants in mammalian cells

hGFP-M4, hGFP-M3, hGFP-M2 and hGFP-M1, as discussed above, showed strong fluorescence in Cos7 cells. To examine and compare their efficiency in mammalian cells, hGFP and GFP mutants were subcloned into the pCI vector, a CMV promoter based eukaryotic expression vector, and linked to IRES-βgeo. The resulting constructs were named pCIhGIZ4, pCIhGIZ3, pCIhGIZ2, pCIhGIZ1, pCIG2IZ, pCITIZ, pCICIZ and pCIGIZ (**Fig.3.13**). These dicistronic constructs allowed a coexpression of both GFP fluorescence and β-galactosidase activity in the same cells. Thus GFP fluorescent activity could be analysed against a background of expression. Although there was no indication to the contrary, this assumes IRES-βgal expression was the

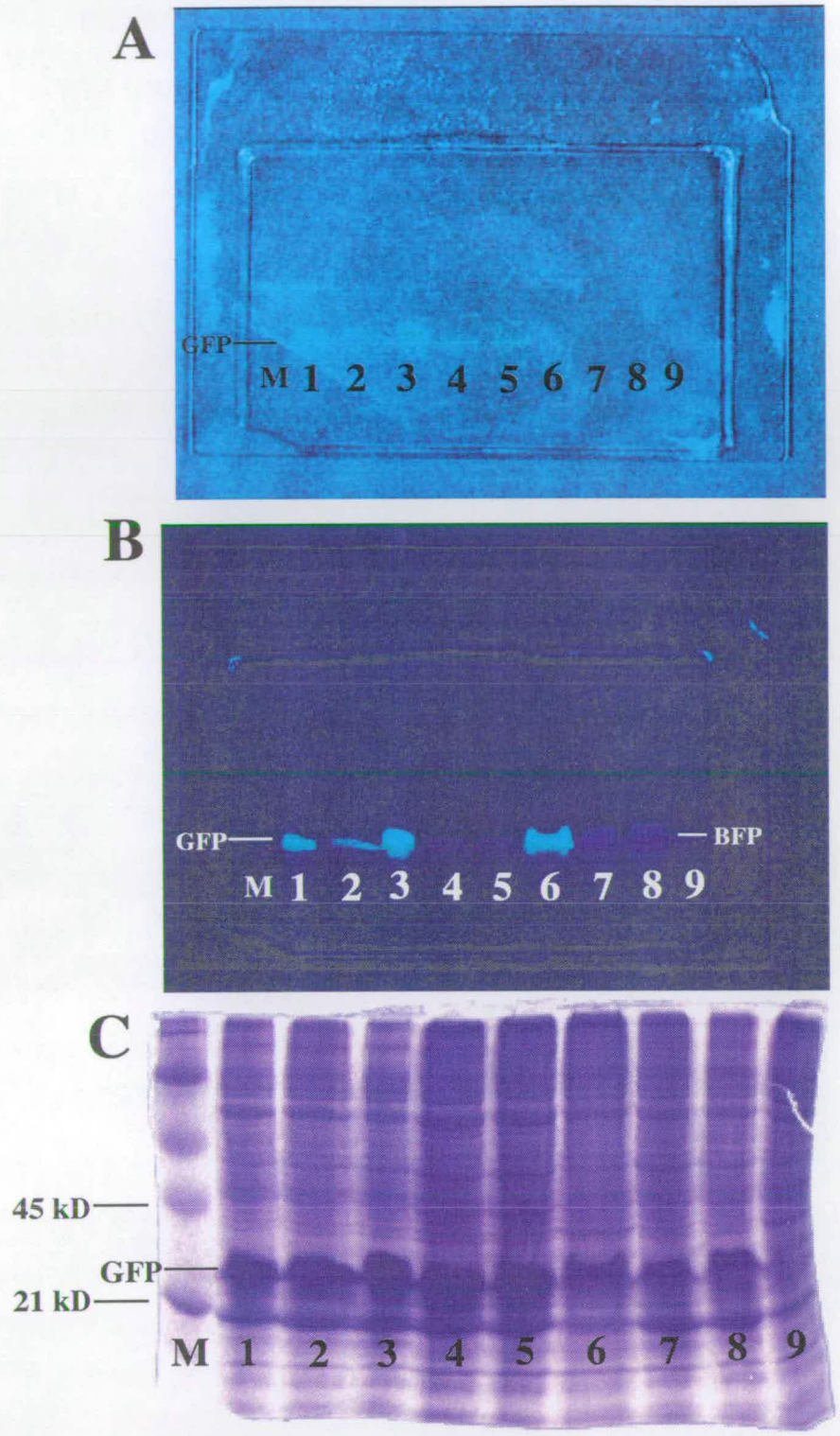

Fig.3.12 Quantitative measurement of relative fluorescent intensity of GFP mutants. 10 µg/well of BL21(DE)3 protein lysate was loaded into a 8% non-denaturing gel. The gel was then visualised under **A)** visible light, **B)** UV light and **C)** coomassie blue staining. Lane 1, GFP-C4; Lane 2, GFP-C3; Lane 3, GFP-C2; Lane 4, TFP; Lane 5, CFP; Lane6 , GFP; Lane 7, BFP; Lane 8, BFP-C3; 9. Bl21(DE)3 (control); M, protein size marker

same in each construct. The expression efficiency of each construct was measured by calculating the ratio of the number of green fluorescent cells to the number of blue x-gal stained cells

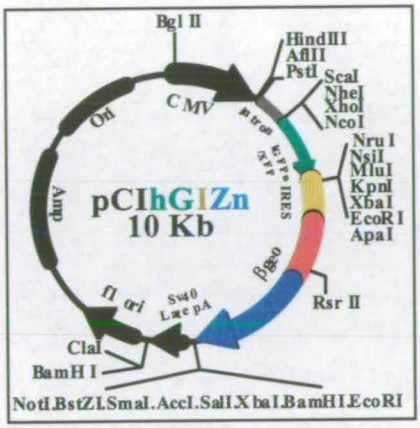

Fig.3.13 Plasmid vector used to transiently and stably express GFP variants under the control of the human cytomeglovirus immediate early promoter (CMVIE) in mammalian cells, hGFPn, n=M1, M2, M3, & M4,. XFP=TFP (GFP-S65T), CFP (GFP-S65C) or GFP.

These constructs and a β-galactosidase control construct were then transiently transfected into G7 cells, a mouse myoblast cell line. The number of GFP fluorescent cells expressing each construct were first counted. Then the same transfected cells were counted for blue cells following x-gal histochemistry staining. By using this measurement, hGFPs constructs showed more efficient production of active GFP than those containing the wild-type codon usage except for the GFP-C2 construct **(Table 3.2)**. In the FITC filter range, the ratios of TFP and CFP were about 10 fold higher than wild-type GFP and GFP-C2 was about 6 folds higher than TFP and CFP. The ratio of hGFP variants was only two fold higher than GFP-C2. However, the ratio of hGFP-M4 was 152 fold higher that of wild-type GFP.

To compare the expression efficiency with other mammalian cell lines, three different lines were used in a similar analysis and the ratios were very similar to those in Table 3.2 (**Table 3.3**). Similarly, TFP or CFP had a mild effect compared with wild-type GFP. The change to mammalian codon usage also had a mild effect with a two fold difference between GFP-C2 and hGFP variants. However, the limitation of this assay are two-fold. First, as the ratio of GFP to β–gal expressing cells approach 1 the assay is probably not linear. Secondly, the relative fluorescence cell is not taken into account.

To examine relative GFP levels, a western analysis of the protein in transiently transfected Cos7 cells was done. Most of the hGFP variants had high expression levels of protein under the same transfection conditions as compared to GFP variants (**Fig.3.14**). This suggested that the mutations of the variants did not affect GFP production. Thus, the mutations and the change of codon usage introduced into wild-type GFP caused a dramatic increase in GFP production and fluorescent activity. Interestingly, hGFP-M4 which was higher percentage of the cells showed lower protein production then hGFP-M3 and hGFP-M2.

Table 3.2 The expression efficiency of hGFP variants in mammalian cells (G7)

Constructs	Plasmid DNA Concentration(ng)[a]								
	1000			500			100		
	Green	Blue	Green /Blue	Green	Blue	Green /Blue	Green	Blue	Green/ Blue
hGFP-M4	188	246	0.76	41	51	0.78	17	21	0.8
hGFP-M3	142	211	0.70	30	46	0.65	14	18	0.77
hGFP-M2	108	179	0.60	19	33	0.57	9	15	0.60
hGFP-M1	101	192	0.52	25	45	0.55	12	25	0.48
GFP-C2	82	281	0.30	15	65	0.23	7	30	0.23
TFP	10	186	0.05	2	35	0.06	0	15	0
CFP	8	201	0.04	3	45	0.06	1	21	0.05
GFP[b]	2	177	0.005	0	30	0	0	12	0
βgeo		302			66			23	

a. 100ng, 500ng, 1000ng of each GFP constructs (Fig.3.13) were transfected with 10,000 G7 cells and then incubated at 37°C for 36 hrs. **b.** GFP expressing cells were detected under FITC light for the comparison.

Table 3.3 The comparison of expression efficiency of hGFP variants in three mammalian cells[a]

Constructs	NIH3T3			Cos7			G7		
	Green	Blue	Green /Blue	Green	Blue	Green /Blue	Green	Blue	Green/ Blue
hGFP-M4	177	253	0.70	181	223	0.81	179	239	0.75
hGFP-M3	157	216	0.60	179	257	0.7	149	241	0.62
hGFP-M2	151	301	0.50	121	197	0.61	127	271	0.47
hGFP-M1	107	219	0.49	189	287	0.66	134	209	0.64
GFP-C2	75	241	0.31	116	269	0.43	97	276	0.35
TFP	9	289	0.03	17	276	0.06	9	224	0.04
CFP	5	207	0.02	10	231	0.04	8	281	0.03
GFP[b]	2	275	0.007	0	244	0	0	194	0
βgeo		322			265			311	

a. 2mg of each GFP constructs (Fig.3.13) were transfected with 20,000 of each cells and then incubated at 37°C for 24 hrs. **b.** GFP expressing cells were detected at 490 nm light for comparison.

Table 3.4 The summary of characteristic of GFP variants

GFP variants	Expression efficiency[a]	Fluorescent intensity[a]	Fluorescent stability (toxicity)	Green fluorescent cell lines
hGFP-M4	70-80 %	High	Yes(NO)	Yes
hGFP-M3	60-70 %	High	Yes(NO)	Yes
hGFP-M2	50-60 %	High	Yes(NO)	Yes
hGFP-M1	50-60 %	High	Yes(NO)	Yes
GFP-C2	30-40 %	High	Yes(NO)	Yes
TFP	3-6 %	Weak	Yes(NO)	Yes
CFP	2-4 %	Weak	Yes(NO)	Yes
GFP	0-0.1 %	Weak[b]	No(NO)	No

a. This was measured by transient transfection and counted at all of the detectable fluorescent cells. **b.** Wild-type GFP expressing cells could only be seen under UV light.

According to this analysis, these mutants could be divided into four groups, A (hGFP-M4), B (hGFP-M3), C (hGFP-M2 and hGFP-M1, and GFP-C2) and D (TFP, CFP and GFP). The rank order of these groups in terms of their fluorescent intensity was : A>B>C>D (**Table 3.4**). In group D, the excited spectral mutations, S65T or S65C, only slightly increased fluorescent activity compared to wild-type GFP when illuminated with FITC filter (490 nm). In group C, the mutants showed strong fluorescence presumably resulting in a dominant contribution of the F64L mutation. However, there was no additive effect of combining F64L and S176G, as shown by there being no

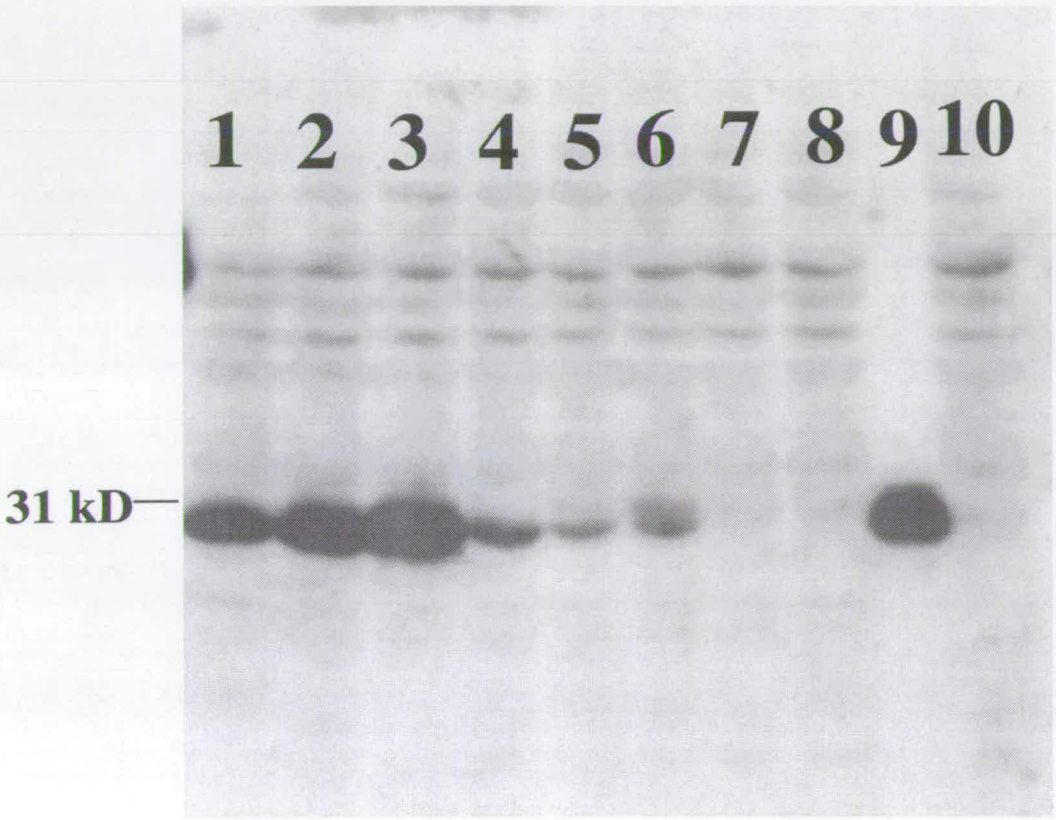

Fig.3.14 Western blot analysis of the translation efficiency of GFP variants in mammalian cells. 1 μg of each GFP construct was transiently transfected into $1x10^5$ Cos7 cells. After incubating for 48 hours, 20 μg/well of total protein from each transfectant were run by 12% SDS-PAGE. 1, hGFP-M4; 2, hGFP-M3; 3, hGFP-M2; 4, hGFP-M1; 5, TFP; 6, CFP; 7, wild type GFP; 8 ,wild type GFP; 9, purfied GFP (10ng); 10, Cos7.

significant difference between the level of expression of hGFP-M1 and hGFP-M2. In group B, hGFP-M3 gave a higher level of fluorescence than hGFP-M2 or hGFP-M1. This may suggest that the S147P and S176G had a synergistic effect and resulted in a higher level of fluorescence than the F64L. The most successful class of mutations was A, hGFP-M4 showed the highest GFP activity. Although hGFP-M4 contained a combination of mutations there seemed to be no effect on protein structure. Thus, F64L and S147P/S176G must have had a mutual effect or contributed individually to the fluorescence of hGFP-M4 without any negative interactions. Thus, hGFP-M4 produced a highly fluorescent GFP.

3.5.3 Comparison of the altered wavelength of GFP mutants.

There are three classes of wavelength shifted GFP mutants, GFP with S65T, GFP with Y66H or (BFP) and GFP with T203I or GFP-UV (**Fig.3.7B**). The GFP-C2, containing S65T, showed a maximal fluorescence at 490 nm wavelength (or blue light) but had also a weak fluorescence in the UV light range in bacteria (**Fig.3.15**). Interestingly, the BFP and GFP had a similar level of fluorescent activity in bacterial cells (**Fig.3.16A**) but the blue fluorescence was weak and unstable in mammalian cells compared to green fluorescence (**Fig.3.16B**). The weak fluorescent activity of BFP is due to the weak intensity of the proteins and sensitive to photobleaching. However, targeting BFP to subcellular organelles may increase the blue fluorescent signals.

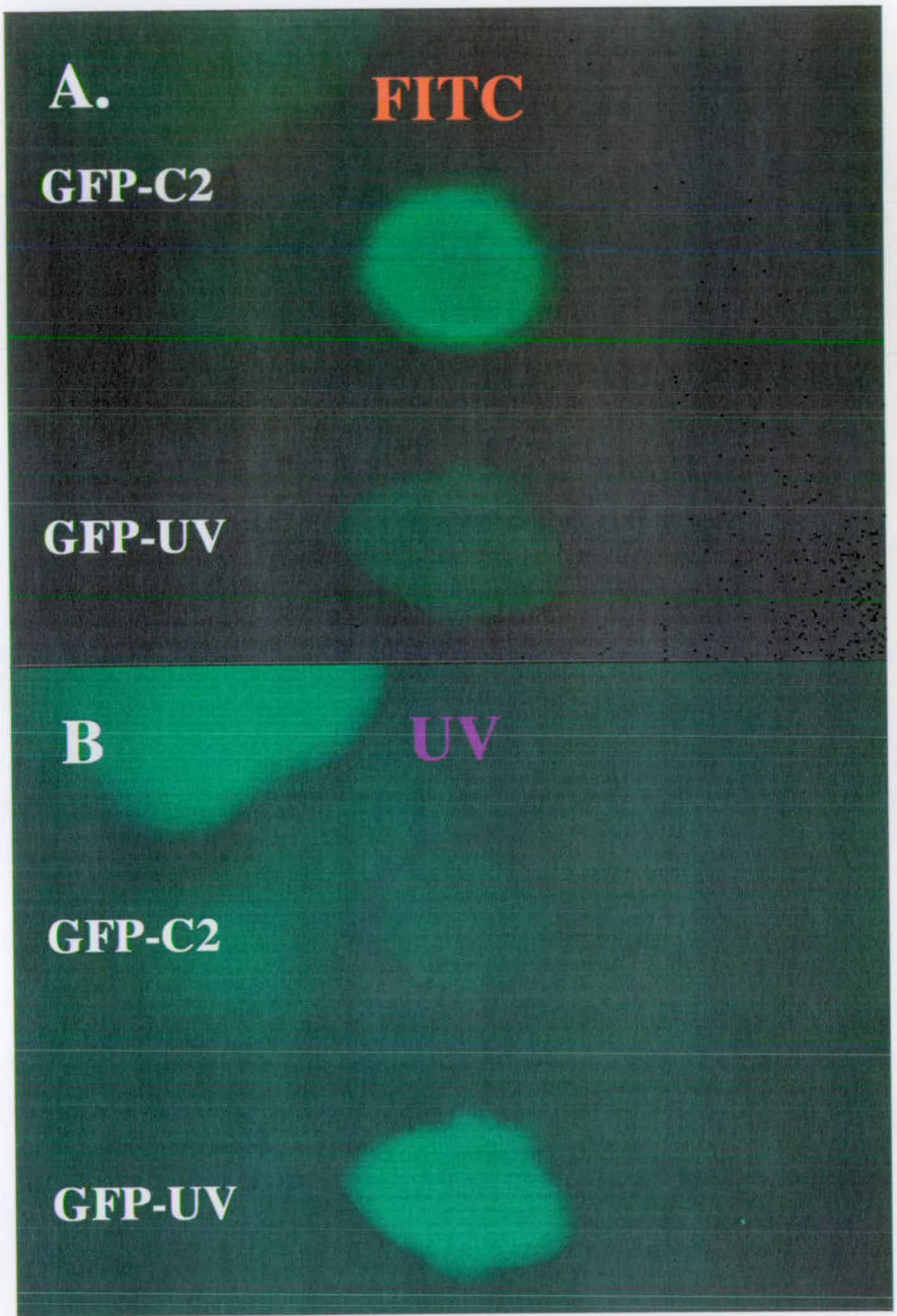

Fig.3.15 Comparison of GFP-C2 and GFP-UV expressing bacterial colonies illumated with **A**) FITC filter and **B**) UV light (100X).

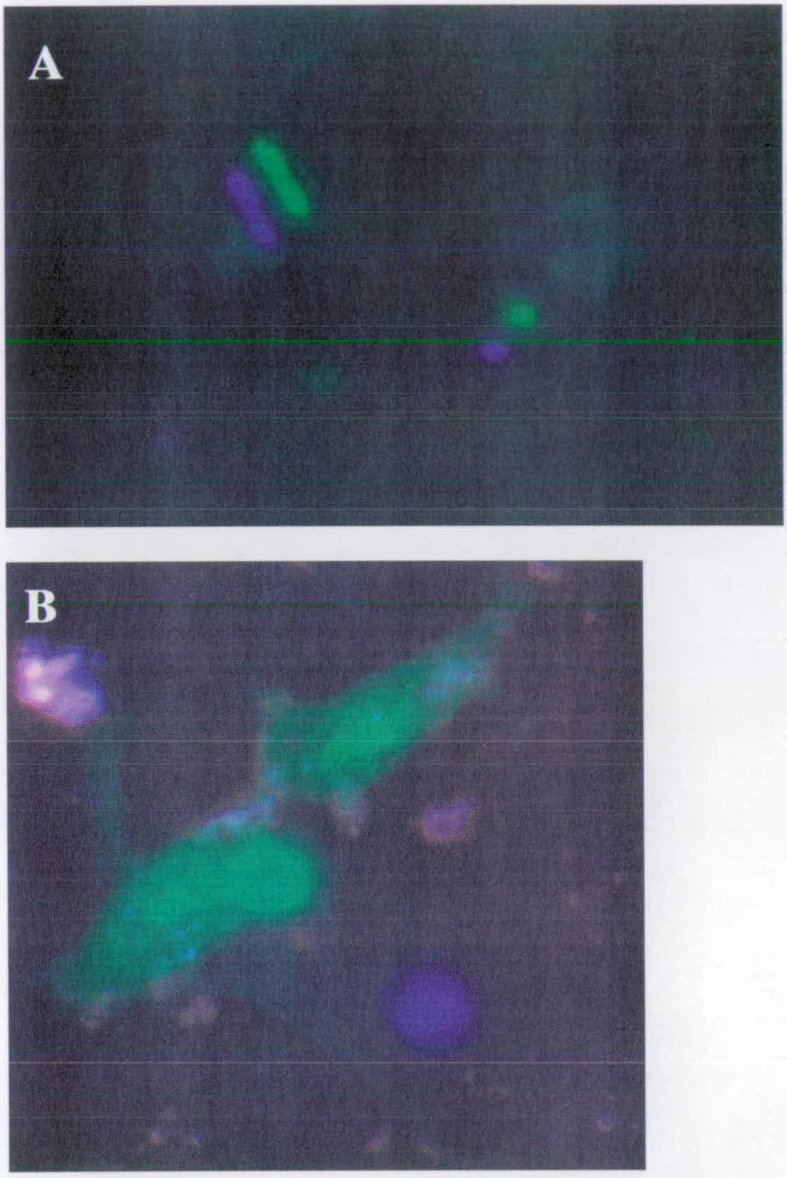

Fig.3.16 Comparison of fluorescent intensity of GFP and BFP mutants in prokaryotic and eukaryotic cells. **A)** GFP and BFP expressing bacterial cells (BL21) (250X). **B)** αGFP and EBFP expressing mammalian cells (Cos 7)(100X). GFP fluorescence was visualised under FITC filter and BFP fluorescence was visualised under uv light.

3.5.4 Stable expression in mammalian cells

The next question addressed was that of long term toxicity (or the possibility of negative effects on cell physiology) and fluorescent stability in mammalian cells. Although several stable GFP cell lines have been reported (Chishima et al. 1997; Giorgi et al. 1996) there is still no clear evidence that GFP is not toxic to mammalian cells. In particular, the mutations giving rise to hGFP variants might cause cytotoxicity in mammalian cells. Also, the mutations might alter the three-dimensional structure of the GFP molecule and expose the tightly folded structure of the GFP chromophore (β-can) (Yang et al. 1996) resulting in an unstable GFP molecule and a reduced half-life.

To address these possibilities, the GFP mutant constructs described in **Fig.3.13** were transfected into two different mammalian cell lines, Cos7, and NIH3T3. Generally, Cos7 cells stably transfected with hGFPs displayed many green fluorescent clones after a two-week G418 selection but fewer clones expressed a detectable level of green fluorescence in NIH3T3 cells transfected under similar conditions. There was no detectable fluorescence with wild-type GFP transfected into NIH3T3 or Cos7 cells. Ten independent clonal cell lines were isolated and named hG4Cos-5, hG43T3-19, hG3Cos-14, hG2Cos-23, hG1Cos-9, G4Cos-28, G3Cos-11, G2Cos-5, TCos-34, CCos-9. These cell lines expressed stable, but varying levels of green fluorescence **(Table 3.5)**.

Table 3.5 The stable GFP expressing cell lines				
Cell lines[a]	GFP construct	Cell type	Fluorescent activity	stability
hG4Cos-5	hGFP-M4	Cos 7	very strong	Yes
hG43T3-19	hGFP-M3	NIH3T3	Strong	Yes[b]
hG3Cos-14	hGFP-M3	Cos 7	very strong	Yes
hG2Cos-23	hGFP-M2	Cos 7	very strong	Yes
hG1Cos-9	hGFP-M1	Cos 7	Strong	Yes
G4Cos-28	GFP-C4	Cos 7	Strong	Yes
G3Cos-11	GFP-C3	Cos 7	Strong	Yes
G2Cos-5	GFP-C2	Cos 7	Strong	Yes
TCos-34	TFP	Cos 7	detectable	Yes
CCos-9	CFP	Cos 7	detectable	Yes

a. 1 mg of each GFP constructs (Fig.3.13) were transfected into 50,000 cells. The clonal cells were isolated from the G418 resistant clones which were selected by G418 at the concentration of 500mg/ml for 2 weeks. **b.** The cell growth rate was lower than the untransfected NIH3T3 cells.

There were no obviously toxic effects in these cell lines stably transfected with the hGFPs except for a lower growth rate seen for hG43T3-19 cells. This was a NIH3T3 cell line which expressed the hGFP-M4 construct. After several months in culture, three clonal cell lines, hG4Cos-5, hG3Cos-14 and hG2Cos23, still had very strong and stable fluorescent activity as compared to transiently transfected cells (**Fig.3.17**). However, two Cos7 clonal cell lines named TCos-34 and CCos-9 expressing TFP and CFP respectively, only showed a low level of expression of green fluorescence and gradually lost their activity. These results suggest that hGFP and to a lesser extent GFP over extended period in cell lines continue to stably express at detectable levels and those with the highest fluorescent activity are not toxic to mammalian cells.

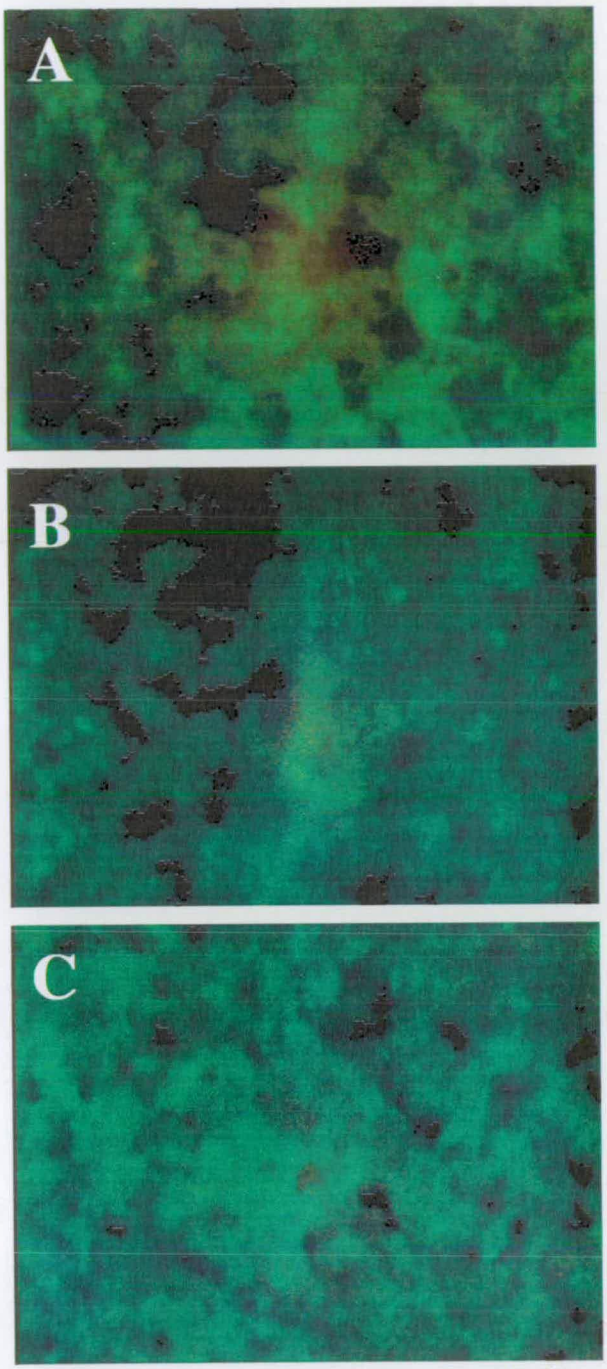

Fig.3.17 Three clonal Cos7 cell lines showing strong and stable GFP fluorescence was illuminated at 490 nm after culturing for 2-3 months. **A)** hG2Cos-23, a Cos7 cell line expressing hGFP-C2 (40X); **B)** hG3Cos-14, a Cos7 cell line expressing hGFP-C3 (40X); **C)** hG4Cos-5, a Cos7 cell line expressing hGFP-C4 (40X).

3.5.5 The green fluorescence in two-cell stage of embryos

To test the fluorescent activity and toxicity of hGFP-M4 in mouse embryos, the hGFP-M4 (called αGFP in Chapter 6) and GFP-C2 mutants were sucloned into pCAG vector (Niwa et al. 1991) to produce pCAGhG4 (pCAGαGFP) and pCAGG2 (**Fig.3.18**). In these constructs the GFP mutants were under control of the chicken β–actin promoter. 50 ng/ml of supercoiled plasmid DNA of pCAGhG4 and pCAGG2 were microinjected into fertilised mouse oocytes and cultured at 37°C overnight (24-27 hours). After overnight incubation these cultured oocytes grew to two-cell stage embryos which were then examined for green fluorescence. Green fluorescence was seen throughout a significant proportion of the embryos injected. hGFP-M4 (αGFP) showed a stronger fluorescent activity than GFP-C2 (**Fig.3.19**). In addition, there were more injected eggs expressing hGFP-M4 (40%) than GFP-C2 (16%) (**Table 3.6**). This implies that hGFP-M4 is the better variant for production of transgenic mice and is active and nontoxic to mouse early embryos.

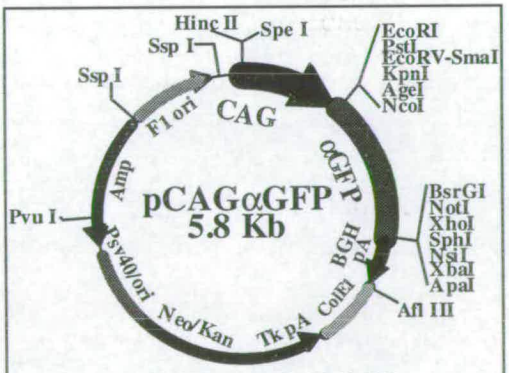

Fig.3.18 The map of pCAGαGFP

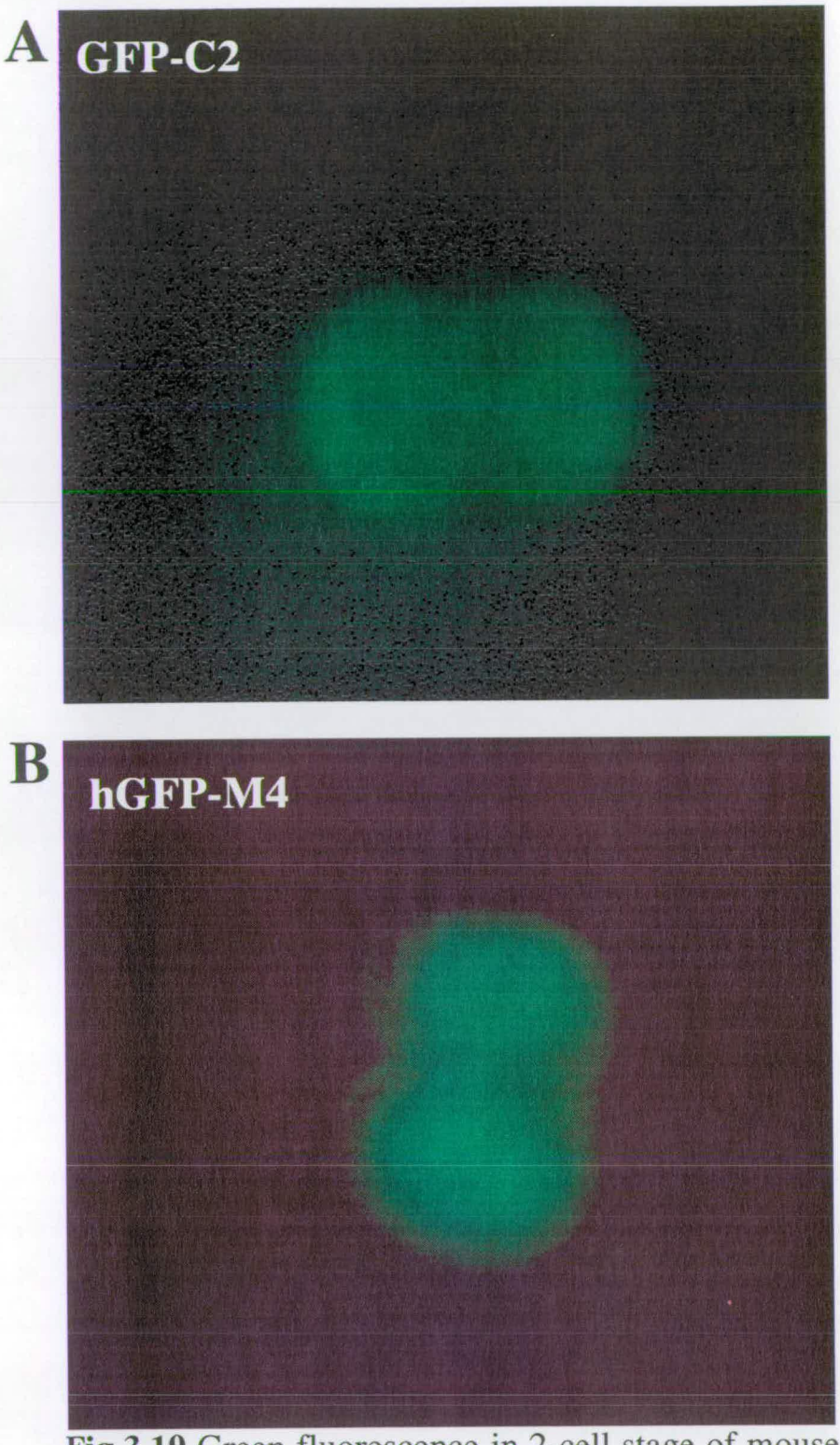

Fig.3.19 Green fluorescence in 2-cell stage of mouse embryos. 10ng/ml of pCAGG2 (in **A**) and pCAGhG4 (in **B**) were microinjected into fertilized eggs and incubated at chamber slide for overnight. The expression constructs were described in **Fig.3.18**. Green fluorescence was detected at 490 nm under a magnification of 40X.

Table 3.6 The transient expression of hGFP-M4 and GFP-C2 in two cell stage of mouse embryos			
Constructs	**No of injected eggs**	**No of surviving eggs (2 cell embryos)**	**No of green fluorescent embryos**
pCAGhG4	35	27(77%)[a]	11(40%)[b]
pCAGG2	40	30(75%)	5(16%)

a. The percentage indicates the survival rate. **b.** The percentage indicates the expression rate of green fluorescence.

3.6 Discussion

3.6.1 F64L mutation has a critical role for increasing GFP activity

In this study, after bacterial transformation, GFP-C4, GFP-C3 and GFP-C2 showed a green colour in bacterial colonies which was detected under visible light, whereas GFP-C1 and wild-type GFP only produced a very faint green color. This is consistent with the suggestion that the mutations contribute to a change of GFP structure making the proteins (GFP-C2-4) less hydrophobic (Crameri et al. 1996), more soluble thus reducing the formation of inactive protein (Cormack et al. 1996) or insoluble inclusion bodies (Crameri et al. 1996) in bacterial cells. The S65T and S65C mutations, however, appeared to have little or no effect on the solubility of the proteins.

The F100S/M154T/V163A mutations in GFP-C3 and the F64L mutation in GFP-C2 or GFP-C4 did result in more soluble protein than TFP, CFP and wild-type GFP. In fact, the comparision of fluorescent activity in both bacterial colonies (in vivo) and bacterial lysates (in vitro) and the quantitative analysis of the relative fluorescent intensity implied that the fluorescent activity was GFP-C2>wild-type

GFP=GFP-C4>GFP-C3>TFP=CFP illuminated on the UV transillumator. According to previous reports, wild-type GFP had better fluorescent intensity in UV light (380 nm) (Chalfie et al. 1994). GFP-S65T (Heim et al. 1995) had a preferred excitation at blue light (490 nm). However, wild-type GFP and GFP-S65T had a similar fluorescent activity when excited with their preferred excitation wavelength. There was no evidence of the F100S/M154T/V163A mutations affecting spectral features in GFP while the F64L mutation in GFP could retain from 20 to 80 % fluorescent intensity compared to wild-type GFP excited at UV light (Cormack et al. 1996). Thus, using the wide range of UV light may not be an optimal wavelength to compare their fluorescent activity or intensity. However, GFP-C3 > TFP=CFP was due to more active protein. GFP-C2> wild-type GFP was for the similar reason even GFP-C2 had only 80% of fluorescent intensity of wild-type protein. GFP-C4 did not show the strongest fluorescence. Perhaps, the mutations (F64L / S65T / F100S / M154T / V163A) together may alter the protein structure (Gura 1996; Ormo et al. 1996; Yang et al. 1996; Youvan et al. 1996) to such an extent as to have a negative effect on overall GFP activity. Thus, the fluorescent activity was: GFP-C2>GFP-C4 & GFP-C3>TFP=CFP> wild-type GFP excited at blue light. However, there was no comparable analysis of the fluorescent activity between GFP-C4 and GFP-C3 in this study.

Thus, the F64L mutation in GFP-C2 is a simple replacement but increase the capacity in GFP variants. In fact, the other F64L containing mutants (GFP-UV, and hGFPs) displayed the enhancement of GFP fluorescent activity without interference with other spectral features.

3.6.2 The requirement for the optimal levels of GFP expression in mammalian cells

Production of wild-type GFP is temperature-sensitive, causing problems when expressing the protein in various cells that require incubation at 37°C, resulting in reduced fluorescence (Kaether et al. 1995; Lim et al. 1995; Ogawa et al. 1995; Pines 1995; Webb et al. 1995). Previous reports agree with this aspect of GFP fluorescent intensity (Cormack et al. 1996; Kimata et al. 1997; Siemering et al. 1996). In addition, GFP production could be hindered by the translational efficiency of the protein. By optimising codon usage (Yang et al. 1996) or creating a humanised GFP (Zolotukhin et al. 1996), higher levels of expression of GFP protein leading to enhance sensitivity of green fluorescence could be obtained in mammalian cells.

Taking these into consideration, to get high GFP fluorescence in mammalian cells, a large amount of active proteins needs to be produced in cells. Thus, the modifications of the wild-type protein which optimised fluorescence included those which enhanced stability and solubility, increased fluorescent intensity, increased translation efficiency, and remained nontoxic. In addition, a change of excitation wavelength was also considered. In fact, four mutations, F64L, S65T, S147P and S176G, in combination with the humanised GFP gene seem to be the most important mutations involved in the enhancement of GFP fluorescent activity.

hGFP mutants, hGFP-M4 (hGFP-F64L/S65T/S147P/S176G), hGFP-M3 (hGFP-S65T/S147P/S176G), hGFP-M2 (hGFP-F64L/S65T/S147P) and hGFP-M1 (hGFP-F64L/S65T), were generated based on the considerations discussed above. Western blot analysis of the translation efficiency of these protein in transiently transfected Cos7 cells showed that most of the hGFP variants had high levels of protein using the same transfection conditions compared to wild-type GFP variants. This suggests that the mutations introduced into hGFP and GFP variants did not interfere with protein production. Thus, the high expression level obtained from hGFP variants was due to codon usage and the dominant mutations. The hGFP variants are therefore suitable for maximal expression of GFP fluorescence.

3.6.3 The stability of hGFP variants in mammalian cells

To test the life-span and the toxicity of hGFP variants in mammalian cells, pCIhGIZ4 was transfected into Cos7 and NIH3T3 cells and G418 resistant clones were selected. Ten clonal cell lines were established. The pCIhGIZ4 transfected cell lines showed stable green fluorescence for several weeks while three of the transfected lines contained strong green cells after three months of culture. In fact, all hGFP's cell lines continued to express hGFP. However, TFP and CFP containing cell lines which did not show fluorescence.

The GFP variants generated in this study show four classes of fluorescent activity in mammalian cells. These mutant proteins gave very different levels of fluorescence in mammalian cells, compared to the native protein. Generally, the mammalian codon usage increased the

amount of protein in mammalian cells and resulted in increasing fluorescent activity 10-fold compared to wild-type protein. Furthermore, hGFP-M4 and GFP-C2 also showed a strong and stable fluorescence in two-cell mouse embryos. This suggests that high levels of GFP proteins (hGFP-M4) are not toxic to early developing mouse embryos (This will be discussed in more detail in Chapter 6). Thus, hGFP-M4 shows optimal features (strong and stable fluorescence) in a mammalian cell environment and this makes it an excellent marker for applications in both mammalian cells and transgenic mice.

Chapter 4 Visualisation of subnuclear localisation of WT1 isoforms by using GFP as a vital fluorescent tag

4.1 Introduction

Immunohistochemistry is a useful technique to detect gene expression in cells but does not enable monitoring of biological processes in living cells or animals. For example, the localisation of splicing factors in the nucleus show highly dynamic events. Many nuclear factors may associate or dissociate with splicing factors at different times and different processes (Huang et al. 1997; Misteli et al. 1997; Zeng et al. 1997). Using antibody techniques chemical fixation may disturb the subcellular structures making analysis of complex cellular processes difficult. Therefore techniques which more closely represent the situations in living cells are required. Recently, proteins fused with fluorescent GFP moieties have been used to analyse protein locations or examine dynamic events in living cells.

Recently, Larsson et al. (1995) demonstrated that the different WT1 isoforms localise to distinct nuclear compartments. The WT1-KTS isoform (lacking the three amino acids KTS) mainly displayed a diffuse pattern and was associated with some transcription factors such as Sp1 and TFIIB. The WT1+KTS isoform preferentially associated with splicing factors forming speckled structures. However, the nuclear patterns could be interrupted by some chemical or physical treatments. For example, the affinity of WT1 and nuclear proteins could be interrupted by actinomycin D or heat shock resulting in a relocalisation (Charlieu et al. 1995). On the other hand, a deletion of the

zinc finger domain could damage the protein function and result in altering the subnuclear localisation (Englert et al. 1995).

All these results were obtained using immunofluorescent techniques. Direct labelling or vital labelling of the WT1 proteins in unfixed or living cells may provide a more detailed analysis of the nuclear localisation process. In Chapter 3, hGFP variants were designed which were efficient fluorescent markers in mammalian cellular environment. These GFP variants were used to make GFP- WT1 fusion proteins (GW isoforms) to look at the subnuclear localisation or nuclear behaviour of WT1 in living cells.

4.2 Construction of GW expression vectors

In order to make the GFP fusion with WT1 protein isoforms (GW isoforms), a 1.3 kb Sma I/Xba I restriction fragment for four cDNAs encoding WT1 isoforms (WT1+/+, WT1-/+, WT1+/- and WT1-/-) were obtained from the pRC/CMVWT1 expression constructs (Larsson et al. 1995). The four WT1 protein isoforms result from two different splicing variations. These produce proteins with or without exon 5 and with or without three amino acids KTS resulting in the four isoforms. Specifically, the WT1+/+ contains the both exon 5 and the KTS, the WT1-/- has neither. WT1-/+ contains the KTS and the WT1+/- has exon 5 (**Fig.4.1**). These cDNA fragments of WT1 were subcloned into the Nru I / Xba I sites of pCIhGFP-M1 vector to crease a fusion protein. The resultants were named pCGW+/+, pCGW+/-, pCGW-/- and pCGW-/+. All the constructs contained a synthetic intron at the 5' end and were oriented such that the C-terminus of hGFP-M1

was fused to the N-terminus of WT1 **(Fig.4.2)**. The fusion regions of GW isoforms were checked by DNA sequencing and restriction enzyme digestion.

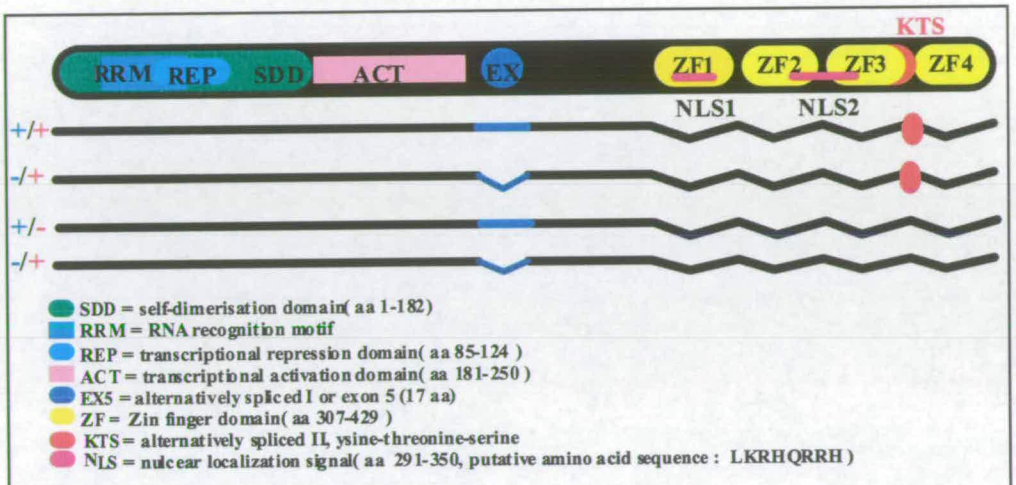

Fig.4.1 Scheme of WT1 functional motifs and their spliced isoforms. WT1 functional motifs were referred from Wang et al., 1993; Bruening et al., 1996; Kennedy et al.,1996.

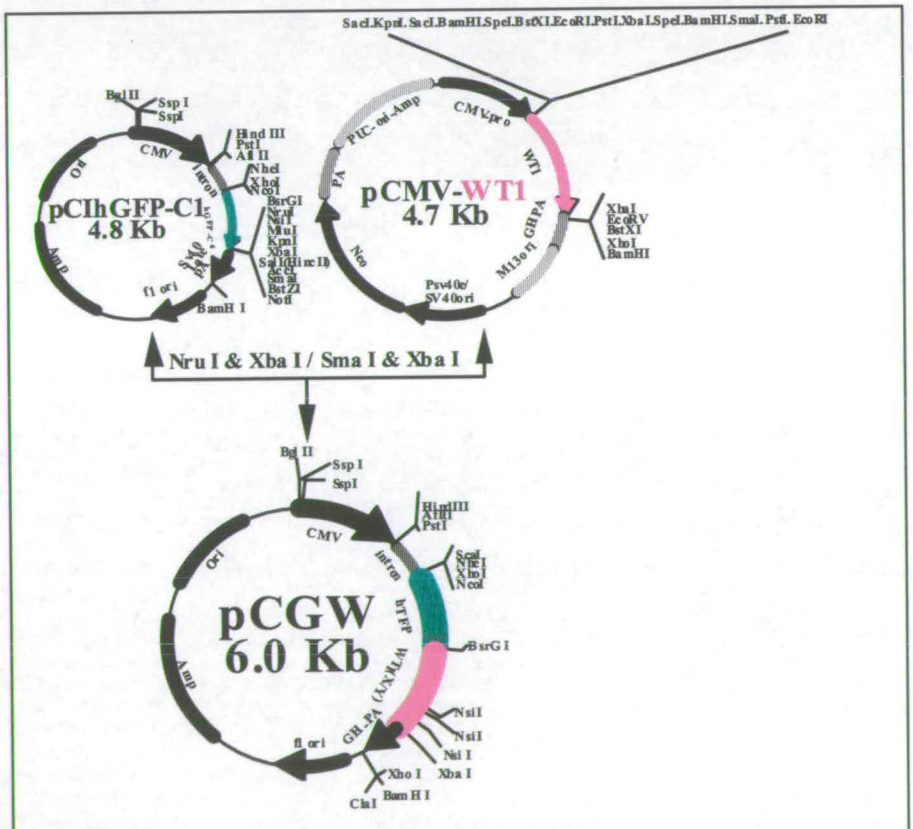

Fig.4.2 The cloning scheme of pCGW expression vectors.

4.3 Green fluorescent GW chimeras expressed in Cos7 cells

The four WT1 isoforms displayed three classes of subnuclear patterns in Cos7 cells using immuohistochemistry analysis (Larsson et al. 1995). The WT1+/+ and -/+ forms showed speckled patterns (the strongly stained irregular foci set against a diffuse nuclear background), +/- form showed domains (distinct areas of stain with little or no background) and -/- form showed diffuse stain (a general stain in the nuclei). The GW isoform were predicted to retain similar biological properties as the wild-type proteins. In two independent transient transfections, each GW isoform expression construct was transiently transfected into Cos7 cells and incubated for 24 to 36 hours. For each construct, 50 cells expressing green fluorescence in the nucleus were counted and three classes of nuclear patterns were seen under the fluorescence microscopy (**Table 4.1**). Both GW+KTS (GW+/+ and GW-/+) containing constructs in Cos7 cells showed predominantly green fluorescent speckles (**Fig.4.3 A1-A5, B1-B4**) but some cells in addition contained a faint green fluorescent background (**Fig.4.3 A6, B5 &B6**). The GW-/- transfected cells showed only a small proportion with a speckled pattern as most were either in domains (**Fig.4.3 C1, C2 & C3**) and or diffuse (**Fig.4.3 C4, C5 & C6**). The patterns of most GW+/- was diffuse (**Fig.4.3 D4, D5, & D6**) but a significant proportion showed domains or big clots (**Fig.4.3, D1, D2 & D3**). In fact, 43% of the GW+/+ and 36% of the GW-/+ expressing cells showed speckles. GW -/- expressing cells showed 33% domains and 42% diffuse. GW +/- expressing cells showed 46% domains and 18% diffuse. The proportion of GW+KTS is similar to WT1+KTS and the proportion of GW-KTS are higher than WT-KTS (Larsson et al. 1995). However, in all cases

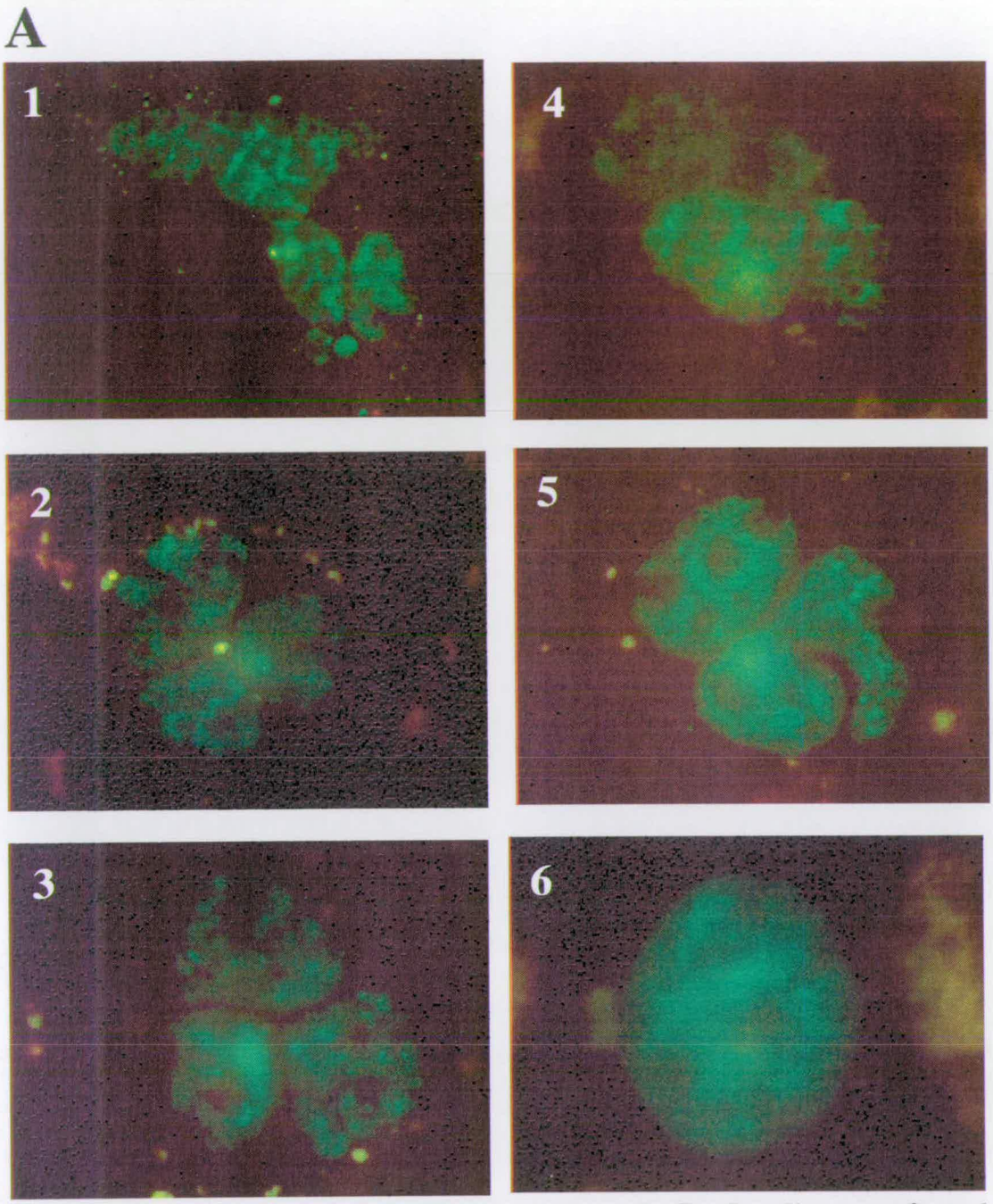

Fig.4.3 Green fluorescent nuclear patterns of Cos7 cells transfected with GW isoforms. 100 ng of each construct was transfected into 5x 10^4 cells and incubated for 36 hours at 37 °C. The transfected cells were then fixed in 4% paraformaldehyde (PFA) and visualised at 490 nm. **A**) GW+/+. **B**) GW-/+. **C**) GW-/-. **D**) GW+/-.

B

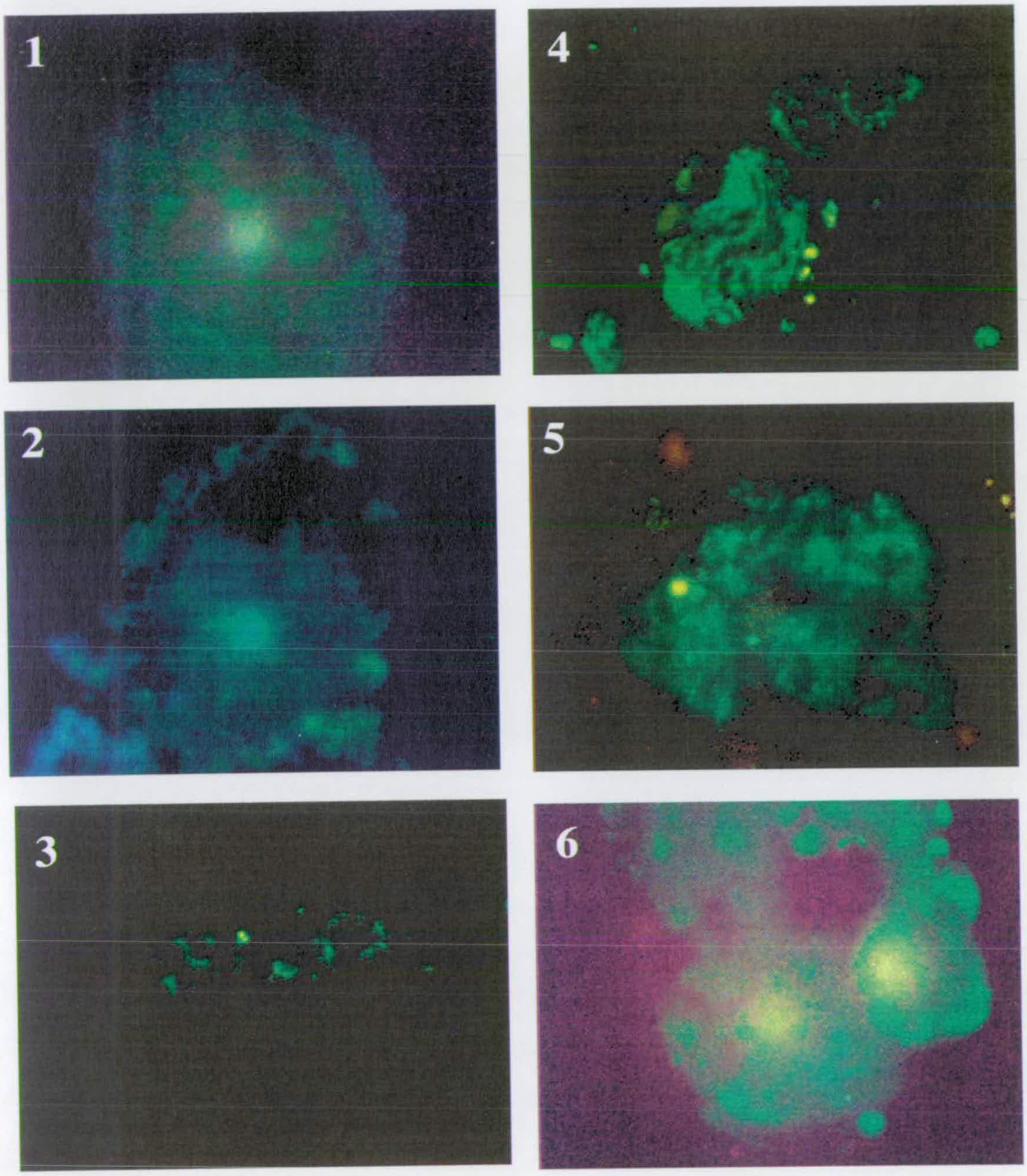

C

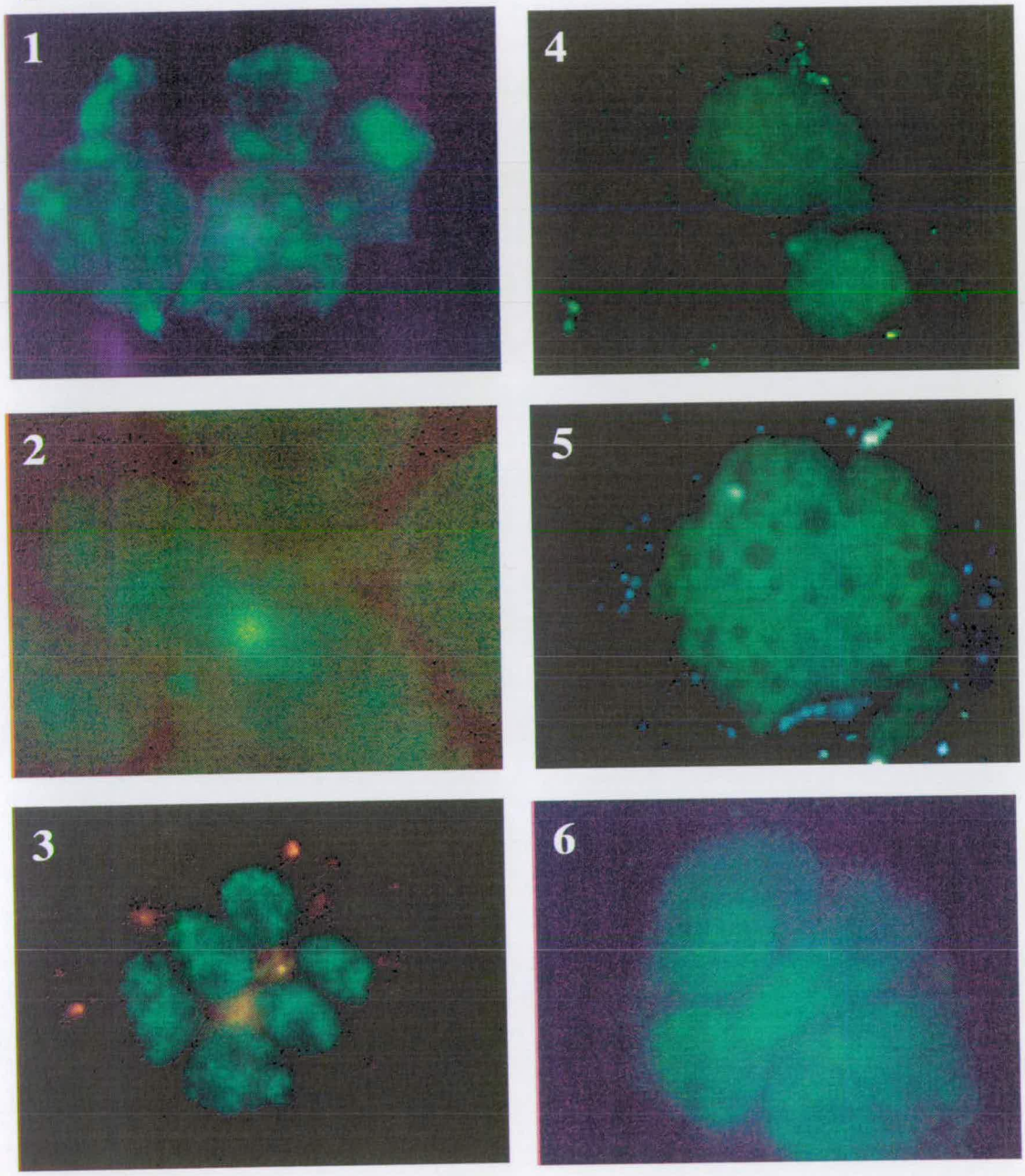

D

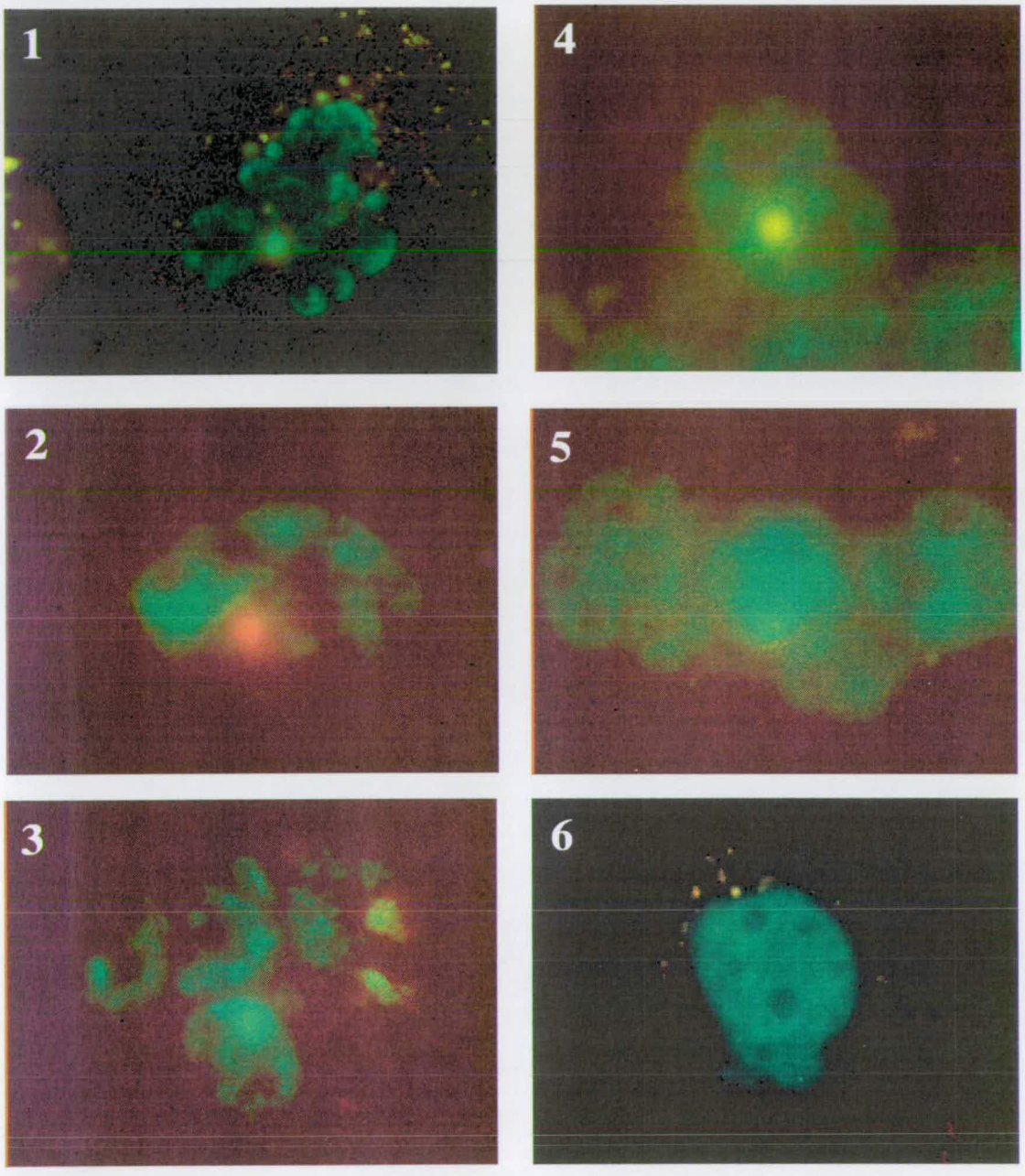

there was a proportion of an unpredicted pattern that showed nuclear and cytoplasm localisation (43% for GW+/+, 49% for GW-/+, 21% for GW-/- and 31% for GW+/-). These results are summarised in **Table 4.1.** Thus, the GW isoforms showed a similar nuclear localisation but GW proteins may be less efficient than the wild-type WT1 at a nuclear translocation.

Table 4.1 Green fluorescent nuclear patterns of GW isoforms transfected Cos7 cells

GW isoforms	Nuclear pattern[a]				
	Speckles	Domains	Diffuse	Other[b]	Total
GW+/+	20, 23	2, 3	5, 4	23, 20	100
GW-/+	17, 19	1, 4	7, 3	25, 24	100
GW-/-	1, 3	16, 17	19, 23	14, 7	100
GW+/-	3, 2	10, 8	25, 21	12, 19	100

a. The number of cells with nuclear patterns were counted by 2 independent transfections. **b.** Those were leaked patterns (green fluorescence was seen in nucleus and cytoplasm)

However, PFA treatment may alter the cellular morphology of the cells and hence the localisation of proteins. Thus, to compare green fluorescence in unfixed or living cells, transiently transfected cells without any treatment were directly examined for their fluorescent signals. Similarly, GW+/+ and GW-/+ expressing cells showed speckled patterns while GW-/- and GW+/- showed diffuse patterns mixed with some showing a domain pattern (**Fig.4.4A**). The patterns from the unfixed cells were not obviously different to the fixed cell (**Fig.4.3**). The green fluorescent signals provided a high resolution means for detecting nuclear sublocalisation at high magnification (250X). Especially, GW+/+ or GW-/+ showed the "web" like structures in the nucleus (**Fig.4.4 A1**) and these were expected to the speckles viewing at low magnification. A similar nuclear pattern was seen in GW transiently transfected Cos7 cells after following immunostain by

GFP antibody (**Fig.4.4B**). However, the resolution of immunofluorescence was lower than the GFP fluorescence under the same transfection conditions. This may be due to fluorescein (Texas Red) artificially creating strong signals whereas GFP direct labelled proteins show an intensity proportional to the number of protein molecules.

These results suggest that GW fusion proteins may behave like wild-type WT1 and provides a non-invasive means to monitor the subnuclear localisation of WT1 isoforms.

4.4 Molecular characteristic of GW isoforms

The predicted GW isoforms were analysed by western blots. There were four clear protein bands (GW+/+, GW-/+, GW+/- and GW-/-) which were immunoreactive against both the GFP and WT1 antibodies (H7). The protein bands showed molecular weights of approximately 90 kd (**Fig.4.5 A &B**). The protein bands indicating GW+/+ or GW+/- were slightly bigger than GW-/- or GW-/+. In addition, there was no cross reaction between GFP and the WT1 antibodies seen on the GFP and WT1 control. To confirm the previous results, GW transfected cells were followed by immunocytochemistry stained with antibodies against GFP and WT1. Double immunofluorescence (FITC and Texas Red) showed identical nuclear patterns (**Fig.4.6**). These results indicated that GW isoforms are the 90 kD proteins in transiently transfected Cos7 cells and the GFP moiety provided the green fluorescent signal while the WT1 moiety provided the nuclear sublocalisation.

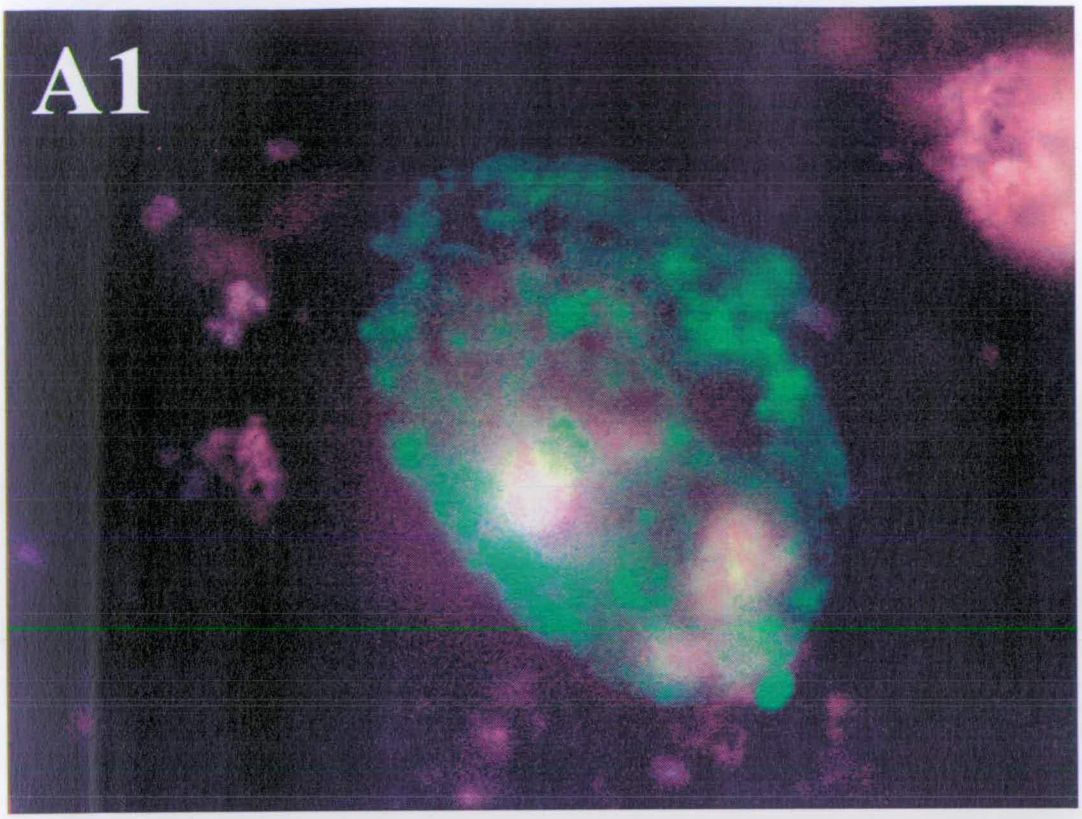

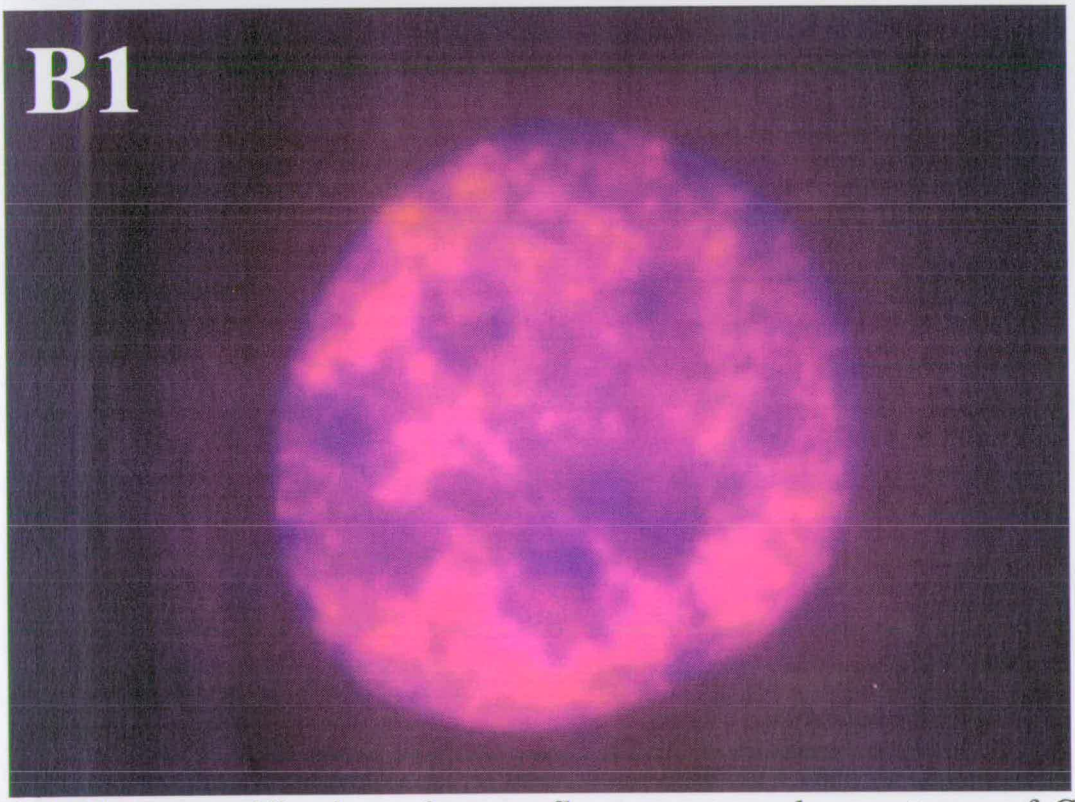

Fig.4.4 High magnification of green fluorescent nuclear patterns of GW isoforms transfected into Cos7 cells. **A)** Living specimens (without any fixation) were prepared from the transiently transfected cells without fixation and was directly visualised at 490 nm (250X). **B)** Immunochemistry staining of the transfectants with GFP antibody (red; Texas red). Blue staining in the nucleus was DAPI staining. The immunofluorescence was detected using Texas Red and DAPI filter (250X). **1**, GW+/+; **2**, GW-/+; **3**, GW-/-; **4**, GW+/-.

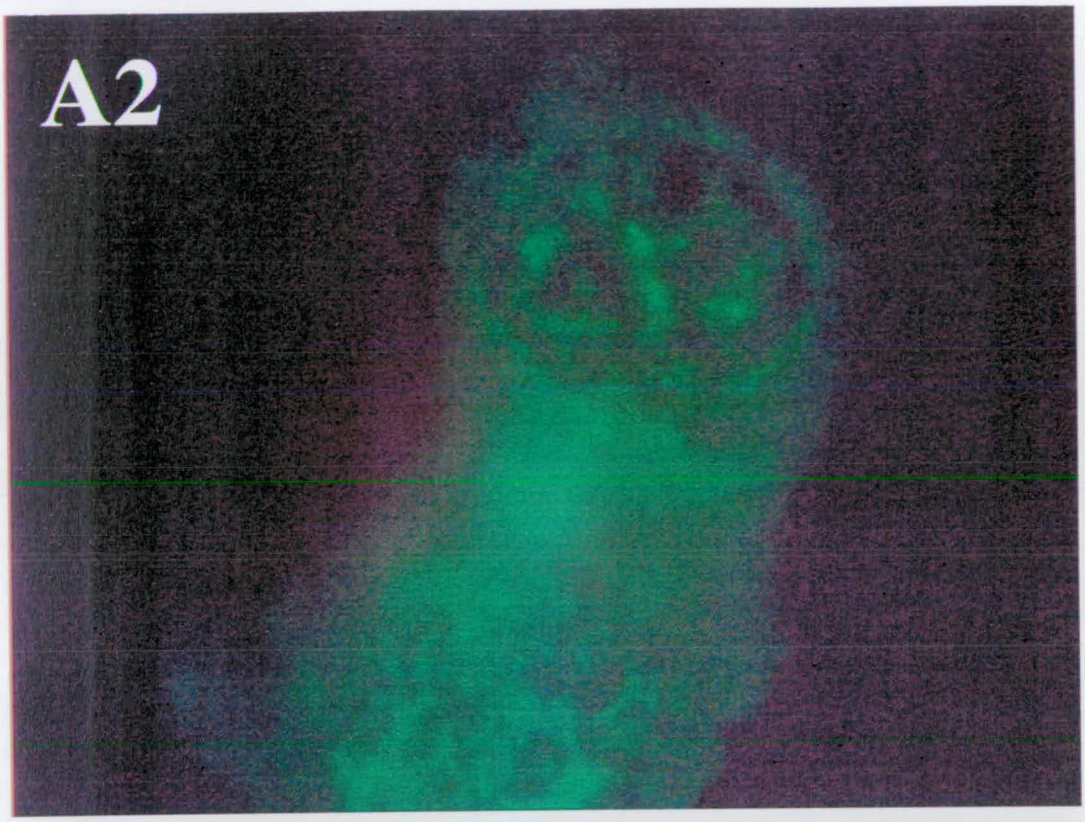
A2

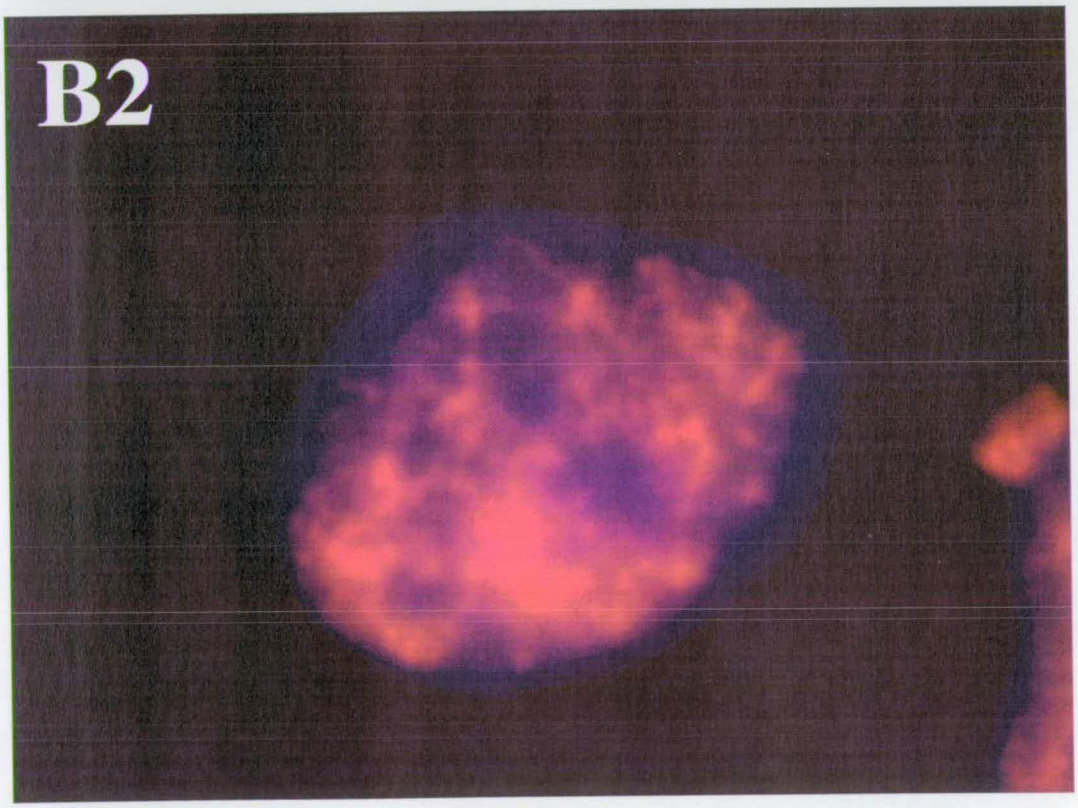
B2

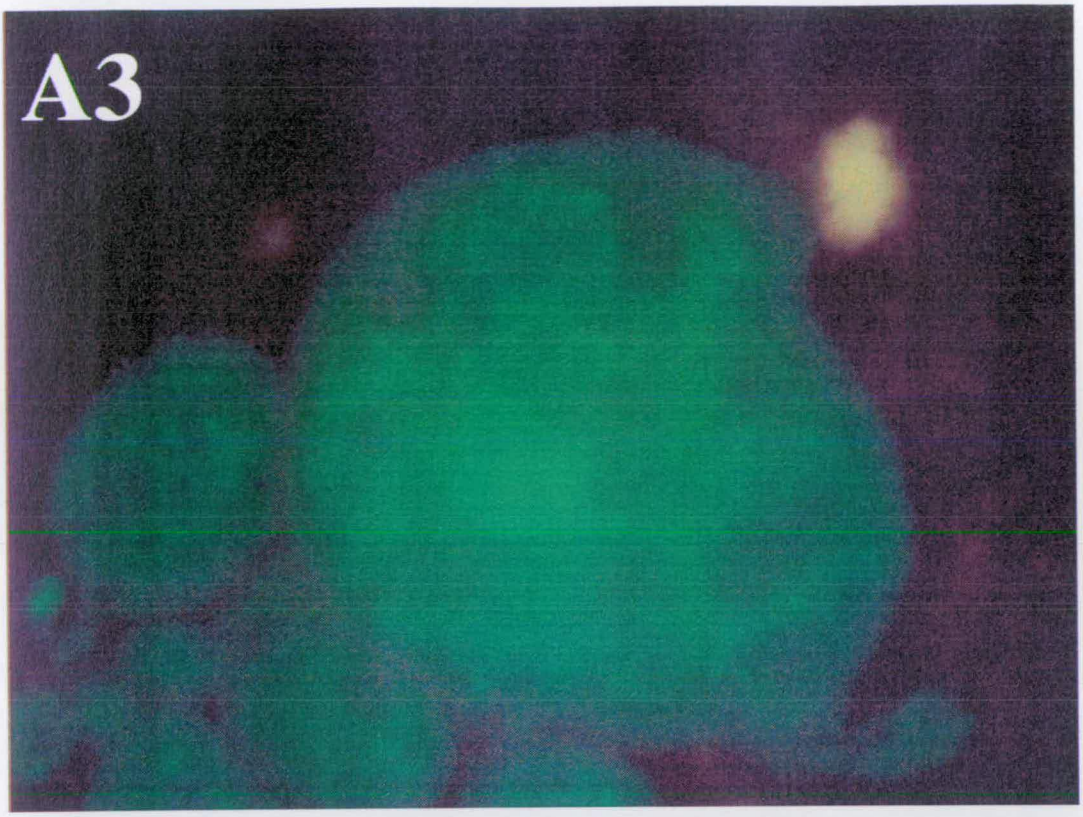
A3

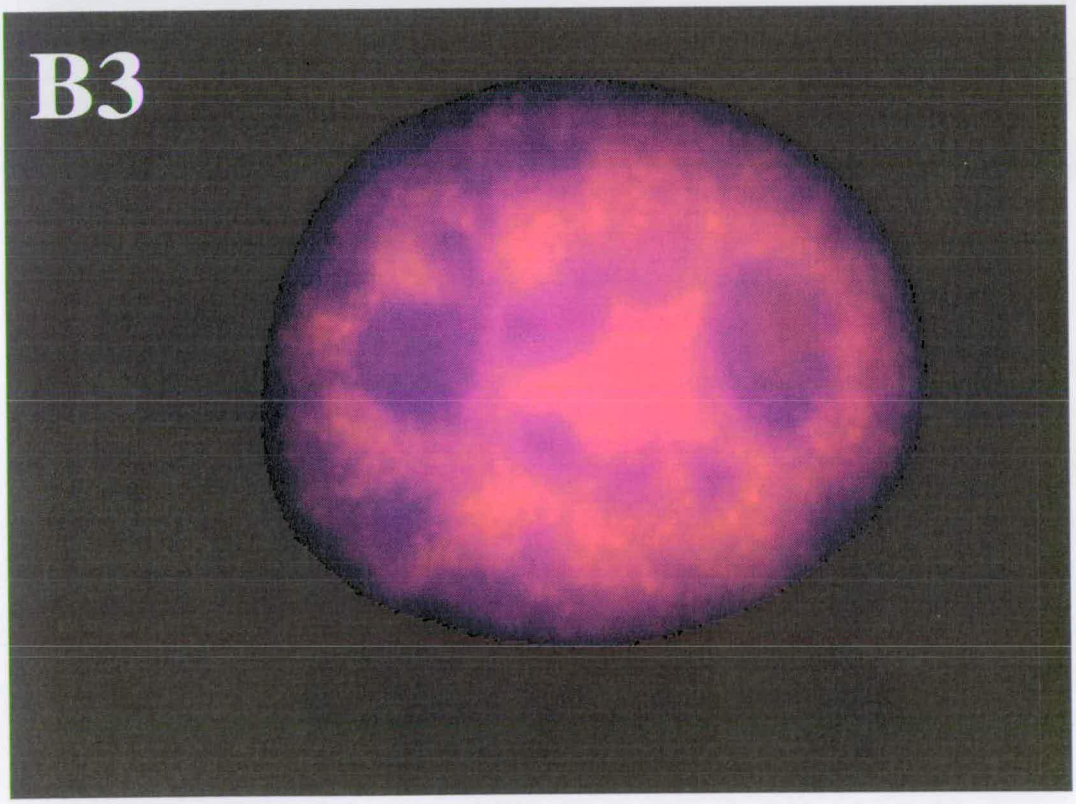
B3

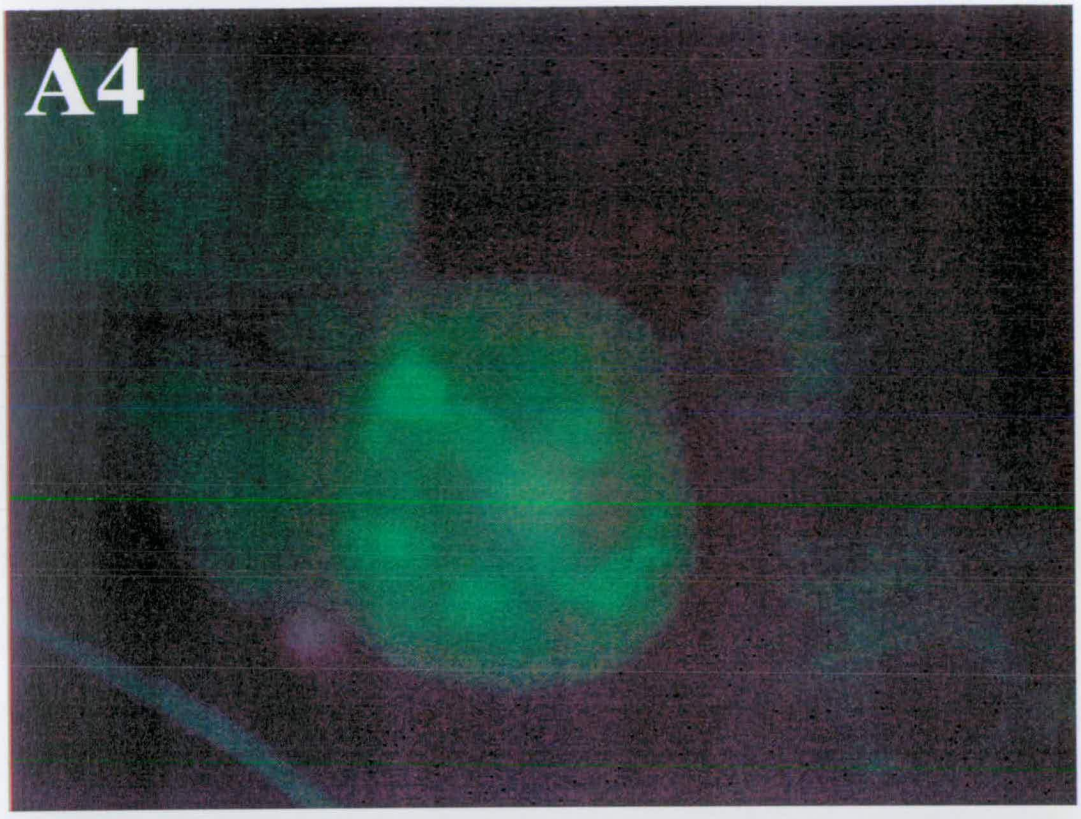
A4

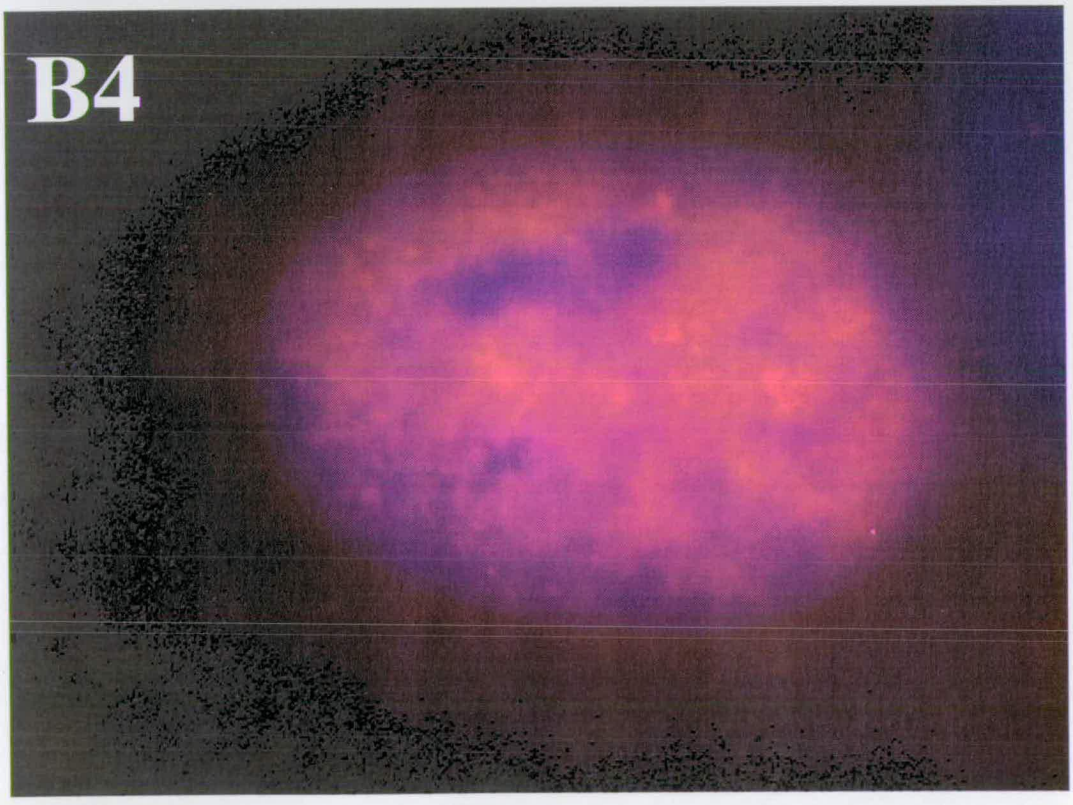
B4

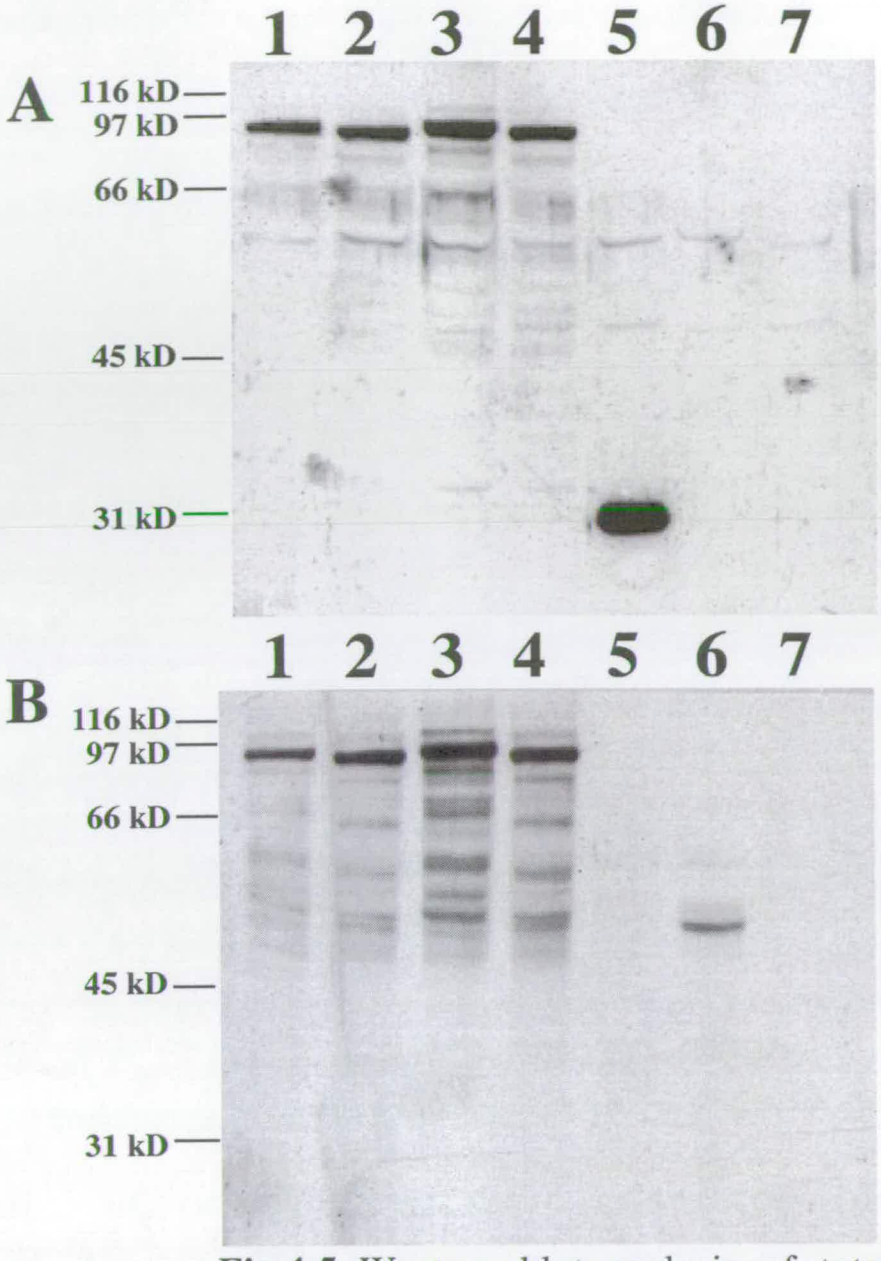

Fig.4.5 Western blot analysis of total protein for pCGW+/+, pCGW-/+, pCGW+/- and pCGW-/- transiently transfected Cos7 cells. **A)** first antibody against GFP. **B)** first antibody against WT1 (C19). 2μg of each construct was transiently transfected into 1 X 10^6 Cos7 cells. Total protein was extracted from 48 hour posttransfection. 20μg/well of total protein from each transfectant was used for the 12% SDS gel and followed by western bolt analysis. 1, GW+/+; 2, GW-/+; 3, GW+/-; 4, GW-/-; 5, GFP; 6, total protein of M15 cells; 7, total protein of Cos7 cells.

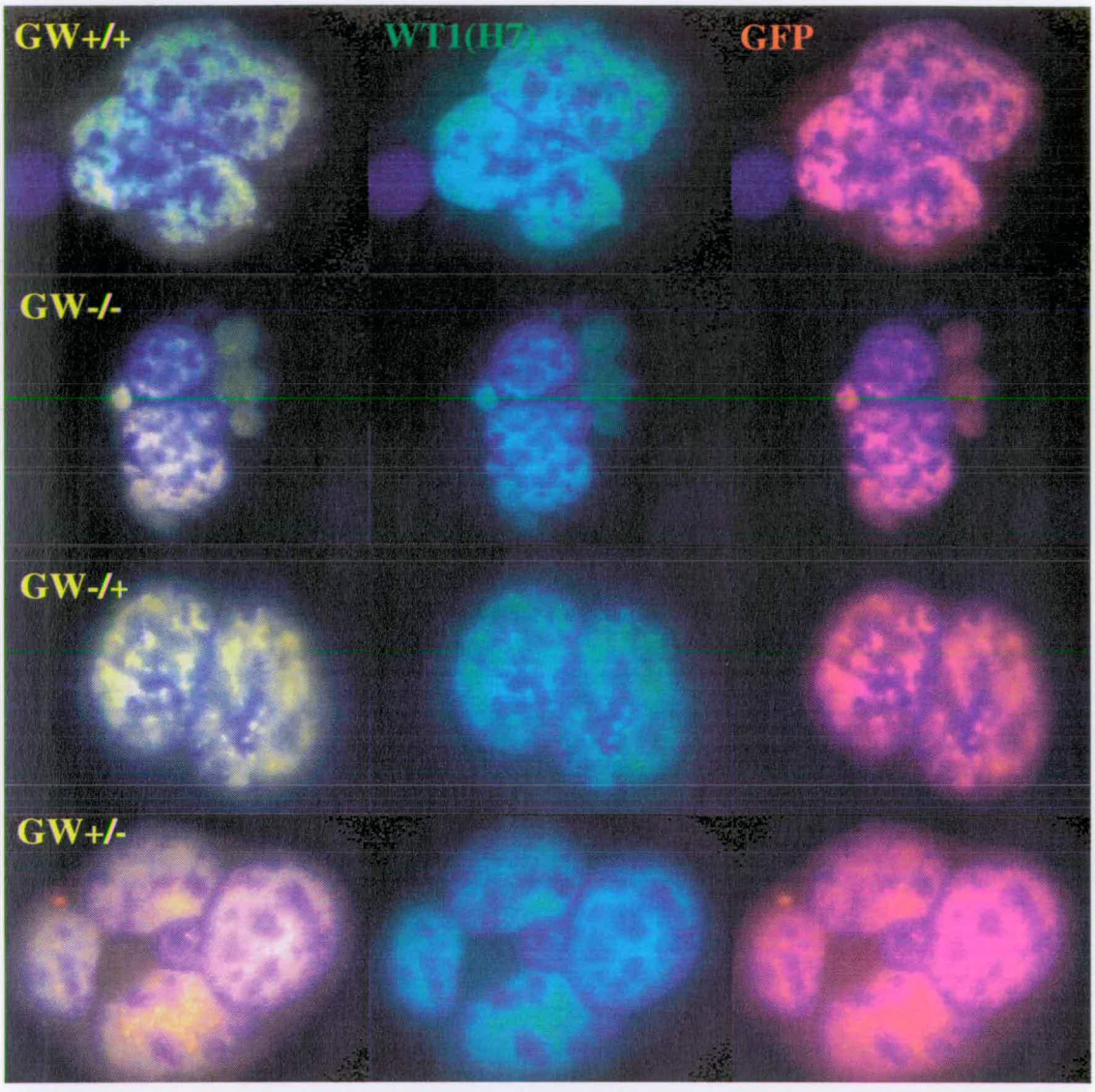

Fig.4.6 Double-labeled GW transfected Cos7 cells using antibodies against GFP and WT1 (H7). Texas red (Red fluorescence) nuclear patterns indicates the GFP motiety. FITC (Green fluorescence) nuclear patterns indicates the WT1 moteiy. Yellow nuclear patterns show co-localisation of the red and green fluorescence.

4.5 The functional analysis of GW isoforms

4.5.1 Comparison of subnuclear localisation of GW isoforms and WT1s

GW isoforms had the expected biological activities; however, the protein structure (WT1 functional motifs) might be altered in the fusion proteins. Thus, the nuclear function of GW proteins might have some different properties compared to the WT1 isoforms. The subnuclear localisation of GW isoforms and WT1 isoforms were then compared by immunocytochemistry staining and compared to GFP fluorescence. Cos7 cells were transiently transfected with WT1 expression vectors which were followed by immunocytochemistry staining using a WT1 monoclonal antibody (H7) and a WT1 polyclonal antibody (C19). In support of previous results (Larsson et al. 1995), the WT1+KTS isoforms (WT1+/+ and WT1-/+) predominantly showed the speckled patterns while the WT1 -KTS isoforms (WT1-/- and WT1+/-) mainly showed a diffuse pattern or domain (**Fig.4.7A**). Although the nuclear fluorescent background could also be seen in the nucleus, the subnuclear patterns were still very similar to the results of Larsson et al. (1995). Immunofluorescence of GW isoforms transfected Cos7 cells showed a very similar nuclear pattern as the unfixed green fluorescent patterns (**Fig.4.7B**). This comparison suggested that the WT1 and GW isoforms kept most of the assailable nuclear functions. However, immunofluorescence gave higher background than GFP fluorescence and had a lower resolution (**Fig.4.8**). In summary, GW isoform nuclear patterns were comparable to WT1 immunofluorescent patterns. In addition, they provided a higher resolution and a direct way to visualise subnuclear localisation.

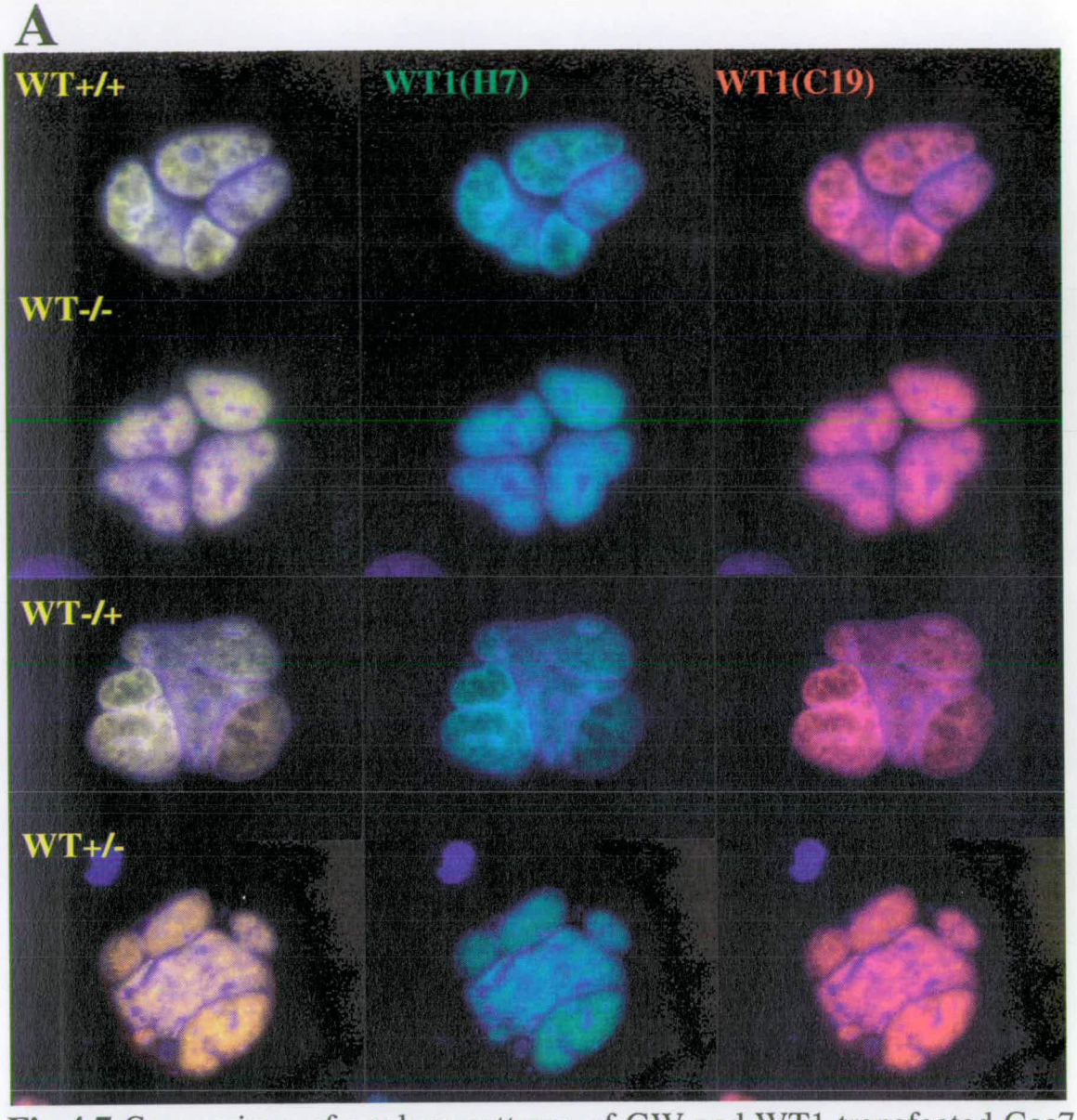

Fig.4.7 Comparison of nuclear patterns of GW and WT1 transfected Cos7 cells. **A**) Immunofluorescence of WT1 transfected Cos7 cells; **B**) Immunofluorescence of GW transfected Cos7 cells. Red: Texas red conjugated with C19 antibody; Green: FITC coniugated with H7 antibody; Yellow ,the combination of immunofluorescence of Texas red and FITC.

B

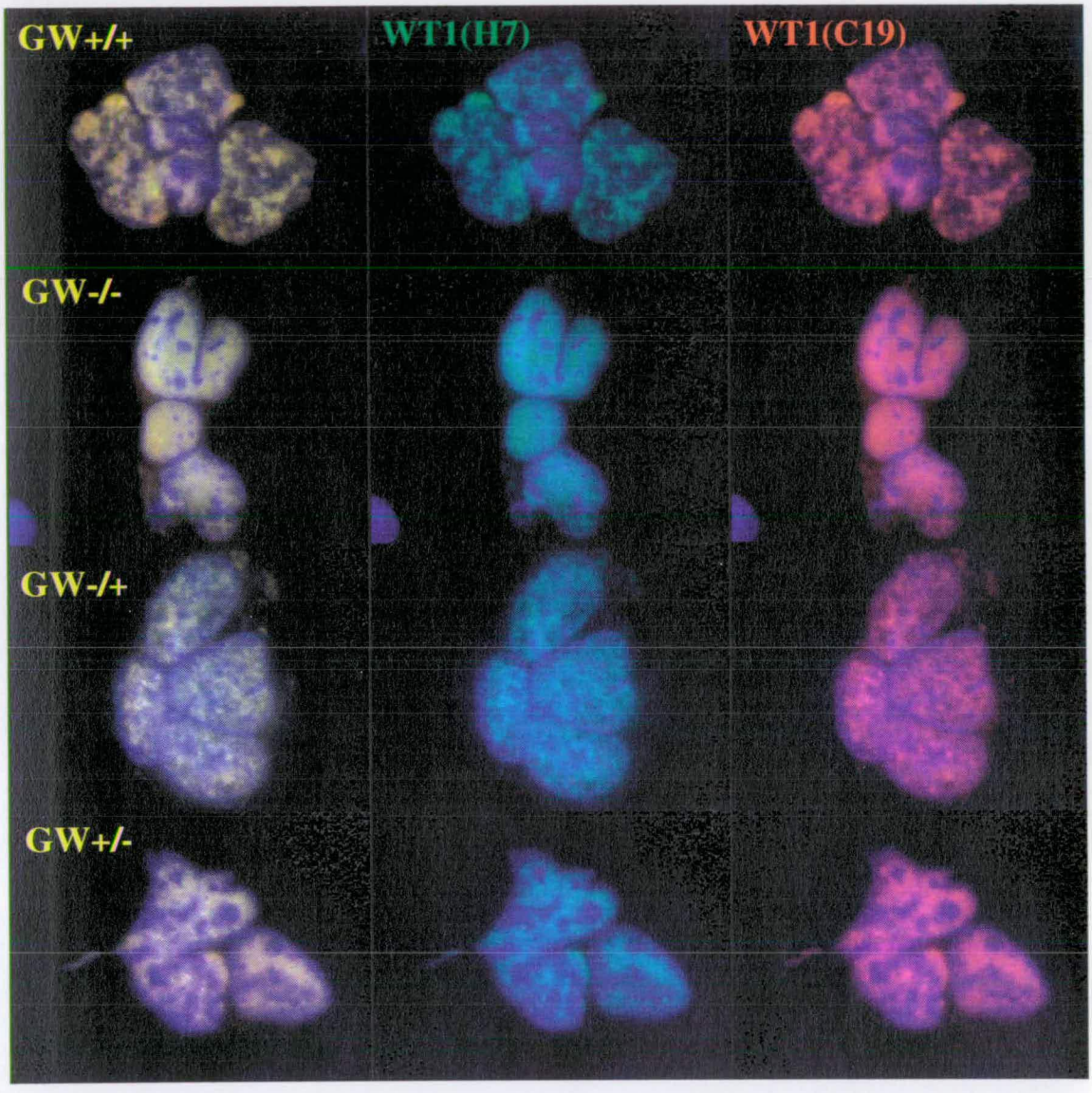

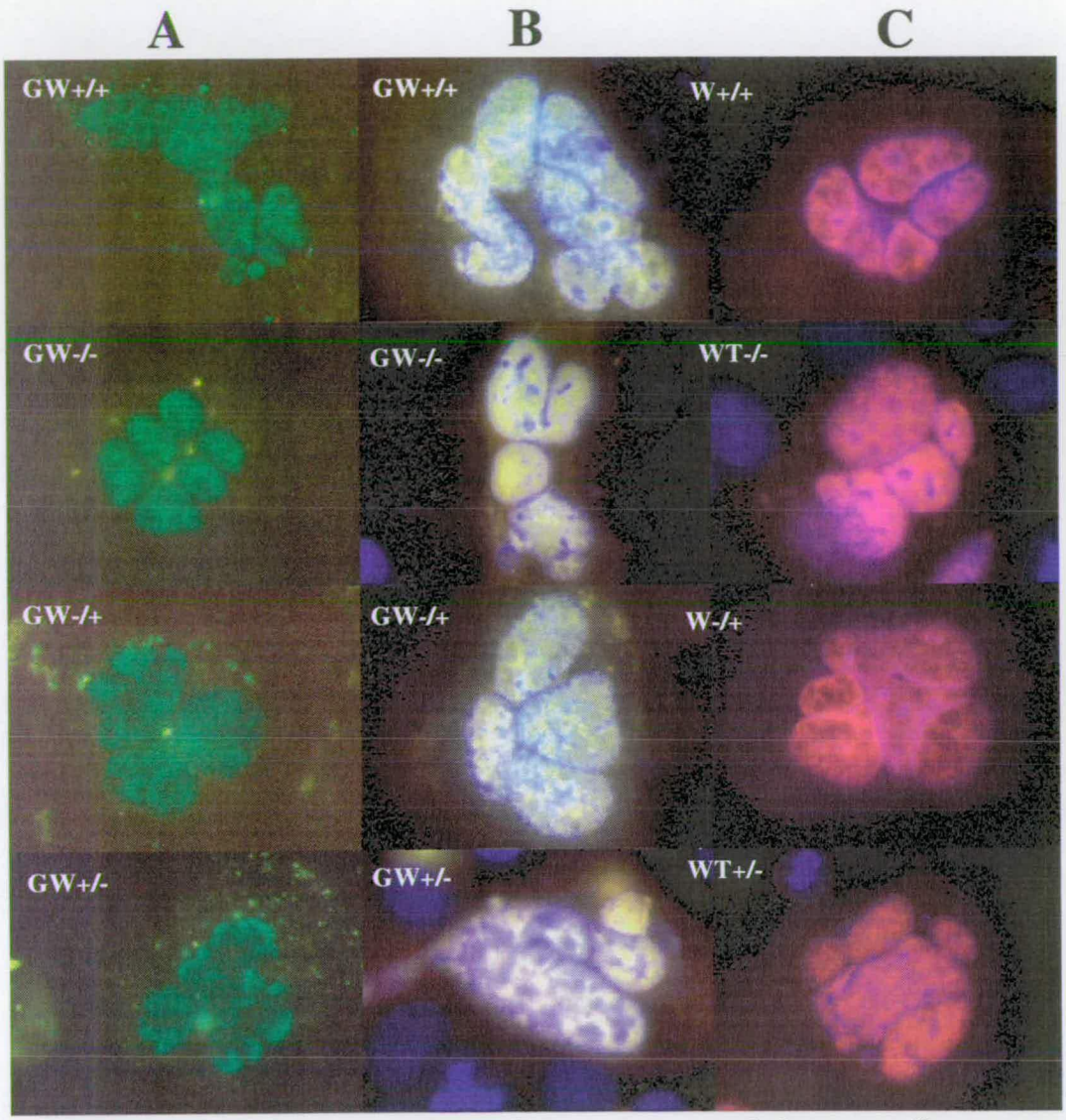

Fig.4.8 Comparison of green fluorescent and immunofluorescent signals between the GW and WT1 transfected Cos7 cells. GW expression vectors were transiently transfected into Cos7 cells. **A)** The unfixed transfectants showed GFP green fluorescent nuclear patterns using FITC filter for each GW isoforms. **B)** The transfectants were followed by immunochemistry staining using GFP antibody (yellow is a synthetic color by computer prograrm). **C)** The transfectants were followed immunochem istry staining using WT1 antibody (C19) (Red / Texsa red).

4.5.2 The unique nuclear patterns in Cos7 cells

The unique nuclear pattern of WT1 has been defined by transiently expressing its four isoforms in Cos7 cells (Larsson et al. 1995). Similar speckled nuclear patterns were also seen in two osteosarcoma cell lines (Saos-2 and U2OS) (Englert et al. 1995). To determine weather other mammalian cell lines had similar properties to the Cos7 cells, GW expression constructs were transiently transfected into two other mammalian cell lines, CHO-K1 (Chinese hamster ovary, epithelial cell) and NIH3T3 (rat, fibroblast cell). In the control of transfected Cos7 cells, again, the +KTS isoforms (GW+/+ and GW-/+) showed the speckled patterns and the -KTS isoforms showed diffusion and domain patterns (**Fig.4.9A**). However, in the transfected CHO-K1 (**Fig.4.9B**) and NIH3T3 cells (**Fig.4.9C**), all the GW isoforms showed a diffuse nuclear pattern. Thus, GW isoforms may only be allowed to enter into the nucleus of CHO-K1 and NIH3T3 cells (this will be more discussed in Chapter5) but the cell are not responsive to sublocalisation signals. Obviously, GW isoforms locate in the nucleus of mammalian cells and sublocalise with unique nuclear patterns in Cos7 cells but not in CHO-K1 and NIH3T3 cells. Thus, Cos7 cells provide a better cellular environment to visualise subnuclear localisation.

4.5.3 GW isoforms may also associate with some nuclear proteins

The nuclear patterns of WT1 in Cos7 cells suggested that WT1 associates with some nuclear proteins (splicing factors or transcription factors) (Charlieu et al. 1995; Larsson et al. 1995). The +KTS isoforms of WT1 colocalize with some splicing factors whereas

A (Cos7)

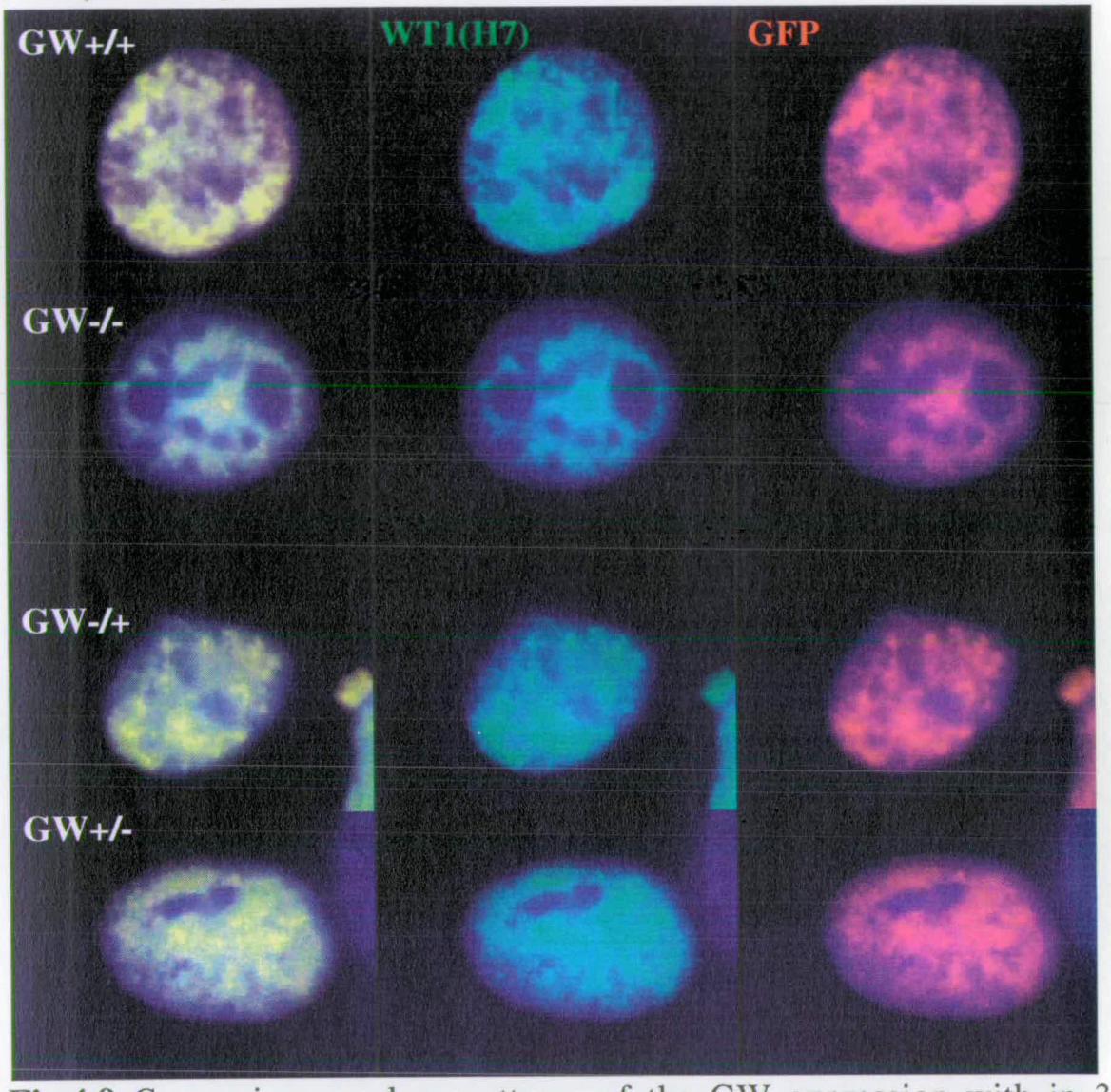

Fig.4.9 Comparison nuclear patterns of the GW expression with in 3 different mammalian cells **A)** Cos7 cells. **B)** CHO-K1 cells. **C)** NIH3T3 cells: Red, Texas red conjugated with GFP antibody; Green, FITC coniugated with H7 antibody; Yellow,the combination of immunofluorescence of Texas red and FITC.

B (CHO-K1)

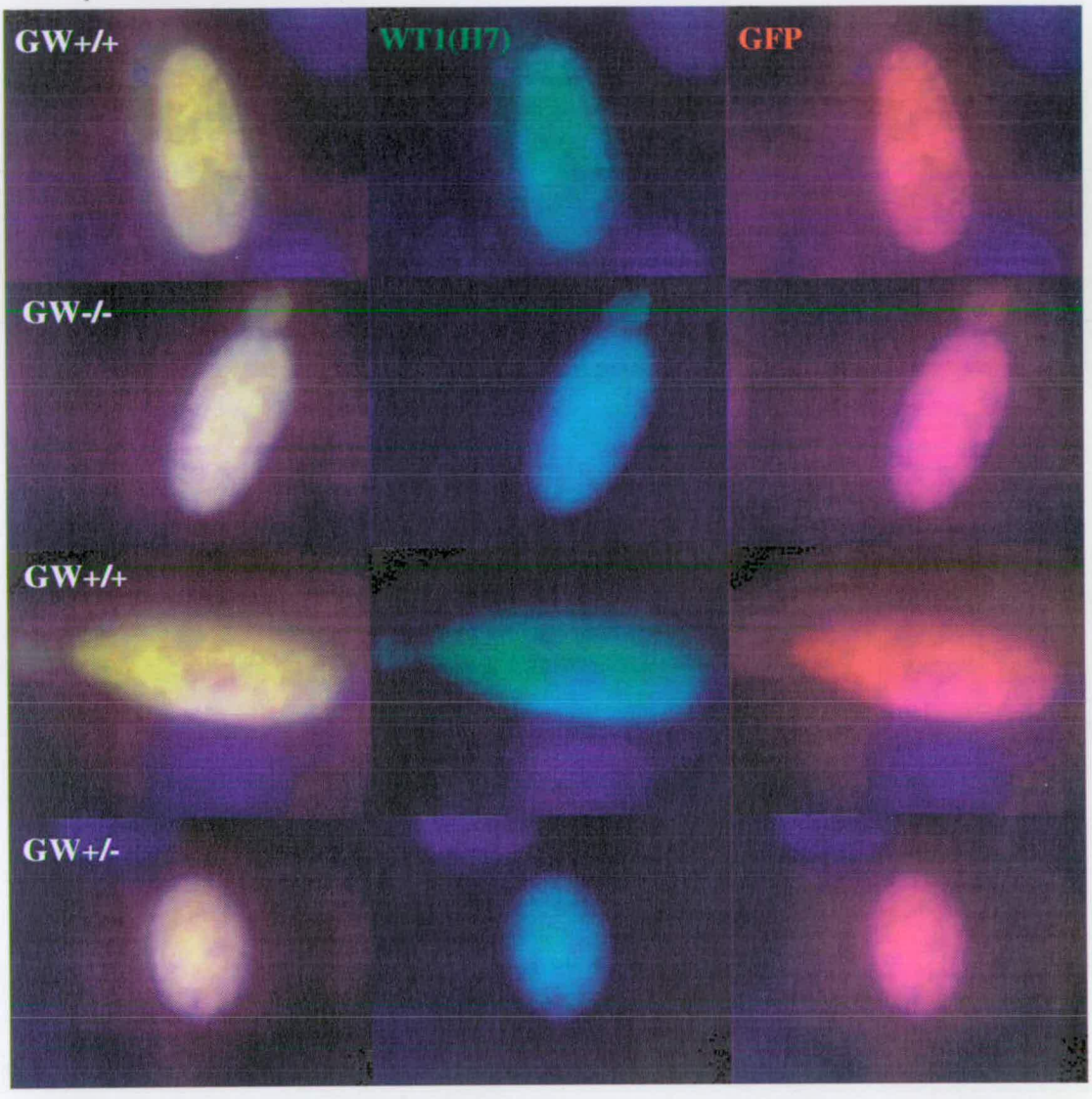

C (NIH3T3)

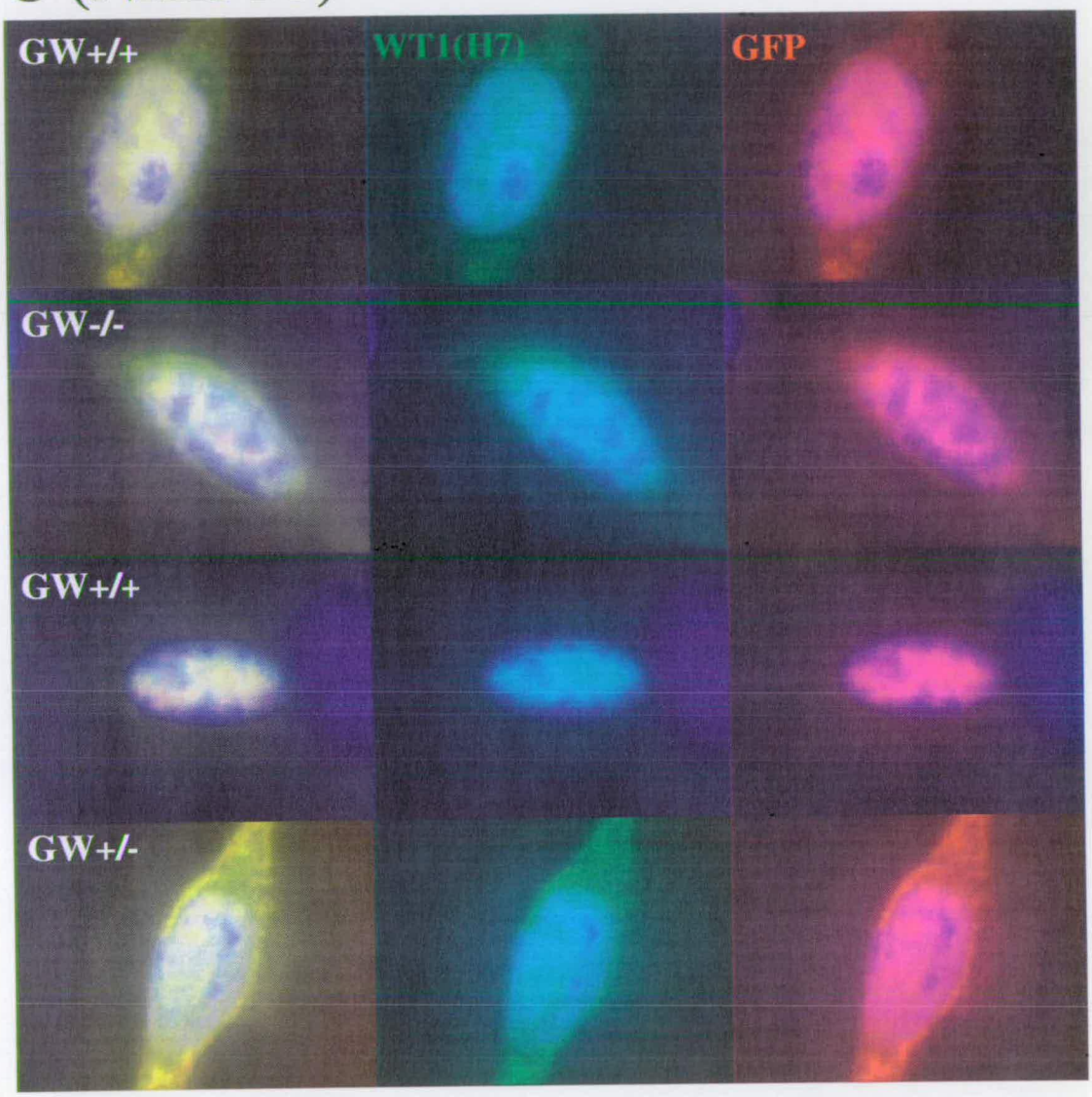

the -KTS isoforms of WT1 colocalize with transcription factors. Thus, the next question is to ask whether GW isoforms also associate with these factors. In the analysis of colocalisation with nuclear proteins, GW+/+ and GW-/+ showed a strong but not complete colocalisation with the splicing factor Sm (**Fig.4.10A**) and poor colocalisation with a component of ribonucleoprotein (RNP) complex, hnRNPC (**Fig.4.10B**). However, GW-/- and GW+/- showed poor colocalisation with either transcription or splicing factors. Interestingly, GW-KTS and GW-/+ isoforms in stably transfected Cos7 cells inhibited cell growth and changed the cellular morphology (**Fig.4.11**). These results suggest that GW still remain in association with some nuclear proteins; however, the structural conformation of GW isoforms may be slightly altered compared to wild-type WT1 resulting in loss of some affinity in these protein associations.

4.6 Discussion

4.6.1 The consideration for design of GW constructs

In generally, GFP fused to ether the C or N terminus showed similar fluorescent properties. However, in making a functional fluorescent fusion protein, the orientation of the functional motif might be very important for biological activity. Dobson et al. (1996) showed that there was a difference in behavior of insulin-stimulated translocation between N-terminal and C-terminal GFP fused transporter (Dobson et al. 1996). The products of the WT1 gene exhibit structural features common to transcription factors, including a C-terminal DNA binding domain composed of the four zinc finger and an N-terminal

A

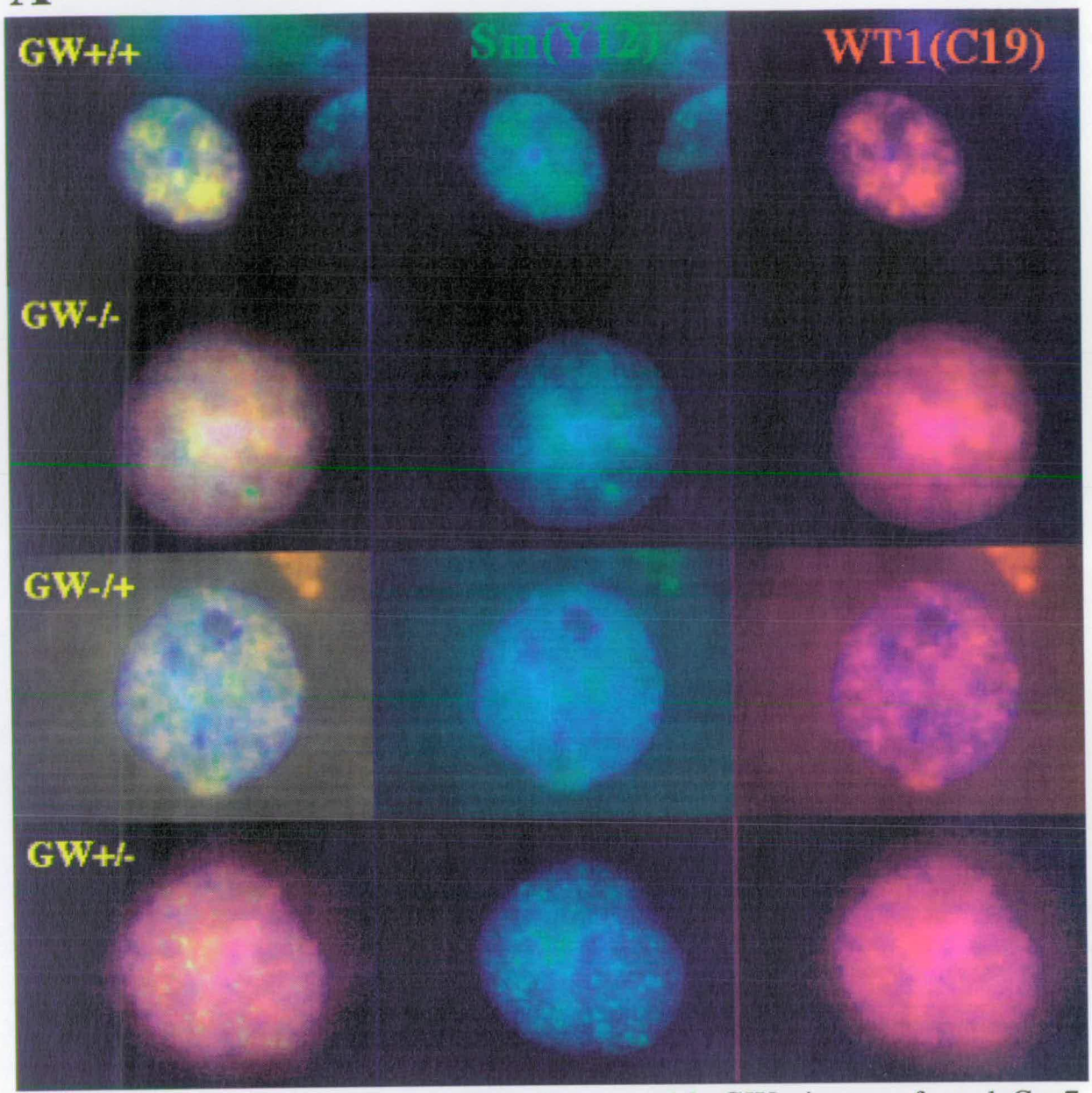

Fig.4.10 Colocalisation of nuclear factors with GWs in transfected Cos7 cells. **A)** Immunofluorescence of GW transfected Cos7 cells with antibodies against WT1(C19) and splicing factor,Sm,(Y12) or **B)** with antibodies against WT1(C19) and hnRNPC. Red: Texas red conjugated with C19 antibody; Green: FITC conjugated with Y12 or hnRNPC antibody; Yellow ,the combination of immunofluorescence of Texa red and FITC.

B

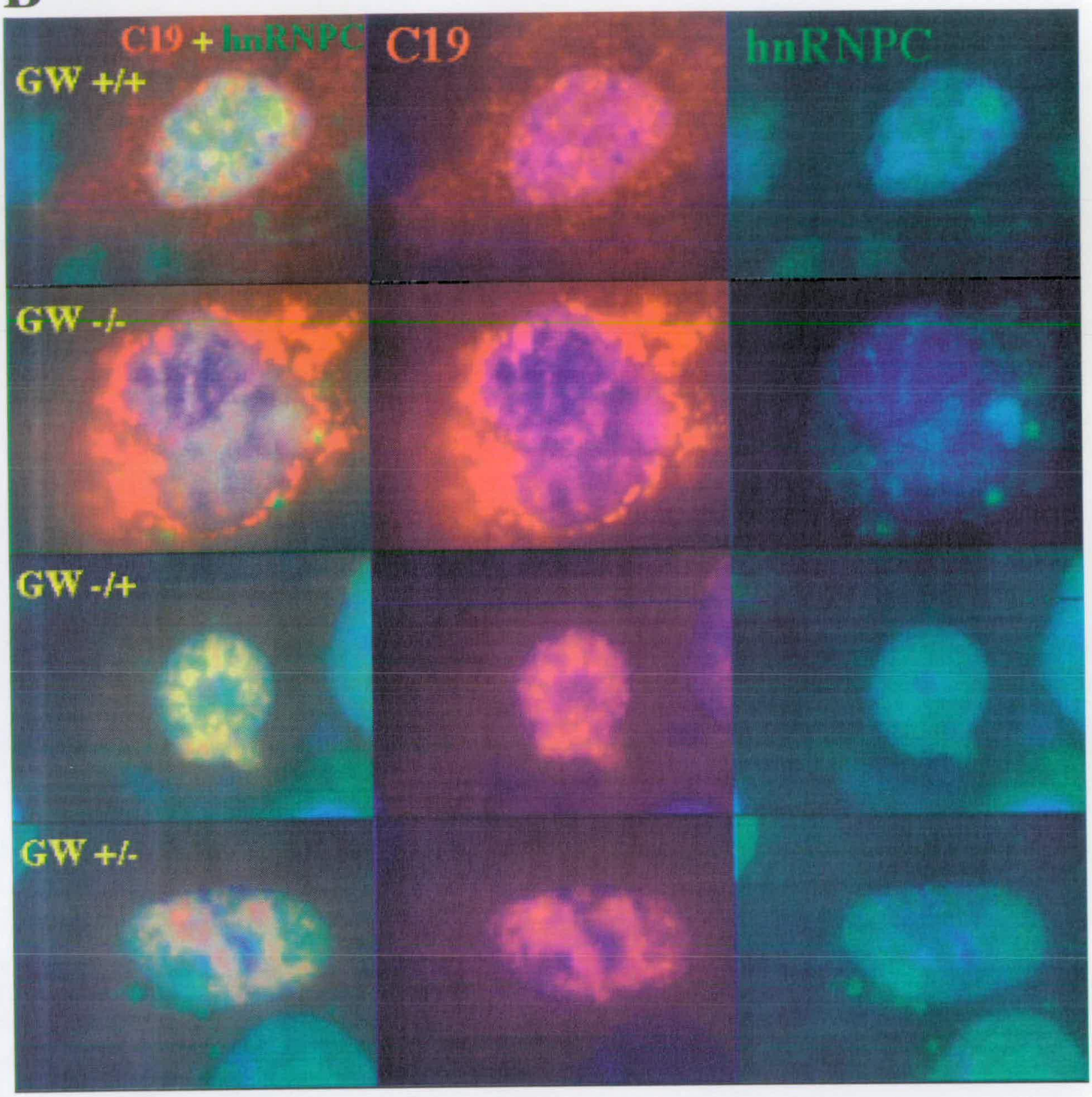

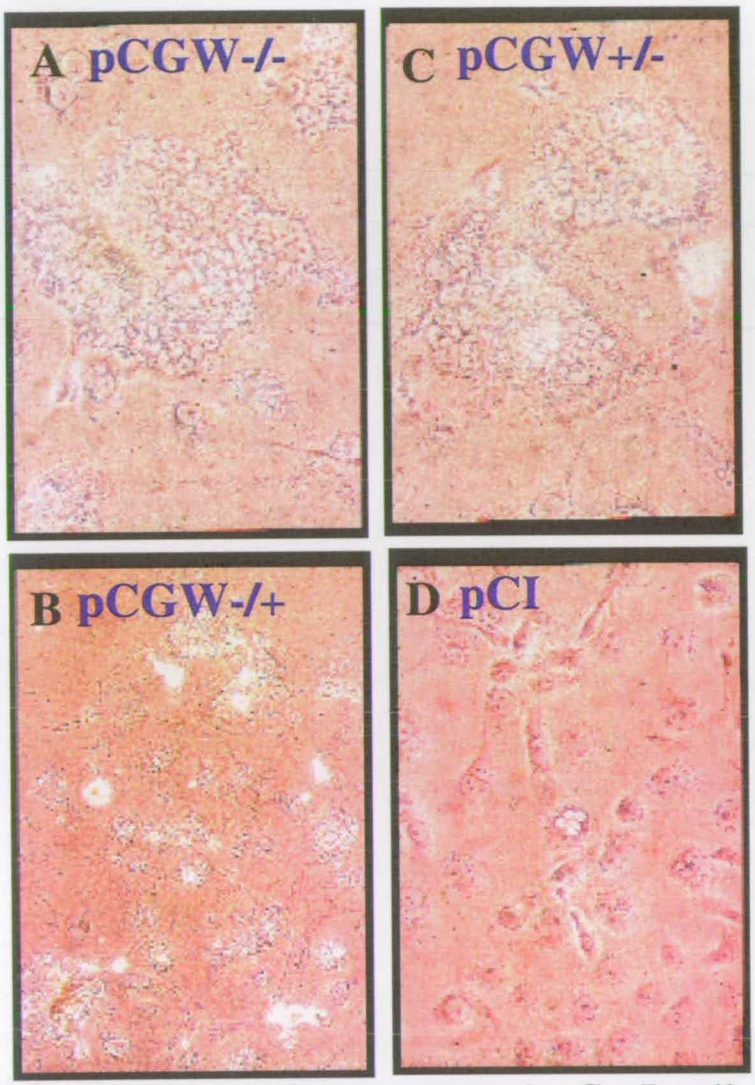

Fig.4.11 Morphology change in Cos7 cells stably transfected with GFP-WT1 fusion constructs as described in **Fig.4.2 A)** pCGW-/-, **B)** pCGW-/+, **C)** pCGW+/-, **D)** pCI (control). These images were visualised by phase contrast microscopy (100X).

regulatory domain. The C-terminal domain has in addition the DNA binding domain (Hewitt et al. 1996), putative NLS signals (Boulikas 1994; Bruening et al. 1996; Ye et al. 1996) and functional motifs important for associating with nuclear proteins (Wang et al. 1995). Thus, the C-terminus may be involved in determining the nuclear sublocalisation. For these consideration , GW isoforms were generated such that C-terminus of GFP was fused with the N-terminus of WT1.

All these considerations were put into the final construct. In line with the expectation, GW isoforms transiently transfected into Cos7 cells, showed a quite detectable level of green fluorescent signals in the nucleus with low fluorescent background levels.

4.6.2 A functional comparison of GW isoforms compared to WT1s

The comparison of subnuclear localisation of transiently transfected GW isoforms and WT1 isoforms showed very similar patterns. This strongly suggest that the GW isoforms have similar biological activities as WT1 expressed in Cos7 cells. The +KTS of GW isoforms (GW+/+ and GW-/+) showed only a partial colocalisation with a splicing factor, Sm, and poor colocalisation with the component of ribonucleoprotein (RNP) complex, hnRNPC. However, the -KTS of GW isoforms showed a low affinity to these nuclear proteins compared to wild-type WT1. Some GW isoforms were found to alter cellular morphology in stably transfected Cos7 cells. Similar results were found when WT1 was ectopically expressed in mammalian cells resulting in an altered morphology of retinoic acid induced F9 cells (Kudoh et al. 1996). This may be due to other activities attributed to overexpression

of WT1 in mammalian cells such as blocked cell cycle at the G1 phase (Kudoh et al. 1995) or induced apoptosis (Englert et al. 1995; Kudoh et al. 1996).

4.6.3 Cos7 cells may provide an similar environment for GW and WT1 isoform expression

In GW expressing Cos7 cells, three kinds of nuclear patterns (speckle, domain and diffuse) were seen in the nuclei. However, there was no typical nuclear pattern when GW isoforms were transiently transfected into two other mammalian cells, NIH3T3 and CHO-K1B. There was also no obviously different pattern between +KTS and -KTS of GW isoforms in their nucleus. Perhaps, WT1 needs an optimal cellular environment for expressing the appropriate nuclear pattern. NIH3T3 or CHO-K1 cells, on the other hand, allows the nuclear entry of GW proteins by a NLS dependent process (Bruening et al. 1996) but does not provide the biological environment for sublocalisation of GW isoforms. In fact, WT1+/+ showed no obvious speckled patterns in the nucleus of CHO-K1 (personal observation). In agreement the functional role of WT1 is in kidney development. Cos7 cells (a kidney cell line from Africa green monkey) may provide an appropriate biological environment for expressing appropriate function.

4.6.4 The natural fluorescence of GW isoforms provide a detailed and sensitive signal

Green fluorescence of the GW isoforms gave a more sensitive signal than immunofluorescence. At high magnification,

GW+/+ and GW-/+ expressing Cos7 cells showed a more detailed fluorescent speckled pattern within a low fluorescent background. GW-/- and GW+/- expressing Cos7 cells showed a clear diffuse signal with strong fluorescent domains. In contrast, immunohistochemical analysis showed that all GW isoforms showed a strong fluorescent background in the nucleus. Obviously, GW isoforms provided not only an easy way to visualise the WT1 isoforms but also gave high resolution. This may be due to the fluorescent intensity reflecting the local concentration of GW proteins. However, in the immunohistochemical analysis, the epitopes may be saturated by immunoreactive fluorescent molecules and cause strong immunofluorescent signals (intensity).

Chapter 5 Analysis of WT1 functional domains and the altered subnuclear localisations of mutated WT1

5.1 Introduction

Wilms' tumour development is associated with two syndromes; The WAGR (Wilms Tumour / Aniridia / Genitourinary abnormalities / Retardation) syndrome and the Denys-Drash syndrome (DDS) (Pelletier et al. 1991; Rausher et al. 1990). In the WAGR syndrome, one allele of WT1 is deleted and these patients develop mild genitourinary problems. In DDS patients, WT1 is found to be mutated. These patient develop more severe genitourinary abnormalities than would be expected of the inactivation of a single allele. Most WT1 mutations in DDS patients are missense mutations within the zinc finger region. However, a mutation has been described which results in deleting the whole zinc finger region of the WT1 protein (Pelletier et al. 1991). These mutant isoforms may therefore dimerise with wild-type WT1 proteins resulting in dominant-negative effects. In fact, truncated WT1 mutants alter the subnuclear localisation of wild-type WT1 in some mammalian cells (Englert et al. 1995). Specifically, the N terminal domain (1-160/182 aa) of WT1 mediated the self-association of WT1 isoforms (Moffett et al. 1995; Reddy et al. 1995). Perhaps, this association causes the dominant negative action of the WT1 mutation in DDS.

So far, to investigate the protein expression in the nucleus, immunonhistochemistry staining is widely used. However, there are many drawbacks with this type of analysis; it is laborious to obtain

suitable antibodies, the chemical fixation may lead to artificial results, and indiscernible immunofluorescent intensity result in low resolution of image. The WT1 isoforms have very discernible nuclear patterns (Larsson et al. 1995). There are many antibodies against WT1 but no specific antibody can recognise the individual WT1 isoforms. In chapter 4, the expression patterns of GW isoforms (GFP-WT1 fusion isoforms) showed similarity to that of wild-type WT1 proteins. The fluorescent signal provided high resolution and reflected the expression status in the living cells.

In this chapter, GW isoforms were use as vital markers for developing a cellular system to examine the behavior of WT1 mutants. Thus, taking advantage of GW isoforms, nuclear patterns of these WT1 mutants were directly examined in living Cos7 cells. A series of C-terminal deletions was used to determine the putative signal for nuclear localisation of GW proteins and a synthetic NLS was ligated at the C-terminal end of these truncated proteins and used to analyse the functional domain for the nuclear localisation. In addition, a competitive pattern was seen in cotransfecting GW+/- with a truncated WT1+/+ or by a coexpression construct which expressed GW+/- and truncated WT1 proteins through IRES. Furthermore, three individual missense mutations as have been described in WT1 from rat embryonic kidney tumor cells (S365F, H372Y) (Sharma et al. 1994) and WT1 mutation that cause DDS (R394W) (Pelletier et al. 1991) were introduced into GW to examine the nuclear pattern.

5.2 Identification of putative NLS sequence for GW isoforms

Usually, transportation of a protein molecule across the nuclear membrane is mediated by nuclear pore complexes that allow small proteins such as GFP to enter the nucleus by passive diffusion. However, a large protein like GW (> 80 kDs) needs a nuclear localisation signal for translocation from the cytoplasm to the nucleus. In Chapter 3, GFP was shown to localise throughout the mammalian cell, including the nucleus and cytoplasm. However, GFP can also be found in subcellular locations when linked to specific localisation sequences. In chapter 4, GW isoforms were visualised in subnuclear localisation with patterns similar to wild-type WT1 proteins. Thus, defining the localisation sequences in the WT1 moiety of GW proteins will be useful in the analysis of WT1 cellular sequestration.

The C-terminus containing zinc fingers may play an important role in determining the subnuclear localisation. The zinc fingers show DNA binding activity but may also contain a nuclear localisation signal(s) (Bruening et al. 1996; Charlieu et al. 1995; Englert et al. 1995; Larsson et al. 1995). Taken together, WT1 should play a critical part in determining the localisation of the GW proteins assuming that GFP does not interfere in that process.

5.2.1 The construction of the truncated GW isoforms

Serial C-terminal deletions of GW isoforms were made by using the GW expression vector, pCGW+/- (**Fig.4.1**), as a template. An adaptor containing the human lamin NLS sequence (hN) or a polylinker were used to make the coding sequences in frame. To generate GW-dC1/GW-dC1+hN, amino acid 193 to 438 of the coding sequences of

GW+/- was deleted by restriction digestion of the Sca I and Nsi I sites, GW-dC2/GW-dC2+hN, amino acids 236 to 438 were deleted by restriction digestion of Nsi I sites, GW-dC3/GW-dC3+hN, amino acids 256 to 438 were deleted by restriction digestion of Sac I and Nsi I sites, GW-dC4, amino acids 283 to 438 were deleted by restriction digestion of NlaI V and Nsi I sites, and GW-dC5, amino acids 326 to 438 were deleted by restriction digestion of Nsi I sites. For the GW-dN, pCGW was partially digested with BsrG I and Pvu II to remove 100 amino acids of the WT1 N-terminus and religated by adding polylinker. The constructs are summarised in **Fig.5.1& Fig.5.2**.

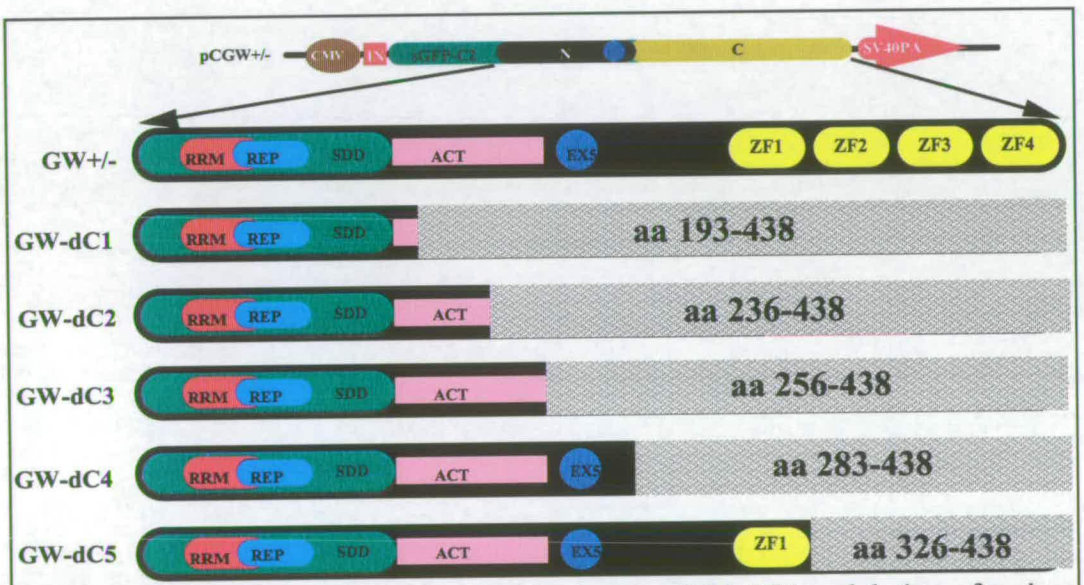

Fig. 5.1 Summary maps of the GW mutants. **GW-dC1**, a deletion of amino acid 193-438 in GW+/-; **GW-dC2**, a deletion of amino acid 236-438 in GW+/-; **GW-dC3**, a deletion of amino acid 256-438 in GW+/-; **GW-dC4**, a deletion of amino acid 283-438 in GW+/-; **GW-dC5**, a deletion of amino acid 326-438 in. GW+/-;

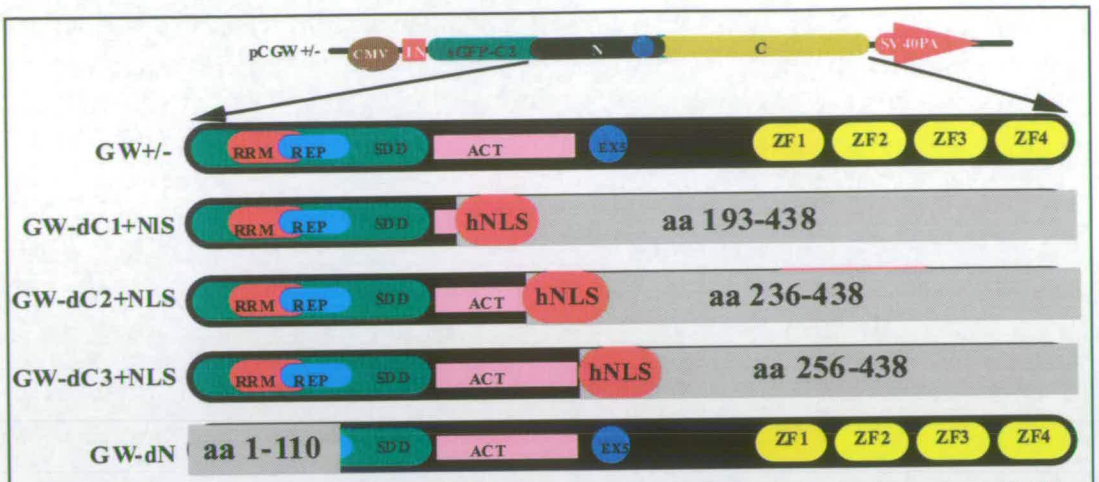

Fig.5.2 Summary maps of the GW deletion mutants containing human nuclear laminar NLS. GW-dC1+hN, a replacement of amino acid 193-438 in GW+/- by hNLS; GW-dC2+hN, a replacement of amino acid 236-438 in GW+/- by hNLS; GW-dC3+hN, a replacement of amino acid 256-438 in GW+/- by hNLS; GW-dN, a deletion of amino acid 1-110 in GW+/-.

5.2.2 A putative NLS within the zinc finger regions

To analyze the functional domains responsible for nuclear localisation, truncated GW+/- mutants and GW-dC1-5 were transiently transfected to Cos7 cells. As a result, GW-dC1-3 could not be detected in the nucleus but was found in cytoplasm and perinuclear region (out side of the nuclear membrane). GW-dC4 showed a few small fluorescent spots in the nucleus while GW-dC5 showed many aggregated fluorescent spots accumulated to one side of the nucleus **(Fig.5.3)**. Thus, GWd-C1-3 must have lost the nuclear localisation signal and stayed in the cytoplasm.

A weak nuclear signal was detected for the GW-dC4 protein whereas the GW-dC5 protein had a strong nuclear signal. Because both GW-dC4 and GW-dC5 proteins are still too big (>60 kDa), they could

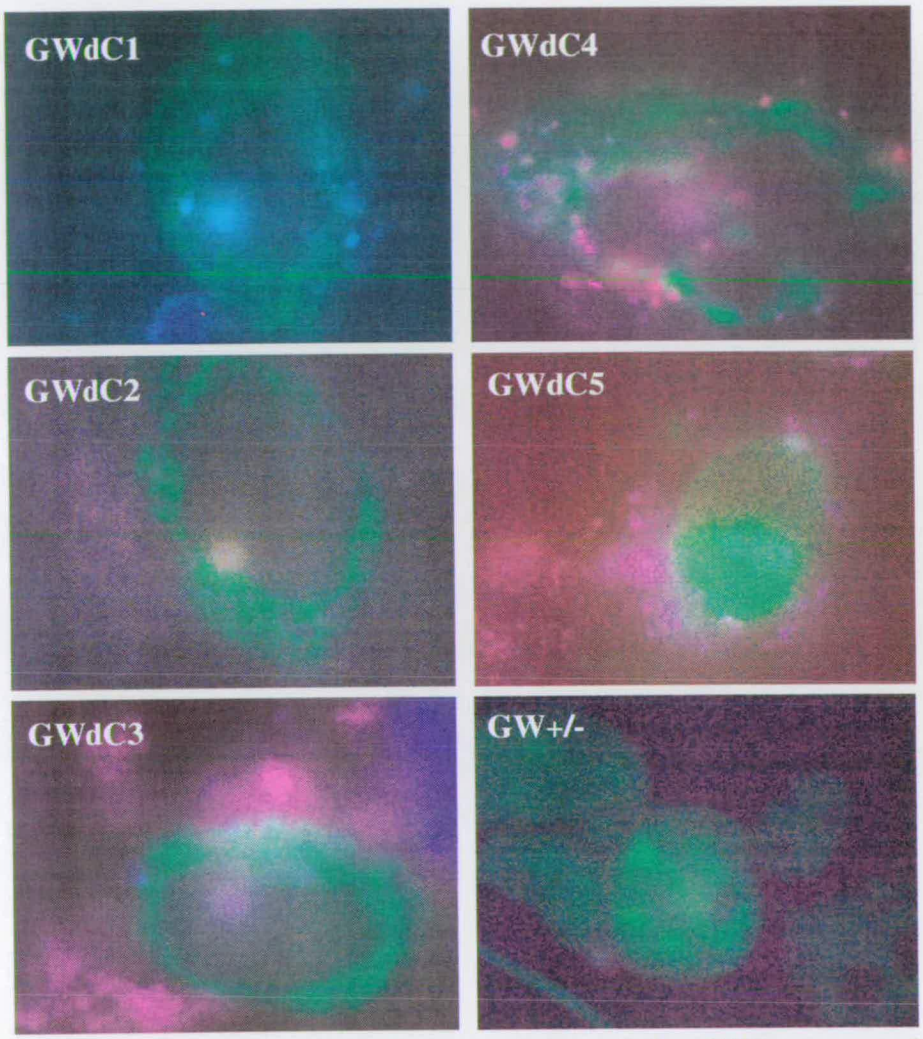

Fig.5.3 Fluorescent nuclear patterns of the GW truncated constructs (GW-dC1-5). pGW-dC1-5 were transiently transfected into Cos7 cells and green fluorescence was visualised using FITC filter (250X). The delection of GW of these expression vectors were described in **Fig. 5.1**.

not get into nucleus by simple diffusion. Hence, there is at least one NLS sequence between amino acid 283 and 326. In addition, this region may also affect the efficiency of nuclear transportation as the large aggregated fluorescent domains were seen in GW-dC5 expressing cells but not in GW-dC4 expressing cells.

5.3 The zinc fingers are required for the nuclear patterns

Although GW-dC4 and GW-dC5 showed nuclear localisation, the signals were not diffuse but resided in a few spots or granules in the nucleus. This suggests that GW-dC4 and GW-dC5 may still have some NLS signals but the disruption of the zinc fingers led to loss of the appropriate nuclear patterns. To test this, the nuclear localisation of GW-dC1-3 was restored by ligating the human lamin NLS (Boulikas 1994) to the C-terminal end of GW-dC1, GWdC2 and GWdC3. The resultants were named GWdC1+hN, GWdC2+hN and GWdC3+hN (**Fig.5.2**). The relocalisation of GW-dC1-3 proteins were seen in the nucleus but they did not show the normal patterns however irregular shaped fluorescent dots were found (**Fig.5.4**). Thus, GWdC1+hN, GWdC2+hN and GWdC3+hN restores nuclear translocation through the human lamin NLS while the nuclear sublocalisation may be interrupted by the C-terminal deletion. Interestingly, GW-dN, 100 amino acids of N-terminus deleted from GW+/- was found to have similar nuclear patterns (diffuse) compared to GW+/- (**Fig.5.4**). Obviously, the normal nuclear pattern is dependent on the C-terminus of GW, including the NLS and functional domains (zinc fingers).

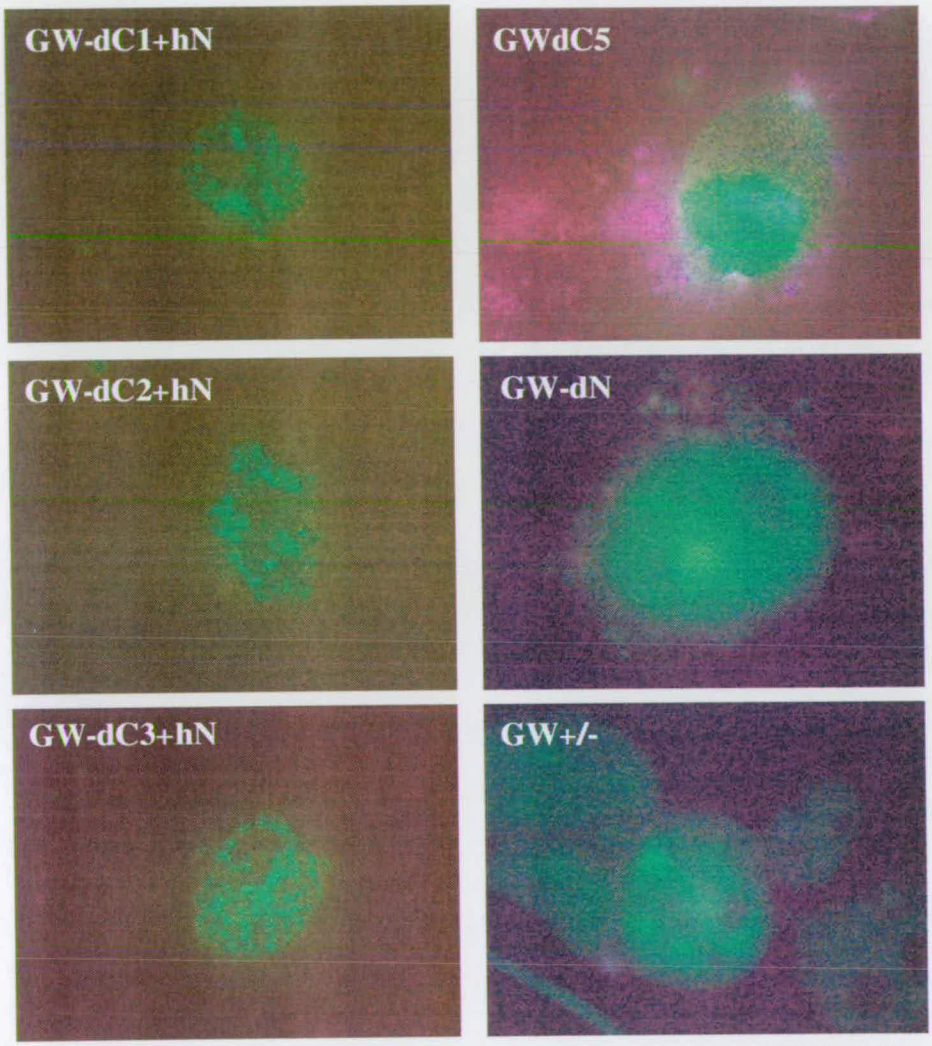

Fig.5.4 Fluorescent nuclear patterns of the GW-dC1-3+hN,GW-dN and GW-dC5. These GW constructs were transiently transfected into Cos7 cells and green fluorescence was visualised using FITC filter (250X). The modification of GW for these expression vectors were described in **Fig. 5.2**.

Taken together, these results suggest that there are putative nuclear localisation signals between amino acid 283 and 326. The zinc finger domain is required for the nuclear pattern. Deletion of zinc fingers may not only affect nuclear localisation but may also a effect the efficiency of translocation as there was a gradual increase of subnuclear localisation in Cos7 cells expressing these deletion constructs.

5.4 Altered nuclear patterns caused by GW mutants

In vitro analysis of WT1 functional domains indicate that the N-terminal region plays a regulatory role while the C-terminus or zinc finger region is responsible for DNA binding activity (Drummond et al. 1994; Hamilton et al. 1995; Kennedy et al. 1996; Reddy et al. 1995; Wang et al. 1993; Wang et al. 1995; Wang et al. 1995). In fact, some mutations or truncations of WT1 result in the development of Wilms' tumour (Pelletier et al. 1991). Perhaps, these mutations may affect the nuclear behaviour of WT1 and then interfere normal cellular functions of wild-type proteins.

5.4.1 Dimerisation via the self-association domain of WT1 may cause a dominant negative behavior in the nucleus

According to previous results, a truncated WT1 mutant in which the four zinc fingers are detected can interfere with the nuclear pattern of WT1-KTS (Ehrig et al. 1995). These may be due to the N terminal region containing a self-association domain (Moffett et al. 1995; Reddy et al. 1995) resulting in a dimerization between the wild-type and truncated proteins. To investigate whether the binding domain

of mutant WT1 to wild-type WT1 is responsible for the dominant negative behavior in mammalian cells three C-terminal truncated WT1 mutants (WT1-dC1, WT1-dC2 and WT1-dC3) and variants (WT1-dC1-3+hN and WT1-dN) were generated using similar strategies as for the truncated GW constructs described in **Fig.5.1 & 5.2**.

The truncated constructs were cotransfected with GW+/- expression constructs. GW+/- was cotransfected with WT1-dC1-3+hN into Cos7 cells and displayed many spots or granules (**Fig.5.5**) while GW+/- cotransfected with WT1-dC1 displayed little or no effect (**Table 5.1**). These results suggest that WT1-dC1-3+hN constructs act to interfere with the nuclear sublocalisation. In fact, the dimerisation of WT1 proteins has been shown in a yeast two-hybrid system (Ehrig et al. 1995). Although WT1-dC1-3 was similar to WT1-dC1-3+hN; the lack of a nuclear localisation signal reduced dimerisation in the nucleus. The nuclear pattern was also affected by cotransfecting GW1+/- and wild-type WT1+/+ but was not affected by cotransfecting GW1+/- and WT1-dN (a deletion of the N-terminal region which may contain the dimerisation domain). This implies that the dimerisation domain is required for this interference effect in the nucleus. In fact, pCGWIWT1-dC1+hN, a coexpression construct, expressed GW+/- and WT1-dC1+hN via IRES (**Fig.5.6**) and showed a similar high efficiency of this interference effect. Twenty Cos7 cells expressing green fluorescent nuclear patterns were counted in each cotransfections at the results are summarised in **Table 5.1**.

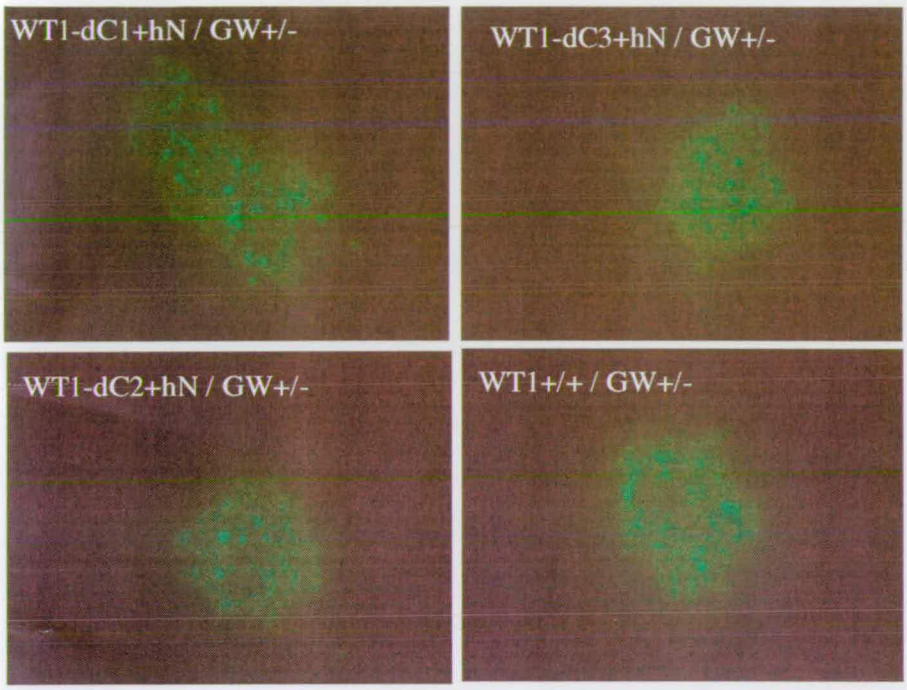

Fig.5.5 The dominant negative patterns in nucleus of cotransfectedCos7 cells. 1 μg WT1 constructs and 100ng GW constructs were used to cotrasfected into 10^5 cells. After 36 hours of incubation, the transfected cells were directely visualized by fluorescent microscopy .

5.4.2 The missense mutations of zinc fingers result in an altered subnuclear localisation

Table 5.1 The dominant negative effect of GW+/- nuclear patterns by coexpression[a] with truncated WT1 mutants

Constructs	Spots	Diffuse	Other[b]
GW+/-	0	18	2
pCGWIWT1-dC1+hN[c]	15	5	0
GW+/- / WT1+/+	6	12	2
GW+/- / WT1-dC1+hN	10	9	1
GW+/- / WT1-dC2+hN	11	6	3
GW+/- / WT1-dC3+hN	14	4	2
GW+/- / WT1-dC1	3	14	4
GW+/- / WT1-dC2	1	15	5
GW+/- / WT1-dC3	0	18	2
GW+/- / WT1-dN	0	19	1

a. The ratio of transfected concentration of GW+/- and WT1 constructs is 1/10 and 20 expressing cell of each cotransfection were examined for the nuclear pattern **b.** Those were speckled patterns or nuclear leaked patterns(they showed green fluorescence both in nucleus and cytoplasm). **c.** see **Fig.5.6**.

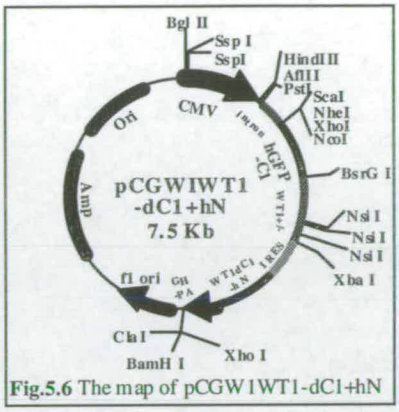

Fig.5.6 The map of pCGW1WT1-dC1+hN

Pelletier et al. (1991) had reported that there were several "hot spot" mutations on the third zinc finger domain of one WT1 allele in DDS patients. They found ten DDS patients with the Arg366His (1patient), Arg394Trp (7 patients) and Asp396Gly/Asn (2 patients) mutations. Sharma et al. (1994) proposed an animal model for Wilms tumor by using the alkylating agent N-nitroso-N'-methylurea (NMU)-induced rat kidney tumors. They analyzed WT1 cDNA from the kidney tumors and two point mutations (S364F and H372Y) were found in zinc finger 2. The R394W in WT1 caused low DNA binding activity (Pelletier et al. 1991). The S365F may affect the phosphorylation of WT1 resulting in a reduced ability of nuclear translocation (Ye et al. 1996). It was also suggested that the S365F in WT1 may interrupt the second zinc finger resulting in the loss of DNA binding activity (Sharma et al. 1994). These mutations were introduced into the GW+/- (**Fig.5.7**) to examine their effect on the subnuclear localisation. The mutated GW+/- were named GW-S365F, GW-H372Y and GW-R394W and were transfected with Cos7 cells.

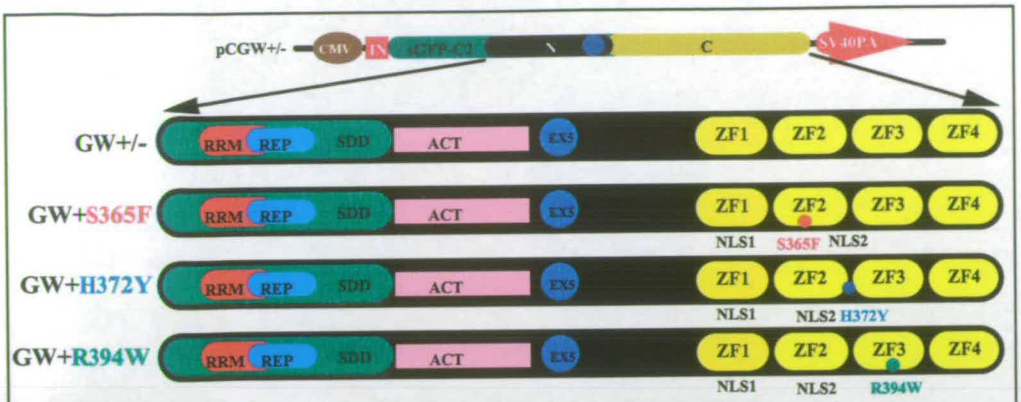

Fig.5.7 Summary maps of the GW mutants. **GW+S365F**, a replacment of amino acid Ser 365 by Phe in GW+/-; **GW+H371Y**, a replacment of amino acid His 372 by Tyr in GW+/-; **GW+R394W**, a replacment of amino acid Arg394 by Trp in GW+/-.

Interestingly, the GW-S365F expressing cells showed a poor nuclear localisation pattern. In fact, green fluorescent signals remained primarily in the cytoplasm and surrounded the nuclear membrane **(Fig.5.8A&B)**. However, some green fluorescent signal was seen in the nucleus so all GW-S365F was not excluded **(Fig.5.8A&C)**. This result implies that the S365F interrupts GW nuclear localisation. In expression of the GW-H372Y mutant, many clear big fluorescent spots with a low fluorescent background were seen in the nucleus **(Fig.5.8D, E&F)**. The mutation may alter the DNA binding specificity or activity of GW resulting in different patterns in nucleus. The GW-R394W mutant showed different levels of fluorescence in nuclear spots **(Fig.5.8F,G&H)**. There was also some nuclear "leakage" of signal to the cytoplasm **(Fig.5.8F)**. These results suggest that the missense mutants alter nuclear translocation and sublocation resulting in cytoplasmic retention and altered nuclear patterns.

Fig.5.8 GW+/- mutants with zinc finger missense mutations were transiently transfected into Cos7 cells. All green fluorescence was visualised using FITC and Texas Red filters. Nuclear patterns of the GW-S365F were shown in **A**, **B** and **C**. Nuclear patterns of the GW-H372W were shown in **D**, **E** and **F**. Nuclear patterns of the GW-R394W were shown in **G**, **H** and **I**.

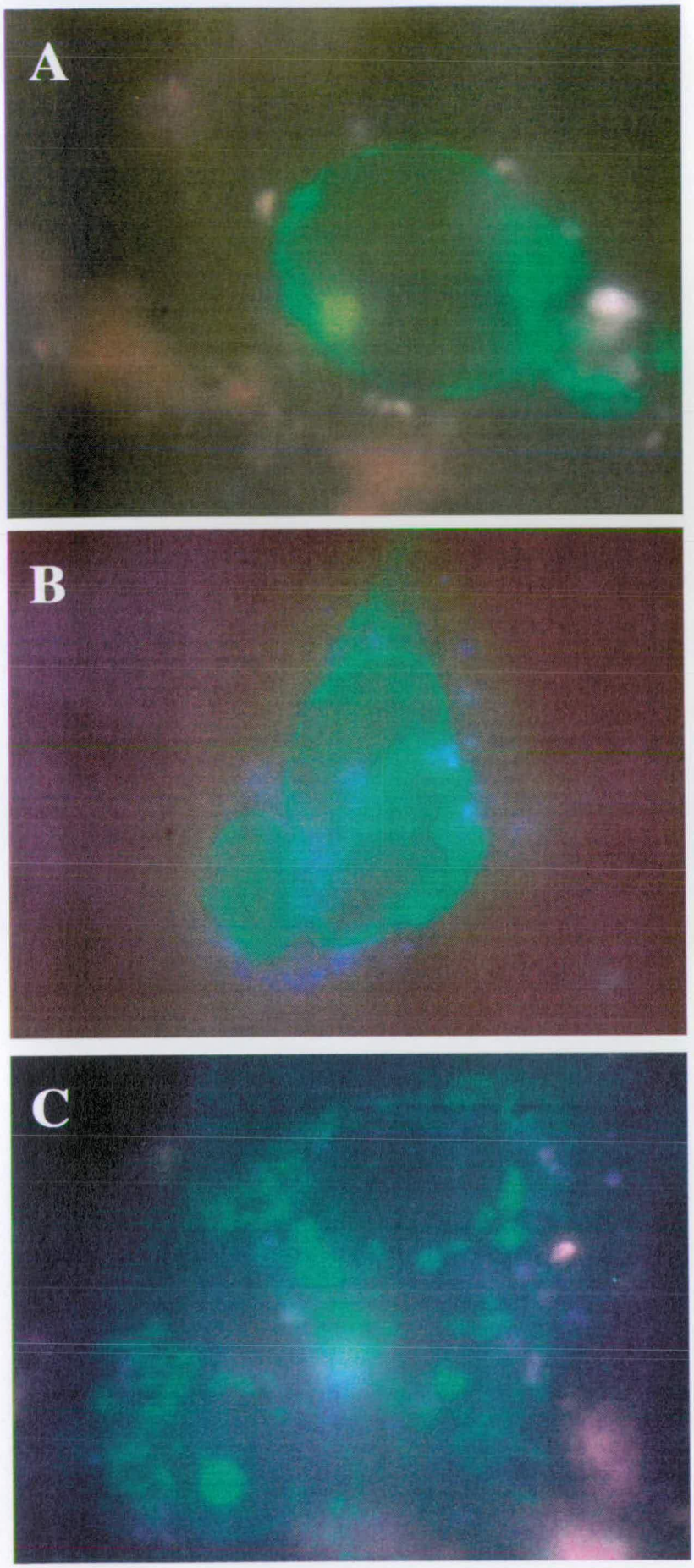
A
B
C

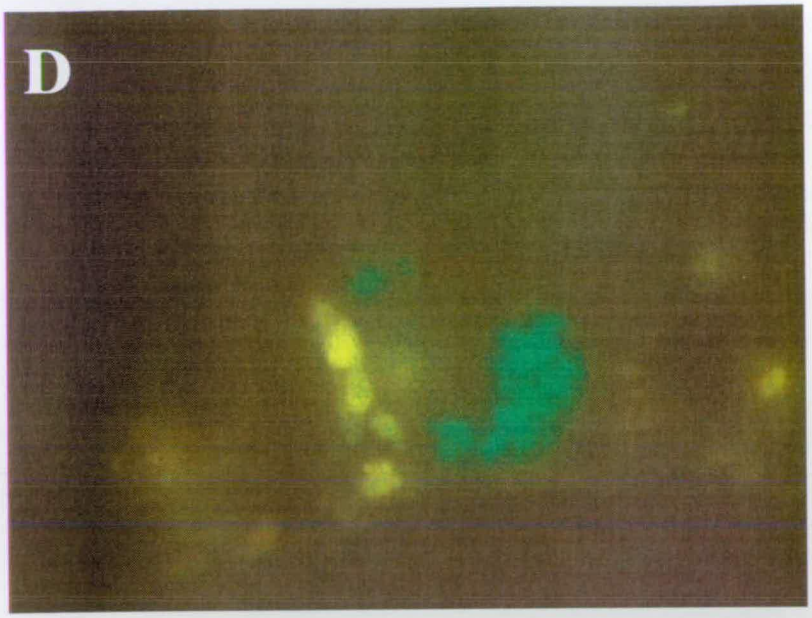
D

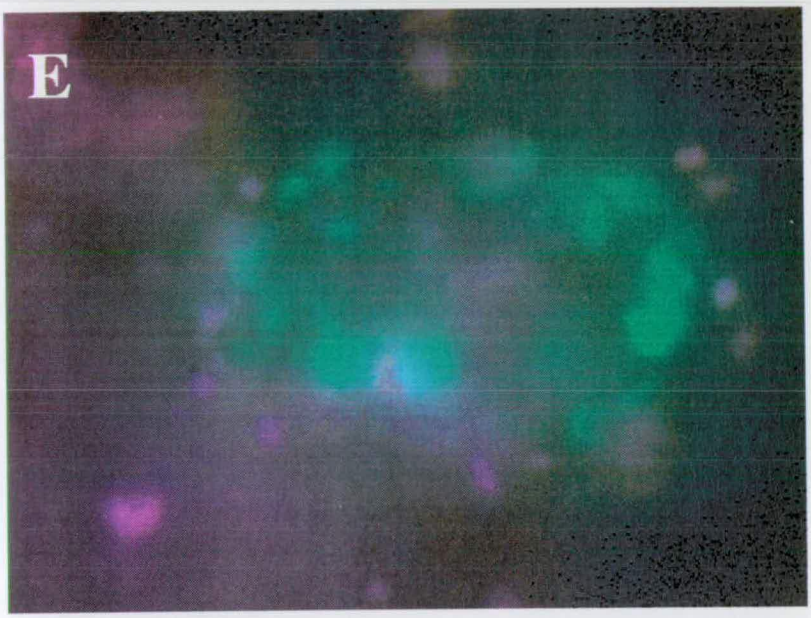
E

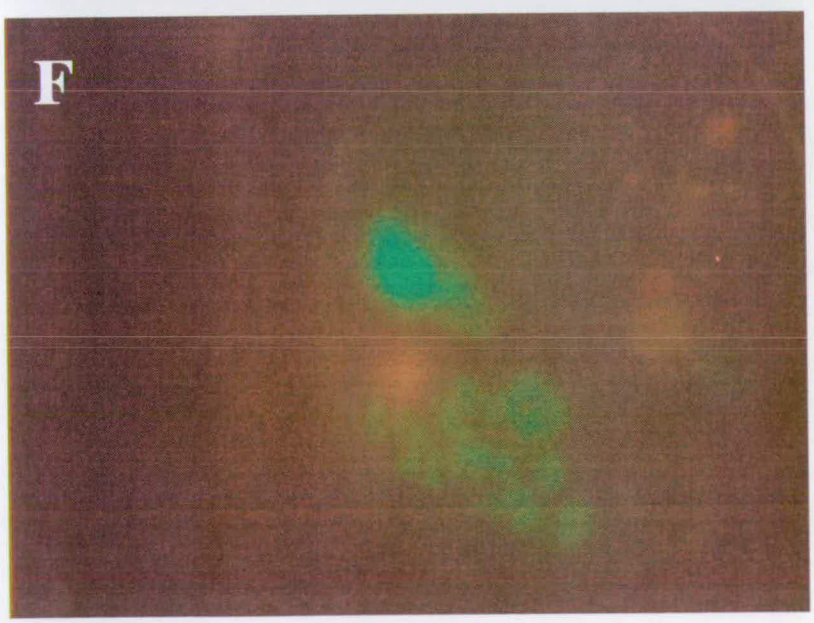
F

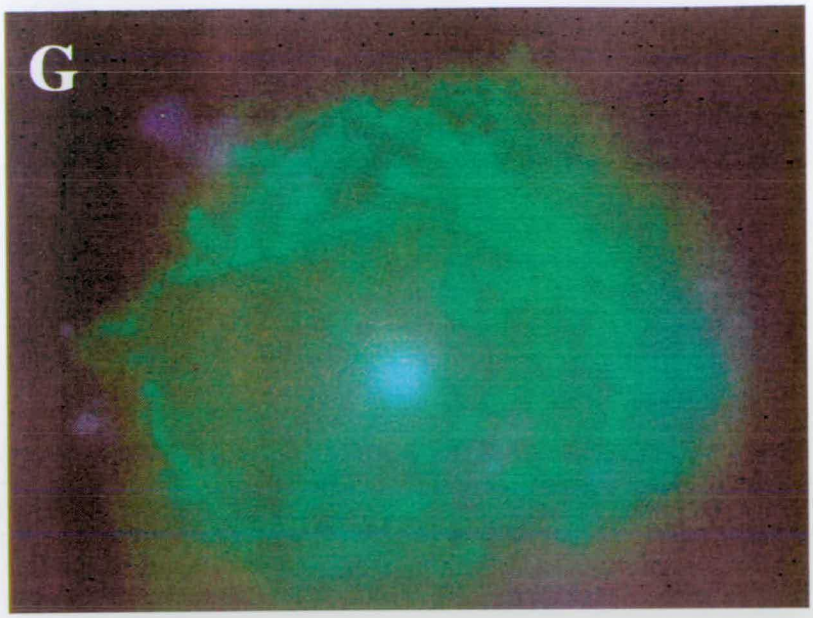
G

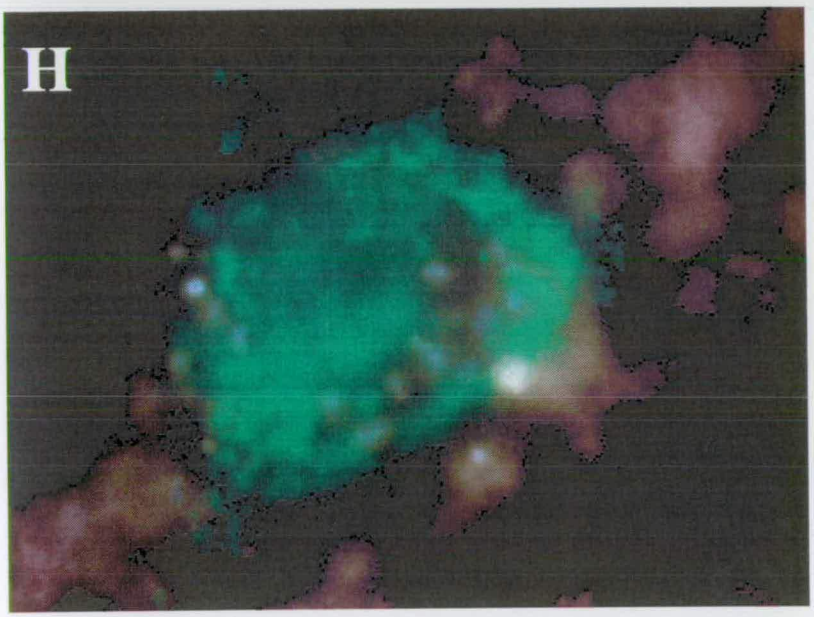
H

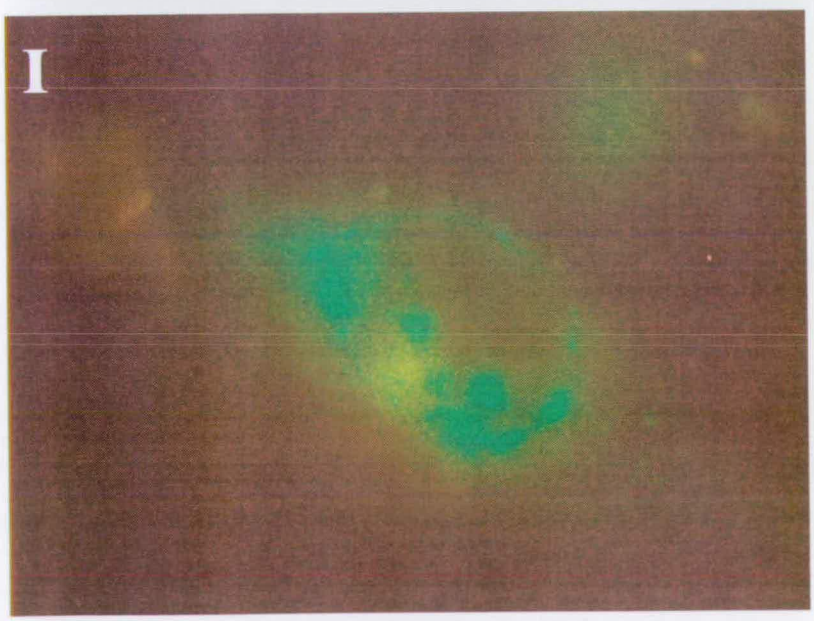
I

5.5 Discussion

5.5.1 The functional motifs for the nuclear localisation

In general, proteins > 45 kd require a nuclear localisation signal (NLS) in order to be targeted to the nucleus (Boulikas 1993; Boulikas 1994). Bruening et al. (1996) made C-terminal truncated WT1 proteins resulting in a localisation in both the nucleus and cytoplasm. In order to determine the signals for nuclear localisation, they compared the deleted region of the truncated proteins and proposed that WT1 zinc fingers contain target signals required for nuclear localisation of the protein. Further analysis making fusions between the putative NLS with β-galactosidase, proved that there were two independent signals that lie within zinc fingers I and within zinc fingers II and III. In fact, a putative core sequences of NLS, LKRHQRRH (Boulikas 1994; Buckler et al. 1991; Ye et al. 1996), was located within zinc fingers II and III as described by Bruening et al. (1996). This implies that the NLS signals are required for WT1 nuclear localisation.

To test these results in the GW protein, C-terminal truncated GW+/-mutants (GW-dC1-5) were generated by a sequential deletion of the WT1 C-terminus. As expected, GW-dC1, GW-dC2 and GW-dC3, showed cytoplasmic localisation with a clear dark background in the nucleus. GW-dC4 showed a low degree of nuclear localisation while GW-dC5 showed a strong patchy signal in one side of the nucleus. Thus, the amino acids between 193 and 326 has nuclear localisation activity for transportation of GW in agreement with the putative WT1 NLS proposed by Bruening et al. (1996). In addition, the cytoplasmic

localisation of GW-dC1-3 suggested that the GFP moiety did not contribute to nuclear translocation.

The domain containing the zinc fingers of WT1 also plays a role in subnuclear localisation. The nuclear localisation of GW-dC1-3 were restored by adding the human lamin NLS at their C-terminus. The resultant genes (GWd-C1-3+hN) were reappeared in the nucleus but showed different amounts of green fluorescent spots depending on the construct. Similarly, a WT1 mutant containing a deleted zinc finger 3 of the wild-type protein, showed a spotted pattern with a strong diffuse background in the nucleus (Englert et al. 1995). However, GW-dC5 contained the WT1 NLS and zinc finger 1 and showed a big accumulated domain in the nucleus. Thus, the deleted zinc fingers may interrupt the nuclear sublocalisation and the human lamin NLS restored nuclear translocation without restoration of specific nuclear sublocalisation.

To analyze the contribution of the N-terminal region of WT1, the GW+/- construct, pGW-dN, was generated by a short N-terminal deletion (100 amino acids) of the WT1 moiety. However, the GW-dN proteins did not give an obviously altered nuclear pattern but remained in similarly diffuse like GW+/-. This suggests that the small N-terminal domain has little effect on the nuclear pattern.

5.5.2 The altered nuclear patterns caused by dominant negative mutations or missense mutations of the zinc finger regions of WT1

Deny Drasch syndrome (DDS) patients usually have severe developmental disorders of the reproductive system, and have a predisposition to development Wilms' tumor. DDS mutations were proposed to act in a dominant negative manner. The mutated alleles harbor missense mutations within zinc fingers or truncated zinc finger domains and it was proposed that these interfere with the function of the wild-type allele (Pelletier et al. 1991; Reddy et al. 1995). Reddy et al. (1995) and Moffett et al. (1995) proposed that WT1 C-terminal truncations have the ability to oligomerise in vitro. Thus, WT1 C-terminal mutations may dimerise with native WT1 protein resulting in the DDS phenotype. Englert et al. (1995) showed that when truncated WT1 proteins formed dimers with the wild-type protein that the subnuclear localisation of WT1 was altered (Englert et al. 1995). Thus, the normal function of WT1 may be disrupted by the association of the mutated protein in DDS patients resulting in a altered subnuclear localisation.

Three missense GW mutants caused a change in subnuclear specificity, including poor nuclear localisation, cytoplasmic retention and altered (random) nuclear patterns. The GW-S365F protein remained in the cytoplasm surrounding the nuclear membrane. Ye et al. (1996) showed that the zinc fingers of WT1 proteins could be phosphorylated by protein kinase A (PKA), protein kinase C (PKC) and casein kinase II (CKII), which led to an inhibition of WT1 DNA binding in vitro. The Ser365 was a potential phosphorylation site for both PKC and PKA. It was additionally shown that the wild-type pattern was altered by treating with forskolin, a strong PKA activator, resulting in the cytoplasmic retention of WT1. The cytoplasm localisation was

presumably due to the inhibition of PKA phosphorylation. They concluded that the role of phosphorylation was important to the regulation of WT1 nuclear functions (the DNA binding or nuclear translocation). This suggested that the GW-S365F lost the ability to translocate to the nucleus due to failure of proper phosphorylation. The Ser365 site may be an important phosphorylation site which interacts with the zinc finger NLS sequences to mediate nuclear translocation.

In the GW-H372Y mutant, the mutation was in the core NLS sequence (Boulikas 1994; Buckler et al. 1991) but GW-H372Y still targeted into the nucleus with an altered nuclear sublocalisation. However, the H372Y mutation may interrupt the second zinc finger causing the loss of DNA binding activity (Sharma et al. 1994). There were different levels of fluorescent spots with a low fluorescent background in the nucleus. A faint signal was also seen in the cytoplasm. Obviously, the H372Y mutation did not completely impede the nuclear localisation but did affect the specificity of subnuclear localisation. Similarly, GW-R394Y also showed a poor nuclear localisation but many small fluorescent spots also could be seen in a diffuse background in the nucleus. The R394Y mutation is a hot spot mutations in DDS patients and may also interrupt the zinc fingers causing the loss of WT1 protein function. In fact, the nuclear patterns of GW-R394Y looks like a combination of GW-S365F and GW-H372Y.

Any alteration within functional motifs will result in a dysfunctional protein. In fact, the most significant mutations resulting in a disease phenotype were due to truncation or mutations of the zinc fingers. The change in the nuclear pattern is, thus, common to these

mutations and sequences of the protein to abnormal locations may be at least, part of the basis for DDS.

Chapter 6 Green fluorescent protein as a lineage specific marker in transgenic mouse embryos

6.1 Introduction

Making transgenic mice is one of the approaches to understanding complex development processes during embryogenesis. So far, the β-glactosidase gene is the most popular marker in transgenic mice. Expression of the β-galactosidase gene under the control of any given promoter can be examined by histochemical x-gal staining. Thus, the β-galactosidase gene is a useful marker for monitoring developmentally regulated gene expression in embryos. However, this approach can only provide a static report of gene expression during development. Some chemicals such as fluorescent β-galactosidase (fluorescein di-β-D-galactosidase{FDG} and resorufin β-galactoside bis-aminopropyl polyethylene glycol 1900{RGPEG}) have been reported as vital substrates of β-galactosidase activity and the fluorescent products shown to have high stability and sensitivity in living mammalian cells (Zhang et al. 1991), *Drosophila* embryos (Minden 1996) and transgenic mice (Jasin et al. 1992). However, these fluorescent vital dyes only label a limited cell population resulting in a quick dilution of fluorescent signals in dividing cells during embryogenesis. This reduces the ability of using the fluorescent vital dye to visualise stained embryonic structures.

As described in Chapter 1, GFP labelling techniques have caused a revolution in the field of gene expression in many biological systems. However, there are only a few reports using GFP in mammals

(Akagi et al. 1997; Ikawa et al. 1995; Ikawa et al. 1995; Z.-Goetz et al. 1997). Ikawa et al. (1995) first demonstrated that GFP could be as a marker in transgenic mice. Ikawa et al. (1995) used wild-type GFP as a reporter gene under the control of the chicken beta-actin ubiquitous promoter and showed green fluorescence in various tissues of adult mice, including, muscle, pancreas, kidney, heart, lung. An enhanced fluorescent GFP, EGFP (Yang et al. 1996), was used as a reporter under the control of the same promoter to produce much stronger fluorescent mice (Okabe et al. 1997) and green fluorescence was found in many tissues previously detected which had either weak or no fluorescence, including brain, liver, kidney, heart, spleen, thymus, adrenal gland, testis, testicular cells, adipose tissue and the skin of new born mice. They also showed that the GFP is non-toxic by examining a 12 week old transgenic mouse using histochemical analysis and found no abnormality in any examined section. Recently, Peel et al. (1997) had demonstrated GFP as a marker gene under the control of the tissue specific promoters, neuron-specific enolase and platelet-derived growth factor B chain promoter, in adult rats. Similarly, a humanised GFP, hGFP-S65T, was used as a marker under the control of the astrocyte-specific glial fibrillary acidic protein (GFAP) promoter giving green fluorescent patterns in the optic nerve, brain, and retina tissues of adult mice (Zhuo et al. 1997). These reports show that GFP is useful for both ubiquitous and tissue specific expression in adult mice and embryos. These results also suggest that some GFP mutants can enhance the sensitivity of green fluorescent activity even under the control of weak promoters or embryonic specific promoters.

MacKenzie et al. (1997) reported transgenic analysis of the Msx-1 embryonic expression pattern using LacZ as a reporter. To examine the involvement of the Msx-1 gene in the complex events generating the body plan of the mouse embryo and also to develop GFP as a cell lineages marker in developing mouse embryos, GFP derivatives including wild-type GFP, TFP, αGFP and βGFP (αGFP/β-galactosidase gene fusion) were used as reporter genes. Particularly, βGFP was seen to be the most useful marker of specific cell types at various developmental stages of mouse embryos. This successful approach should provide a way of further analysing the dynamic events of cell lineages in the developing mouse embryo.

6.2 αGFP and β-GFP constructs

αGFP (previously named hGFP-M4 in chapter 3) was based on hGFP-S65T(Clontech) and was generated as described in Materials and Methods (Section 2.2). The fluorescent features were discussion in Chapter 3. In order to generate a more versatile GFP marker, the αGFP /β–gal chimeric reporter was generated by fusing αGFP to the N terminus of construct β–galactosidase (**Fig.6.1A**). The resultant construct was named β-GFP (**Fig.6.1B**). Because the molecular features of both GFP and β–galactosidase allow fusion to foreign proteins without losing biological activity and their biochemical features are tolerant to many harsh environments, the β–GFP was expected to be a double functional marker which has both fluorescence and enzymatic activity. In fact, as shown between green fluorescence and x-gal blue stain were simultaneously detected in a single cell expressing the β-GFP construct (PCIβ-GFP) (**Fig.6.2**).

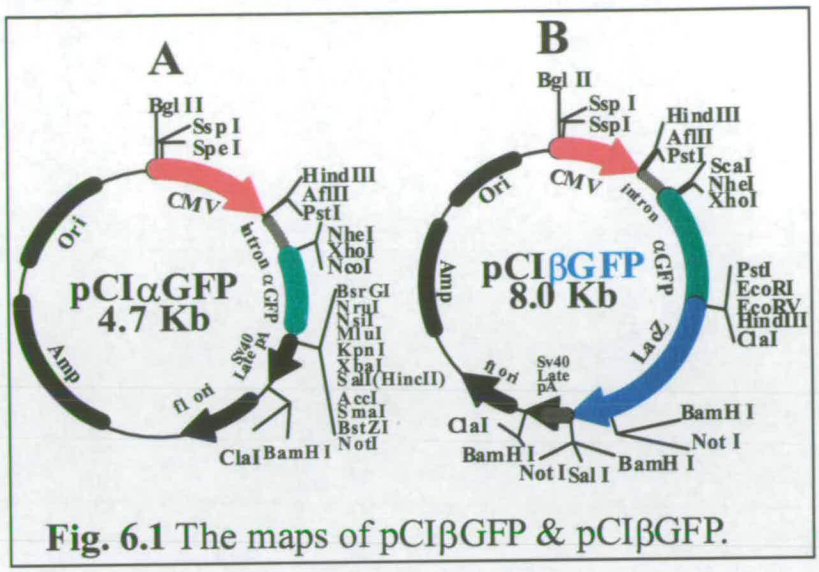

Fig. 6.1 The maps of pCIβGFP & pCIβGFP.

6.3 Construction of transgenic vector

During initial experiments with wild-type GFP transgenic mice, there was no evidence of green fluorescence in any mouse tissues. According to previous results, GFP mutants showed a higher fluorescent activity in mammalian environment. However, only a limited number of reports suggest that GFP could be used as a marker in mice. and may be unreported limitations using GFP in mice.

I have used a secondary marker to control for GFP activity. β-galactosidase is the most common reporter , showing both high stability and non toxicity in transgenic mice. To compare the possibility of using GFP variants as a marker in transgenic mice, the double reporter constructs were generated for expressing the two protein in same embryonic tissues. First, GFP or TFP (GFP-S65T) and β-galactosidase gene were linked by IRES (Ghattas et al. 1991; Mountford et al. 1995) to produce a dicistronic vector. The GFP and TFP (GFP-S65T)

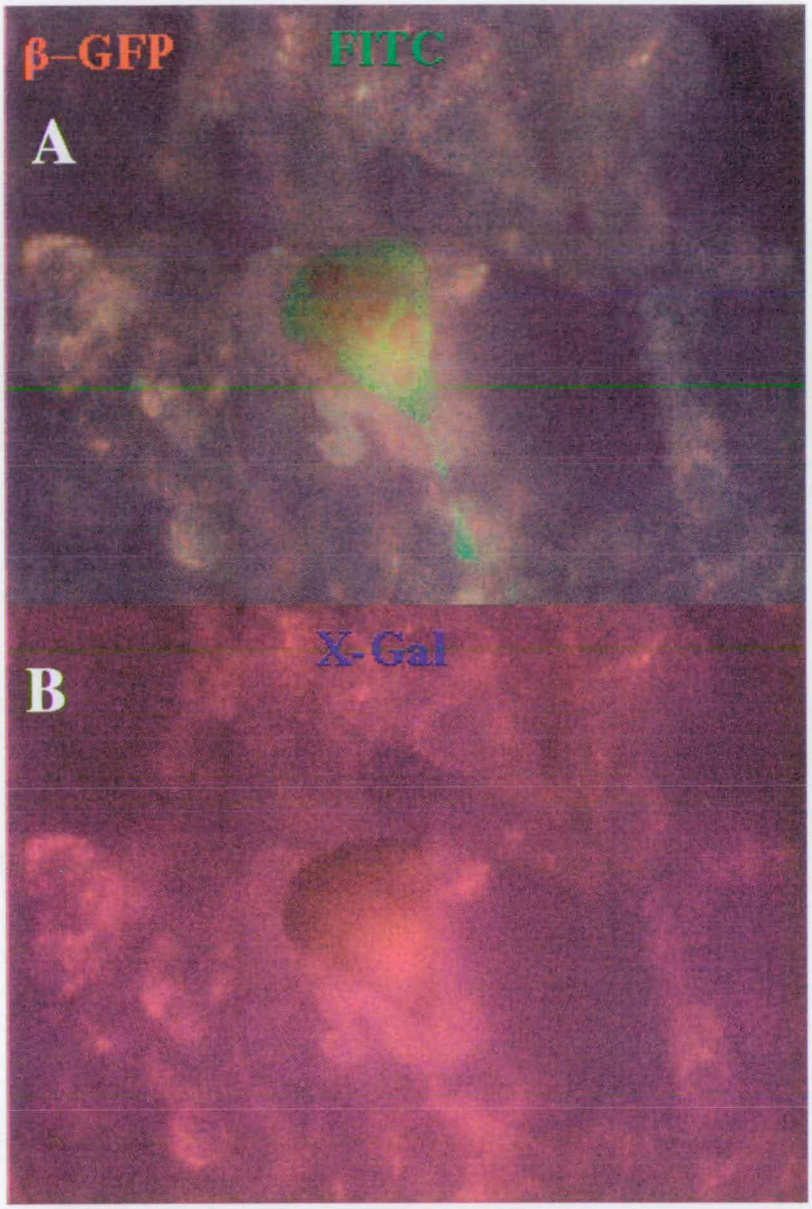

Fig.6.2 pCIβGFP transfected Cos7 cell showing both (**A** green fluorescence (125X) and (**B** blue staining (125X) following histochemical X-gal treatment The green fluorescence was visualised using FITC and Texas Red filters and the the blue staining was visualised using a Texas Red filter. The expression constructs were described in **Fig.6.1**.

described in Chapter 3 were subcloned into the pTA vector (Invitrogene) and named pTATFP and pTAGFP. A 0.72 kb Xba I/Hind III fragment of pTATFP was subcloned into the Nhe I/ Hind III digested pJ4Ω vector to produce pTFP. The 5 kb Not I/Nco I fragment of pCosλNco5' (MacKenzie et al. 1997) containing the Msx-1 promoter was cloned into the Not I/Nco I of pTFP to produce pMT. Then the 5.7 kb Nsi I/ Sal I fragment of pMT was cloned into the Nsi I/Xho I site of pIRESβgal to produce pMTZ (**Fig.6.3**). The same cloning strategy was also used to generate pMGZ. A control transgenic vector, pMZ, was generated by a replacement of the TFP of pMT with the Msx-1 cDNA. Second, βGFP was introduced into similar constructs to compare the dicistronic vectors. 3' Sal I-*-NruI (* indicates a stop codon between SalI and Nru I) /5' Nco I sites were introduced into αGFP by PCR and the digested fragment was ligated into Nco I/Sal I digested pMT to generated pMαG. To generate a β–galactosidase fusion, a Sma I/ Sal I digestion of 3.4 kb fragment of bacterial lacZ gene from pNASSβ (Biolabs) was subcloned into the Sma I/Sal I sites of pBluescript® II KS vector (Stratagene) named placZSV40pA. The 3.3 kb Sma I/BamH I fragment of placZSV40pA was cloned into the Nru I/Bgl II site of pMαG to produce pMβG (**Fig.6.4**). To examine the green fluorescent activity, the β-galactosidase was used as an internal control to monitor the GFP expression. These double reporter constructs were introduced into transgenic mouse embryos.

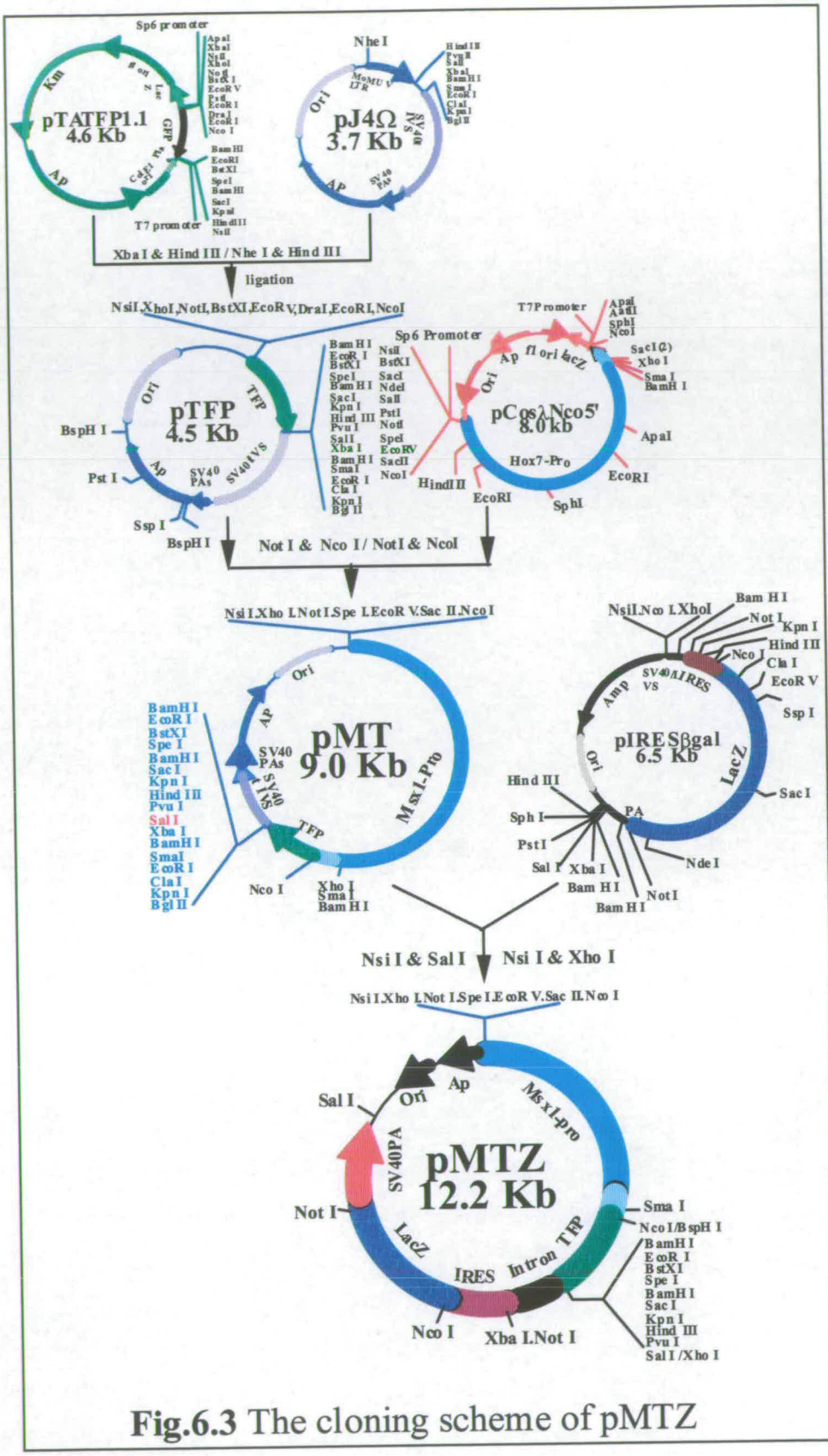

Fig.6.3 The cloning scheme of pMTZ

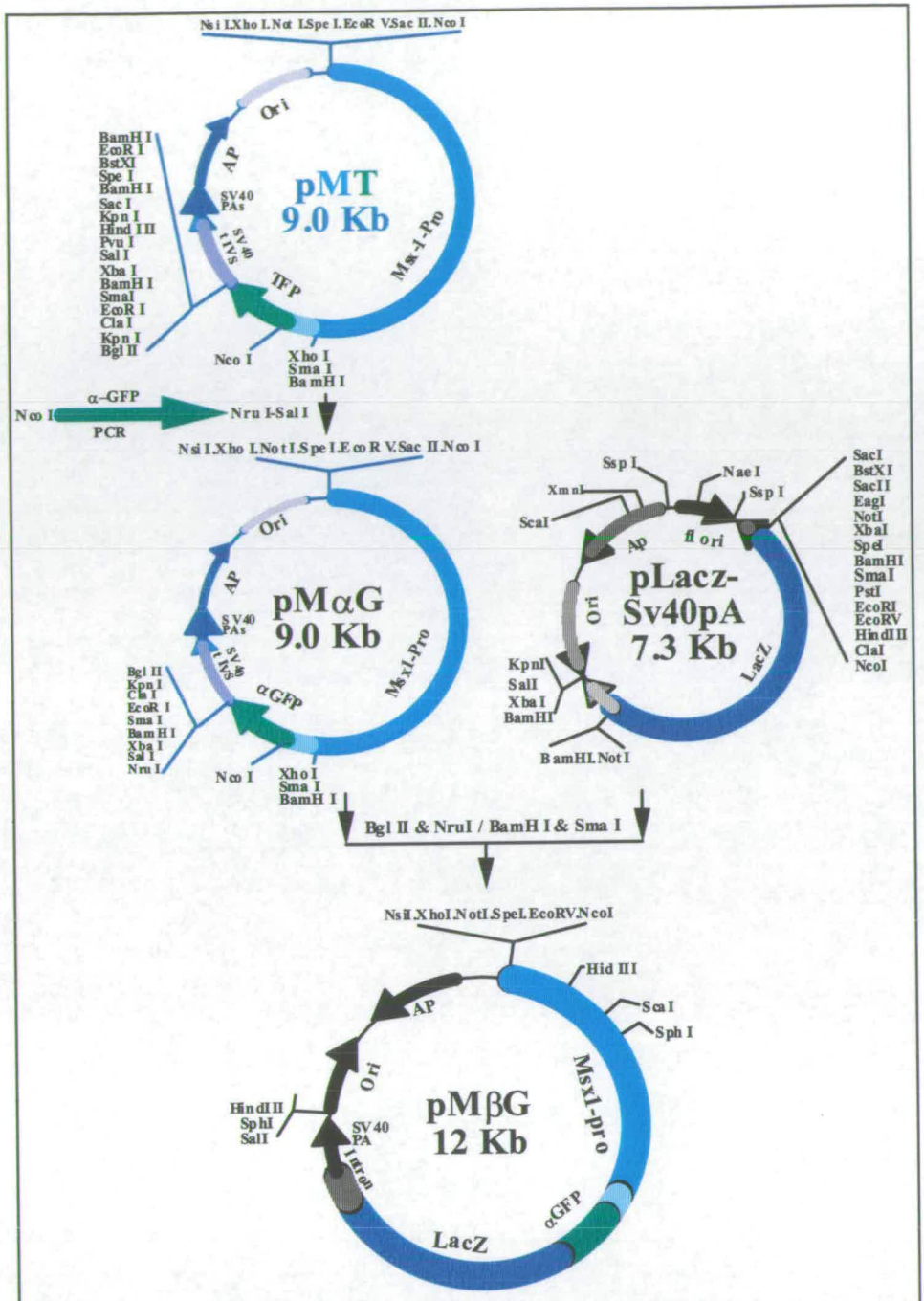

Fig.6.4 The cloning scheme of pMβG.

6.4 The production of GFP transgenic mice

GFP transgenic lines were obtained by microinjecting the following constructs into fertilised oocytes: A) pMGZ; wild-type GFP and β–galactosidase linked by IRES and driven by the 5 kb Msx1

promoter, B) pMTZ; TFP and β–galactosidase linked by IRES and driven by the 5 kb promoter, C) pMZ; the Msx1 cDNA and β–galactosidase linked IRES and driven by the 5 kb promoter, D) pM5βG; βGFP driven by the 5 kb promoter, E) pM3βG; βGFP driven by the 3.5 kb Msx1 promoter, F) pMαG; αGFP driven by the 5 kb promoter. To improve the expression of the transgene, all of these constructs also contained an SV40 intron (Brinster et al. 1988; Choi et al. 1991) and polyadenylation signal **(Fig.6.5)**.

Five lines of transgenic mice were obtained carrying by the 5MβG transgene; each line designated 5βGn (n=1,2,3,4& 5). Likewise, the three lines carrying 3MβG transgene were designed 3βGn (n=1,2,& 3); four lines carrying MαG transgene were designed αGn (n=1,2,3,&4); three lines carrying MTZ transgene were designed TZn (n=1,2&3); four lines carrying MGZ transgene were designed GZn (n=1,2,3&4). Two lines carrying MZ transgene were designed Zn (n=1&2). The production rate of transgenic mice was between 8-10% **(Table 6.1)**.

Table 6.1 The production rate of transgenic mice[a]

Constructs[b]	No. transferred eggs / recipients	No. Pregnant mice	No. mice born	No. transgenic mice (%)
pM5βG	50/8	7	61	5 (8.2%)
pM3βG	50/3	3	30	3 (10%)
pMαG	50/6	4	42	4 (9.5%)
pMTZ	50/4	4	35	3 (8.6%)
pMGZ	50/6	5	40	4 (10%)
pMZ	50/2	2	26	2 (8%)

a. The transgenic mice were identified by PCR analysis of genomic DNA from tail tip samples.
b. The constructs were described in Fig.6.5.

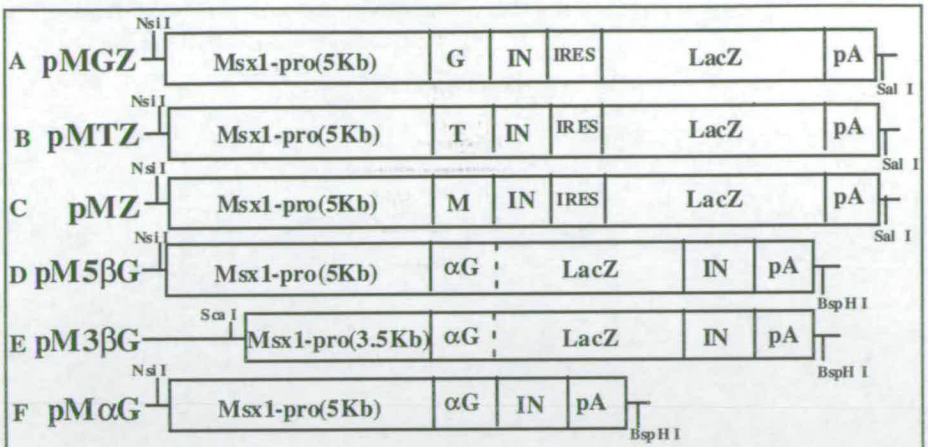

Fig.6.5 Structure of the transgenes. **A).** pMGZ. **B).** pMTZ. **C).** pMZ. **D).** pM5βG. **E).** pM3βG. **F).** pαG. Msx1-pro, Msx1 promoter; G,GFP; T, GFP-S65T; M, Msx1 cDNA; αG, αGFP; IRES, encephalomyocarditis virus internal ribosome entry site; LacZ, bacterial lacZ gene; INS, SV40 intron; pA, SV40 polyadenylation signal. All of GFP constructs were fused with the 44 amino acidsof the N-terminu of Msx-1 exon 1 contining in the 5 Kb promoter. The transgenes of pMGZ, pMTZ and pZ were digested with Nsi I/Sal I and the transgenes of pMβG and pMαG were digested with Nsi I/BspH I to remove the bacterial sequences.

6.5 Identification of GFP transgenic embryos

The internal positive control of the double reporter constructs (**Fig.6.5**), β–galactosidase, was used to score transgenic embryos. In the constructs, pMGZ, pMTZ and pMZ, the transcription of β–galactosidase occurred in a cap independent manner through the IRES while in the βGFP constructs the β–galactosidase activity correlated directly to the GFP fluorescent activity. Thus, examination of β–galactosidase activity in whole mount transgenic embryos would rapidly screen lines for the further analysis of GFP fluorescent activity.

The β–galactosidase activity in the transgenic lines (Table 6.1) was mainly located in the frontonasal process, limb buds,

mandibular component of the first arch, maxillary component of the first arch, and the somites during embryogenesis. 5βG lines had slightly stronger x-gal staining patterns compared to IRES-lacZ transgenic lines (two TZ, three GZ and two Z lines). However, the three 5βG lines (the transgenes were driven by the 3.5 kb Msx-1 promoter) showed detectably stronger blue staining patterns than IRES-lacZ lines. This implies that IRES dependent translation gave less efficient expression in transgenic embryos. 5βG-1 embryos were carefully examined for their expression patterns from E9.5 to E12.5. The main expression pattern included limb buds, the mandibular component of the first arch, maxillary component of the first arch, and somites and was first detected in E9.5 embryos. The expression level of these patterns increased at E10.5 and E11.5. There were strong blue stained forelimb and hindlimb buds in E10.5 and E11.5 embryos, but these were only weakly stained at E9.5 and E12.5. The mandibular and maxillary component of the first arch were strongly stained in E10.5 and 11.5 embryos. However, there was a particularly strong activity in the mandibular component of the first arch at E11.5. In E12.5 embryos, strong staining was only in the mandibular component of the first arch **(Fig.6.6A)**. E9.5 embryos started to show the main activity of transgene. Obviously, the 5 kb Msx-1 promoter had a strong activity in developing limb buds between E10.5 and E11.5 but decreased in activity after E11.5 and also had different activity in the other regions from E10.5 to E12.5.

The 3βG-1 line of transgenic embryos showed a strong activity in the midbrain, hindbrain limb buds, mandibular component of the first arch, and the somites from E9.5 to E12.5 **(Fig.6.6B)**. In

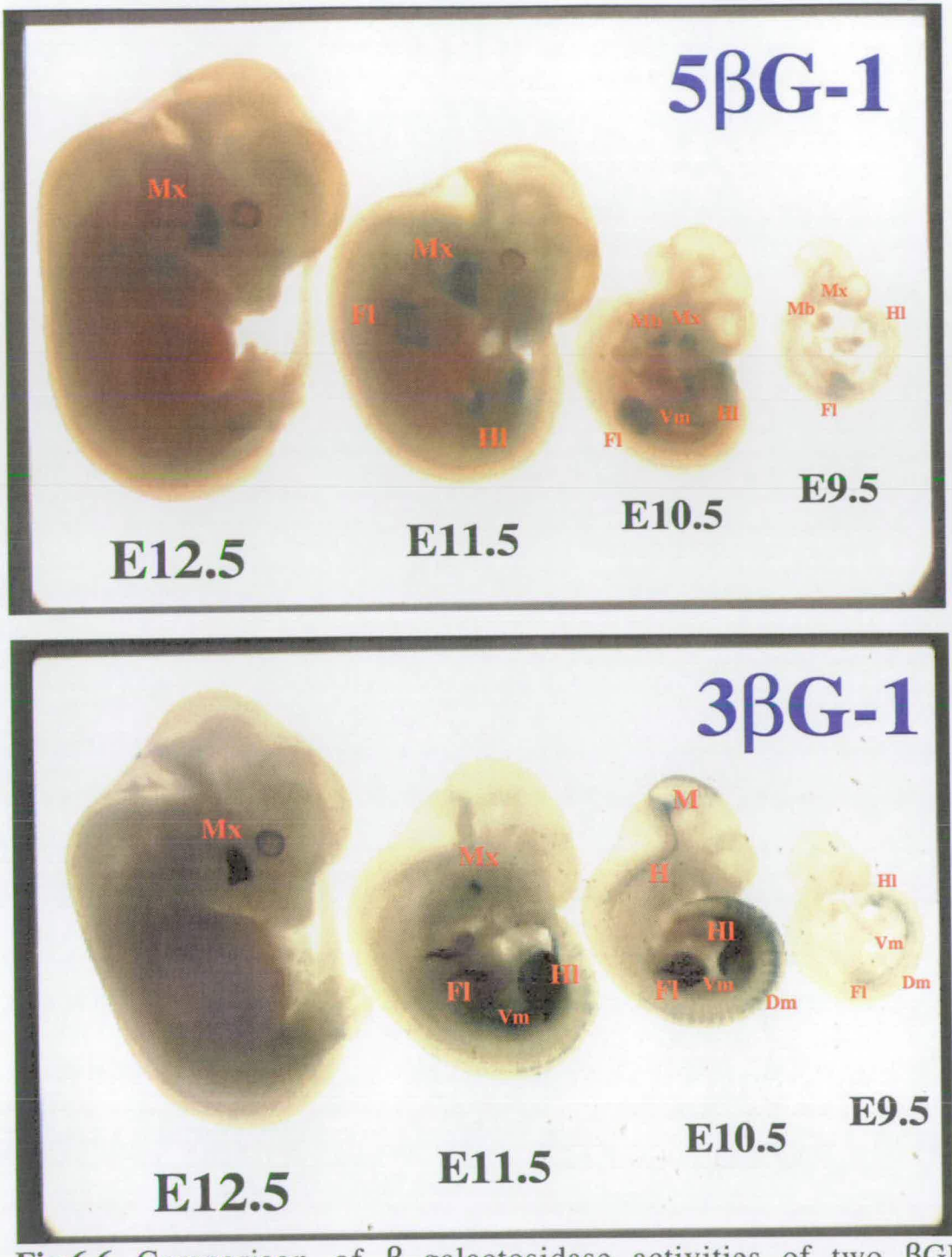

Fig.6.6 Comparison of β–galactosidase activities of two βGFP transgenic linesat E9.5, E10.5, E11.5 and E12.5. A). 5βG-1 line, expression ofβGFP under the control of 5 kb Msx1 promoter. B). 3βG-1 line, expression of βGFP under the control of 3 Kb Msx1 promoter. All embryos were fixed by 4% paraformaldehyde (PFA) and followed histochemistry x-gal staining. Mx, maxillary component of the first branchial arch; Mb, mandibular component of the first branchial arch; Fl, forelimb bud; Hl, hindlinb bud; M, mid brain, H, hind brain; Dm, dorsal mytome; Vm, ventral mytome.

addition, there was a very clear staining in ventral and dorsal myotome and somites from E9.5 to E11.5 embryos. The staining pattern in the mandibular component of the first arch was only seen at E11.5 and E12.5 embryos. Interestingly, a particularly strong staining pattern in the mid brain, somites and hind limb buds was seen in E10.5 embryos (**Fig.6.7**). The 5.0 kb and 3.0 kb Msx-1 promoters gave a different activity from E9.5 to E11.5 but showed a similar activity after E12.5.

The Msx-1 promoters thus showed spatial specific embryonic activity between E9.5 to E12.5. To more precisely understand the activity of βGFP at these stages, E10.5 embryos of 5βG-1 and 3βG-1 lines were examined as vibratome sections. In sagittal sections of x-gal stained E10.5 5βG-1 embryos, βGFP was detected at high levels in the mesenchyme of mandibular and maxillary arches (**Fig.6.8A & B**), the neuroepithelium of mid brain (**Fig.6.8C**), urogenital structures (**Fig.6.8D**), the neural retina layer of eye (**Fig.6.8E & F**), the apical ectodermal ridge (AER) of forelimb bud (**Fig.6.8G & H**), and the mesenchyme of hindlimb bud (**Fig.6.8I & J**). In sections of E10.5 3βG-1 embryos, analysis of whole embryos and sections showed no detectable βGFP activity in the mandibular and maxillary arches (**Fig.6.9A & D**) but did show particularly strong expression patterns in the hindlimb buds and somites (**Fig.6.9B & E**). There were also very similar x-gal staining patterns in TZ-1, GZ-1 and Z-1 lines and their patterns are summarised on Table 6.3 to Table 6.6.

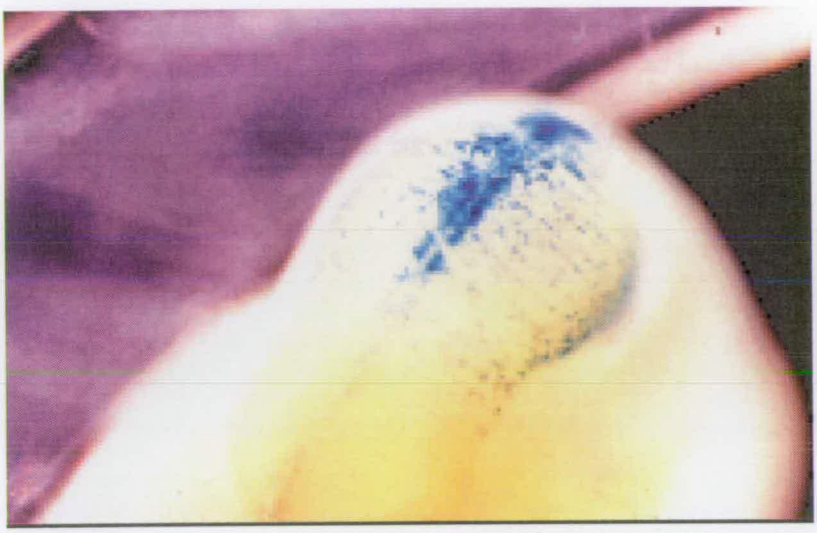

Fig.6.7A Whole mount x-gal staining in mid brain of E10.5 3βG-1 embryo.

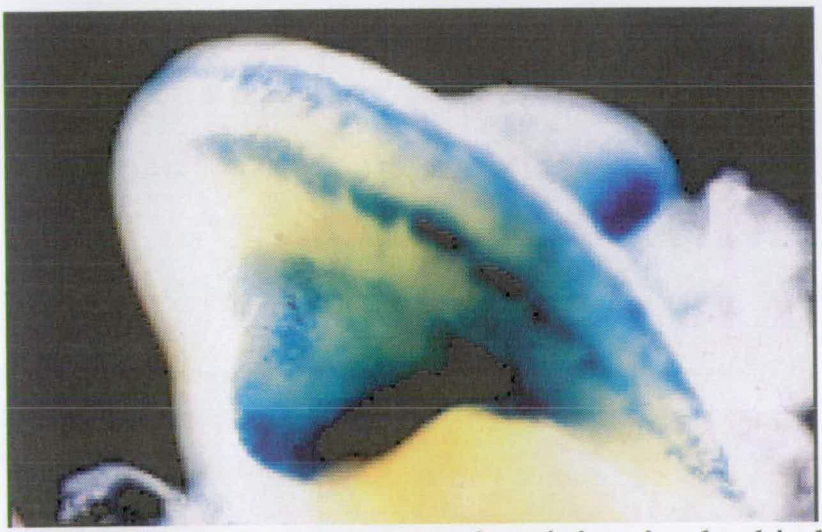

Fig.6.7B Whole mount x-gal staining in the hind limb buds and somites of E10.5 3βG-1 embryo.

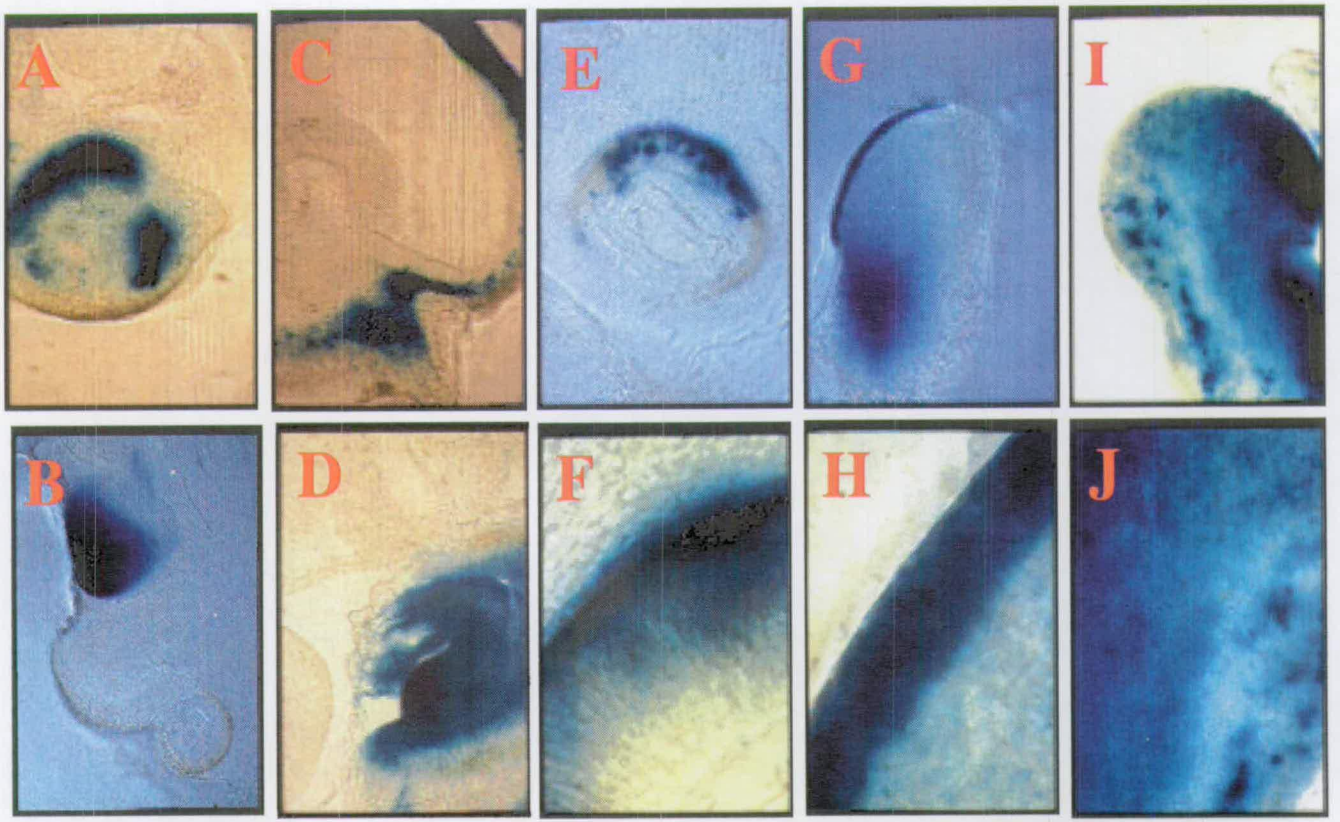

Fig.6.8 Vibratome sections (150 nm) of x-gal stained 5βG-1 embryo. Sagittal sections shown in **A)** mandibular arch; B). maxillary arch; C). mid brain; D). ureogenital ridge; E). eye (5X); F). neural retina layer (100X in E); G). forelimb bud (5x); H). apical ectodermal ridge (100x in G); I). hind limb bud(5x); J). mesenchyme (100X in I).

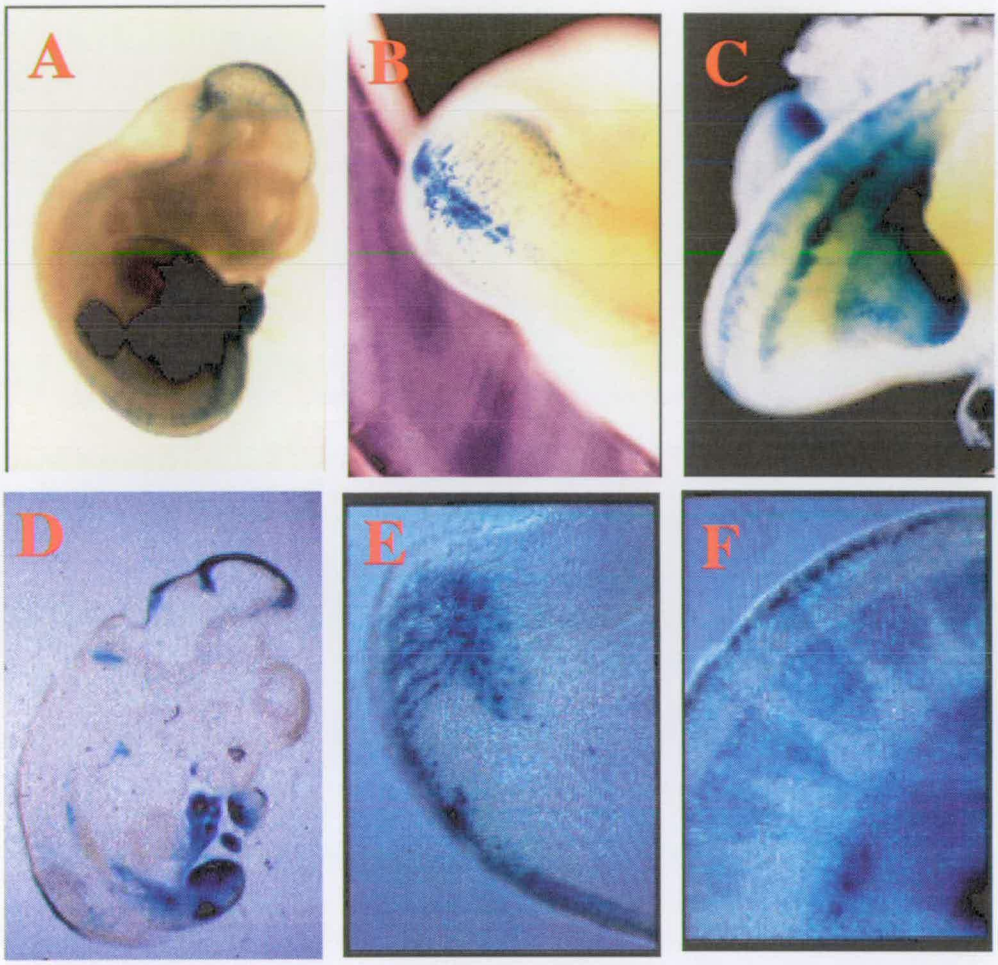

Fig.6.9 x-gal staining of expression in 3βG-1 embryos. **A)** Whole mount E10.5 embryos. High magnification view of midbrain **B)** and **C)** hindlimbs and somites. Vibratome sections (100μm) of the same embryo shown in **D)** Sagittal section of the same embryo in A. **E)** Sagittal section of the same region in B. **F)** Sagittal section of the somites in C.

Table 6.3 The summary of β–galactosidase staining patterns E9.5 transgenic embryos

	βGFP(β–galactosidase stating)									
Lines	Fpb	Mx	Mb	Fl	Hl	AER	Dm	Vm	E	M
5βG-1[a]	-	+	+	+	+/-	-	-	+	-	-
5βG-2[b]	-	-	-	+	+	-	-	+	-	-
3βG-1[b]	-	-	-	+/-	+	-	++	++	-	-
TZ-1[b]	-	+	+	++	+	-	-	+	-	-
TZ-2[b]	-	+	+	++	+	-	-	+	-	-
GZ-1[b]	ND	ND	ND	ND	ND	ND	ND	ND	ND	ND
Z-1[b]	-	+	+	++	+	-	-	+	-	-

Table 6.4 The summary of β–galactosidase staining patterns E10.5 transgenic embryos

	βGFP(β–galactosidase stating)										
Lines	Fpb	Mx	Mb	Fl	Hl	AER	Dm	Vm	E	M	Ge
5βG-1[a]	-	++	++	++	++	+++	-	+	-	+	-
5βG-2[a]	-	++	++	++	++	++	-	+	-	-	-
3βG-1[a]	-	-	-	+++	+++	-	+++	+++	-	++	++
TZ-1[a]	-	+	+	++	+	-	-	+/-	-	-	-
TZ-2[a]	-	+	+	+	+	-	-	+/-	-	-	-
GZ-1[a]	-	+	+	++	++	-	-	+	-	+	+
Z-1[a]	-	+	+	++	++	-	-	+	-	-	-

Table 6.5 The summary of β–galactosidase staining patterns E11.5 transgenic embryos

	βGFP(β–galactosidase stating)										
Lines	Fpb	Mx	Mb	Fl	Hl	AER	Dm	Vm	E	M	Ge
5βG-1[a]	-	+++	++	+	+	+	-	+/-	+	-	+/-
5βG-2[b]	-	+++	++	+	+	+	-	+	-	-	-
3βG-1[a]	-	++	-	++	++	-	+	++	-	+	++
TZ-1[b]	-	+	+/-	+	+	-	-	-	-	-	-

Table 6.6 The summary of β–galactosidase staining patterns E12.5 transgenic embryos

	βGFP(β–galactosidase stating)										
Lines	Fpd	Mx	Mb	Fl	Hl	AER	Dm	Vm	E	M	Ge
5βG-1[a]	+	+++	-	+/-	+/-	-	-	-	-	-	-
5βG-2[b]	+	+++	-	+/	+/-	-	-	-	-	-	-
3βG-1[a]	-	+++	-	+/-	+/-	-	-	-	-	-	-
TZ-1[b]	+	++	-	-	-	-	-	-	-	-	-

a. Those patterns were obtained from the x-gal histochemical stain of whole mount embryo and vibratome sections of each lines. **b.** Those patterns were only obtained from the x-gal histochemical stain of whole mount embryo . -, No expression; +/-, low expression; +, moderate level of expression; ++, high level of expression. +++, highest level of expression. d. Fp, frontonasal process; Mx, maxillary component of the first branchial arch; Mb, mandibular component of the first branchial arch; Fl, forelimb; Hl, hindlimb; AER, apical ectodermal ridge; Dm, dorsal myotome; Vm, ventral myotome; E, the neural retina layer of developing eye, M, mid brain; Ge, genital structure.

Taken together, these results imply that the Msx-1 promoter has a high level of activity at embryonic stages from E9.5 to E12.5 and is expressed in specific tissues. The developmentally regulated activity of the 5 kb Msx-1 promoter implies that the expression of the Msx-1 gene provides different levels of Msx-1 proteins resulting in dynamic and morphological changes in embryonic tissues during embryogenesis. In fact, the expression of the 5 kb and 3.5 kb Msx-1 promoter is comparable to that recently published (MacKenzie et al. 1997).

6.6 Detection of GFP expression in transgenic mice

As stated previously, β-galactosidase activity in these lines of mice predicted the location of GFP activity in the dicistronic transgenic (TZ, GZ, and Z) and the fusion βGFP lines (5βG-1, 5βG-2 & 3βG-1). In both constructs, β-galactosidase activity would directly indicate the GFP activity and signal intensity of these transgenic lines.

6.6.1 A comparison of GFP fluorescent activity in βGFP, TFP and wild

type GFP

Embryos from the 5βG-1, 5βG-2, 3βG-1, TZ1, TZ2, GZ1 and Z1 lines were first analysed by β–galactosidase staining and then were prepared for 150μm vibratome sections. Fluorescent images were captured on a photometric cooled charge-coupled device (CCD) camera using IPlab imaging software and a standard fluorescein filter cube. As shown in sections of 5βG-1 embryo **(Fig.6.10)**, a strong green fluorescence was seen in the ventral myotome, somites and dorsal myotome at E9.5 **(Fig.6.10A)**. The E10.5 embryo showed green fluorescence in maxillary and mandibular arches, mid brain, limbs and somites **(Fig.6.10B)**. Fluorescent signals were more easily detectable in the frontonasal process **(Fig.6.10C&D)** in E11.5 and E12.5 embryos. In the 3βG-1 E10.5 embryos, a particularly strong fluorescence was seen in the ventral myotome, urogenital ridge and hind limb bud **(Fig.6.10E)**. Interestingly, there were similar fluorescent patterns between 5βG-1 **(Fig.6.10B)** and TZ-1 **(Fig.6.10F)** E10.5 embryos. However, TZ-1 embryos gave a weaker and less stable fluorescence and no detectable fluorescent signals was seen in GZ-1 E10.5 embryos **(Fig.6.10G)** and Z1 E10.5 embryos **(Fig.6.10H)**.

Both GFP fluorescence and β-galactosidase activity in βGFP transgenic embryos was stable after a series of gentle chemical treatments. Comparison of GFP green fluorescence and blue staining

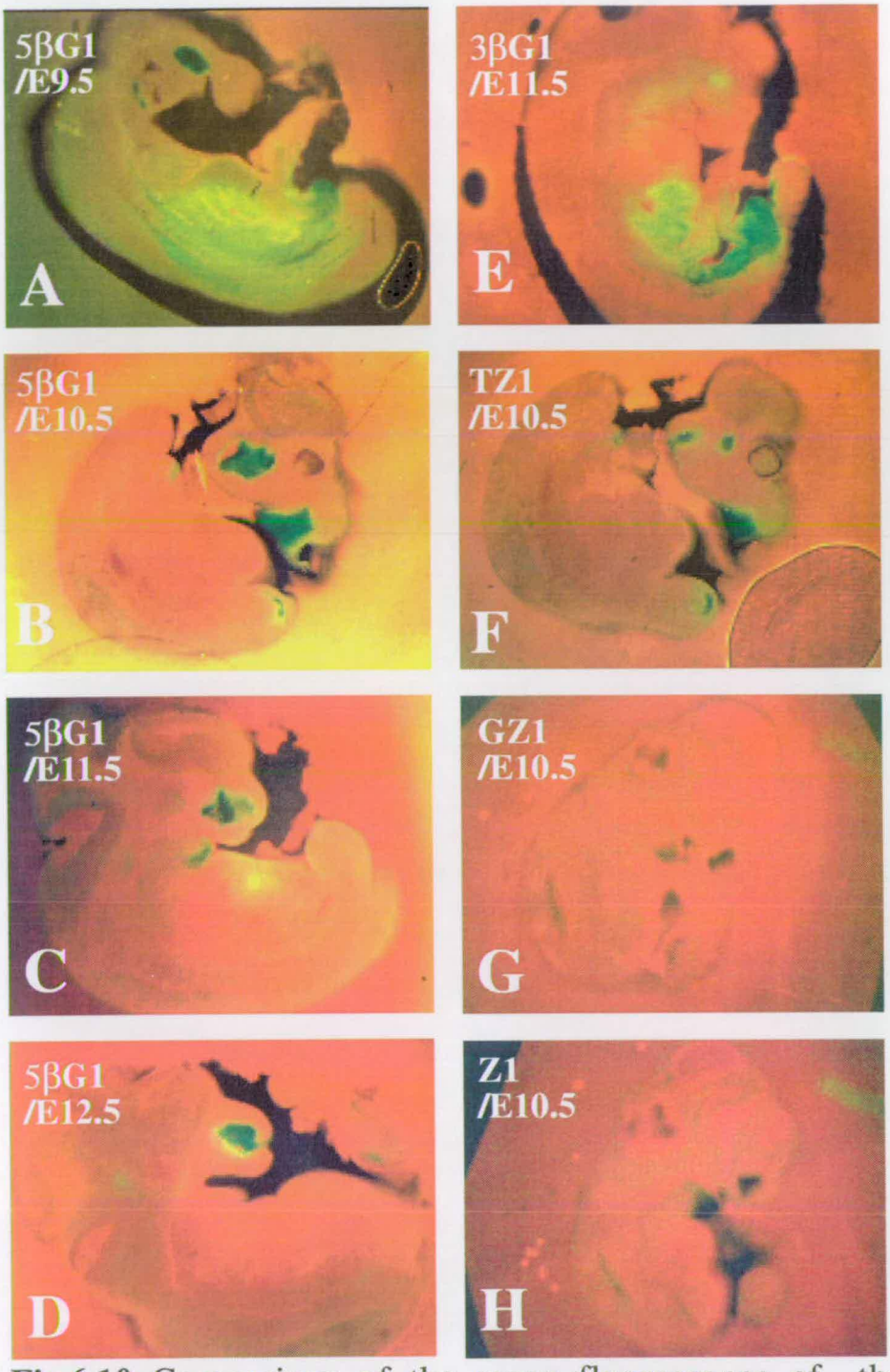

Fig.6.10 Comparison of the green fluorescence of the transgenic lines. 5βG-1 (E9.5-E12.5) **A-D**), 3βG-1 (E11.5) **E**),TZ1(E10.5) **F**) and GZ-1 lines (E10.5)**G**). The E10.5 Z-1 embryo was a negative control of green fluorescenceshown in **H**). The embryos were fixed at 4% paraformaldehyde and were followed by histochemistry x-gal staining. The stained embryos were prepared for vibratome sections (100 μm). The fluorescent images was visualised by a CCD camera conjugated fluorescence microscopy using using FITC and Texas Red filter.

showed identical patterns in the 5βG-1 and TZ-1 embryos (**Fig.6.11**). Using a fluorescent (FITC& Texas red) field, 5βG-1 embryos showed superimposed images(**Fig.6.11A,C&D**) which were overlapped by green fluorescence and blue shadow (x-gal blue products were not responsive to FITC and Texas red wavelength (**Fig.6.10G&H**). Similarly, in bright field (visible light), a blue patterns was seen at exactly same positions but no fluorescent signals (**Fig.6.11E,G&H**). In bright field, the TZ1 embryo showed strong blue stain. However, in the fluorescent field, it showed weak GFP fluorescence (the weak fluorescence was seen after 5-10 min exposured under the 450-490 nm light sources). This might be due to the lower fluorescent activity and stability of TFP than βGFP.

GFP fluorescence was more sensitive than β-galactosidase activity in most transgenic embryos. X-gal substrates perhaps penetrated poorly into embryonic tissues giving weak histochemical blue staining. In fact, in 5βG-1 embryos, there was a patchy green fluorescent signal in the eye but no blue stain in the same section (**Fig.6.12A**). The β-galactosidase only showed a sporadic activity in the forelimb (**Fig.6.12C**), hindlimb, (**Fig.6.12G**) mandibular arch (**Fig.6.12F**) and maxillary arch (**Fig.6.12A**). However, the surface embryonic tissue such as mid brain showed relatively stronger blue stain than GFP fluorescence (**Fig.6.12D**). In deep sections, inner tissues showed only very weak blue staining but strong green fluorescence such as the same maxillary position of Fig.6.13A in **Fig.6.12E** and somites (**Fig.6.12H**).

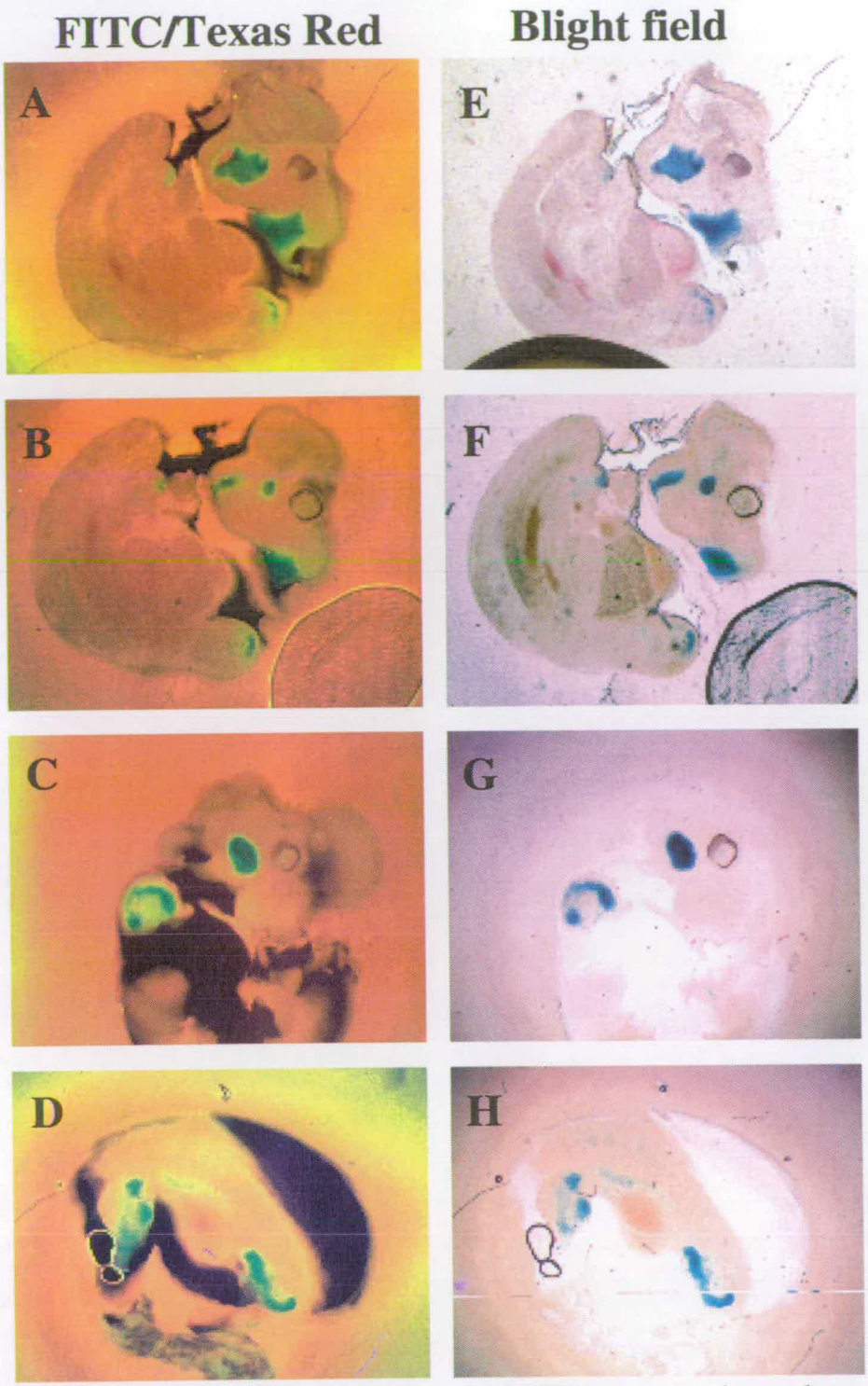

Fig.6.11 Superimposed images of GFP transgenic embryos. Vibratome sections (150μm) of 5βG-1&2 and TZ-1 transgenic embryos showing identical GFP fluorescent and x-gal blue stain patterns. The green fluorescence was visualised using FITC and Texas Red filters in the fluorescent field and shown in **A)** βG-1/E10.5, **B)** TZ-1/E10.5, **C)** βG-2/E11.5, **D)** βG-1/E10.5. The same sections were visualised using normal light for full colour images in the bright field and shown in **E)** the same embryo in A, **F)** the same embryo in B, **G)** the same embryo in C, **H)** the same embryo in D.

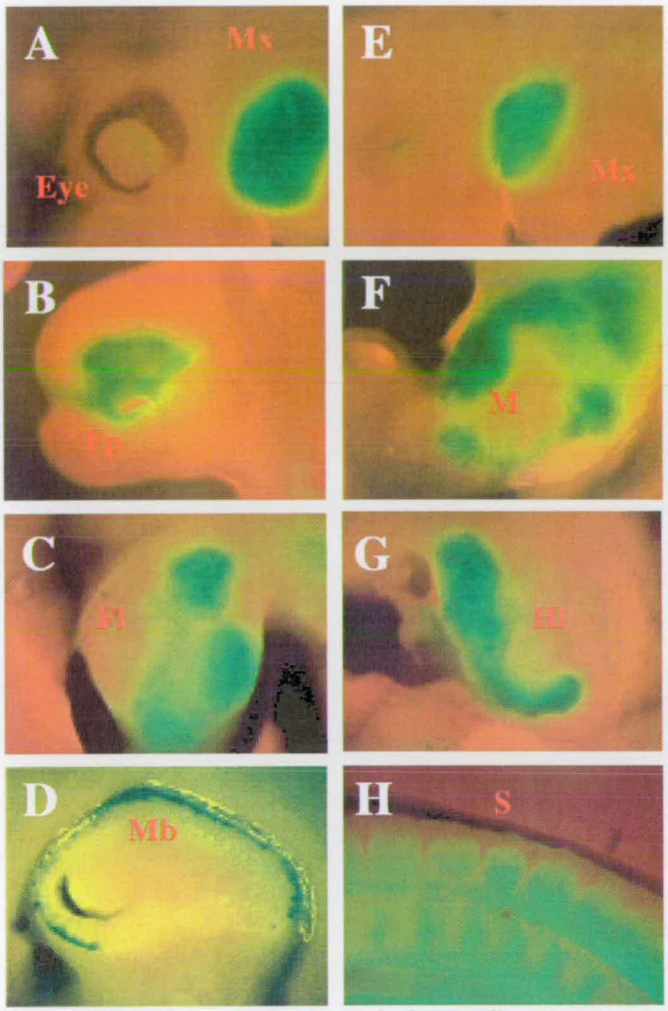

Fig.6.12 Comparison of GFP fluorescence and β-galactosidase activity of βGFP in 150 μm vibratome sections of 5βG-1 embryos. Green fluorescence was visualised using FITC and Texas Red filter and shown in **A)** eye and maxillary arch (Mx), **B)** frontonasal process (Fp), **C)** forelimb (Fl); **D)** midbrain (Mb)(frontal section), **E)** the same position in A, **F)** mandibular arch (M), **G)** hindlimb (Hl), **H)** somites (S). The fluorescent images was visualised by a CCD camera conjugated fluorescence microscopy using using FITC and Texas Red filter.

Thus, the double-reporter transgenic constructs did provide a more efficient way to check the GFP activity in transgenic embryos. Compared with the β-galactosidase activity, the wild-type GFP was not sensitive enough as a fluorescent marker under the control of the Msx-1 promoter but TFP (GFP-S65T) had detectable fluorescent signals. Most interestingly, βGFP was more stable and sensitive than the TFP/IRESLacZ transgene (TZ-1 line) in vivo. By using these strategies, the green fluorescent patterns of 3 βG lines (5βG-1,5βG-2 & 3βG-1) and 2TZ lines were defined (**Table 6.7**) for further analysis and application.

Table 6.7 The expression of transgenes in transgenic (tg) lines.

Line No. (No of TG)	Green fluorescence		Blue stain		pattern similarity[a]
	+	-	+	-	
5βG(5)	3	2	3	2	3
3βG(3)	1	2	1	2	1
αG(4)	1	3	0	0	1
TZ(3)	2	1	3	0	2
GZ(3)	0	3	2	1	2
Z(2)	0	2	2	0	2

a. The pattern similarity was compared by the green fluorescence and blue stain more than one embryos for each lines.

6.6.2 Identification of single green fluorescent cells in embryonic tissues

To identify green fluorescent cells in embryonic tissues in βGFP transgenic embryos, cryosections were prepared from E10.5 and E11.5 5βG-1 embryos.

In the facial region, vibratome sections (150μm) of E11.5 5βG-1 embryos showed strong green fluorescence in patches including maxillary (**Fig.6.13A**) and mandibular (**Fig.6.13D**) components of the

first branchial arches and frontonasal process (**Fig.6.13G**). However, cryosections (10μm) of similar embryonic tissues showed many green fluorescent spots indicating many GFP labelled cells (5X) (**Fig.6.13B, E &H**). Further, many individual mesenchymal cells (**Fig.6.13C, F &I**) expressing different levels of GFP were seen under high magnification (40X) of fluorescence microscopy.

In genital structures, vibratome sections (150μm) of E10.5 3βG-1 embryos showed a particular strong green fluorescence (**Fig.6.14A**) and blue stain (**Fig.6.8D**) in the urogenital ridge and its relative embryonic structures. Cryosection of the same region also showed a strong fluorescence in the urogenital ridge (**Fig.6.14B & C**). Strong fluorescent cells could be clearly visualized in the urogenital tissue at higher magnification (40X) (**Fig.6.14D**).

In somites, green fluorescence was more clearly detectable in cryosection (**Fig.6.15A & B**) than vibratome section (**Fig.6.12H**). Single cells highly expressed GFP protein in the E10.5 3βG-1 embryo (**Fig.15C&D**). Similarly, strong green fluorescence was also seen in the mesenchymal cells of the limb of E9.5 3βG-1 embryos (**Fig.6.16**).

Cryosections of βGFP transgenic embryos gave a detailed analysis of green fluorescence in embryonic structures. Clear fluorescent signals could be seen at the single cell level indicating that βGFP was highly expressed under the control of Msx-1 promoter in those tissues and its fluorescent activity was also very stable. Green fluorescent patterns of other GFP transgenic lines were also examined as above and are summarised on **Table 6.8-6.11**.

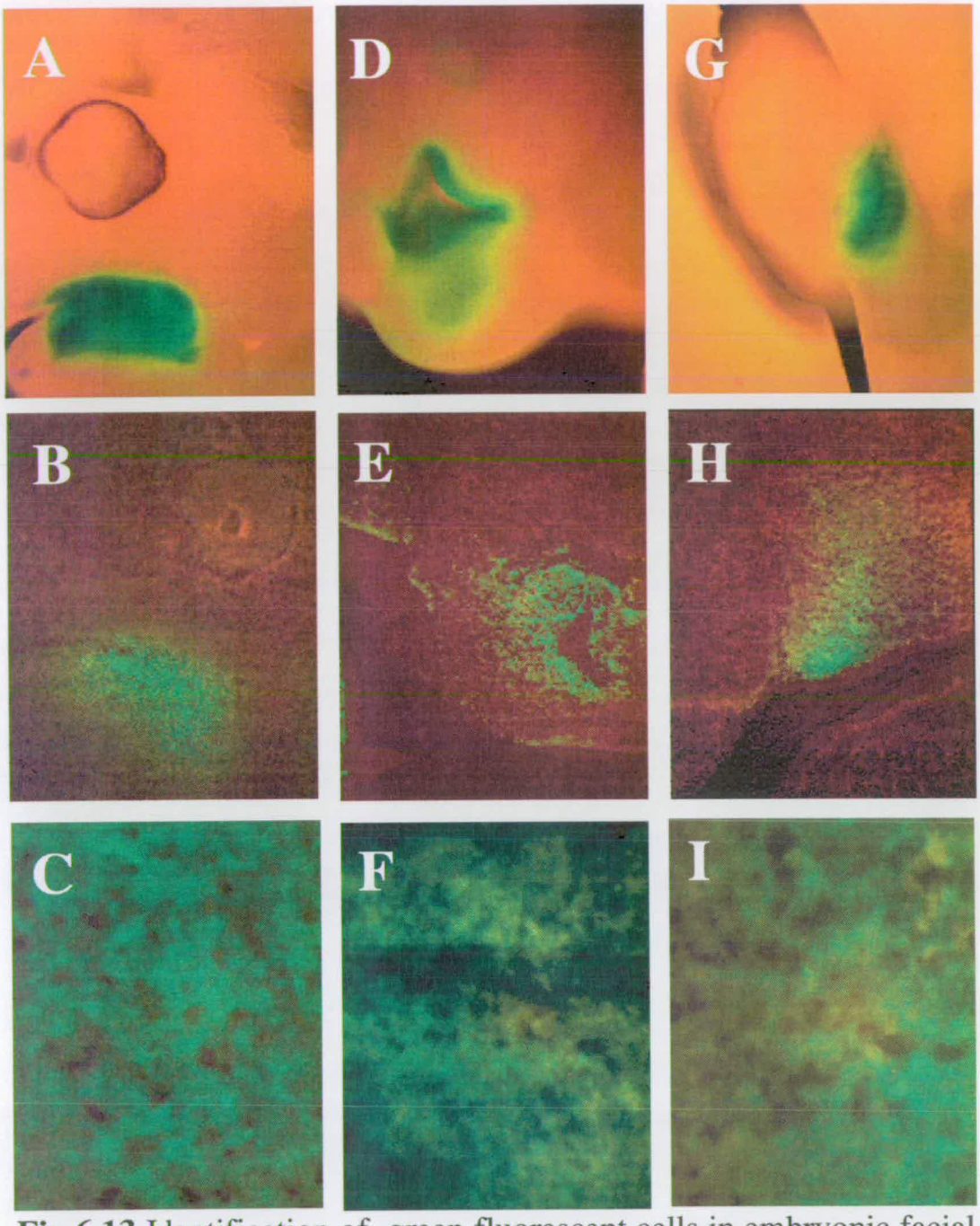

Fig.6.13 Identification of green fluorescent cells in embryonic facial structures of E11.5 5βG-1 embryos. **A-C** Maxillary arch, **D-F** fronotonasal process, **G-I** mandibular arch. **A, D & G,** 150μm vibratome section at 5X magnification. **B, E & H**, 10μm cryosections at 5X magnification. **C, F & I,** 10μm cryosections at 40X magnification. The fluorescent images was visualised by a CCD camera conjugated fluorescence microscopy using using FITC and Texas Red filter. .

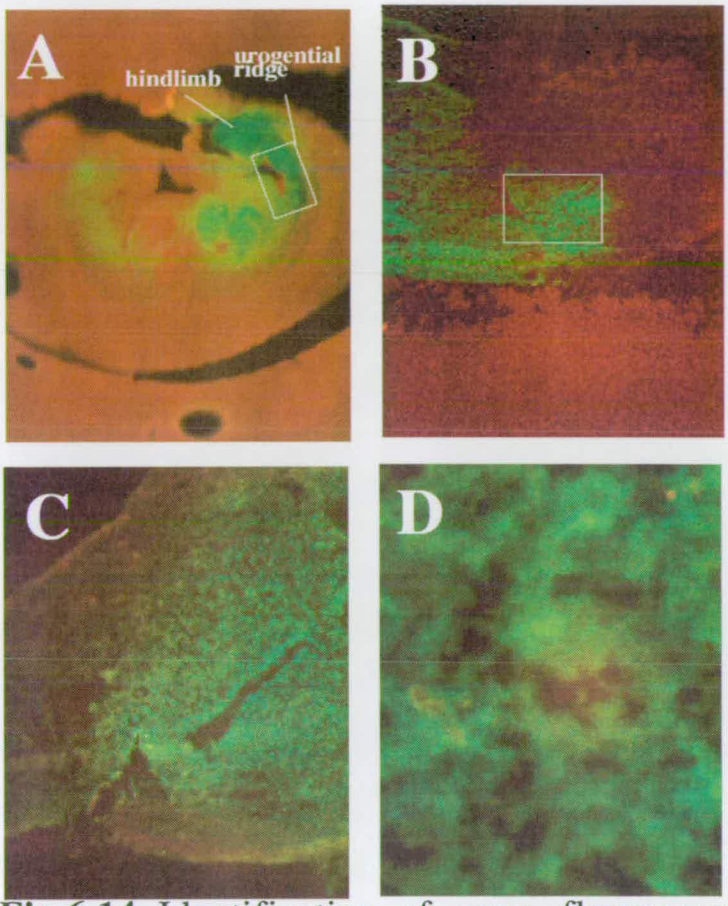

Fig.6.14 Identification of green fluorescent cells in embryonic genital structures ofβG-1 embryos. **A)** Sagittal vibratome section (150μm) of a E10.5 embryo showing the strong fluorescence in urogential ridge (1.25X). Sagittal cryostat section (10μm) at **B)** 2.5X, **C)** 5X and **D)** 40X magnification. The fluorescent images was visualised by a CCD camera conjugated fluorescence microscopy using using FITC and Texas Red filter.

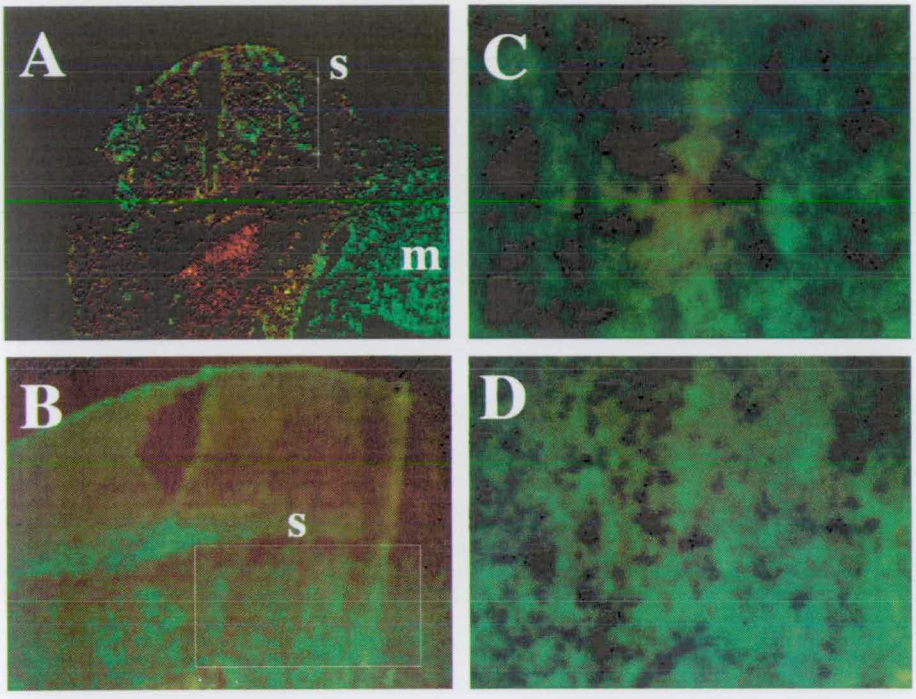

Fig.6.15 Identification of green fluorescent cells in somites of 3βG-1 embryos. **A**). transvere cryostat section (10μm) of a E10.5 embryo showing strong fluorescence in somite(S) and limb mesenchyme(m) (2.5X), **B)** Sagittal cryostat section (10 μm) (2.5 X), **C**) fluorescent cells in the selected area in A (40X). **D**) fluorescent cells in the selected area in B (20X). The fluorescent images was visualised by a CCD camera conjugated fluorescence microscopy using using FITC and Texas Red filter.

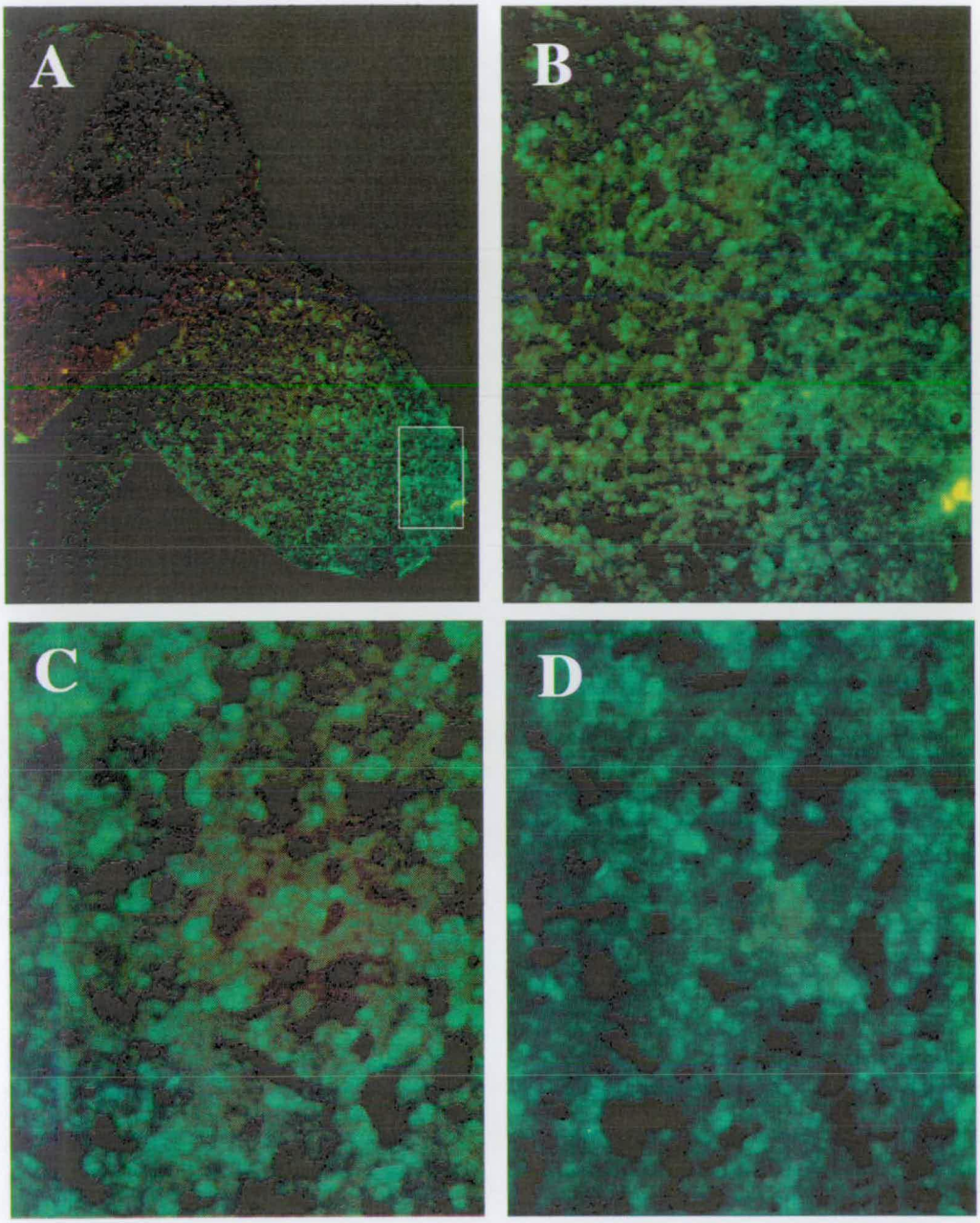

Fig.6.16 Identification of green fluorescent cells in the limb mesenchyme of 5βG-1 embryos. **A**) traverse cryostat section (10μm) of a E9.5 embryo showing strong fluorescence in limb mesenchyme (2.5X).Fluorescent cells in the selected area in A at **B**) 10X, **C**) 20X and **D**) 40X maganification. The fluorescent images was visualised by a CCD camera conjugated fluorescence microscopy using using FITC and Texas Red filter.

Table 6.8 The summary of green fluorescent patterns E9.5 βGFP embryos

	βGFP(green fluorescence)									
Lines	Fpb	Mx	Mb	Fl	Hl	AER	Dm	Vm	E	M
5βG-1[a]	-	+	+	+	+	-	++	++	-	-
3βG-1[a]	-	-	-	+/-	+	-	+	++	-	-

Table 6.9 The summary of green fluorescent patterns E10.5 GFP embryos

	βGFP(green fluorescence)										
Lines	Fpb	Mx	Mb	Fl	Hl	AER	Dm	Vm	E	M	Ge
5βG-1[a]	-	++	++	++	++	++	-	+/-	+	+/-	+/-
5βG-2[a]	-	++	++	++	++	+	-	+	+/-	-	-
3βG-1[a]	-	-	-	+/-	+	-	+++	+++	-	+	+++
αG-1[b]	-	+	+	++	+	-	-	-	-	-	-
TZ-1[a]	-	+/-	+/-	+	+	-	-	-	-	-	-
TZ-2[c]	-	+/-	+/-	+/-	+/-	-	-	-	-	-	-
GZ-1[c]	-	-	-	-	-	-	-	-	-	-	-
Z-1[c]	-	-	-	-	-	-	-	-	-	-	-

Table 6.10 The summary of green fluorescent patterns E11.5 βGFP embryos

	βGFP(green fluorescence)										
Lines	Fpb	Mx	Mb	Fl	Hl	AER	Dm	Vm	E	M	Ge
5βG-1[a]	-	+++	++	+	+	+	-	+/-	+	-	+/-
3βG-1[a]	-	++	-	++	++	-	+	++	-	+	++

Table 6.11 The summary of green fluorescent patterns E12.5 βGFP embryos

	βGFP(green fluorescence)										
Lines	Fpb	Mx	Mb	Fl	Hl	AER	Dm	Vm	E	M	Ge
5βG-1[a]	+	+++	-	+/-	+/-	-	-	-	-	-	-
3βG-1[a]	-	+++	-	+/-	+/-	-	-	-	-	-	-

a These patterns were obtained from the analysis of vibratome , and cryosections of mouse embryo of each lines. **b** These patterns were only obtained from crystal sections. **c** Those patterns were only obtained from vibratome sections. -, No expression; +/-, low expression; +, moderate level of expression; ++, high level of expression. +++, highest level of expression. Fp, frontonasal process; Mx, maxillary component of the first branchial arch; Mb, mandibular component of the first branchial arch; Fl, forelimb; Hl, hindlimb; AER, apical ectodermal ridge; Dm, dorsal myotome; Vm, ventral myotome; E, the neural retina layer of developing eye, M, mid brain; Ge, genital structure.

6.7 GFP fluorescence in living or unfixed transgenic embryos

To visualize green fluorescence in living or unfixed tissue and also to consider the optic resolution, a limb bud was taken from E10.5 TZ-1 embryos and the cultured E8.5 5βG-1 embryo were examined by the CCD chimera. However, the green fluorescent signals could only be seen in the surface tissues of limb **(Fig.6.17A)** and a blurry signal was detected in E8.5 5βG-1 embryo **(Fig.6.17B)**. To obtain fluorescent images from these embryos, optical sections were taken by confocal microscopy.

In the confocal images of 5βG-1 and TZ-1 embryos, clear green fluorescence was detected in many embryonic structures of E10.5 /9.5 embryos, including mid brain **(Fig.6.18A)**, surrounding mesenchyme of forelimb bud **(Fig.6.18B)**, apical ectodermal ridge (AER) of limb **(Fig.6.18C)**, neural retina of eye **(Fig.6.18D)**, mandibular arches **(Fig.6.18E)** and somites **(Fig.6.18F&G)**. The nontransgenic embryos did not show significant fluorescent signals **(Fig.6.18H)**. The extensive fluorescence was found in the mid brain region surrounding by neural ectoderm and continuous fluorescent signals were also detected in whole brain tissues **(Fig.6.19)**. To detect GFP expression in a living embryos, E8.5 5βG-1 embryos were cultured for 3-6 hours and then were reexamined by fluorescence confocal microscopy. Fluorescent signals could only be detected on the head fold region of the cultured embryo **(Fig.6.20)**

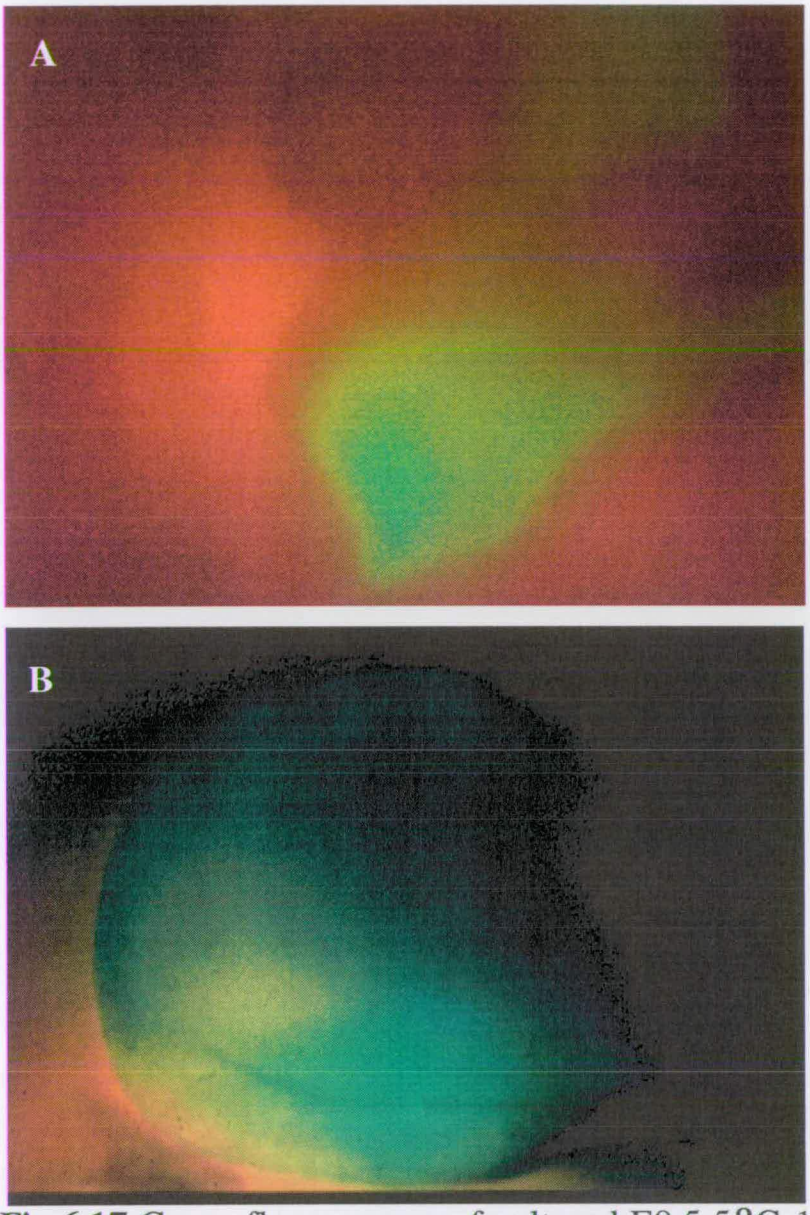

Fig.6.17 Green fluorescence of cultured E8.5 5βG-1 embryo in **A** and unfixed hindlimb of E10.5 3βG-1 embryo in **B**. The embryo was cultured for 6 hours at DMEM containing 50% rat serium. The fluorescent images was visualised by a CCD camera conjugated fluorescence microscopy using FITC filter.

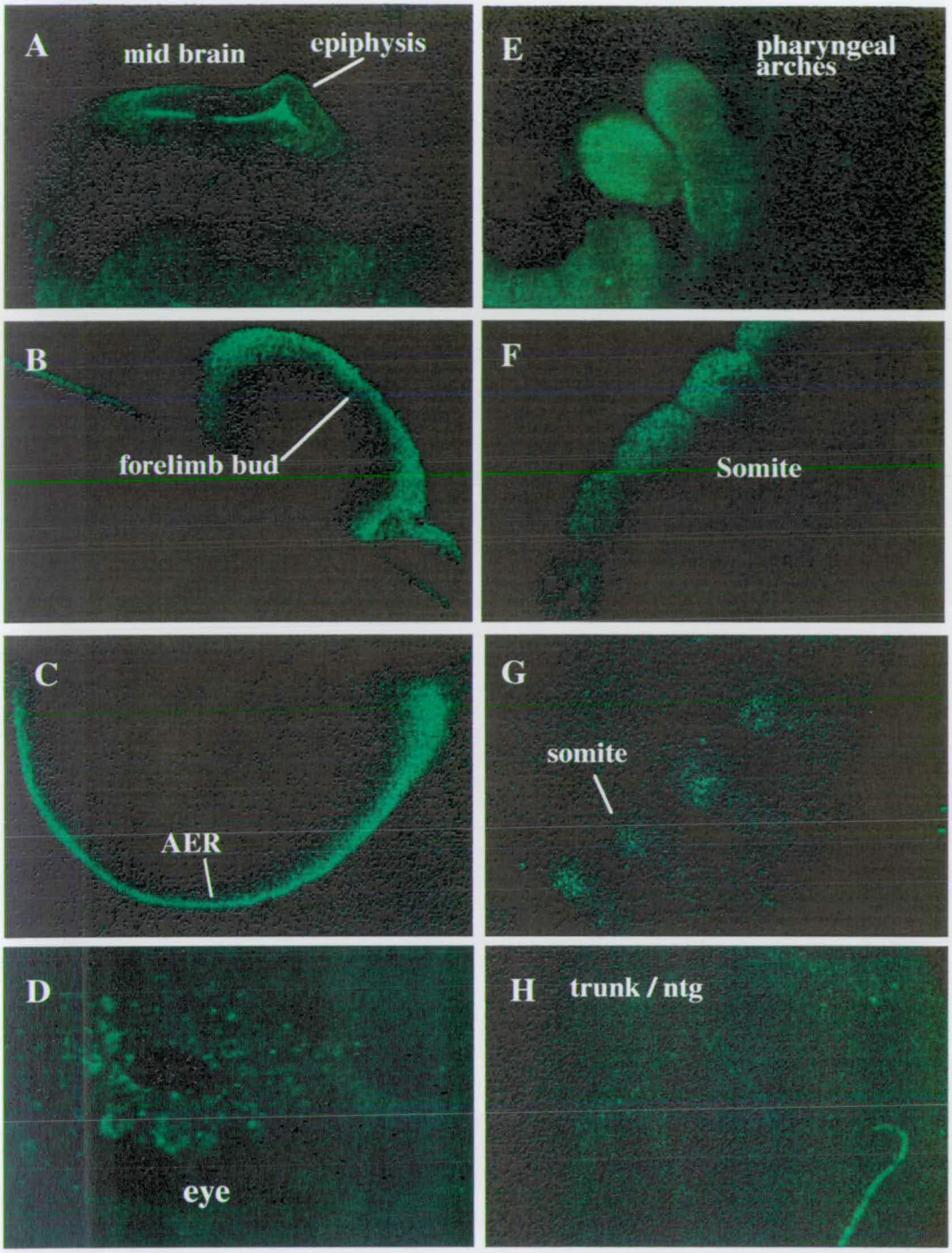

Fig.6.18 Optical sections (10μm) of images from fresh (unfixed) 5βG-1/ TZ-1 embryos obtained by confocal microscopy (10X). **A)** mid brain (E10.5/TZ-1). **B)** forelimb bud (E10.5/TZ-1). **C)** apical ectodermal ridge (AER) (E10.5/TZ-1). **D)** neural retina layer of eye (E10.5/ 5βG-1). **E)** pharyngeal arches (E10.5/5βG-1). **F)** somites (E10.5/ 5βG-1). **G)** somites (E9.5/5βG-1). **H)** trunk of nontransgenic embryo (E10.5).

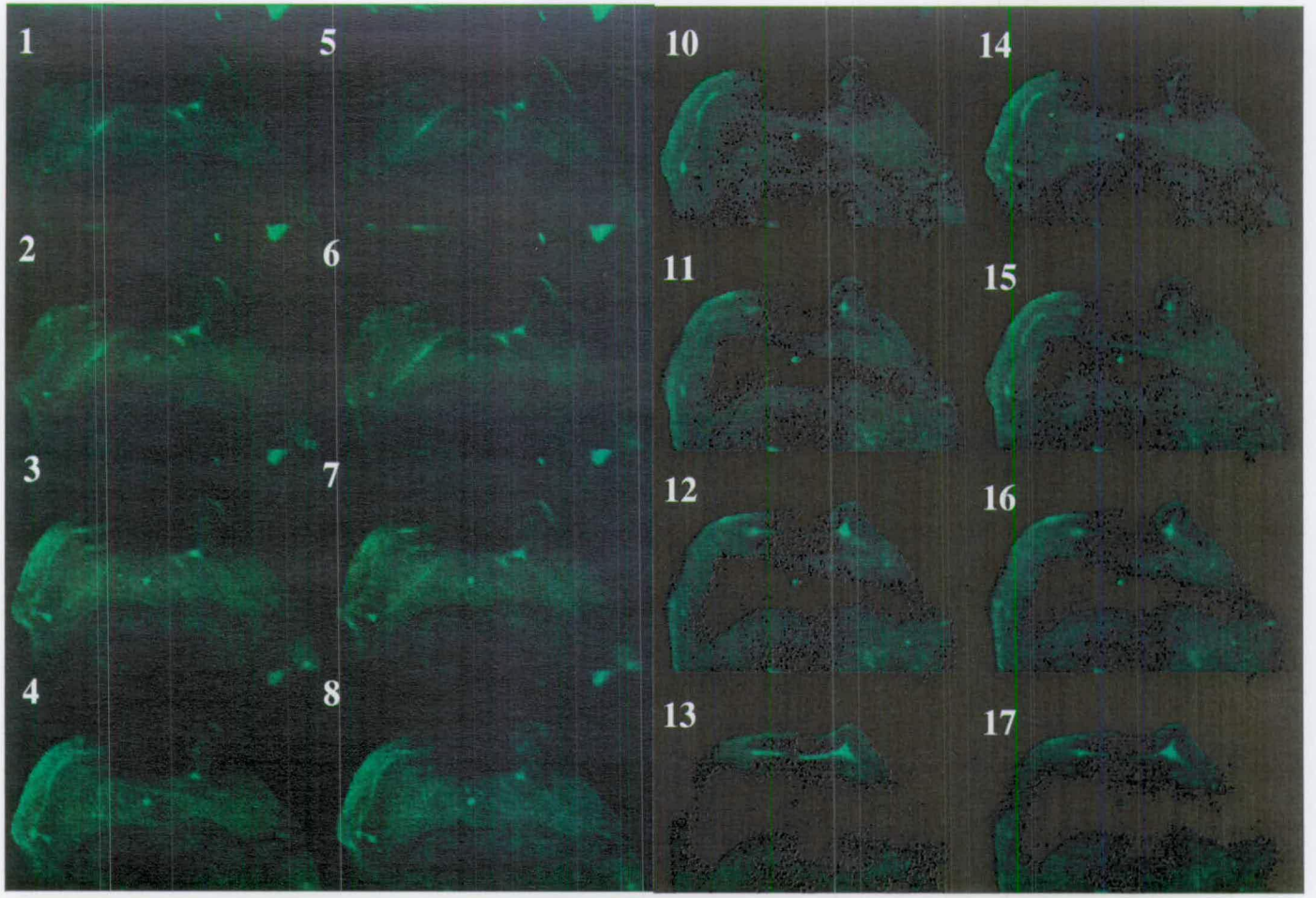

Fig.6.19 A series of optical sections (10μm) through the brain region of E10. 5 TZ-1 embryos.

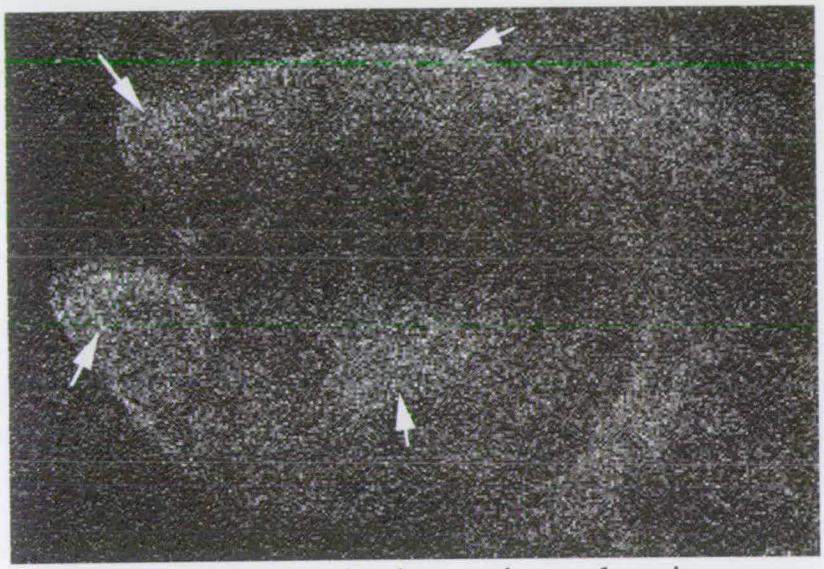

Fig.6.20 10μm optical section showing green fluorescence in the brain region (arrow) of a cultured E8.5 5βG-1 embryo (10X). The embryo was cultured for 6 hours at DMEM containing 50% rat serum. The fluorescent signal was visualised by confocal microscopy using FITC filter.

These results suggested that those transgenic embryos can efficiently express GFP at a developmentally regulated level driven by an embryonic specific promoter. GFP is also nontoxic and stable in embryos.

6.8 Discussion

6.8.1 β–GFP behaves as a dual functional marker

βGFP (5βG1-2 or 3βG-1) embryos and TZ-1 embryos showed both GFP fluorescence and β–galactosidase activity in mammalian cells and embryos. This implies that the βGFP and the dicistronic reporter gene were stably produced in transgenic embryos. Although both types of double reporter constructs could express the activities of GFP and β–galactosidase in a single cell, βGFP consistently gave higher expression levels of the two reporter proteins. Perhaps, the cap independent translation via the viral IRES sequence was not as efficient during mouse embryogenesis. A similar activity of GFP / β–galactosidase fusion protein has been successfully shown in *Drosophila embryos* and gave both green fluorescent signals and blue stain (Shiga et al. 1996; Timmons et al. 1997). These results indicate that βGFP behaves like a dual function reporter. The β–galactosidase provides a valuable control which may be important in setting up the reporter assay or used as substitute in cases which expression is low and GFP is not easily assayed.

6.8.2 Sensitivity of green fluorescence in βGFP transgenic embryos

There were different sensitivities between GFP fluorescence and β–galactosidase activity when the double reporter constructs were used as markers in transgenic embryos. In general, the expression patterns of GFP and β–galactosidase were similar in many embryonic tissues of transgenic lines. However, GFP fluorescence in some tissues was more sensitive than β–galactosidase blue staining, such as internal tissues of maxillary and mandibular arches, limbs and somites. In cryosection analysis, a single fluorescent cell was particularly easy to detect by fluorescence microscopy but the β–galactosidase blue staining was almost invisible. In optical sections, green fluorescent signals were very clear in tissues of whole mount unfixed embryos. In fact, green fluorescent signals from the fresh (living or unfixed) embryos were also particularly stable compared with the fixed embryo. This may be due to de novo GFP production in the tissues and compensation for the lost fluorescent activity caused by photobreaching (Heim et al. 1994; Kaether et al. 1995; Lim et al. 1995; Ogawa et al. 1995; Pines 1995; Webb et al. 1995). In addition, there were some tissues which showed weak fluorescence, including the AER and surface tissues in midbrain. Perhaps, GFP may not mature or unstable in some mouse embryonic tissues. Some *Drosophila* tissues may inhibit GFP maturation and interfere with GFP fluorescence to varying degrees through unknown mechanisms (Timmons et al. 1997). On the other hand, Msx1 promoter may have varying activity dependent on the tissue.

These results suggest that the histochemical process of x-gal staining (the pentration, enzymatic catalysis and fixation) may not penetrate into internal embryonic tissues resulting in low blue products.

6.8.3 The Msx1 promoter expressed in a similar embryonic patterns during embryogenesis as the endogenous Msx1 gene.

Although the initial characterisation of the mouse Msx-1 promoter showed its activity in E9.5 to E12.5 embryos, Msx-1 endogenous gene expression showed embryonic activity between E6.5 and E16.5 (Hill et al. 1989; Houzelstein et al. 1997; Robert et al. 1989). This difference may be due to a lack of some regulatory elements far from the 5' or 3' untranslated regions of the Msx-1 gene (Kuzuoka 1994; MacKenzie et al. 1997). Actually, two enhancer domains, DE and PE, have been identified within the 5 kb Msx-1 promoter (MacKenzie et al. 1997). Although the developmental role of the DE and PE is still unclear, they activate independent transcription via a heterologous promoter (MacKenzie et al. 1997). The different expression patterns driven by 5.0 kb and 3.5 kb of the Msx-1 promoter was probably due to the "DE" enhancer located at the 5' end of 5 kb promoter. This enhancer element is lacking in the 3.5 kb promoter.

6.8.4 The requirement of GFP fluorescent detection in the transgenic mouse embryos

Wild-type GFP in the cytoplasm must be at a concentration of 1.0 μM to obtain a fluorescent signal (under blue light) in mammalian cells (Hela cells) (Niswender et al. 1995). For other GFP derivatives, 0.2 μM of GFP-S65T and 0.03 μM of EGFP is needed for the same level of detection compared to wild-type GFP illuminated at 490 nm (Clontech 1997).

In this study, βGFP (a humanised GFP containing the enhanced fluorescent mutations), TFP (a wild-GFP containing a S65T mutation) and wild-type GFP were used as markers under the control of the Msx-1 promoter in transgenic mice. All fluorescent signals were detected in three of five βGFP transgenic lines, two of three TFP transgenic lines but no detectable fluorescence in wild-type GFP. βGFP showed a strong fluorescence in mammalian cells (Chapter 3) and βGFP transgenic lines showed easily detectable fluorescence in embryos. TZ-1 line also showed detectable fluorescence in embryos but its photostability was less than βGFP transgenic lines due to it being more sensitive to photobleaching (the TFP fluorescent signals dimmed more quickly than βGFP fluorescent signals). However, the detected fluorescence in the TFP lines (TZ-1 and TZ-2) was perhaps due to transgene insertion position resulting in optimal TFP expression as the fluorescence of TFP in mammalian cells was obviously weaker than βGFP fluorescence. Besides, βGFP may also increase the protein stability as the β–galactosidase may increase the half-life of the fusion molecules in cell (Kain 1997). Although the transgene copy number in those fluorescent lines was not determined in this study, there was no correlation between transgene copy number and GFP fluorescent expression in other GFP trangenic animals (Amsterdam et al. 1996; Chiocchetti et al. 1997). The fact that strong fluorescent cells in the cryosections of βGFP embryos could be detected in many embryonic tissues expressing βGFP implied that βGFP did provide a strong and stable fluorescent protein in these cells.

To detect fluorescent signals in living or unfixed whole embryos from βGFP and TFP lines, confocal images were used to show that GFP substantially labelled in many embryonic tissues. Actually, fluorescent signals in the eye of E10.5 and the head of E8.5 embryos could be only detected in βGFP embryos. Comparison of GFP signal in brain optic section from the E10.5 TFP embryos showed that fluorescence was specifically seen in the developing brain.

Taken together, the double-reporter transgene constructs provide a versatile way to monitor the Msx-1 gene regulation in developing embryos. Strong fluorescence in many fixed or living embryonic tissues suggested that GFP was stable and nontoxic during embryogenesis. Thus, these GFP transgenic lines can be used for real time studies of Msx-1 gene regulation during morphogenetic changes in the near future (Chapter 7).

Chapter 7 Conclusion and Perspective

In this thesis, at least three GFP mutant genes (hGFP-M4/M3/M2) showed promising features, such as high levels of expression which were stable, non-toxic. These GFP mutants were successfully developed to be used as a marker in living cells so as to visualise the expression of developmentally regulated genes in both mammalian cells and mouse embryos.

In summary, GW (GFP-WT1 fusion) constructs expressed in Cos7 cells showed the unique nuclear patterns which were previously examined by immunohistochemistry. GW isoforms provided a simple *in* vivo means to dissect WT1 cellular destination. In transgenic embryos, GFP fluorescence was found in a similar expression pattern as previously reported (MacKenzie et al. 1997) using β-gal as reporter.

GFP fluorescence is a simple and sensitive way to label proteins in cells providing a means to study living systems in real time. Recently, Misteli et al. (1997) examined the dynamic properties of the splicing factors SF2/ASF by making a GFP-SF2/ASF fusion and expressing in several mammalian cell lines. In their study, the movements and responses of GFP-SF2/ASF to other nuclear proteins in living BHK cells were seen by time-lapse fluorescent microscopy. Huang et al. (1997) visualised the dynamic structure of the PNC (perinuclear compartment) by making a fusion protein between one component of the PNC, and GFP for time lapse studies.

In previous results (Chapter4 and 5), the nuclear patterns of GW isoforms and their derivatives in living Cos7 cells showed clear subnuclear structures (speckles, domains /coil bodies). However, GW isoforms may be used as a novel tool to gain further insights into the complex nuclear behaviors (properties and formation of these nuclear bodies, events of the association between WT1 isoforms and nuclear proteins and the interaction among WT1 isoforms) of WT1 isoforms in living cells. Thus GW may allow to study the following :

1) Spatial organization of GW nuclear localisation

WT isoforms interact with other nuclear proteins through functional motifs and display unique nuclear patterns (Ehrig et al. 1995; Hewitt et al. 1996; Maheswaran et al. 1993; Wang et al. 1995). However, there are no isoform-specific antibodies for WT1 and the individual function of each isoforms is unclear. Thus, it is difficult to investigate the different cellular functions of WT1 isoforms at same physiological conditions. GW has provided a valuable tool to follow WT1 in living cells. Thus, WT1 isoforms can be individually labelled with GFP variants which have different excitation or emission maxima **(Table 7.1)** and these may provide a means to distinguish individual WT1 isoforms within the same cell. For example, a GW can be made by the fusion of EBFP or GFP_{UV} to the N-terminus of the WT1+KTS isoform (the speckle patterns) and EGFP, ECFP or EYFP can be used for the WT1-KTS isoform (the diffuse or domain pattern). It may be possible to distinguish these GW fusion isoforms due to the blue fluorescence of EBFP or the green fluorescent of GFP_{UV} excited by UV light and the green fluorescent of EGFP, ECFP and EYFP excited by

blue or visible light **(Table 7.1)**. One of the possible nuclear patterns is schematised in **Fig.7.1**. All possible combinations of individual GFP/WT1 fusions are summarised at **Table 7.2**. This strategy would allow the direct visualisation of individual nuclear behaviors of WT1 isoforms in a given cell.

Table 7.1 GFP variants for multiple labelling

Variants	Excitation maxima(nm)	Excitation maxima(nm)	Fluorescent intensity & colour	references
EGFP	488	507	Strong/ Green	(Cormack et al. 1996; laboratory 1996(October); Yang et al. 1996)
ECFP	433	507	Strong/ Green	(Miyawaki et al. 1997; Olmsted et al. 1994)
EYFP	513	513	Strong/ Yellow	(Miyawaki et al. 1997)
EBFP	380	440	weak/ Blue	(laboratory 1997(April))
GFP_{UV}	~400	509	mild/ Green	(laboratory 1996(October))

Table 7.2 Optimal combination of GFP/WT1 fusions[a]

Combinations	WT1+/+	WT1-/+	WT1+/-	WT1-/-
1	BW+/+	UW-/+	CW+/-	YW-/-
2	UW+/+	BW-/+	YW+/-	CW-/-
3	BW+/+	UW-/+	CW+/-	YW-/-
4	UW+/+	BW-/+	YW+/-	CW-/-

a. BW, EBFP-WT1 fusion protein; UW, GFPUV-WT1 fusion protein; CW, ECFP-WT1 fusion protein; YW, EYFP-WT1 fusion protein.

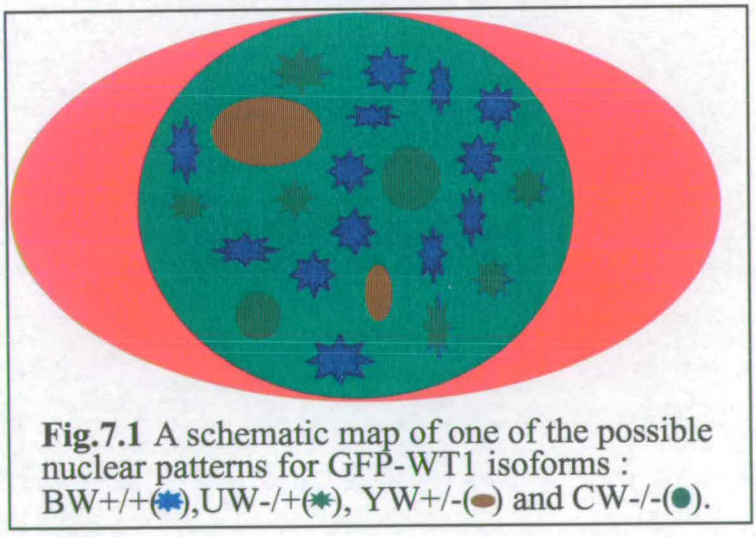

Fig.7.1 A schematic map of one of the possible nuclear patterns for GFP-WT1 isoforms : BW+/+(✸),UW-/+(✸), YW+/-(⬬) and CW-/-(●).

2) To investigate endogenous expression of WT1 isoforms in normal cell physiology

In normal physiological conditions, the WT1 gene expresses four major mRNA splice variants at given ratios during development (Reddy et al. 1995). Although the ectopic expression of GFP/WT1 fusion proteins may highlight some of the behavior in living cells, this approach may not mimic the complete spectrum of events that occur in this highly regulated system. To gain a more realistic impression of endogenous WT1 expression, a GFP 'knock-in' could be attempted inserting GFP in frame with the N-terminal exon of the WT1 gene in cells expressing endogenous WT1. The successful GFP knock-in cells can easily be sorted out by FACS and used to establish cell lines. Such GFP 'knock-in' cell lines would be a valuable source for a more accurate analysis of the WT1 in normal cell physiological condition.

3) Tracing the cell fate of developing embryos

The Msx-1 gene is involved in control of embryonic tissue development, affecting differentiation (Song et al. 1992), and epithelial-mesenchymal interactions (Jowett et al. 1993; Wang et al. 1995). In vivo, Msx-1 expression has also been associated with neural crest cell migration and most recently with myoblast migration during embryogenesis (Houzelstein et al. 1997). In my previous results, fluorescent signals was found in GFP transgenic embryos (Chapter 6). Most interestingly, strong green fluorescent cells were found in a subset of specific embryonic tissues, such as dorsal neural crest cells, spinal ganglion, somites and limb mesenchyme (**Fig.7.2**). Thus, GFP

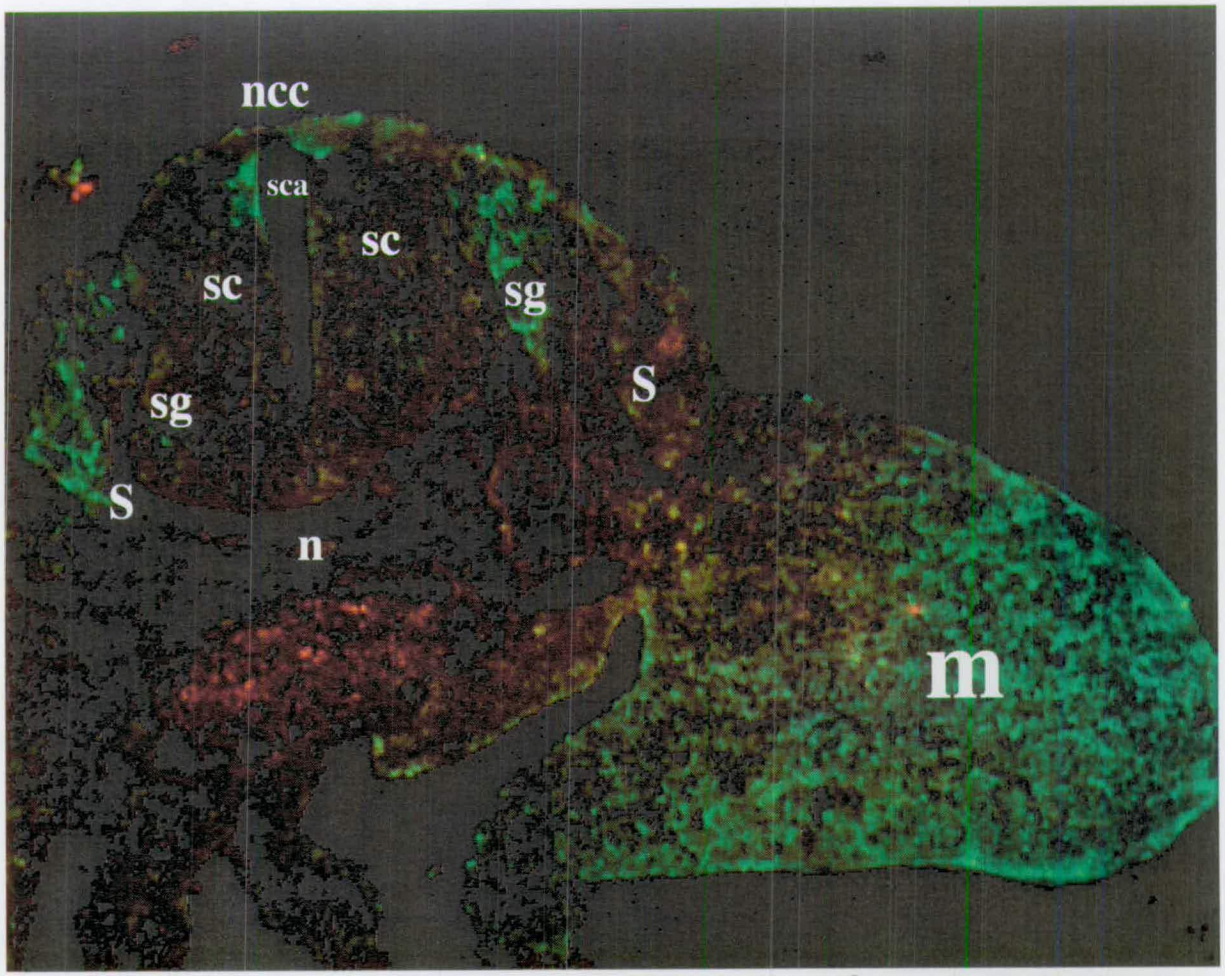

Fig.7.2 Transverse cryosection through the hindlimb of E10.5 3βG-1 embryo showing strong GFP fluorescence in the dorsal neural tube and hindlimb. s, somites; sg, spinal ganglion; ncc, neural crest cells; sc, spinal cord ; sca, spinal canal; n, notochord; m, mesenchy me of hindlimb. The fluorescent images was visualised by a CCD camera conjugated fluorescence microscopy using using FITC and Texas Red filter.

fluorescence in these embryonic tissues may become a valuable resource to establish whole embryo or organ (tissue) culture systems to investigate the developmental role of Msx1 expressing cells. These system may be useful for the following:

a) The sensitivity of GFP detection in living embryos may permit a study to follow Msx1 in trunk neural crest cells which migrate from the dorsal neural tube.

b) Living embryos may also allow the study of limb development by analysis of migration in limb mesenchyme and subsequent cell differentiation by visualising those cell types in cultured embryonic tissues.

c) In embryo culture, GFP transgenic mouse cells may be grafted into wild type mouse embryos for the examination of the contribution of donor cells to embryonic tissues of interest. Perhaps, GFP vital marker may be used to ascertain the role that a specific cell type makes to embryonic tissues such as maxillary and mandibular arches, limb buds and brain etc.

Bibliography

Akagi, Y., Y. Isaka, A. Akagi, M. Ikawa, M. Takenaka, T. Moriyama, A. Yamauchi, M. Horio, N. Ueda, M. Okabe and E. Imai (1997). "Transcriptional activation of a hybrid promoter composed of cytomegalovirus enhancer and β-actin/β-globulin gene in glomerular epithelial cells in vivo." Kidney International 51: 1265-1269.

Amsterdam, A., S. Lin and N. Hopkins (1995). "The aequprea victoria green fluorescent protein can be used as a reporter in live zebrafish embryos." Developmental Biology 171: 123-129.

Amsterdam, A., S. Lin, L. G. Moss and N. Hopkins (1996). "Requirement for green fluorescent protein detection in transgenic zebra fish embryos." Gene 173: 99-103.

Anderson, M. T. and I. M. Tjioe (1996). "Simultaneous fluorescence-activated cell sorter analysis of two distinct transcriptional elements within a single cell using engineered green fluorescent proteins." Proc. Natl. Acad. Sci. 93: 8508-8511.

Barthmaier, P. and E. Fyrberg (1995). "Monitoring development and pathology of *Drosophila* Indirect flight muscles using green fluorescent protein." Development Biology 169: 770-774.

Baulcombe, D. C., S. Chapman and S. S. Cruz (1995). "Jellyfish green fluorescent protein as a reporter for virus infections." The plant Journal 7(6): 1045-1053.

Boevink, P., S. S. Cruz, C. Hawes, N. Harris and K. J. Oparka (1996). "Virus-mediated delivery of the green fluorescent protein to the endoplasmic reticulum of plant cells." The Plant Journal 10(5): 935-941.

Bokman, S. H. and W. W. Ward (1981). "Renaturation of Aequorea green-fluorescent protein." Biochem. Biophys .Res. Comm 101: 1372.

Boulikas, T. (1993). "Nuclear location signals." Critical Reviewes in Eukaryotic Gene Expression 3(3): 193-227.

Boulikas, T. (1994). "Putative nuclear localization signals (NLS) in protein transcription factors." Jounal of Cellular Biochemistry 55: 32-58.

Brinster, R. L., J. M. Allen, R. R. Behringer and R. E. Gelinas (1988). "Introns increase transcriptional efficiency in transgenic mice." Proc. Natl. Acad. Sci. 85: 836-840.

Brown, J. M., S. E. Wedden, G. H. Millburn, L. G. Robson, R. E. Hill and D. R. D. &. C. Tickle (1993). "Experimental analysis of the control of expression of the homeobox-gene Msx-1 in the developing limb and face." Development 119: 41-48.

Bruening, W., P. Moffett, S. Chia, G. Heinrich and J. Pelletier (1996). "Identification of nuclear localization signals within the zinc finger of the WT1 tumor suppressor gene product." FEBS Letters 393: 41-47.

Bruening, W. and J. Pelletier (1996). "A non-AUG translation initiation event generates novel WT1 isoforms." J. Biol. Chem 271: 8646-8654.

Buckler, A. J., J. Pelletier, D. A. Haber, T. Glaser and D. E. Housman (1991). "Isolation, characterization, and expression of the murine Wilms' Tumor gene(WT1) during kidney development." Mol. and Cell. Biol. 11(3): 1707-1712.

Call, M. K., T. Glaser, Y. C. Ito, J. A. Buckler, J. Pelletier, A. D. Haber, A. E. Rose, A. Kral, H. Yeger, H. W. Lewis, C. Jones and E. D. Housman (1990). "Isolation and characterisation of a zinc finger polypeptide gene at the human chromosome 11 Wilms' tumor locus." Cell 60: 509-520.

Carey, K. L., S. A. Richards, K. M. Lounsbury and I. G. Macara (1996). "Evidence using a green fluorescent protein-glucocorticoid receptor chimera that the RAN/Tg4 GTPase mediates an essential function independent of nuclear protein import." J. Cell Bio. 133(5): 985-996.

Casper, S. J. and C. A. Holt (1996). "Expression of the green fluorescent protein-encoding gene from a tobacco mosaic virus-based vector." Gene 173: 69-73.

Catron, K. M., H. Wang, G. Hu, M. M. Shen and C. A.-Shen (1996). "Comparison of Msx-1 and Msx-2 suggests a molecular basis for functional redundancy." Mechanisms of Development 55: 185-199.

Chalfie, M., Y. Tu, G. Euskirchen, W. W. Ward and D. C. Prasher (1994). "Green fluorescent protein as a marker for gene expression." Science 263(11): 802-805.

Charlieu, J.-P., S. Larsson, K. Miyagawa, V. v. Heyningen and N. D. Hastie (1995). "Does the Wilms' tumor suppressor gene, WT1, play roles in both splicing and transription." J. Cell. Sci. 19: 95-99.

Chiocchetti, A., E. Tolosano, E. Hirsch, L. Silengo and F. Altruda (1997). "Green fluorescent protein as a reporter of gene expression in transgenic mice." Biochimica et Biophysica Acta 1352: 193-202.

Chishima, T., Y. Miyagi, X. Wang, H. Yamaoka, H. Shimada, A. R. Moossa and R. M. Hoffman (1997). "Cancer invasion and micrometastasis visualized in live tissue by green fluorescent protein expression." Cancer Research 57: 2042-2047.

Chiu, W.-L., Y. Niwa, W. Zeng, T. Hirano, H. Kobayashi and J. Sheen (1996). "Engineered GFP as a vital reporter in plants." Current Biology 6(3): 325-330.

Choi, T., M. Huang, C. Gorman and R. Jaenisch (1991). "A generic intron increases gene expression in transgenic mice." Mol. Cell. Biol. 11: 3070-3074.

Clontech (1997). "GFP application notes." Protocol (Clontech) PT2040-1: 10.

Coburn, C. M. and C. I. Bargmann (1996). "A putative cyclic nucleotide-gated channel is required for sensory development and function in *C.elegans*." Neuron 17: 695-706.

Cody, C. W., D. C. Prasher, W. M. Westler, F. G. Prendergast and W. W. Ward (1993). "Chemical structure of the hexapeptide chromophore of the Aequorea gren-fluorescent protein." 32: 1212-1218.

Coelho, C. N. D., W. B. Upholt and R. A. Kosher (1993). "Ectoderm from various regions of the developing chick limb bud differentially

regulates the expression of the chicken homeobox-containing genes GHox-7 and GHox-8 by limb mesenchymal cells." Developmental Biology 156: 303-306.

Cormack, B. P., R. H. Valdivia and S. Falkow (1996). "FACS-optimized mutants of the green fluorescent protein (GFP)." Gene 173: 33-38.

Cormack, B. P., G. Bertram, M. Egerton, N. A. R. Gow, S. Falkow and A. J. P. Brown (1997). "Yeast-enhanced green fluorescent protein (yEGFP): a reporter of gene expression in *Candida albicans*." Microbiology 143: 303-311.

Coxon, A. and T. H. Bestor (1995). "Proteins that glow in green and blue." Chemistry & Biology 2(3): 119-121.

Crameri, A., E. A. Whitehorn, E. Tate and W. P. C. Stemmer (1996). "Improved green fluorescent protein by molecular evolution using DNA shuffling." Nature Biotechnology 14: 315-319.

Cubitt, A. B., R. Heim, S. R. Adams, A. E. Boyd, L. A. Gross and R. Y. Tsien (1995). "Understanding, improving and using green fluorescent proteins." TIBS 20: 448-455.

Davidson, D. R., A. Crawley and R. E. H. &. C. Tickle (1991). "Position-dependent expression of two related homeobox genes in developing vertebrate limbs." Nature 352:

Davidson, D. R. and R. E. Hill (1991). "Msh-like genes: a family of homeobox genes with wide-ranging expression during vertebrate development." seminars in Development Biology 2: 405-412.

Delagrave, S., R. E. Hawtin, C. M. Silva, M. M. Yang and D. C. Youvan (1995). "Red-shifted excitation mutants of the green fluorescent protein." Biotechnology 13: 151-154.

Dhandayuthapani, S., L. E. Via, C. A. Thomas, P. M. Horowitz, D. Deretic and V. Deretic (1995). "Green fluorescent protein as a marker for gene expression and cell biology of mycobacterial interactions with macrophages." Molecular microbiology 17(5): 901-912.

Dobson, S. P., C. Livingstone, G. W. Gould and J. M. Tavare (1996). "Dynamics of insulin-stimulated translocation of GLUT4 in single living cells visualised using green fluorescent protein." FEBS Letters 393: 179-184.

Dorrell, N., V. G. Gyselman, S. Foynes, S.-R. Li and B. W. Wren (1995). "Improved efficiency of inverse PCR mutagenesis." BioTechniques 21(4): 604-606.

Drummond, I. A., H. D. Rupprecht, P. R.-N., J. M. L.-Guisa, S. L. Madden, F. J. R. III and V. P. Sukhatme (1994). "DNA recognition by splicing variants of the Wilms' tumor suppressor, WT1." Molecular and Cellular Biology 14(6): 3800-3809.

Ehrig, T., D. J. O'Kane and F. G. Prendergast (1995). "Green-fluorescent mutants with altered fluorescence excitation spectra." FEBS Letters 367: 163-166.

Endow, S. A. and D. J. Komma (1996). "Centrosome and spindle function of the Drosophila Ncd microtuble motor visualized in live embryos using Ncd-GFP fusion protein." Jounal of Cell Science 109: 2429-2442.

Englert, C., X. Hou, S. Maheswaran, P. Bennett, C. Ngwu, G. G. Re, A. J. Garvin, M. R. Rosher and D. A. Haber (1995). "WT1 suppresses synthesis of the epidermal growth factor receptor and induces apoptosis." The EMBO Journal 14(19): 4662-4675.

Englert, C., M. Vidal, S. Maheswaran, Y. Ge, R. M. Ezzell, K. J. Isselbacher and D. A. Haber (1995). "Truncated WT1 mutants alter the subnuclear localization of the wild-type protein." Proc. Natl. Acad. Sci. 92: 11960-11964.

Epel, B. L., H. S. Padgett, M. Heinlein and R. N. Beachy (1996). "Plant virus movement protein dynamics probed with a GFP-protein fusion." Gene 173: 75-79.

Fire, A. and S. W. H. &. D. Dixon (1990). "A modular set of lacZ fusion vectors for studying gene expression expression in Caenorhabditis elegans." Gene 93: 189-198.

Gage, D. J., T. Bobo and S. R. Long (1996). "Use of green fluorescent protein to visualize the early events of symbiosis between *Rhizobium meliloti* and *Alfalfa(Medicago sativa)*." J. Bacteriol. 178(24): 7159-7166.

Galbraith, D. W. (1995). "Flow Cytometric analysis of transgene expression in higher plants: green-fluorescent protein." Method in Cell Biology 50: 3-14.

Gaunt, S. J. (1991). "Expression patterns of mouse Hox genes: clues to an understanding of developmental and evolutionary strategies." BioEssays 13: 505-513.

Gerdes, H. H. and C. Kaether (1996). "Green fluorescent protein: applications in cell biology." FEBS letters 389: 44-47.

Gerisch, G., R. Albrecht, C. Heizer, S. Hodgkinson and M. Mana]iak (1995). "Chemoattractant-controlled accumulation of coronin at the leading edge of *Dictyostelium* cells monitored using a green fluorescent protein-coronin fusion protein." Current Biology 5(11): 1280-1285.

Gessler, M., A. Poustka, W. Cavenee, L. R. Neve, H. S. Orkin and P. A. G. Bruns (1990). "Homozygous deletion in wilms' tumors of a zinc-finger gene identified by chromosome jumping." Nature 343: 774-778.

Ghattas, I. R., J. R. Sanes and J. E. Majors (1991). "The encephalomyocarditis virus internal ribosome entry site allows efficient coexpression of two genes from a recombinant provirus in cultured cells and in embryos." Mol. Cell. Biol. 11(12): 5848-5859.

Giorgi, F. D., M. Brini, C. Bastianutto, R. Marsault, M. Montero, P. Pizzo, R. Rossi and R. Rizzuto (1996). "Targeting aequorin and green fluorescent protein to intracellular organelles." Gene 173: 113-117.

Grantham, R., C. Gautier, M. Gouy, M. Jacobzone and R. Mercier (1981). "Codon catalog usage is a genome strategy modulated for gene expressivity." Nucleic Acids Res. 9: r43-rt4.

Gui, F. J., S. W. Lane and X.-D. Fu (1994). "A serine kinase regulates intracellular localization of splicing factors in the cell cycle." Nature 369: 678-682.

Gura, T. (1996). "Structure of gene-tag protein solved." Science 273: 1336.

Haas, J., E.-C. Park and B. Seed (1996). "Codon usage limitation in the expression of HIV-1 envelope glycoprotein." Current Biology 6(3): 315-324.

Haber, A. D., J. A. Buckler, T. Glaser, M. K. Call, J. Pelletier, L. R. Sohn, C. E. Douglass and E. D. Housman (1990). "An internal deletion within an 11p13 zinc finger gene contributes to the development of Wilms' tumor." Cell 61: 1257-1269.

Haber, A. D., L. R. Sohn, J. A. Buckler, J. Pelletier, M. K. Cell and E. D. Housman (1991). "Alternate splicing and genomic structure of the Wilms' tumor gene WT." Proc. Natn. Acad. Sci. 88: 9618-9622.

Haber, D. A. and D. E. Housman (1992). "Role of the WT1 gene in Wilm's tumour." Cancer Surveys 12: 105-117.

Hamilton, T. B., K. C. Barilla and P. J. Romaniuk (1995). "High affinity binding sites for the Wilms' tumour suppressor protein WT1." Nucleic Acids Res. 23(2): 277-284.

Hampton, R. Y., A. Koning, R. Wright and J. Rine (1996). "In vivo examination of membrane protein localization and degradation with green fluorescent protein." Proc. Natl. Acad. Sci. 93: 828-833.

Hanahan, D. (1985). "Techniques for transformation of *E.coli.*" In DNA cloning a practical approach, IRL press, Oxford 1: 109.

Hanakam, F., R. Albrecht, C. Eckerskorn, M. Matzner and G. Gerisch (1996). "Myristoylated and non-myristoylated forms of the pH sensor protein hisactophilin II: intracellular shuttling to plasma membrane and nucleus monitored in real time by a fusion with green fluorescent protein." The EMBO Journal 15(12): 2935-2943.

Haseloff, J. and B. Amos (1995). "GFP in Plants." TIG 11(8): 328-329.

Heim, R., D. C. Prasher and R. Y. Tsien (1994). "Wavelength mutations and posttranslational autoxidation of green fluorescent protein." Pro. Natl. Acad. Sci. USA 91: 12501-12504.

Heim, R., A. B. Cubitt and R. Y. Tsien (1995). "Improved green fluorescence." Nature 373: 663-664.

Heim, R. and R. Y. Tsien (1996). "Engineering green fluorescent protein for improved brightness, longer wavelengths and fluorescence resonance energy transfer." Current Biology 6(2): 178-182.

Heinlein, M., B. L. Epel, H. S. Padgett and R. N. Beachy (1995). "Interaction of tobamovirus movement proteins with the plant cytoskeleton." Science 270: 1983-1985.

Hewitt, J. E., L. N. Clark, A. Ivens and R. Williamson (1991). "Structure and sequence of the human homeobox gene HOX7." Genomics 11: 670-678.

Hewitt, S. M., G. C. Fraizer, Y.-J. Wu, F. J. Rauscher and G. F. Saunders (1996). "Differential function of Wilms' tumor gene WT1 splice isoforms in transcriptional regulation." J. Biol. Chem. 271(15): 8588-8592.

Heyningen, V. V. and N. D. Hastie (1992). "Wilms' tumour:reconciling genetics and biology." Trends Genet. 8: 16-21.

Higgs, S., D. Traul, B. S. Davis, K. I. Kamrud, C. L. Wilcox and B. J. Beaty (1996). "Green fluorescent protein expressed in living mosquitoes-without the requirement of transformation." BioTechniques 2(660-664):

Hill, R. E., P. F. Jones, A. R. Rees, C. M. Sime, M. J. Justice, N. G. Copeland, N. A. Jenkins, E. Graham and D. R. Davidson (1989). "A new family of mouse homeo box-containing genes: molecular structure, Chromosomal location, and developmental expression of Hox-7.1." Gene & Development 3: 26-37.

Hodgkinson, S. (1995). "GFP in Dictyostelium." TIG 11(8): 327-328.

Houzelstein, D., A. Cohen, M. E. Buckingham and B. Robert (1997). "Insertional mutation of the mouse Msx1 homeobox gene by an nlacZ reporter gene." Mechanisms of Development 65: 123-133.

Htun, H., J. Barsony, I. Renyi, D. L. Gould and G. L. Hager (1996). "Visualization of glucocorticoid receptor translocation and intranuclear organization in living cells with a green fluorescent protein chimera." Proc. Natl. Acad. Sci. 93: 4845-4850.

Huang, S., T. J. Deerinck, M. H. Ellisman and D. L. Spector (1997). "The dynamic organization of the perinucleolar compartment in the cell nucleus." Journal of Cell Biol. 137(5): 965-974.

I.-Belmonte, J.-C. and D. Duboule (1992). "Homeobox genes and pattern formation in the vertebrate limb." Developmental Biology 152: 26-36.

Ikawa, M., K. Kominami, Y. Yoshimura, K. Tanaka, Y. Nishimune and M. Okabe (1995). "Green fluorescrnt protein as a marker in transgenic mice." Develop. Growth Differ. 37: 455-459.

Ikawa, M., K. Kominami, Y. Yoshimura, K. Tanaka, Y. Nishimune and M. Okabe (1995). "A rapid and non-invasive selection of transgenic embryos before implantation using green fluorescent protein (GFP)." FEBS Letters 375: 125-128.

Inouye, S., M. Noguchi, Y. Sakaki, Y. Takagi, T. Miyata, S. Iwanaga, T. Miyata and F. I. Tsuji (1985). "Cloning and sequence analysis of cDNA for the luminescent protein aequorin." Pro. Natl. Acad. Sci. 82: 3154-3158.

Inouye, S., S. Zenno, Y. Sakaki and F. I. Tsuji (1991). "High-level expression and purificaton of apoaequorin." Protein expression and purification 2: 122-126.

Inouye, S. and F. I. Tsuji (1994). "Aequorea green fluorescent protein: expression of the gene and fluorescence characteristics of the recombinant protein." FEBS Letters 341: 277-280.

Ivens, A., N. Flavin, R. Williamson, M. Dixon, G. Bates, M. Buckingham and B. Robert (1990). "The human homeobox gene HOX7 maps to chromosome 4p16.1 and may be implicated in wolf-Hirschhorn Syndrome." Hum. Genet. 84: 473-476.

Jasin, M. and P. Zalamea (1992). "Analysis of *Escherichia coli* b-galactosidase expression in transgenic mice by flow cytometry of sperm." Proc. Natl. Acad. Sci. 89: 10681.

Jowett, A. K., S. Vainio, M. W. J. Ferguson, P. T. Sharpe and I. Thesleff (1993). "Epithelial-mesenchymal interactions are required for msx 1 and msx 2 gene expression in the developing murine molar tooth." Development 117: 461-470.

Kaether, C. and H. H. Gerdes (1995). "Visualization of protein transport along the secretory pathway using green fluorescent protein." FEBS Letters 369: 267-271.

Kain, S. (1997). "dEGFP." GFP meeting summary of international symposium on GFP :

Kalish, J. E., G.-A. Keller, J. C. Morrell, S. J.Mihalik, B. Smith, J. M. Cregg and S. J. Gould (1996). "Characterization of a novel component of the peroxisomal protein import apparatus using Fluorescent peroxisomal protein." The EMBO Iournal 15(13): 3275-3285.

Kennedy, D., T. Ramsdale, J. Mattick and M. Little (1996). "An RNA recognition motif in Wilms' tumor protein (WT1) revealed by structural modelling." Nature Genetics 12: 329-332.

Kimata, Y., M. Iwaki, C. R. Lim and K. Kohno (1997). "A novel mutation which enhances the fluorescence of green fluorescent protein at high temperature." Biochemical and Biophysical Research Communications 232: 69-73.

Kitts, P., M. Adams, A. Kondenpudi and D. G. &. S. Kain (1995). "Green fluorescent protein (GFP): A novel reporter for monitoring gene expression in living organisms." CLONTECHniques X(1): 1-3.

Komatsu, H., I. Mori, J.-S. Rhee, N. Akaike and Y. Ohshima (1996). "Mutations in a cyclic nucleotide-gated channel lead to abnormal thermosensation and chemosensation in *C.elegans*." Neuron 17: 707-718.

Kreidberg, A. J., H. Sariola, M. J. Loring, M. Maeda, J. Pelletier, D. Housman and R. Jaenisch (1993). "WT-1 is required for early kidney development." Cell 74 (679-691):

Kudoh, T., T. Ishidate, M. Moriyama, K. Toyoshima and T. Akiyama (1995). "G1 phase arrest induced by Wilms tumor protein WT1 is abrogated by cyclin ? CDK complexes." Proc. Natl. Acad. Sci. 92: 4517-4521.

Kudoh, T., T. Ishidate, K. Toyoshima, K. Toyoshima and T. Akiyama (1996). "Constitutive expression of the Wilms tumor suppressor gene WT1 in F9 embryonal carcinoma cells induces apoptotic cell death in response to retinoic acid." Oncogene 13: 1431-1439.

Kuzuoka, M. (1994). "Murine homeobox-containing gene, Msx-1: analysis of genomic organization, promoter structure, and potential autoregulatory cis-acting elements." Genomics 21: 85-91.

laboratory, C. (1996, October). "Living colors pEBFP vector." CLONTECHniques XI(4): 18.

laboratory, C. (1997,April). "Living colors pEBFP vector." CLONTECHniques XII(2): 16-17.

Larsson, S. H., J.-P. Charlieu, K. Miyagawa, D. Engelkamp, M. Rassoulzadegan, A. Ross, F. Cuzin, V. v. Heyningen and N. D. Hastie (1995). "Subnuclear localization of WT1 in splicing or transcription factor domains is regulated by alternative splicing." Cell 81: 391-401.

Lim, C. R., Y. Kimata, M. Oka, K. Nomaguchi and K. Kohno (1995). "Thermosensitivity of green fluorescent protein fluorescence utilized to reveal novel nuclear-like compartments in a mutant nucleoporin Nsp1." J. Biochem. 118: 13-17.

Ludin, B., T. Doll, R. Meili, S. Kaech and A. Matus (1996). "Application of novel vectors for GFP-tagging of proteins to study microtuble-associated proteins." Gene 173: 107-111.

Luo, Y., A. S. Vasi, X. Chen, W. C. Dewolf and M. A. O'Donnell (1996). "A novel method for monitoring *Mycobacterium bovis* BCG trafficking with recombinant BCG expressing green fluorescent

protein." Clinical and Diagnostic laboratory immunology 3(6): 761-768.

Lybarger, L. (1996). "Rapid generation and flow cytometric analysis of stable GFP-expressing cells." Cytometry 25: 211-220.

Lyons, G. E., D. Houzelstein, D. Sassoon, B. Robert and M. E. Buckingham (1992). "Multiple sites of Hox-7 expression during mouse embryogenesis: Comparison with retinoic acid receptor mRNA localization." Molecular reproduction and development 32: 303-314.

Mackenzie, A., M. W. J. Ferguson and P. T. Sharpe (1991). "Hox-7 expression during murine craniofacial development." Development 113: 601-611.

Mackenzie, A., G. L. Leeming, A. K. Jowett, M. W. J. Ferguson and P. T. Sharpe (1991). "The homeobox gene Hox7.1 has specific regional and temporal expression patterns during early murine craniofacial embryogenesis, especially tooth development in vivo and in vitro." Development 111: 269-285.

Mackenzie, A., M. W. J. Ferguson and P. T. Sharpe (1992). "Expression patterns of the homeobox gene Hox 8 in the mouse embryo suggest a role in specifying tooth initiation and shape." Development 115: 403-420.

MacKenzie, A., L. Purdie, D. Davidson, M. Collinson and R. E. Hill (1997). "Two enhancer domains control early aspects of the complex expression pattern of Msx1." Mechanisms of development 62: 29-40.

Maheswaran, S., S. Park, A. Bernard, J. F. Morris, F. J. Rauscher, D. E. Hill and D. A. Haber (1993). "Physical and functional interactional interaction between WT1 and p53 proteins." Proc. Natl. Acad. Sci. 90: 5100-5104.

Maniak, M., R. Rauchenberger, R. Albrecht, J. Murphy and G. Gerisch (1995). "Coronin involved in phagocytosis: dynamic of particle-induced relocalization visualized by a green fluorescent protein tag." Cell 83: 915-924.

Marshall, J., R. Molloy, G. W. J. Moss, J. R. Howe and T. E. Hughes (1995). "The jellyfish geen fluorescent protein: A new tool for studying ion channel expression and function." Neuron 14: 211-215.

Matayoshi, E. D., G. T. Wang, G. A. Krafft and J. Erickson (1990). "Novel fluorogenic substrates for assaying retroviral proteases by resonance energy transfer." Science 247: 954-958.

Matheson, J. M., A. Miyawaki, A. Muto, T. Inoue and K. Mikoshiba (1996). "Expression of the green fluorescent protein deruvate S65T in *Xenopus laevis* oocytes." Biomedical Research 17(3): 221-225.

Matsumura, I. and A. D. Ellington (1996). "DNA shuffling brightens prospects for GFP." Nature Biotechnology 14: 366.

Minden, J. S. (1996). "Synthesis of a new substrate for detection of lacZ gene expression in live *Drosophila* embryos." BioTechniques 20: 122-129.

Misteli, T., J. F. Caceres and D. L. Spector (1997). "The dynamics of a pre-mRNA splicing factor in living cells." Nature 387: 523-527.

Misteli, T. and D. L. Spector (1997). "Protein phosphorylation and the nuclear organization of splicing factors of pre-mRNA splicing." Trends Cell Biol 7: 135-138.

Mitra, R. D., C. M. Silva and D. C. Youvan (1996). "Fluorescence resonance energy transfer between blue-emitting and red-shifted excitation derivatives of the green fluorescent protein." Gene 173: 13-17.

Miyagawa, K., J. Kent, A. Schedl, V. V. Heyningen and N. D. Hastie (1994). "Wilms' tumour- a case of disrupted development." J. Cell Science Suppl. 18: 1-5.

Miyawaki, A., J. Liopis, R. Heim, J. M. McCaffery, J. A. Adams, M. Ikura and R. Y. Tsien (1997). "Fluorescent indicators for Ca^{2+} based on green fluorescent proteins and calmodulin." Nature 388: 882-887.

Moffett, P., W. Bruening, H. Nakagama, N. Bardeesy, D. Housman, D. E. Housman and J. Pelletier (1995). "Antagonism of WT1 activity by protein self-association." Proc. Natl. Acad. Sci. 92: 11105-11109.

Monaghan, A. P., D. D. Davidson, C. Sime, E. Graham, R. Baldock, S. S. Bhattacharya and R. E. Hill (1991). "The msh-like homeo box genes define domains in the developing eye." Development 112: 1053-1061.

Monosov, E. Z., T. J. Wenzel, G. H. Luers, J. A. Heyman and S. Subramani (1996). "Labelling of peroxisomes with green fluorescent protein in living *P. pastoris* cells." The Journal of Histochemistry and Cytochemistry 44(6): 581-589.

Morgenstern, J. P. and H. Land (1990). "A series of mammalian expression vectors and characterization of their expression of a report gene in stably and transiently transfected cells." Nucleic Acids Res. 18(4): 1068.

Morise, H., O. Shimomura, F. H. Johnson and J. Winant (1974). "Intermolecular energy transfer in tne bioluminescent system of aequorea." Biochemistry 13(12): 2656-2662.

Moriyoshi, K., L. J. Richards, C. Akazawa, D. D. M. O'Leary and S. Nakanishi (1996). "Labelling neural cells using adenoviral gene transfer of membrane-targeted GFP." Neuron 16: 255-260.

Moss, J. B., A. L. Price, E. Raz, W. Driever and N. Rosenthal (1996). "Green fluorescent protein markers skeletal muscle in murine cell line and zebrafish." Gene 173: 89-98.

Mountford, P. S. and A. G. Smith (1995). "Internal ribosome entry sites and dicistronic RNAs in mammalian transgenesis." TIG 11(5): 179-184.

Mundlos, S., J. Pelletier, A. Darveau, M. Bachmann, A. Winterpacht and B. Zabel (1993). "Nuclear localization of the protein encoded by the wilms' tumor gene WT1 in embryonic and adult tissues." development 119: 1329-1341.

Niswender, K. D., S. M. Blackman, L. Rohde, M. A. Magnuson and D. W. Piston (1995). "Quantitative imaging of green fluorescent protein in cultured cells: comparison of microscopic techniques, use in fusion proteins and detection limits." Journal of Microscopy 180(2): 109-116.

Niwa, H., K.-I. Yamamura and J.-I. Miyazaki (1991). "Efficient selection for high-expression transfectants with a nove eukaryotic vector." gene 108: 193-200.

Niwa, H. (1996). "Chemical nature of the light emitter of the Aequorea green fluorescent protein." Proc. Natl. Acad. Sci. 93: 13617-13622.

Ogawa, H., S. Inouye, I. F. Tsuji, K. Yasuda and K. Umesono (1995). "Localization, trafficking, and temperature-dependence of the *Aequorea* green fluorescent protein in culture vertebrate cells." Proc. Natl. Acad. Sci. 92: 11899-11903.

Okabe, M., M. Ikawa, K. Kominami, T. Nakanishi and Y. Nishimune (1997). "'Green mice' as a source of ubiquitous green cells." FEBS Letters 407: 313-319.

Olmsted, J. B. and K. R. O. &. J. R. Mclntosh (1994). "Green fluorescent protein (GFP) chimeras as repoters for MAP4 behavior in living cells." Molecular biology of the Cell 5: 167a #973.

Olson, K. R., J. R. Mcintosh and J. B. Olmsted (1995). "Analysis of MAP4 function in living cells using green fluorescent protein(GFP) chimeras." The Journal of Cell Biology 130(3): 639-650.

Oparka, K. J., P. Boevink and S. S. Crus (1996). "Studying the movement of plant viruses using green fluorescent protein." Trens in plant Science 1(12): 412-420.

Oparka, K. J., A. G. Roberts, I. M. Roberts, D. A. M. Prior and S. S. Crus (1996). "Viral coat protein is targeted to, but does not gate, plasmodesmata during cell-to cell movement of potato virus X." The Plant Journal 10(5): 805-813.

Ormo, M., A. B. Cubitt, K. Kallio, L. A. Gross, R. Y. Tsien and S. J. Remington (1996). "Crystal structure of the *aequorea victoria* green fluorescent protein." Science 273: 1392-1395.

Pang, S.-Z., D. L. DeBoer, Y. Wan, G. Ye, J. G. Layton, M. K. Neher, C. L. Armstrong, J. E. Fry, M. A. W. Hinchee and M. E. Fromm (1996). "An improved green fluorescent protein gene as a vital marker in plants." Plant Physiol. 112: 893-900.

Peel, A. L., S. Zolotukhin, G. W. Schrimsher, N. Muzyczka and P. J. Reier (1997). "Efficient transduction of green fluorescent protein in spinal cord neurons using adeno-associated virus vectors containing cell type-specific promoters." Gene Therapy 4: 16-24.

Pelletier, J., W. Bruening, C. E. Kashtan, S. M. Mauer, J. C. Manivel, J. E. Striege, D. C. Houghton, C. Junien, R. Habib, L. Fouser, R. N. Fine, B. L. Silverman, D. A. Haber and D. Housman (1991). "Germline mutations in the Wilms' tumor suppressor gene are associated with abnoral urogenital development in Denys-Drash syndrome." Cell 67: 437-447.

Pelletier, J., M. Schalling, A. J. Buckler, A. Rogers, A. D. Haber and D. Housman (1991). "Expression of the Wilms' tumor gene WT1 in the murine urogenital system." Genes Dev. 5: 1345-1356.

Peter, K. G., P. S. Rao, B. S. Bell and L. A. Kindman (1995). "Green fluorescent fusion protein: powerful tools for monitoring protein expression in live zebrafish embryos." Developmental Biology 171: 252-257.

Pines, J. (1995). "GFP in mammalian cells." TIG 11(8): 326-327.

Plautz, J. D., R. N. Day, G. M. Dailey, S. B. Welsh, J. C. Hall, S. Halpain and S. A. Kay (1996). "Green fluorescent protein and its derivatives as versatile markers for gene expression in living *Drosophila melanogaster* , plant and mammalian cells." Gene 173: 83-87.

Potter, S. M. (1996). "Intravital imaging of green fluorescent protein using two-photon laser-scanning microscopy." Gene 173: 25-31.

Prasher, D. C., V. K. Eckenrode, W. W. Ward, F. G. Prendergast and M. J. Cormier (1992). "Primary structure of the *Aeqorea victoria* green-fluorescent protein." Gene 111: 229-233.

Prasher, D. C. (1995). "Using GFP to see the light." TIG 11(8): 320-323.

Prendergast, F. G. and K. G. Mann (1978). "Chemical and physical properties of aequorin and the green-fluorescent protein isolated from *Aequorea forskalea*." Biochemistry 17: 3448-3453.

Pritchard-Jones, K., S. Fleming, D. Davidson, W. Bickmore, D. Porteous, C. Gosden, J. Bard, A. Buckler, J. Pelletier, D.Housman, V. v. Heyningen and N. Hastie (1990). "The candidate Wilms' tumor gene is involved in genitourinary development." Nature 346: 194-197.

Rausher, I. J. F., F. J. Morris, E. O. Tournay, M. D. Cook and T. Curran (1990). "Binding of the Wilms' tumor locus zinc finger protein to the EGR1 consensus sequence." Science 250: 1259-1262.

Reddy, J. C., J. C. Morris, J. Wang, M. A. English, D. A. Haber, Y. Shi and J. D. Licht (1995). "WT1-mediated transcriptional activation is inhibited by dominant negative mutant proteins." J. Biol. Chem. 270(18): 10878-10884.

Richman, J. M. and C. Tickle (1992). "Epithelial-mesenchymal interactions in the outgrowth of limb buds and facial primordia in chick embryos." Developmental Biology 154: 299-308.

Rietdorf, J., F. Siegert and C. J. Weijer (1996). "Analysis of optical density wave propagation and cell movement during mound formation in *Dictyostelium discoideum*." *Developmental Biology* 177: 427-438.

Rizzuto, R., M. Brini, P. Pizzo, M. Murgia and T. Pozzan (1995). "Chimeric green fluorescent protein as a tool for visualizing subcellular organelles in living cells." Current Biology 5(6): 635-642.

Rizzuto, R., M. Brini, F. D. Giorgi, R. Rossi, R. Heim, R. Y. Tsien and T. Pozzan (1996). "Double labelling of subcellular structure with organelle-targeted GFP mutants in vivo." Current Biology 6(2): 183-188.

Robart, F. D. and W. W. Ward (1990). "Solvent perturbations of aequorea green fluorescent protein." Photochem. Photobiol. 51: 92s.

Robert, B., D. Sassoon, B. Jacq, W. Gehring and M. Buckingham (1989). "Hox-7, A mouse homeobox gene with a novel pattern of expression during embryogenesis." The EMBO J. 8(1): 91-100.

Robert, B., G. Lyons, B. K. Simandl, A. Kuroiwa and M. Buckingham (1991). "The apical ectodermal ridge regulates Hox-7 and Hox-8 gene

expression in developing chicl limb buds." Genes & development 5: 2363-2374.

Rosenberg, A. H., B. N. Lade, D.-S. Chui, S.-W. Lin, J. J. Dunn and F. W. Studier (1987). "Vectors for expression of cloned DNA by T7 RNA polymerase." Gene 56: 125-135.

Royer-Pokora, B., S. Ragg, B. H.-Ostreicher, M. Held, U. Loos, K. Call, T. Glaser, D. Housman, G. Saunders, B. Zabel, B. Williams and A. Poustka (1991). "Direct pulsed field gel electrophoresis of wilms' tumors shows that DNA deletions in 11p13 are rare." Genes, Chromosomes 3: 89-100.

Satokata, I. and R. Maas (1994). "Msx1 deficient mice exhibit cleft palate and abnormalities of craniofacial and tooth development." Nature Genetics 6: 348-356.

Schackwitz, W. S., T. Inoue and J. H. Thomas (1996). "Chemosensory neurons function in parallel to mediate a pheromone response in *C.elegans*." Neuron 17: 719-728.

Sharma, P. M., M. Bowman, B.-F. Yu and S. Sukumar (1994). "A rodent model for wilms tumor: embryonal kidney neoplasms induced by N-nitroso-N'-methylurea." Pronc. Natl.Acad.Sci. 91: 9931-9935.

Shiga, Y., M. T.-Matakatsu and S. Hayashi (1996). "A nuclear GFP/b-glactosidase fusion proteion as a marker for morphogenesis in living *Drosophila*." Develop. Growth Differ. 38: 99-106.

Sidorova, J. M., G. E. Mikesell and L. L. Breeden (1995). "Cell cycle-regulated phosphorylation of Swi6 controls its nuclear localization." Molecular Biology of the Cell 6: 1641-1658.

Siemering, K. R., R. Golbik, R. Sever and J. Haseloff (1996). "Mutations that suppress the thermosensitivity of green fluorescent protein." Current Biology 6(12): 1653-1663.

Song, K., Y. Wang and D. Sassoon (1992). "Expression of Hox-7.1 in myoblasts inhibits terminal differentiation and induces cell transformation." Nature 360: 477-481.

Spelling, T., A. Bottin and R. Kahmann (1996). "Green fluorescent protein(GFP) as new vital marker in the phytopathogenic fungus *Ustilago maydis*." Mol. Gen. Genet. 252: 503-509.

Studier, F. W. and B. A. Moffatt (1986). J. Mol. Biol. 189: 113-130.

Studier, F. W. (1990). Methods Enzymol. 185: 60-89.

Studier, F. W., A. H. Rosenberg and J. J. D. &. J. W. Dubendorff (1990). "Use of T7 RNA polymerase to direct expression of cloned gene." Method in enzymology 185: 60-89.

Suzuki, H. R., B. J. Padanilam, E. Vitale, F. Ramirez and M. Solursh (1991). "Repeating developmental expression of G-Hox7, a novel homeobox-containing gene in the chicken." Dev. Biol. 115: 403-420.

Tabin, C. J. (1991). "Retinoids, homeoboxes, and growth factors: toward molecular models for limb development." Cell 66: 199-217.

Takahashi, Y. and N. LeDourin (1990). "cDNA cloning of a quail homeobox gene and its expression in neural crest-derived mesenchyme and lateral plate mesoderm." Proc. Natl. Acad. Sci. 87: 7482-7486.

Tanahashi, H., T. Ito, S. Inouye, F. I. Tsuji and Y. Sakaki (1990). "Photoprotein aequorin : use as a reporter enzyme in studying gene expression in mammalian cells." Gene 96: 249-255.

Tannahill, D., S. Bray and W. A. Harris (1995). "A Drosophila E(spl) gene is " neurogenic " in Xenopus: a green fluorescent protein study." Devel. Biol. 168: 694-697.

Terasaki, M., L. A. Jaffe, G. R. Hunnicutt and J. A. Hammer (1996). "Structural change of the endoplasmic reticulum during fertization: Evidence for loss of membrane continuity using the green fluorescent protein." Developmental Biology 179: 320-328.

Terry, B. R., E. K. Matthews and J. Haseloff (1995). "Molecular characterisation of recombinant green fluorescent protein by fluorescence correlation microscopy." Biochemical and Biophysical Research Communications 217(1): 21-27.

Timmons, L., J. Becker, P. Barthmaier, C. Fyrberg, A. Shern and E. Fyrberg (1997). "Green fluorescent protein/β-galactosideas double reporters for visualizing *Drosophila* gene expression patterns." Developmental Genetics 20: 338-347.

Troemel, E. R., J. H. Chou, N. D. Dwyer, H. A. Colbert and C. I. Bargmann (1995). "Divergent seven transmembrane receptors are candidate chemosensory receptors in *C.elegans*." Cell 83: 207-218.

Valdivia, R. H. and S. Falkow (1996). "Bacterial Genetics by flow cytometry: rapid isolation of *Salmonella typhimurium* acid-inducible promoters by differential fluorescence induction." Molecular Microbiology 22(2): 367-378.

Valdivia, R. H., A. E. Hromockyj, D. Monack, L. Ramakrishnan and S. Falkow (1996). "Applications for green fluorescent protein(GFP) in the study of host-pathogen interactions." Gene 173: 47-52.

Venerando, R., G. Miotto, P. Pizzo, R. Rizzuto and N. Siliprandi (1996). "Mitochondrial alterations induced by aspirin in rat hepatocytes expressing mitochondrially targeted green fluorescent protein (mtGFP)." FEBS Letters 382: 256-260.

Vilardaga, J.-P., E. D. Paolo and A. Bollen (1995). "Improved PCR method for high-efficiency site-directed mutagenesis using class 2s restriction enzymes." BioTechniques 18(4): 605-606.

Wada, K., S. Aota, R. Tsuchiya, F. Ishibashi, T. Gojobori and T. Ikemura (1990). "Codon usage tabulated from the GenBank genetic sequence data." Neuleic Acids Res. 18(Suppl.): 2367-2411.

Wang, Z.-Y., Q.-Q. Qiu and T. F. Deuel (1993). "The Wilms' tumor gene product WT1 activates or suppresses transcription through separate functional domains." J.. Biol. Chem. 268: 9172-9175.

Wang, S. and T. Hazelrigg (1994). "Implications for bcd mRNA location from spatial distribution of exu protein in Drosophila oogenesis." Nature 369: 400-403.

Wang, Y. and D. Sassoon (1995). "Ectoderm-mesenchyme and mesenchyme-mesenchyme interactions regulate Msx-1 expression and

cellular differentiation in the murine limb bud." Developmental biology 168: 374-382.

Wang, Z.-Y., Q.-Q. Qiu, J. Huang, M. Gurrieri and T. F. Deuel (1995). "Products of alternatively spliced transcripts of the Wilms' tumor suppressor gene, wt1, have altered DNA binding specificity and regulate transcription in different ways." Oncogene 10: 415-422.

Wang, Z.-Y., Q.-Q. Qiu, J. Huang, M. Gurrieri and T. F. Deuel (1995). "WT1, the Wilms' tumor suppressor gene product, represses transcription through an interactive nuclear protein." Oncogene 10: 1243-1247.

Ward, W. W. and M. J. Cormier (1976). "An energy transfer in Renilla bioluminescence." J. Phys. Chem. 80: 781-788.

Ward, W. W. (1979). "Energy transfer processes in bioluminescence." Photobiol. Rev. 4: 1-57.

Ward, W. W. and S. H. Bokman (1982). "Reversible denaturation of aequorea green-fluorescent protein: physical separation and characterization of the renatured protein." Biochemistry 21: 4535-4540.

Webb, C., A. Decatur, A. Teleman and R. Losick (1995). "Use of green fluorescent protein for visualization of cell-specific gene expresssion and subcellular protein localization during sporulation in *Bacillus subtilis*." J. Bacteriol. 177: 5906-5911.

Wubbolts, R., M. F.-Borja, L. Oomen, D. Verwoerd, H. Janssen, J. Calafat, A. Tulp, S. Dusseljee and J. Neefjes (1996). "Direct vesicular transport of MHC class II molecules from lysosomal structures to the cell surface." The Journal of Cell Biology 135(3): 611-622.

Yang, F., L. G. Moss, G. N. Phillips and Jr. (1996). "The molecular structure of green fluorescent protein." Nature Biotechnology 14: 1246-1251.

Yang, T.-T., L. Cheng and S. R. Kain (1996). "Optimized codon usage and chromophore mutatipns provide enhanced sensitivity with the green fluorescent protein." Nucleic Acids Research 24(22): 4592-4593.

Yang, T.-T., S. R. Kain, P. Kitts, A. Kondepudi, M. M. Yang and D. C. Youvan (1996). "Dual color microscopic imagery of cells expressing the green fluorescent protein and a red-shifted variant." Gene 173: 19-23.

Ye, Y., B. Raychaudhuri, A. Gurney, C. E. Campbell and B. R. G. Williams (1996). "Regulation of WT1 by phosphorylation: inhibitition of DNA binding, alteration of transcriptional activity and cellular translocation." EMBO J. 15(20): 5606-5615.

Yeh, E., K. Gustafson and G. L. Boulianne (1995). "Green fluorescent protein as a vital marker and reporter of gene expression in *Drosophila*." Proc. Natl. Acad. Sci 92: 7036-7040.

Yokouch, Y., K. Ohsugi, H. Sasaki and A. Kuroiwa (1991). "Chicken homeobox gene Msx-1: structure, expression in limb buds and effect of retinoic acid." Development 113: 431-444.

Youvan, D. C. and M. E. M.-Beyerle (1996). "Structure and fluorescence mechanism of GFP." Nature biotechnology 14: 1219-1200.

Z.-Goetz, M., J. Pines, K. Ryan, K. R. Siemering, J. Haseloff, M. J. Evana and J. B. Gurdon (1996). "An indelible lineage marker for *xenopus* using a mutated green fluorescent protein." Development 122: 3719-3724.

Z.-Goetz, M., J. Pines, S. M. Hunter, J. P. C. Dixon, K. R. Siemering, J. Haseloff and M. J. Evans (1997). "Following cell fate in the living mouse embryo." Development 124: 1133-1137.

Zeng, C., E. Kim, S. L. Warren and S. M. Berget (1997). "Dynamic relocation of transcriptional and splicing factors dependent upon tanscriptional activity." The EMBO J. 16(6): 1401-1412.

Zhang, S., G. Zubay and E. Goldman (1991). "Low-usage codon in *Escherichia coli,* yeast, fruit fly and primates." Gene 105: 61-72.

Zhang, Y. Z., J. J. Naleway, D. K. Larison, Z. Huang and P. R. Haugland (1991). "Detecting lacZ expression in living cells with lipophilic fluorogenic β-galactosidease substrates." FASEB J. 5: 3108.

Zhuo, L., B. Sun, C.-L. Zhang, A. Fine, S.-Y. Chiu and A. Messing (1997). "Live astrocytes visualised by green fluorescent protein in transgenic mice." Developmental biology 187: 36-42.

Zolotukhin, S., M. Potter, W. W. Hauswirth, J. Guy and N. Muzyczka (1996). "A "Humanised" green fluorescent protein cDNA adapted for high-level expression in mammalian cells." J. Viol. 70(7): 4646-4654.

Zylka, M. J. and B. J. Schnapp (1996). "Optimised filter set and viewing conditions for the S65T mutant of GFP in living cells." BioTechniques 21(2): 220-226.